Experimental Transmission of Alzheimer's Disease Endophenotypes to Murine and Primate Models

Charlotte Gary

NNT : 2016SACLS412

THESE DE DOCTORAT
DE
L'UNIVERSITE PARIS-SACLAY
PREPAREE A
L'UNIVERSITE PARIS-SUD

ECOLE DOCTORALE N° 568
Signalisations et réseaux intégratifs en biologie

Spécialité de doctorat : Sciences de la vie et de la santé

Par

Mlle Charlotte Gary

Experimental transmission of Alzheimer's disease endophenotypes to murine and primate models.

Thèse présentée et soutenue à Fontenay-aux-Roses, le 29 novembre 2016 :

Composition du Jury :

Dr. Hauw, Jean-Jacques	Professeur honoraire, Université Pierre et Marie Curie	Président du jury
Dr. Aucouturier, Pierre	Professeur Praticien hospitalier, INSERM Université Pierre et Marie Curie	Rapporteur
Dr. Delatour, Benoit	Chargé de recherche, CNRS Université Pierre et Marie Curie	Rapporteur
Dr. Laude, Hubert	Directeur de recherche honoraire, INRA	Examinateur
Dr. Bousset, Luc	Chargé de recherche, CNRS Université Paris-Saclay	Examinateur
Dr. Dhenain, Marc	Directeur de recherche, CNRS Université Paris-Saclay	Directeur de thèse

"Being a scientist is a special privilege:
for it brings the opportunity to be creative,
the passionate quest for answers to
nature's most precious secrets, and
the warm friendships of many
valued colleagues."
Stanley B. Prusiner

Acknowledgments

Je remercie Pierre Aucouturier, Benoît Delatour, Jean-Jacques Hauw, Hubert Laude et Luc Bousset d'avoir accepté de faire partie de mon jury de thèse. J'adresse particulièrement un remerciement aux deux rapporteurs qui m'ont fait l'honneur de juger ce travail, les Drs Pierre Aucouturier et Benoît Delatour, pour le temps précieux qu'ils y ont accordé et pour leur suivi de ma thèse.

Je tiens à remercier Philippe Hantraye et Emmanuel Brouillet de m'avoir accueillie au sein de MIRCen et du Laboratoire des Maladies Neurodégénératives UMR CEA CNRS Université Paris-Sud Paris Saclay 9199, respectivement, et de m'avoir permis de réaliser ces travaux. En particulier, je remercie Emmanuel Brouillet pour ses conseils et ses encouragements !

Je remercie mon directeur de thèse, Marc Dhenain, pour m'avoir donné l'opportunité de faire cette thèse passionnante. Je voudrais te remercier de toujours t'être rendu disponible pour répondre à mes questions malgré tes nombreux engagements. Egalement, merci de m'avoir fait confiance et de m'avoir accordé une grande liberté pour mener à bien tous ces projets! Merci aussi de m'avoir fait découvrir toutes les facettes du métier de chercheur, depuis l'élaboration du projet en passant par les saisines, les demandes de financement, les mises aux point jusqu'à sa réalisation et sa valorisation orale comme écrite. En bref, c'était vraiment complet ! Je te remercie aussi de la confiance que tu m'as accordée pour communiquer nos résultats et promouvoir notre équipe. J'ai vraiment apprécié ! Merci de m'avoir donné l'opportunité d'encadrer deux stages durant cette thèse. Toutes ces expériences ont été très enrichissantes ! Pour finir, merci pour ton enthousiasme scientifique sans faille même dans les moments de découragement! J'ai trouvé cette petite citation qui, je trouve, te correspond assez: « A pessimist sees the difficulty in every opportunity; an optimist sees the opportunity in every difficulty » (Winston Churchill).

Merci aux collaborateurs du projet Induct'Alz, Jean-Luc Picq, Emmanuel Comoy et Fabien Pifferi. Merci Jean-Luc de m'avoir transmis une partie de ton immense savoir sur le comportement du microcèbe et pour ta gentillesse. Merci Emmanuel de m'avoir fait découvrir les prions et de toujours t'être rendu disponible pour répondre à mes questions ! Merci Fabien pour ton chaleureux accueil à Brunoy, pour ton aide logistique au cours de tous mes transports de microcèbe et ta disponibilité. Merci aussi pour ton écoute et la prévenance dont tu as fait preuve à mon égard tout au long de ces trois ans ! Travailler avec vous aura vraiment été un plaisir et j'espère que nous aurons l'occasion d'interagir à nouveau ! Merci encore !

Merci à toute l'équipe de l'UMR 7179 – CNRS/MNHN de Brunoy, en particulier Martine Perret, Fabienne Aujard, Anisur Rahman, Delphine Champeval et Nicolas Villain, pour leur accueil et pour toute l'aide scientifique, technique et/ou logistique qu'ils m'ont apportée.

Merci à l'équipe INSERM U996 du Dr Nathalie Cartier, en particulier Mickaël Audrain et Jérôme Braudeau pour notre projet AAV.

Merci également à l'école doctorale Biosigne et en particulier à Laurent Surdi pour sa réactivité et d'avoir vraiment facilité toutes les démarches administratives!

Merci à toute mon équipe!

- Merci à Fanny Petit qui aura été des plus grands soutiens, tant sur le plan professionnel que personnel, durant cette thèse ! Merci pour ton professionnalisme et la qualité de ton travail. Merci aussi pour ta motivation et ton enthousiasme toujours débordant pour faire de nouveaux tests ! On aura vraiment formé une super équipe et j'espère que nous pourrons retravailler ensemble un jour! Cette thèse, c'est aussi un peu la tienne car je n'aurai jamais pu la finir sans ton aide et j'ai vraiment été fière d'avoir été ta « première thésarde » ! Merci de m'avoir soutenue (et parfois même portée) pendant ces trois ans (TTT !) ! Tu es vraiment une personne exceptionnelle et j'espère un jour plus te ressembler en étant capable de me dédier autant aux autres et de déployer et d'insuffler autant d'énergie, d'enthousiasme et de bonheur autour de moi ! Merci aussi de m'avoir trainée à la danse avec Pauline, c'était de très bons moments passés toutes les trois ! Merci aussi pour les balades et une caresse à Poker ! Pour finir, merci pour ton amitié précieuse que j'espère garder jalousement durant de très, très longues années !
- Merci aussi à Anne-Sophie Hérard, à la fois conseiller scientifique, maman-poule, dragon et psychologue à ses heures perdues...! Merci de tout le temps que tu as pris pour me former, m'aider à développer des protocoles, revoir mes présentations…! En particulier, merci d'avoir relu ma thèse de manière aussi pointilleuse ! Merci aussi pour tout le soutien personnel et professionnel que tu m'as apporté ! Merci pour ton esprit critique et tes remarques toujours constructives ! C'était un bonheur de travailler avec toi ! Tu es vraiment indispensable à cette équipe et à toute cette foule de petits thésards perdus! J'espère avoir un jour ta rigueur, ton professionnalisme, ta patience, ta compétence, ta gentillesse, ton abnégation et ton dévouement ! A très bientôt pour un projet, un Trivial Pursuit ou un resto indien !

- Merci à Nachiket Nadkarni, ah Nad, qu'aurais-je fait sans toi ? Merci pour ton « angélisme », ta bonne humeur, ton aide, ta motivation, ton rhum et ta gentillesse ! Merci pour toutes ces heures qu'on a passé à gérer les élevages et à passer des souris à l'IRM mais aussi merci d'avance pour toutes celles que tu vas encore consacrer à notre projet Hu! Travailler avec toi aura été fantastique et ça va beaucoup me manquer !
- Merci à mes deux stagiaires Zoé Hanss et Lisa Ciaptacz pour la qualité de leur travail et leur implication. Merci d'avoir été aussi tolérantes face à mon inexpérience ! C'était un plaisir de vous avoir comme stagiaires et bon courage à toutes les deux pour la suite !
- Merci aussi à mes co-thésards, le tout récemment Dr Yaël Balbastre (ne t'en fait pas, tu auras ton paragraphe plus bas !) mais aussi à ceux qui n'ont pas encore fini, Zhen Zhen You, Clément Bouvier, Clémence Dudeffant et Clément Garin, bon courage à tous et accrochez-vous !
- Merci au reste de l'équipe, Thierry Delzescaux pour ton humour, Nicolas Souedet pour ta gentillesse et Cédric Clouchoux pour ta bonne humeur!
- Merci aussi aux anciens, Michel Vandenberghe (dommage que l'on ne se soit croisés que si peu de temps mais... qui sait !), Matthias Vandesquille, Kelly Herbert, Mireilla Peterson et Emmalaurie Baptiste (bon courage pour ta thèse !) pour leur gentillesse !

Merci à l'ensemble du personnel de MIRCen! Ce travail n'aurait pas été possible sans votre aide à tous et vous avez rendu mon séjour à MIRCen très agréable ! Merci à tous d'avoir créé un environnement de travail chaleureux, bon enfant, un peu fou par moments qui permet de toujours revenir au labo avec le sourire !! Merci !

En particulier,

- Merci au reste de l'équipe Histo, Pauline Giptchein et Caroline Jan, pour leur aide et leur gentillesse!
- Merci à l'équipe expérimentation animale, Martine Guillermier, Diane Houite et Sueva Bernier, pour leurs conseils et leur bonne humeur !
- Merci à Charlène Josephine, Gwenaëlle Auregan, Noëlle Dufour, Julie Massonneau, Yasemin Gunes et Aurélie Berniard pour leur sourire! Que ce soit à 7h du matin (Gwen), tout au long de la journée (Charlène, Noëlle, Aurélie, Julie) ou après plusieurs heures au microscope (Yasemin), votre bonne humeur et votre gentillesse à toutes m'a vraiment marquée!
- Gilles Bonvento et Alexis Bemelmans pour leur soutien et leur cuisine au congrès AAIC à Toronto ainsi que leurs conseils.

- Merci à Carole Escartin pour ses questions, ses conseils et ses encouragements !
- Merci à Julien Mitja et Karine Cambon pour leur aide pour le comportement souris.
- Merci à Julien Valette et Julien Flament pour leur accueil des premiers jours ! Merci aussi pour votre aide et de toujours avoir été là pour les bugs comme pour les changements de config !
- Merci à Marie-Claude Gaillard pour sa gentillesse et son aide.
- Merci à Christophe Joubert pour sa bonne humeur matinale !
- Merci à Romina Aron Badin, Joanna Demilly et Claire-Maelle Fovet, c'était toujours un plaisir de vous voir à l'IRM comme à l'animalerie primate !
- Merci à Jean-Marie Héliès pour son soutien et son aide dans le soin des microcèbes.
- Merci à Yoan Moreau et aux animaliers, en particulier Stephen Debucquet et Roxanne Trepier pour leur aide avec les microcèbes, le soin qu'ils leurs apportent, leur motivation et leur gentillesse !
- Merci à l'équipe Servier, Elsa Diguet, Dimitri Cheramy (même si tu soutiens l'ennemi..! A bientôt pour un match !) et Mylène Guerif pour leur gentillesse.
- Merci à toute l'équipe support de MIRCen, Laurent Vincent, Didier Thenadey, Aude Biaut, Kristell Bastide, Pascal Wodling, Marie-Laure Manenti, Marie-Christine Courbeix et Cécile Saintot, sans lesquels ce bel institut ne tournerait pas aussi bien ! En particulier, merci à Laurent d'avoir été aussi compréhensif dans son attribution d'autorisation d'horaires non travaillés (ça m'aura bien aidée !) et à Didier pour toute son aide, sa bonne humeur et la qualité de son support informatique!
- Merci à Sylvie Guigon, Sonia Lavisse, Yann Bramouille, Nadja Van Camp, Lev Stimmer (merci pour tes conseils !), Maria Carillo Conesa, Frédéric Ducongé, Christine Menguy et Che Serguera pour leur gentillesse.
- Merci au mythique bureau 110 pour leur joie de vivre, leur humour et leur amitié! Je n'oublierai pas les vendredis aprèm, les apéros et cette scène mythique de Grease dont je ne désespère pas de récupérer la vidéo ! Merci à Brice Tiret, Chloé Najac et Matthias Vandesquille pour leur accueil chaleureux, vous m'avez aidée à me sentir rapidement chez moi ! Merci à Clémence Ligneul, notre licorne magique, dont la présence et l'amitié m'ont été très précieuses pendant cette thèse et le seront encore après! Pour finir, merci aux petits nouveaux, Jérémy Pépin, toujours tout sourire et volontaire, Clémence Dudeffant et Clément Garin. On compte sur vous pour garder l'esprit du Bureau !
- Merci à Kelly Ceyzeriat (merci pour ton soutien au congrès de Toronto et ces quelques jours de visite qui étaient géniaux !), Laurène Abjean (merci pour ton agréable

compagnie quel que soit le contexte !), Lucie De Longprez, Camille Gardier (garde ta bonne humeur et prend bien soin de No !), Juliette Ledouce, Séverine Maire (ta combativité et ta joie de vivre sont deux de tes qualités les plus inspirantes !), Pierrick Jego, Benoit Gautier, Marco Palombo, Susannah Williams, Marianne Maugard, Marie-Anne Burlot (on ne s'est malheureusement pas croisées assez longtemps.. !), Nam Nguyen Quang (et ses fantastiques pâtisseries), Ioanna Theodorou (bon courage pour le post-doc !), Audrey Vautheny et Anastasie Maté de Gérando! C'était un plaisir de travailler à côté de vous !

- Merci à mes trois co-thésards de choc, Yaël Balbastre, Noémie Cresto et Marie d'Orange ! Je vous ai mis par ordre alphabétique, comme ça, pas de jaloux ! Je commencerai par remercier le CEA pour avoir organisé Porquerolles, voyage sans lequel rien n'aurait été possible ! Vous avez été les meilleurs collègues et amis dont quelqu'un puisse rêver et vous allez terriblement me manquer !! Vous avez toujours été là, pour le meilleur comme pour le pire ! Vous avez toujours su trouver les mots pour me remettre le pied à l'étrier après une chute comme me donner une petite tape derrière la tête ou un coup de pieds aux fesses quand j'en avais besoin ! Votre amitié et votre franchise m'aura permis d'arriver au bout de cette difficile étape qu'est la thèse ! Merci aussi pour votre qualité scientifique et toute l'aide que vous m'avez apportée, chacun dans vos domaines d'expertise ! Merci pour vos remarques toujours constructives et votre regard critique qui m'ont toujours permis de prendre du recul et d'avancer autant scientifiquement que personnellement! Un petit merci spécial à Marie dont les idées « pour rigoler » sont souvent les meilleures ! Vous n'êtes pas officiellement mes co-auteurs voire par moments mes co-encadrants de thèse, mais vous mériteriez de l'être! Merci pour toutes votre aide sur les figures, les stats, la préparation des présentations pour les congrès et surtout pour la préparation de la soutenance ! Merci aussi pour nos pauses café, nos déjeuners mutualisés et nos week-ends qu'ils aient été festifs ou travaillés ! Ecrire nos thèses ensemble a vraiment rendu cette période très agréable ! Merci aussi pour nos fou-rires, nos pêtages de cables (bêêêêh..!), nos aprèm rugby, nos soirées PMU, maison ou Globo et surtout nos voyages ! Ma porte vous sera toujours ouverte pour servir de bibliothèque, vinothèque, charcuthèque, fromathèque..! Un petit mot en particulier pour Noémie qui a rempilé pour 6 mois (« Engagez-vous, rengagez-vous qu'ils disaient! »). Bon courage et surtout prends soin de toi, au moins un petit peu de temps en temps (on a quand même missionné Camille pour veiller au grain) ! On est là pour t'aider, te soutenir, te faire un capuccino, boire une bière, te préparer de bons petits plats, aller pêcher la crevette à 6h du

mat'... N'hésite pas, on est là pour toi! Mais honnêtement, si on pouvait éviter le dimanche à l'aube, ça serait quand même mieux! Pour finir, vous êtes tous les trois des personnes exceptionnelles, tant sur le plan humain que scientifique et je ne doute pas un seul instant que vous allez faire de grandes choses ! J'espère que vos futurs collègues se rendront compte de la chance qu'ils auront de vous avoir dans leur équipe et je les jalouse d'avance... Nous avons vraiment formé une petite famille pendant ces trois ans ! Je sais que notre amitié va continuer de grandir en dehors du labo mais j'espère bien qu'un jour nous pourrons reformer notre équipe au travail! Ne soyons pas tristes, car, même si c'est la fin d'une époque, c'est surtout le début d'une autre ! A tout de suite pour de nouvelles aventures !

Merci aussi à mes anciens directeurs de stage et collègues ! En particulier, merci à Jean-Marc Idée et Nathalie Fretellier, qui ont posé les premières pierres, pour m'avoir donné envie de continuer dans la recherche ! Merci pour votre aide, vos conseils et votre soutien encore aujourd'hui!

Merci à mes amis de lycée ou de pharma ! Merci en particulier à Charlotte, Pauline, Margaux, Mathilde et Fanny pour leur compréhension et leur soutien et à Gayou, Vincent, Guillaume, Jules et Bizuth pour le divertissement du week-end!

Merci à ma « belle-famille » pour leur soutien pendant ces trois ans !

Merci à ma famille ! Merci à mes parents qui m'ont soutenue pendant maintenant… tout récemment 27 ans ! Merci de votre amour, votre éducation, votre accompagnement et de m'avoir permis d'arriver jusqu'ici ! Merci aussi à Marie, Laurence et Pierre-Yves, mes frères et sœurs pour leur soutien et leur écoute ! Merci aussi à nos « deux pièces rapportées » comme dirait l'autre, Christophe et Mahmoud! Enfin, merci à mes nièces Leen et Mina et bien sûr à Maxime, le petit dernier que je n'ai pas encore vu mais qui fait déjà la joie de toute la famille !

Pour finir, merci à toi Joy ! C'est la deuxième thèse que tu subis avec brio, félicitations ! Promis, c'est la dernière ..! Tu n'as pas fui (l'Angleterre ça ne compte pas !) et tu as toujours été là pour moi! Merci pour ta présence, ton écoute, ton soutien, ton conseil, ta franchise et ta tolérance… Dans les bons comme les mauvais moments, tu as été ma lumière et, sans toi, je ne serais jamais arrivée au bout de toutes ces années d'étude! Merci…

Contents

Acronym and Abbreviation list

AAV: Adeno-Associated Virus

AChE: Acetylcholinesterase

AD: Alzheimer's Disease

APOEε4: Apolipoprotein E ε4 allele

Aβ: β-amyloid peptide

CA: Cornu Ammonis

CAA: Cerebral Amyloid Angiopathy

CC: Corpus callosum

CERAD: Consortium to Establish a Registry for Alzheimer's Disease

CGH: Cadaver-derived Growth Hormones

CITES: Conventional on International Trade in Endangered Species

CJD: Creutzfeldt-Jakob Disease

CLU: Clusterin

CR1: Complement Receptor type 1

CSF: CerebroSpinal Fluid

EEG: Electroencephalography

FDG: FluoroDeoxyGlucose

FDR: False Discovery Rate

GM: Gray Matter

GWAS: Genome-Wide Association Studies

HuAPPwt: Human wild-type *APP* gene

IAPP: Islet Amyloid Polypeptide

MAPT: Microtubule-Associated Protein Tau

MCI: Mild Cognitive Impairment

MMSE: Mini-Mental State Evaluation

mpi: months post-inoculation

MRI: Magnetic Resonance Imaging

ND: Neurodegenerative Diseases

NFTs: Neurofibrillary Tangles

NIA-AA: National Institute on Aging and Alzheimer's Association

NINCDS–ADRDA: National Institute of Neurological and Communicative Disorders and Stroke and Alzheimer's Disease and Related Disorders Association

NMDA: N-methyl-D-aspartate

PD: Parkinson's Disease

PET: Positron Emission Tomography

PHFs: Paired Helical Filaments

PrP: Protease resistant Protein

PrP^{C}: Protease resistant Protein Cellular

PrP^{Res}: Protease resistant Protein to proteinase K treatment

PrP^{Sc}: Protease resistant Protein Scrapie

PSD: Post-Synaptic Density

SDS: Sodium Dodecyl Sulfate

TREM2: Triggering Receptor Expressed on Myeloid cells 2

TSE: Transmissible Spongiform Encephalopathies

VBM: Voxel-Based Morphometry

w/v: weight/volume

WM: White Matter

wpi: weeks post-inoculation

Figure list

Table list

Part I – Introduction

Chapter I – Alzheimer's disease

1.1. Overview of Alzheimer's disease

Alzheimer's disease (AD) is the most common form of dementia leading to complete loss of autonomy of the patient. It is a devastating disease both socially and economically in societies in which elderly population is growing (Holtzman et al., 2011).

AD is clinically characterized by a progressive alteration of cognitive abilities including memory loss, impaired judgment and decision-making capacity as well as changes in behavior, mood and personality. These symptoms have a strong impact on daily life activities leading to an increasing dependence of the patients on caregivers.

Neuropathologically, AD is defined by a cerebral atrophy and the deposition of two proteins in the brain: β-amyloid peptide (Aβ) and hyperphosphorylated Tau proteins in extracellular amyloid plaques and intracellular neurofibrillary tangles (NFTs), respectively. In AD, both proteins present a misfolded structure that is enriched in β-pleated sheets (Haass and Selkoe, 2007). The involvement of abnormal proteins in AD has been evident since Alois Alzheimer described the first case in 1906 (Alzheimer, 1907; Alzheimer et al., 1995). Nowadays, the definite diagnosis of AD still requires the identification of these two proteinaceous lesions *post-mortem*.

Today, AD patients can only be treated with symptomatic therapies that provide temporary and limited benefits. As no disease-modifying therapies are available, AD is a major challenge for research.

1.2. Clinical manifestations

1.2.1. Overview of clinical symptoms

Memory dysfunction

Memory is separated into short- and long-term memory, the latter being a consolidation of the short-term memory. It is divided in procedural memory, the memory of motor abilities, and declarative memory, the memory of events and facts, itself subdivided in episodic memory and semantic memory.

AD is characterized by progressive memory dysfunction affecting both subtypes of declarative memory that have a considerable impact on patients' daily life. At early stages, AD patients are aware of such memory deficits but quickly lose this self-awareness (anosognosia). In most cases, episodic memory is the first type to be altered in AD (Nestor et al., 2006). This memory records and recalls biographic memories referenced in a spatio-temporal context. At early stages of the disease, the more recent the memory is, the more affected but, with disease progression, amnesia progressively affects older memories. Semantic memory is the memory of concept-based knowledge unrelated to specific personal experiences, such as word significance. It is also affected in AD, generally at latter stages compared to episodic memory (Giffard et al., 2008).

Other cognitive impairments

Other cognitive deficits are associated with AD. Executive cognitive functions, such as planning or abstract thinking, are quickly impaired in AD leading, for example, to difficulties in decision-making. Aphasia (inability to comprehend and formulate language), apraxia (difficulties in motor planning) or agnosia (inability to process sensory information such as object or face recognition) and spatio-temporal disorientation are also frequent in AD (McKhann et al., 2011).

Other symptoms

Aggressiveness is very frequent and worsens with disease progression. Personality changes, depression, anxiety, emotional blunting, apathy and/or withdrawal from social life, among others, can be observed. Psychotic disorders, resulting mostly in visual hallucinations, can sometimes appear, generally at late stages.

1.2.2. Progression of clinical symptoms

AD is a slowly evolving disease that starts decades before the clinical onset. The development of AD biomarkers has led to the redefinition of criteria for AD diagnosis (McKhann et al., 2011) and the identification of preclinical and prodromal stages of AD.

The **asymptomatic preclinical stage** precedes clinical AD onset by one or two decades. It is divided into three stages with asymptomatic individuals presenting (1) cerebral β-amyloidosis, then (2) signs of neurodegeneration and finally (3) subtle cognitive impairment (Sperling et al., 2011). Progressively, memory impairments can worsen leading to a

symptomatic prodromal or pre-dementia stage called **Mild Cognitive Impairment** (MCI). MCI patients present with a global satisfactory cognition but their performance in memory tests are abnormally low for their age. No other cognitive alterations or major impacts on daily life activities are detected in this stage (Bondi and Smith, 2014). MCI can be defined as a prodromal transitional state between physiological aging and AD and around 50% of MCI cases convert into AD within 5 years (Petersen, 2004). Finally, memory impairments further worsen and are associated to other cognitive impairments in the **AD dementia** phase.

1.3. Clinical diagnosis of Alzheimer's disease

The diagnosis of AD is based on clinical and neuroanatomical criteria (McKhann et al., 1984). The updated criteria of the National Institute of Neurological and Communicative Disorders and Stroke and Alzheimer's Disease and Related Disorders Association (NINCDS–ADRDA) categorize AD as (1) definite, (2) probable or (3) possible (McKhann et al., 2011).

(1) **Definite** diagnosis of AD requires the identification of both clinical AD dementia and neuropathological lesions (see **1.4**.). (2) **Probable** AD requires the identification of progressive memory impairments associated with alterations of, at least, one non-amnestic domain and the exclusion of other causes for dementia. (3) **Possible** AD is diagnosed in case of atypical course of cognitive decline or in presence of comorbidities such as stroke or traumatic brain injury, features of another dementia, neurological or non-neurological disease that could have substantial effects on cognition (McKhann et al., 2011).

Another criterion for AD diagnosis is the Diagnostic and Statistical Manual of Mental Disorders IV (DSM-IV). It is based on the identification of progressive and impacting deficiencies in memory function associated with at least one other cognitive domain with the exclusion of other causes for dementia (American Psychiatric Association, 2004).

Identification of cognitive alterations relies on clinical examination and standardized neuropsychological tests such as the Mini-Mental State Evaluation (MMSE, Folstein et al., 1975) or the Clinical Dementia Rating (Hughes et al., 1982). The clinician can also perform complementary exams if necessary such as Magnetic Resonance Imaging (MRI) to observe cerebral atrophy, in particular in the temporal regions, and/or exclude other causes of dementia.

1.4. Post-mortem diagnosis

The post-mortem diagnosis of AD relies on Aβ and Tau lesions identification and staging.

1.4.1. Evaluation of β-amyloid pathology: Thal phases

Thal *et al.* have characterized parenchymal Aβ deposition in five ''phases'' (**Figure 1**). In phase 1, parenchymal Aβ deposition starts in the neocortex then reaches the hippocampus and the entorhinal cortex in phase 2, the striatum and diencephalic nuclei in phase 3, various brainstem nuclei in phase 4, and finally the cerebellum and other brainstem nuclei in phase 5 (Thal et al., 2002a).

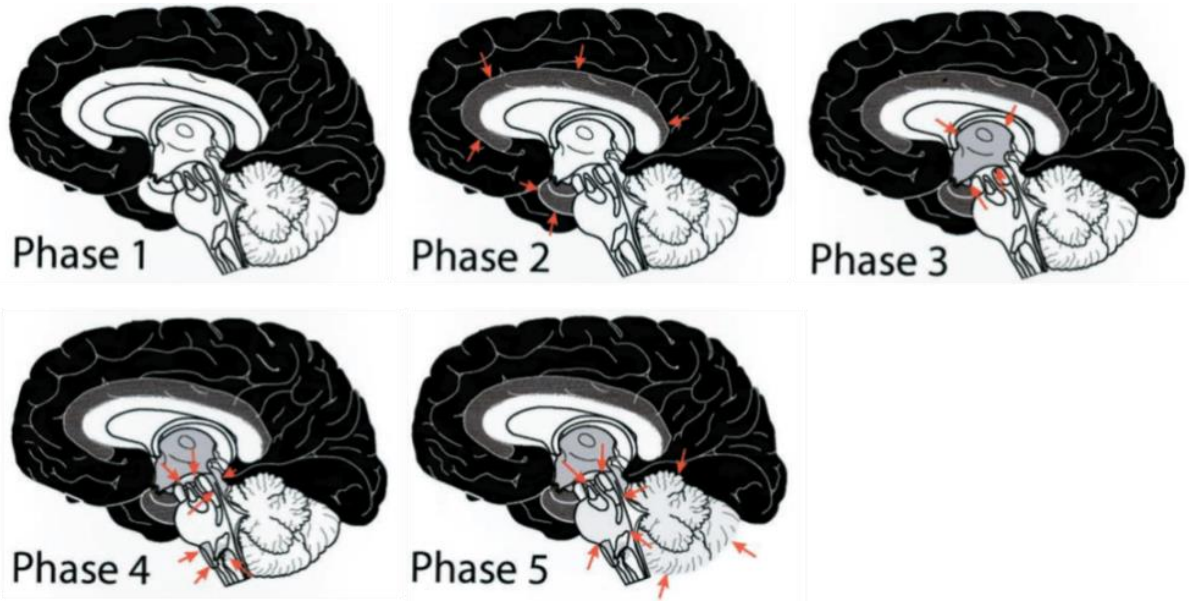

Figure 1. **Thal phases for β-amyloidosis.** Phase 1: neocortex (black). Phase 2: allocortex (red arrows). Phase 3: diencephalic nuclei (red arrows) and striatum (not shown). Phase 4: brainstem nuclei (substantia nigra, superior and inferior colliculus, central gray, red nucleus, inferior olivary nucleus, and intermediate reticular zone) (red arrows). Phase 5: cerebellum and additional brainstem nuclei (locus coeruleus, pontine nuclei, reticulo-tegmental nucleus, dorsal tegmental nucleus, parabrachial nuclei, and oral and central raphe nuclei) (red arrows) adapted from (Thal et al., 2002a).

Aβ deposition in AD may also occur in vessels (cerebral amyloid angiopathy, CAA). Three stages in CAA were described (**Appendix 1**). The vessels are affected in the isocortex at stage 1, in the allocortex, cerebellum and midbrain at stage 2, in the basal ganglia, thalamus, pons and medulla oblongata in stage 3 (Thal et al., 2003, 2008). This staging is not required for

neuropathological diagnosis of AD although the National Institute on Aging and Alzheimer's Association (NIA-AA) guidelines recommends that it should be evaluated and reported systematically (Montine et al., 2012).

1.4.2. Evaluation of Tau pathology: Braak stages

Braak and Braak have characterized the progression of Tau pathology (**Figure 2**). Braak staging of Tau pathology has been adapted to routine pathology (Duyckaerts et al., 1997a) and appears well correlated with the clinical status (Braak et al., 1993).

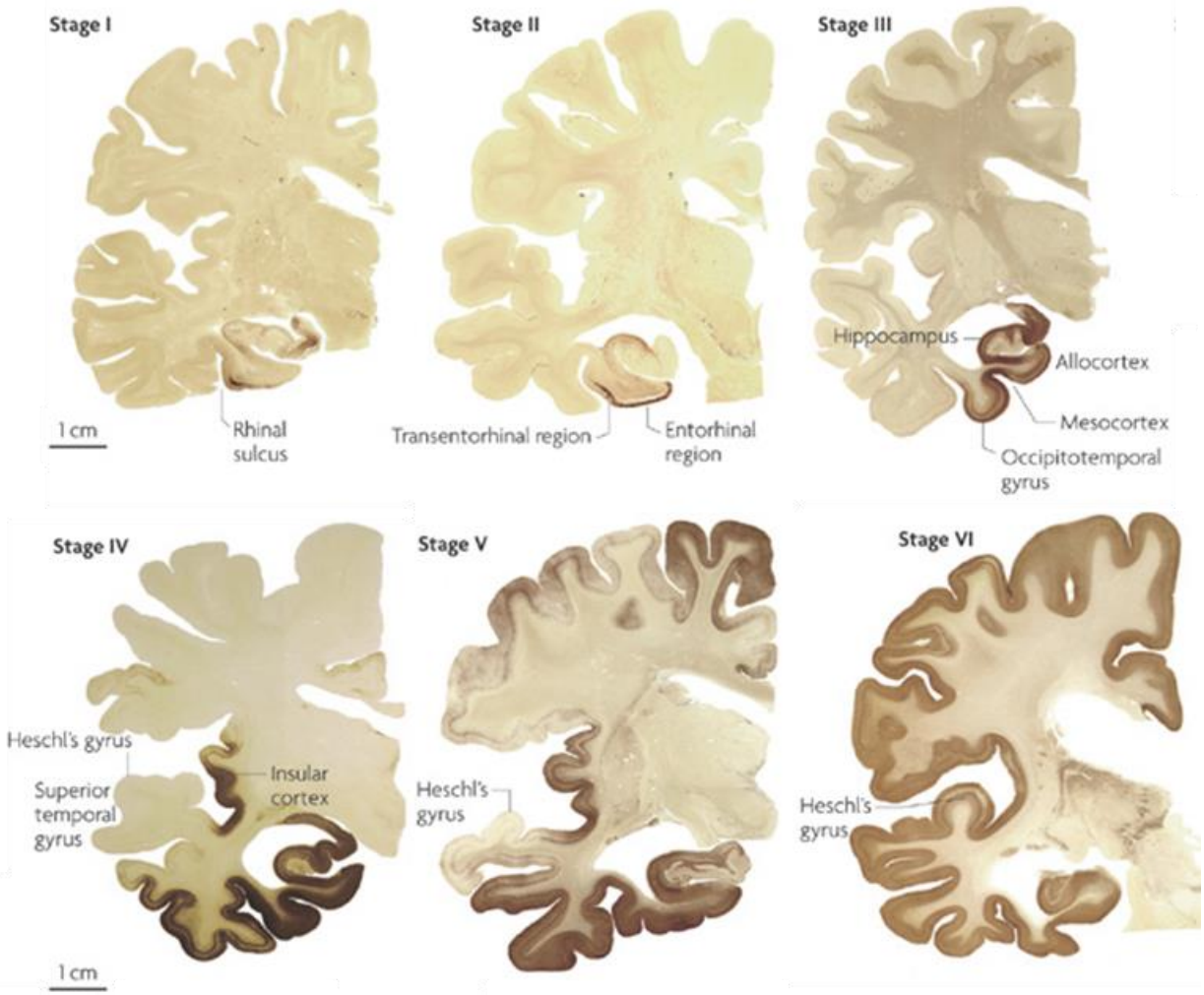

Figure 2. **Braak staging for Tau pathology in AD.** NFT accumulation begins in the transentorhinal cortex (stage I), progresses to the entorhinal cortex (stage II), reaches the hippocampus (stage III) and other limbic areas (stage IV) and finally spreads to neocortical and primary sensory areas (stages V and VI) from (Kretzschmar, 2009).

The staging procedure is based on the localization of NFTs and neuropil threads. In Braak stages I and II, NFTs are present in the transentorhinal and entorhinal cortex without clinical dementia. In stages III and IV, the pathology worsens in these two regions and starts to affect the hippocampus, the fusiform gyrus and the temporal cortex. At these stages, the degree of neuronal damage may determine clinical symptoms. In stages V and VI, representing the neuropathological criteria for the diagnosis of AD, NFTs involve the isocortical association areas and patients are severely demented (Braak and Braak, 1991; Braak et al., 2006).

Interestingly, neuronal Tau inclusions have been detected in the locus coeruleus of children and young adults. These lesions were suggested to be one of the earliest lesions in the evolution of the disease process, although this point is still discussed (Braak et al., 2006).

1.4.3. Evaluation of neuritic plaque pathology: CERAD

Consortium to Establish a Registry for Alzheimer's disease (CERAD) score is a semiquantitative evaluation of neuritic plaques. Neuritic plaques are Aβ deposits associated to thickened neurites stained by silver (Prayson, 2012). CERAD score 0 corresponds to an absence of neuritic plaques, score 1 refers to sparse, score 2 to moderate and score 3 to frequent neuritic plaques (Mirra et al., 1991).

1.4.4. ABC score

NIAAA guidelines (Montine et al., 2012) recommend that AD neuropathologic changes have to be classified along three parameters, (1) Aβ Thal phases (Thal et al., 2002a), (2) NFTs Braak stage using either silver-based histochemistry (Braak and Braak, 1991) or phospho-Tau immunohistochemistry (Braak et al., 2006), and (3) CERAD neuritic plaque score (Mirra et al., 1991) to obtain an "ABC score" (**Appendix 2A**). Evaluation of comorbidity is also recommended as around 60% of AD patients present with neuropathologic comorbidities (Franklin et al., 2015).

The "ABC" ("A" for Amyloid, "B" for Braak, "C" for CERAD) score is based on Thal phases (A), Braak stages (B) and CERAD scores (C) (Kovacs and Gelpi, 2012). ABC score qualifies AD neuropathologic changes as "not", "low", "intermediate" or "high". "Intermediate" or "high" AD neuropathologic changes are considered as a sufficient explanation for dementia (Montine et al., 2012, **Appendix 2B**).

1.5. Epidemiology and etiology of Alzheimer's disease

In 2015, dementia affected around 45 million people worldwide and this number of patients is estimated to triple by 2050 (Baumgart et al., 2015). Around 70% of dementia cases are attributed to AD. The exact prevalence of AD is difficult to determine because, among other reasons, AD is not an obligatory reportable illness. The prevalence and incidence rates for AD increase exponentially with age. For example, AD incidence doubles every 5 years from 65 through the 90 years of age (Reitz et al., 2011).

Based on age of onset, two types of AD can be distinguished, early and late-onset AD (Blennow et al., 2006). **Early-onset AD** is a genetic/familial form of the disease representing around 1% of AD cases. Mean age of onset is 55 year-old although cases have been described as early as the third decade. It is a rare autosomal dominant pathology associated with numerous mutations in three genes implicated in Aβ generation and coding for the Amyloid Precursor Protein (APP, chromosome 21) or presenilin 1 and 2 (PS1 and PS2, chromosomes 14 and 1, respectively) (Goate et al., 1991; Levy-Lahad et al., 1995; Schellenberg et al., 1992). PS1 mutations account for a majority of patients with early-onset AD (Rogaeva et al., 2001).

Sporadic **late-onset** AD is a complex multifactorial disease representing 99% of AD cases and occurs after 65 years old. Multiple genetic susceptibility and interactions among them and with environmental factors likely influence the risk of AD. The ε4 allele of the Apolipoprotein E (**APOEε4**) gene is the main susceptibility gene for late-onset AD (Corder et al., 1993). APOE is a lipid-binding protein encoded by different alleles (APOEε2, APOEε3 and APOEε4). Each inherited APOEε4 allele lowers AD age of onset by 7 years (Kurz et al., 1996). To identify **genetic susceptibilities**, genome-wide association studies (GWAS) are of particular interest as it allows identifying both known and unknown genes. Recent large GWAS have identified additional genes for sporadic AD (Mhatre et al., 2015) mostly involved in endocytosis, lipid metabolism or inflammatory or immune responses (Giri et al., 2016) such as the clusterin gene (CLU), the triggering receptor expressed on myeloid cells 2 (TREM2) or complement receptor type 1 gene (CR1) (Harold et al., 2009; Jonsson et al., 2013; Lambert et al., 2009) (**Appendix 3**). Regarding **environmental risk factors**, age is the main risk factor for AD. Also, cardiovascular risk factors (hypercholesterolemia, arterial hypertension or atherosclerosis), obesity, diabetes, smoking and history of traumatic brain

injury or depression are associated with AD. On the contrary, some factors such as diet with high fish, fruit and vegetable consumption, physical or intellectual activity as well as a high education level have been described as **protective factors** (Reitz et al., 2011).

1.6. Biomarkers of Alzheimer's disease

Biomarker research is a very active domain. A **biomarker** is a "physiological, biochemical, or anatomic parameter that can be objectively measured as an indicator of normal biologic processes, pathological processes, or responses to a therapeutic intervention" (Jack and Holtzman, 2013).

Current AD biomarkers are divided into two classes (1) biomarkers of brain Aβ deposition that include low cerebrospinal fluid (CSF) $A\beta_{1-42}$ and positive positron emission tomography (PET) amyloid imaging, (2) biomarkers of downstream neuronal degeneration or injury that include elevated CSF total and phosphorylated (more AD specific) Tau, decreased ^{18}fluorodeoxyglucose (FDG) uptake on PET in the temporo-parietal cortex and disproportionate atrophy on structural MRI in medial, basal, and lateral temporal lobe as well as medial parietal cortex (McKhann et al., 2011).

Other **potential AD biomarkers** are currently being evaluated such as other CSF (APOE, 24S-hydroxycholesterol…) or plasma (Aβ peptides, cholesterol or inflammation-related proteins) analytes, diffusion MRI, perfusion MRI, resting state and task activation MRI functional MRI as well as Tau PET ligands (Jack and Holtzman, 2013; Reitz et al., 2011). These biomarkers have not yet demonstrated their test-retest precision or their diagnosis efficacy and still require further development.

In patients with probable or possible AD, biomarker tests may increase the certainty of the diagnosis. Presently, it was advocated that **AD biomarker use** should be restrained to investigational studies, clinical trials, and as optional clinical tools when deemed appropriate by the clinician. A specific category of "probable AD with evidence of AD pathophysiological process" was defined to include biomarkers in AD diagnosis and is used for research purposes (McKhann et al., 2011).

Some examples of AD biomarkers will be presented here.

1.6.1. Cerebral atrophy

AD is characterized by a typical symmetric and **widespread cerebral atrophy**. The degree of atrophy is related to disease duration, consistent with an early and sustained disease process. Most impacted structures are the entorhinal cortex, the amygdala and the hippocampus (de la Monte, 1989). Indeed, atrophy affects predominantly the temporal lobe as well as middle frontal cortices with a relative sparing of the primary motor, sensory and visual cortices and total sparing of the inferior frontal lobes (Halliday et al., 2003) and results in ventricle enlargement.

Anatomic MRI allows the longitudinal evaluation of cerebral atrophy in AD at-risk patients. Atrophy starts in the temporal lobe, then reaches the parietal lobes and finally, the frontal lobe (Whitwell, 2010). Measured by MRI, atrophy correlates with neuronal loss (Zarow et al., 2005), Braak stages (Jack et al., 2002; Vemuri et al., 2008; Whitwell et al., 2008) (**Figure 3**) but not well with Aβ load (Josephs et al., 2008) suggesting that it reflects Tau-associated neurodegeneration (Jack and Holtzman, 2013). Also, atrophies of temporal lobe structures correlate with cognitive impairments (Duyckaerts et al., 1985; Jack et al., 2002). In particular, episodic memory impairments are mainly related to the atrophy of the temporal lobe including the entorhinal cortex and the hippocampal formation (Fleischman and Gabrieli, 1999).

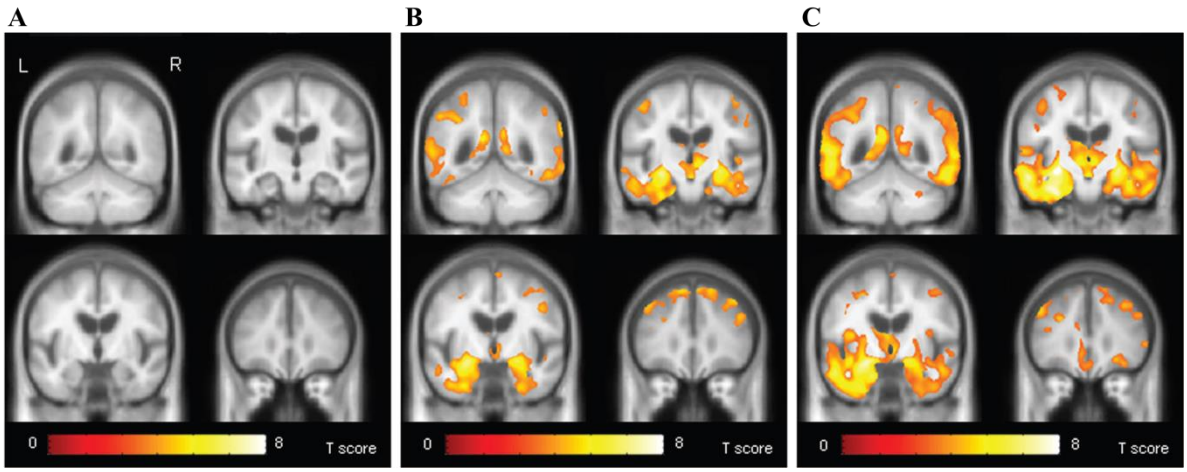

Figure 3. **Atrophy measured by MRI correlates with Braak stages**. Patterns of gray matter loss on MRI in subjects with Braak stage III to IV (A), V (B), or VI (C) when compared with the control group (Braak stages 0–II) adapted from (Whitwell et al., 2008).

1.6.2. Metabolic alterations

In AD, metabolic alterations occurs, for example, with a diminution of glucose carriers (Simpson et al., 1994) and metabolic enzyme activity (Sorbi et al., 1983). **FDG-PET** studies provide a non-invasive measure of cerebral glucose metabolism and revealed a characteristic pattern of symmetric hypometabolism in the posterior cingulate and parieto-temporal regions that then spreads to the prefrontal cortices. The extent of hypometabolism correlates with the degree of cognitive impairment (Nestor et al., 2006; Small et al., 2008).

1.6.3. Electroencephalogram alterations

AD is also associated to neuronal activity alterations. **Electroencephalogram (EEG)** reflects neuronal activity and has been used for many decades as a non-invasive, cost-effective tool for exploring functional brain changes in AD.

During **resting state EEG**, AD patients show a slowing of their EEG frequencies compared with healthy subjects (Giannitrapani et al., 1991; van der Hiele et al., 2007a; Huang et al., 2000; Mattia et al., 2003). AD patients have increased power in slow EEG activity (delta and theta frequency bands) and decreased power in fast EEG activity (alpha and beta frequency bands) and such alterations correlate with the severity of cognitive impairments (Dierks et al., 1991; van der Hiele et al., 2007a, 2007b; Koenig et al., 2005). Additionally, slow EEG activity alterations correlate with other cerebral dysfunctions such as hypoperfusion (Mattia et al., 2003). Also, resting EEG pattern can predict MCI conversion to AD (Jelic et al., 2000). **During eyes open and memory activation EEG**, alterations in alpha frequencies are associated with declines in MMSE scores as well as in memory and language skills in MCI and AD patients (van der Hiele et al., 2007b).

The mechanisms leading to such EEG alterations are not yet well understood. Aβ could play a major role as elevation of Aβ levels elicits epileptiform activity both in mice and AD patients and promotes aberrant neuronal network synchrony (Palop and Mucke, 2010).

1.6.4. Modeling of Alzheimer's disease biomarkers evolution

Various hypotheses have been proposed to model biomarker evolution. In the example presented here, amyloid biomarkers (CSF $A\beta_{1-42}$ and positive PET amyloid imaging) become abnormal first, followed by CSF Tau and then by FDG PET and MRI with cognitive

impairments being the last event in the progression of the disease (Jack and Holtzman, 2013) (**Figure 4**).

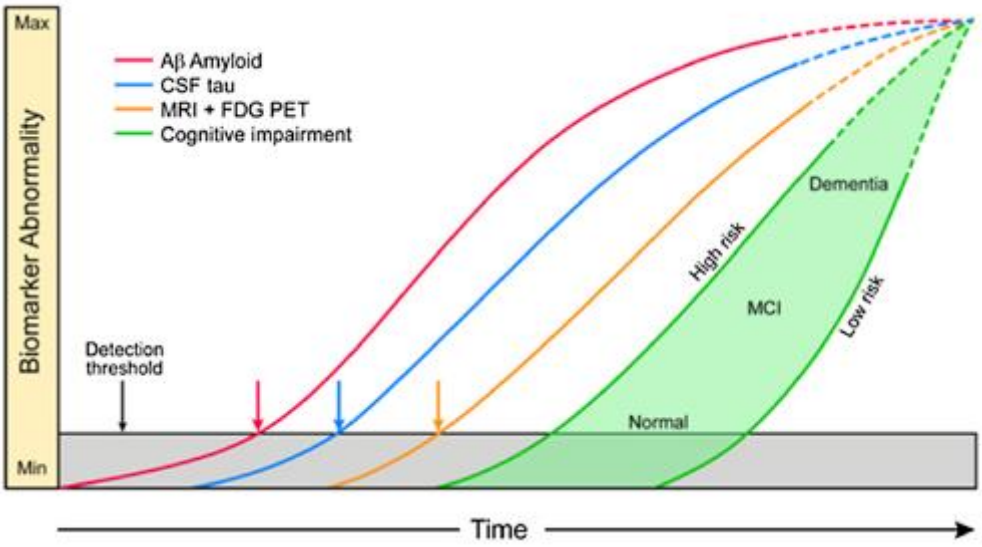

Figure 4. **Hypothesis for the modeling of pure AD biomarker evolution.** The gray area indicates a zone in which abnormal pathophysiology is below the biomarker detection threshold. Cognitive impairments is represented by the green filled area allowing a range of cognitive responses depending on the individual's risk profile that shifts to the high risk for those with low cognitive reserve and to the low risk for those with high cognitive reserve. All biomarker and cognitive impairment curves are modeled as sigmoids but do not reflect reality (Jack and Holtzman, 2013).

1.7. Current therapies for Alzheimer's disease

Current treatments against AD are symptomatic. Four treatments have been approved between 1996 and 2003 and are still commercialized: donepezil (Aricept®), rivastigmine (Exelon®), galantamine (Reminyl®) and memantine (Ebixar® and Namendar®). They are classified in two categories: Acetylcholinesterase (AChE) inhibitors for the three first and the N-methyl-D-aspartate (NMDA) antagonist for the last one.

The **cholinergic hypothesis** for AD physiopathology emerged in the early 80's after the observation that cholinergic neuronal population is especially impacted in AD and significantly contributes to the cognitive decline (Bartus, 2000). This hypothesis oriented the development and use of AChE inhibitors in AD. The AChE inhibitors aim to improve the cholinergic neurotransmission, impaired in AD patients to stabilize cognition (Hansen et al.,

2008; Tan et al., 2014). Also, several studies suggested that excessive activation of NMDA glutamatergic receptors by glutamate plays an important role in the neurodegenerative changes found in AD (Greenamyre et al., 1988; Zhang et al., 2016). Memantine is an **antagonist of NMDA receptors** that aims to target these alterations.

The French Haute Autorité de Santé recommends that the use of AChE inhibitors in patients with mild to moderate AD (MMSE>20), the use of AChE inhibitors or NMDA antagonist for patients suffering from moderate to severe AD (10<MMSE<20) and NMDA antagonist for patients with severe AD (MMSE<10) (Haute Autorité de Santé, 2011). Both therapeutic classes improve cognitive impairments (Cummings, 2000) for a time but, due to progressive neuronal loss, they rapidly lose their efficacy.

1.8. Physiopathology of Alzheimer's disease

1.8.1. β-amyloidosis

1.8.1.1. Generalities on β-amyloid peptides

Aβ is a 38 to 43 aminoacid peptide. Its production results from the sequential cleavages of APP by the enzymatic complexes β- and γ-secretase in neurons. The γ-secretase complex determines the length of Aβ peptides of which 40 and 42 residues are the most common forms. Key proteolytic components of γ-secretase are PS1 and PS2. This processing is called the **amyloidogenic pathway** (**Figure 5**). Physiologically, a non-amyloidogenic pathway for APP processing is predominant involving α-secretase whose cleavage of APP impedes the generation of Aβ (Haass and De Strooper, 1999). Aβ can undergo several post-translational modifications, including N-terminal truncations, pyroglutamate modifications as well as phosphorylation (Thal et al., 2015).

The **function of Aβ** is unknown and its physiological production is often considered a waste product although very low concentrations of Aβ may improve synaptic plasticity and memory (Morley et al., 2010; Puzzo et al., 2008).

In physiological conditions, **Aβ clearance** from the brain is mediated by multiple processes including drainage along perivascular basement membranes, transport across vessel walls into the circulation, microglial phagocytosis, and proteolytic degradation (Miners et al., 2011) and allows limiting its accumulation. Proteolytic degradation is a major route of Aβ clearance and

relies on multiple enzymes such as neprilysin and insulin degrading enzyme (IDE) (Marr and Hafez, 2014).

An imbalance between the production and degradation of Aβ, a shift from the non-amyloidogenic towards amyloidogenic pathways, and/or an alteration in Aβ clearance (Mawuenyega et al., 2010) could contribute to the accumulation of the Aβ in the brain.

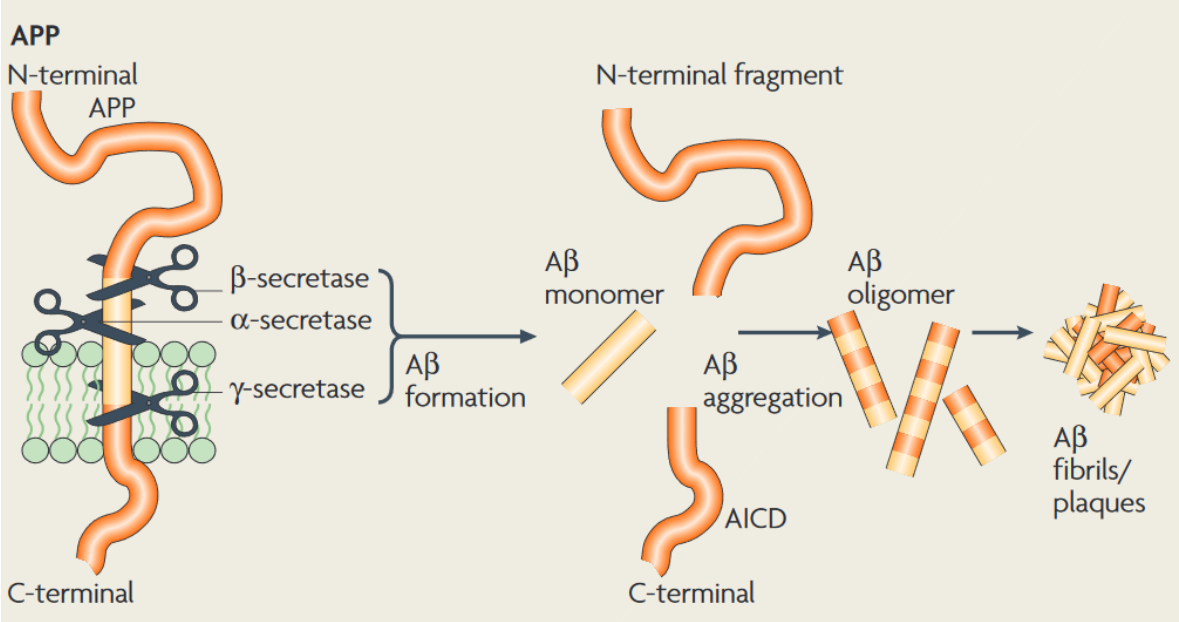

Figure 5. **Amyloidogenic processing of APP leading to Aβ generation and aggregation.** From (Götz and Ittner, 2008).

1.8.1.2. β-amyloid misfolding and aggregation in Alzheimer's disease

Generalities on protein folding

The **conformation** of a protein is the three-dimensional folding of polypeptide chains. It is essential as it defines a protein biological function. Protein folding presents up to four different levels of organization (**Appendix 4**). (1) The primary structure is defined as the linear arrangement of the aminoacid sequence from the amino terminus (N-ter) to the carboxyl terminus (C-ter). (2) The secondary structure is a local folding of the aminoacid backbone chain in two main structures: α-helices or β-pleated sheets (parallel or anti-parallel β-sheets) relying on weak interactions. Other parts of the backbone are ordered without forming any regular structures. (3) The tertiary structure is a three-dimensional structure where α-helix or β-sheets are folded in order to form a compact structure. It is mainly driven

by hydrophobic interactions but other interactions such as salt, hydrogen and disulfide bonds can intervene. (4) Finally, a quaternary structure can be described in multi-subunit proteins and locked by covalent and/or non-covalent interactions.

The **protein homeostasis network** mainly relies on chaperones, that ensure the correct folding of some proteins and prevent their misfolding and/or precipitation, and their degradation by proteases (Landreh et al., 2016).

β-amyloid misfolding and aggregation

Aβ peptides mainly adopt a **random-coil conformation** in their soluble native state (Simmons et al., 1994) although they can also present with α-helix structures in apolar environments or β-pleated sheets in aqueous solutions (Abelein et al., 2014).

The formation of Aβ fibers is dependent on Aβ peptides self-polymerization and seems to require a **conformational transition** from random-coil to β-sheets as they present with substantial β-structures (Barrow et al., 1992; Kirkitadze et al., 2001; McLaurin et al., 2000).

Aβ peptides are **aggregation-prone** and, classically, the longer the sequence, the more aggregation-prone (Jarrett et al., 1993). The hydrophobic regions from the residues 17 to 21 and 29 to 42 are thought to comprise the main β-sheet region and play a major part in the misfolding and aggregation of Aβ peptides (McLaurin et al., 2000). Also, early-onset mutations within Aβ sequence found in familial cases of AD, the Dutch (Glu22Gln), Arctic (Glu22Gly) and Iowa (Asp23Asn) mutations, increase the aggregation-prone character of Aβ by increasing its hydrophobicity and reducing its charge (Kim and Hecht, 2008). This suggests that both hydrophobic and electrostatic interactions are involved in misfolded Aβ aggregation by facilitating the stabilization of β-sheets (Fraser et al., 1994).

1.8.1.3. Characteristics of β-amyloid aggregates in Alzheimer's disease

Amyloid plaques are commonly classified as (1) "diffuse" and (2) "focal", based on their morphology and their affinity to amyloid dyes specific for the β-pleated sheet conformation such as Congo Red and Thioflavin-S. (1) **Diffuse plaques** are usually large deposits, poorly immunoreactive to anti-Aβ antibodies that do not bind amyloid dyes (**Figure 6A**). These plaques are numerous in cognitively healthy elderly subjects (Duyckaerts et al., 2009). (2) **Focal deposits** are dense accumulations of Aβ peptides that do or do not bind amyloid dyes,

that may or may not be associated to a neuritic corona and that are generally surrounded by activated microglia (**Figure 6B**).

Neuritic plaques, focal deposits with a neuritic corona, virtually always present with amyloid dyes binding properties. The core of these plaques is generally composed of $A\beta_{1-42}$ (Güntert et al., 2006) and present a halo and a diffuse zone of immunoreactivity constituting the outermost ring of the deposit. Activated microglial cells are usually present in the halo. The corona of these plaques contains neuritic and astrocytic components. Silver-stained neurites forming the neuritic corona are also called "**dystrophic neurites**" since they are abnormally enlarged and contain paired helical filaments (PHFs) of Tau protein (Duyckaerts et al., 2009). These plaques are most often found in patients with symptomatic AD and associated with deleterious effects on the surrounding neuropil, synaptic and neuronal integrity as well as with the recruitment and activation of both astrocytes and microglial cells (Vehmas et al., 2003).

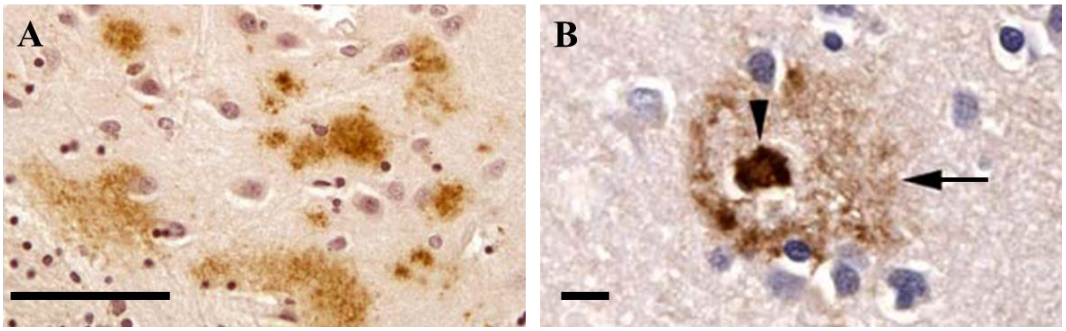

Figure 6. **Aβ plaque morphology.** A. Diffuse amyloid plaques (6F/3D antibody). B. Focal dense-core amyloid plaque. Scale bar 10µm. Adapted from (Duyckaerts et al., 2009).

CAA is frequently detected in sporadic and genetic AD cases (80%) but is also found in elderly cognitively intact individuals (Thal et al., 2008). CAA is an accumulation of Aβ in vessel walls leading to hemorrhages and small cortical infarcts. CAA is mostly composed of $A\beta_{1-40}$ (Güntert et al., 2006) although $A\beta_{1-42}$ can accumulate in capillaries. Aβ first accumulates around the basement membrane and then in the tunica media of arteries and/or capillaries but also in the veins (Thal et al., 2008). The intensity and topography of CAA is variable but the occipital cortex is most massively and frequently involved (Attems et al., 2007). CAA has been separated into two types: with (type 1) (**Figure 7A**) and without capillary involvement (type 2, most frequent) (**Figure 7B**). Capillary involvement is associated with ApoEε4 alleles (Thal et al., 2002b).

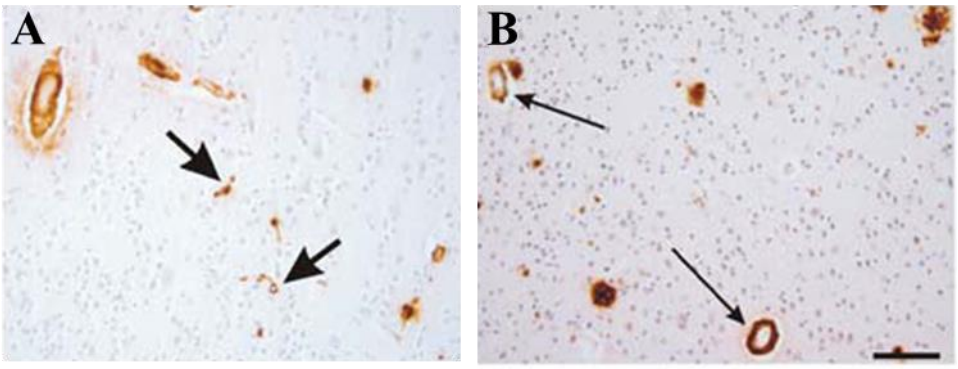

Figure 7. **Types of cerebral amyloid angiopathy.** A. Type 1 CAA, arrows indicate capillary deposits. B. Type 2 CAA, arrows indicate arterial deposits. Scale bar A: 80µm; B: 325µm. Adapted from (Thal et al., 2008).

1.8.1.4. β-amyloid toxicity in Alzheimer's disease

For a long time, the common view has been that Aβ plaques represent the toxic species. However, the frail correlation between the number of aggregates and the cognitive state along with the fact that amyloid plaques are found in cognitively healthy individuals suggests that other players may carry Aβ toxicity.

The assembly of Aβ into amyloid plaques does not occur linearly. Indeed, intermediates between monomers and mature fibrils, that are the main component of amyloid plaques and CAA (Glenner and Wong, 1984; Masters et al., 1985), are various and numerous (Wetzel, 2006) such as protofibrillar (Harper et al., 1997; Walsh et al., 1999) or oligomeric forms (Lambert et al., 1998). These intermediates are found during the lag phase of amyloid formation (Wolff et al., 2015) (see **3.3**).

Although toxic *per se*, plaques might sequester even more toxic species into insoluble and biologically inert materials (Haass and Selkoe, 2007). Reports suggest that most of Aβ toxicity might be mediated by soluble Aβ intermediaries contributing to the disease progression although amyloid plaques might act as a "reservoir" able to release toxic Aβ species (Thal et al., 2015). This hypothesis gained much attention since cortical levels of soluble Aβ assemblies correlate with the extent of neuronal loss and the severity of cognitive impairment in AD patients (McLean et al., 1999). Also, in animal models, some cognitive impairments can develop before β-amyloidosis (Hsia et al., 1999) and oligomeric Aβ assemblies lead to cognitive deficits (Gandy et al., 2010).

Aβ soluble assemblies comprise various numbers of monomers and can exert diverse toxicities. They can induce selective neuronal death, alter synaptic plasticity or deteriorate synapses, favor aberrant Tau phosphorylation, lead to oxidative stress, inflammation, and excitotoxicity, inhibit axonal transport, disrupt membranes by forming toxic pores, disturb ion homeostasis and lead to apoptosis, among others (see Viola and Klein, 2015 for review). Toxicity of Aβ assemblies seems to decrease when they turn into fibrillar forms (Chimon et al., 2007) (**Figure 8**).

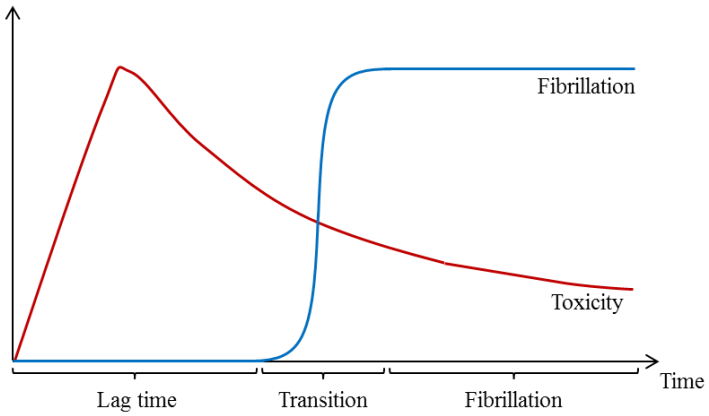

Figure 8. **Scheme representing the evolution of toxicity of Aβ assemblies during amyloid fibrillation.** Adapted from (Luo et al., 2016).

Some Aβ intermediates may be more toxic than others. Several types of oligomers such as Aβ dimers, Aβ trimers, Aβ*56 and Aβ globular oligomers (soluble Aβ oligomers forming protein micelles due to its amphiphilic properties (Kayed et al., 2003)) have been described and it is not yet clear if toxic properties are restricted to oligomers or are exerted by all types of soluble assemblies (Thal et al., 2015).

It has been proposed that Aβ may enter two different pathways: the amyloid formation pathway and the non-amyloid formation pathway (**Figure 9A**). For example, a 60-kDa globular $A\beta_{1\text{-}42}$ oligomer, found in AD patients but not in healthy elderly brains, has been shown to be a persistent structural entity that does not enter the fibrillar aggregation pathway (Gellermann et al., 2008) and exert toxicities interfering with learning and memory processes (Barghorn et al., 2005). This suggests that some oligomers are slowly able to convert into amyloid fibrils whereas others do not (Lee et al., 2011a). Based on this hypothesis, a classification of soluble Aβ oligomers into two classes (**Figure 9B**) was recently proposed. Type 1 oligomers are Aβ assemblies that do not enter the fibril formation process and are

supposed to have a greater toxic potential than type II oligomers. Type II oligomers, supposed to constitute the main pool of Aβ oligomers, are related to the amyloid formation process and therefore are not thought to have limited toxic impacts (Liu et al., 2015) (**Figure 9C**).

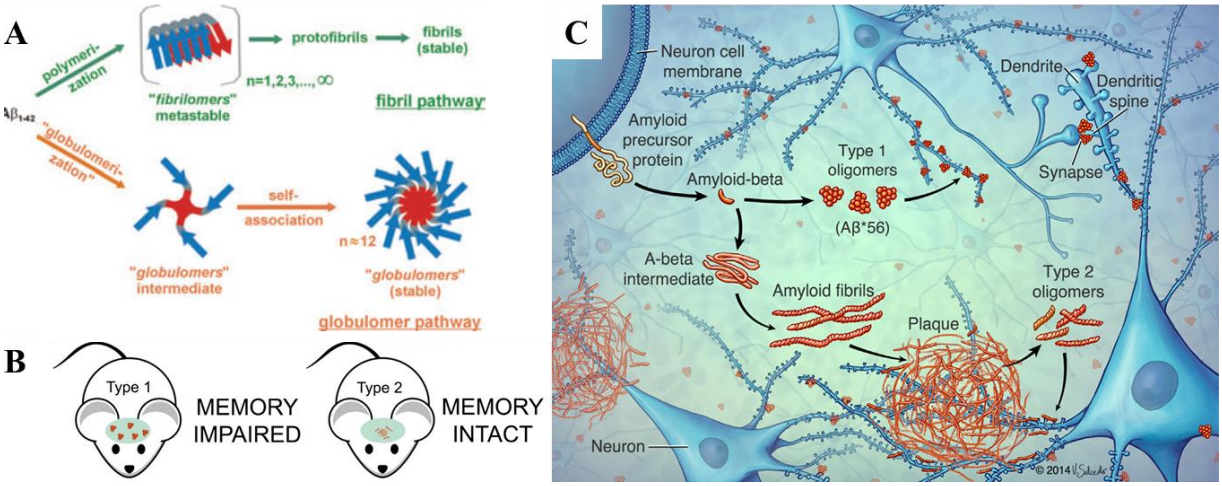

Figure 9. **Hypothesis for the classification of Aβ oligomers according to toxicity in AD.** A. Bi-directional pathway for misfolded Aβ multimerization from (Barghorn et al., 2005). B. Classification of Aβ oligomers based on their relationship with the amyloid formation process. C. Proposed mechanism for oligomer toxicity. B and C from (Liu et al., 2015).

Identifying Aβ assemblies' relative toxicity and their relevance regarding AD pathology will be a critical step for the development of AD-relieving strategies. However, whereas amyloid plaques and CAA are detectable by immunohistochemistry with conventional anti-Aβ antibodies or amyloid dyes, soluble Aβ assemblies, such as oligomers, protofibrils and fibrils, usually escape detection by such methods (Thal et al., 2015) leading to technical issues for their study.

1.8.1.5. Amyloid cascade hypothesis

The **amyloid cascade hypothesis** is the most widely accepted for AD physiopathology. It was proposed in the early 90's and considers Aβ as the main culprit leading to AD (Hardy and Selkoe, 2002). As all AD-related mutations lead to an overproduction of Aβ or shift Aβ production toward more aggregation-prone Aβ peptides, genetic AD provides a strong support to a central role of Aβ in AD. In this hypothesis, elevation of Aβ levels, leading to soluble oligomers, protofibrils, fibrils and amyloid plaques, is supposed to induce subsequent damaging processes such as Tau hyperphosphorylation, NFTs formation, excitotoxic species

generation, oxidative damage, neuroinflammation, and neurotoxicity. Over time, the combination of these events leads to a widespread synaptic dysfunction, neuronal death and AD clinical signs (**Appendix 5)**.

1.8.2. Tauopathy

1.8.2.1. Generalities on Tau protein

Structure

Tau is a 352- to 441-residue protein composed of two major domains: the C-ter microtubule binding domain (containing the repeat domain region) and the N-ter projection domain. A proline enriched region links the two domains (**Figure 10A**). Tau presents with six isoforms depending on the number of the repeat domain regions (R; the presence of repeat R2, yielding 3 or 4 C-ter repeat domain leading to 3R or 4R) and on which near-N-ter exons (N) are included (0N, 1N or 2N) (Wang and Mandelkow, 2016).

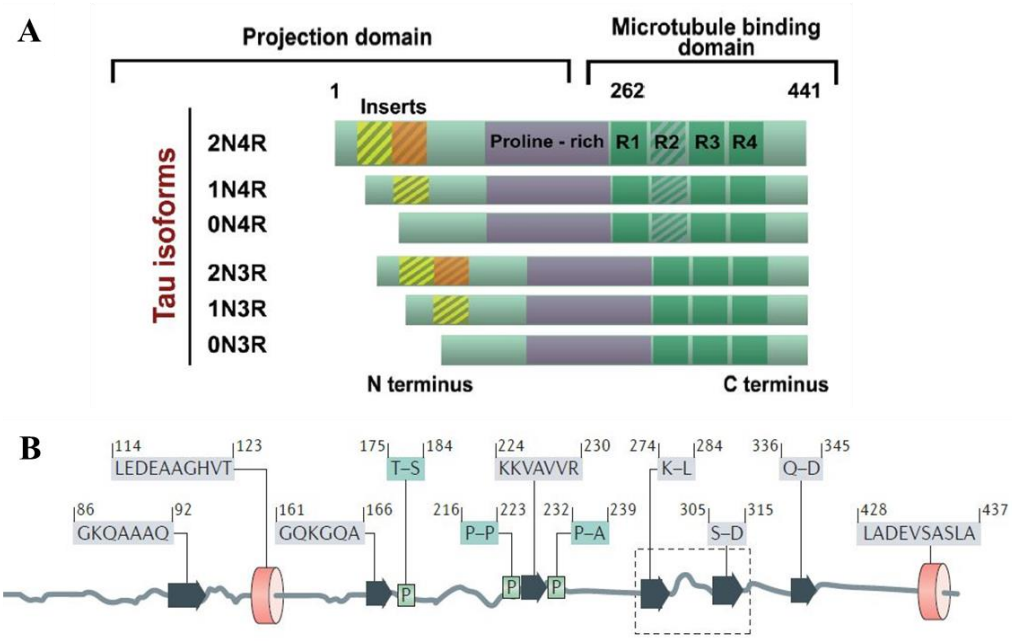

Figure 10. **Structure of Tau protein.** A. Domains of Tau isoforms in the adult human brain from (Šimić et al., 2016). B. Secondary structure of Tau. Gray line: unfolded structures, red cylinders: α-helices, black arrows: β-strands, green boxes: poly-Pro helices, dashed-line box: region containing the two motifs (VQIVYK in R2 and VQIINK in R3) thought to be responsible for Tau aggregation. From (Wang and Mandelkow, 2016)

Physiologically, Tau has little tendency for aggregation (Mukrasch et al., 2009). It is mostly unfold (**Figure 10B**) with a few short and transient secondary structures (α-helices, β-strands and poly-Pro helices (Wang and Mandelkow, 2016) but Tau may also adopt a transient paperclip-like shape (Jeganathan et al., 2006) and local conformations when binding to other partners such as microtubules (Wang and Mandelkow, 2016).

Functions

Tau is a microtubule-associated protein. Depending on its subcellular localization, Tau exhibits different functions. In adult neurons, Tau is mainly localized in axons, where it stabilizes microtubules, promotes their assembly and regulates the reorganization of the cytoskeleton (Feinstein and Wilson, 2005). Small amount of Tau is physiologically present in dendrites and may be involved in the regulation of synaptic plasticity, as activity-dependent translocation of Tau to excitatory synapse is disrupted by exposure to Aβ oligomers, and Tau genetic deficiency protects against Aβ excitotoxicity (Frandemiche et al., 2014). Finally, Tau has been detected in the nucleus of neurons and non-neuronal cells and may play a part in maintaining deoxy- and ribonucleic acids integrity (Violet et al., 2014).

Metabolism

Tau is encoded by Microtubule-associated protein Tau (MAPT) gene located on chromosome 17q21 (Neve et al., 1986). It is subject to alternative splicing producing **6 isoforms**. Tau expression and isoforms ratio are subject to considerable regional variation and these regional differences may contribute to the differential vulnerability of brain regions to Tau pathology (Wang and Mandelkow, 2016).

Many **post-translational modifications** of Tau, such as hyperphosphorylation, truncation or acetylation, have been reported and could play a role in AD (Martin et al., 2011) by promoting Tau aggregation (Wang and Mandelkow, 2016). Physiologically, Tau post-translational modifications are tightly controlled as they are crucial for the regulation of Tau physiological functions, including its binding to microtubules that regulates their stabilization and dynamic assembly (Lu et al., 1999). In AD, Tau is the subject of many post-translational modifications including **hyperphosphorylation** (Köpke et al., 1993) with about 85 sites of phosphorylation and 17 motifs of particular interest (Hanger et al., 2009).

Tau clearance depends on its degradation by many proteases including caspases, calpains and aminopeptidases (Chesser et al., 2013). Also, the ubiquitin–proteasome system (Mori et al., 1987) and the autophagy–lysosomal system (Piras et al., 2016) may participate in Tau clearance but their involvement is still a matter of debate.

1.8.2.2. Tau misfolding and aggregation in Alzheimer's disease

Tau fibril formation may start by **conformational changes** allowing the adoption of β-sheet structures (von Bergen et al., 2001). In AD, all six Tau isoforms (Goedert et al., 1992) fold into an ordered β-structure, that is absent in native Tau proteins (Berriman et al., 2003), during its aggregation in PHFs, a fibrillar structure of around 10nm diameter (Hasegawa, 2016). The sequential process of Tau aggregation seems to start with Tau assembling into dimers or trimers then into small oligomers to larger oligomeric assemblies (Patterson et al., 2011) before slowly assembling into PHFs (Wu et al., 2013). Assembly of PHFs leads to Tau inclusions in neurons, referred to as NFTs in the cell body, and neuropil threads in dendrites and axons (Mukrasch et al., 2009).

The **core of PHFs** is formed of various β-pleated fragments of the repeat domain (Berriman et al., 2003). The C-ter and the N-ter domains form a flexible "fuzzy coat" around the core (Wischik et al., 1988) that may contribute to Tau fibril stabilization (Wegmann et al., 2013). Inside the repeat domain, two short motifs of 6 residues (^{275}VQIINK^{280} and ^{306}VQIVYK^{311} at the beginning of R2 and R3, respectively) show a tendency for β-sheet structures and are essential for Tau aggregation (von Bergen et al., 2000) as they seem to be the basic unit leading to Tau self-assembling (Wille et al., 1992). Indeed, the disruption of these motifs abrogates Tau tendency to aggregate whereas certain mutations (such as ΔK280 or P301L) promote Tau aggregation by enhancing the formation of β-structures in these motifs (von Bergen et al., 2001). Other fragments might also contribute to Tau aggregation such as $Tau_{151–391}$ (Zilka et al., 2006) or truncated $Tau_{1–421}$ (de Calignon et al., 2010).

1.8.2.3. Characteristics of Tau aggregation in Alzheimer's disease

In AD, Tau accumulates exclusively in the somato-dendritic and axonal compartment of neurons. Tau accumulations are called "pre-tangles" and "tangles" in the soma, "neuropil threads" in the dendrites and "neuritic corona" in the axonal processes (**Figure 11**). Tau aggregates undergo a maturation process that can be observed using different antibodies and

colorations (Braak et al., 1994a). In "**pre-tangle" stage**, diffuse or granular Tau aggregates are located in the cytoplasm and around the nucleus, are not usually positive for amyloid staining and show immunoreactivity with several anti-phosphoTau antibodies. In the **"intracellular NFT" stage**, large fibrillar argyrophilic inclusions accumulate in the soma often associated with signs of neuritic deterioration. In the **"extracellular NFT" or "ghost tangle" stage**, extracellular fibrillar Tau is observed with the shape of dead neuronal cell bodies and is highly positive for amyloid dyes with a frequent loss of phospho-Tau immunoreactivity.

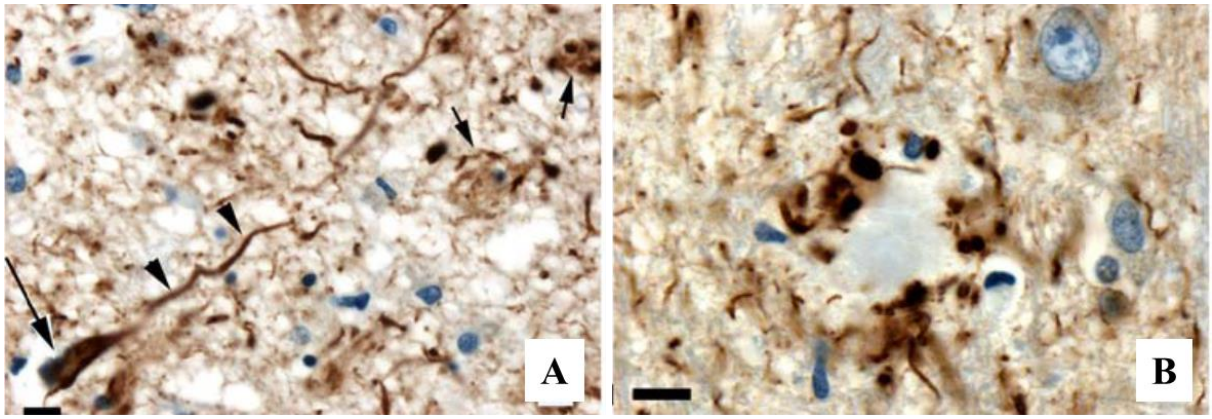

Figure 11. **Tau pathology in Alzheimer's disease.** A. Intracellular NFT (large arrow), extracellular NFT (small arrows) and neuropil threads (arrow heads). B. Neuritic corona. A-B: AT8 antibody. Scale bars 10µm. Adapted from (Duyckaerts et al., 2009).

1.8.2.4. Tau toxicity in Alzheimer's disease

Tau toxicity is supposed to rely on both loss and gain of toxic function. Tau **toxic loss of function** is usually attributed to the aggregation or abnormal hyperphosphorylation of its soluble form. Indeed, reducing Tau binding to the microtubules may lead to disassembly and deficits in axonal transport, contributing to neuronal functions alteration and neurodegeneration (Kimura et al., 2014). However, *in vivo,* Tau deletion is not lethal and only induces some cognitive impairments showing that Tau function can be partially balanced (Lei et al., 2014).

There are two main arguments for Tau **toxic gain of function**. The first one is that Tau hyperphosphorylation is toxic as it disrupts microtubule networks leading to apoptosis (Kondo et al., 2015) and induces its missorting from the axons to the somatodendritic compartment where it can lead to synaptic dysfunction (Wang and Mandelkow, 2016). The

second argument is that NFTs are a better correlate of the severity of the disease than amyloid plaques. However, neuronal loss exceeds NFTs in AD (Gómez-Isla et al., 1997) and strong NFTs pathology can be found in non-demented patients without overt neurodegeneration (Perez-Nievas et al., 2013). Also, in animal models, acute neuronal death (de Calignon et al., 2010), synaptic toxicity and cognitive deficits (Kuchibhotla et al., 2014; Rudinskiy et al., 2014) can occur before NFTs formation. Furthermore, in on/off models, cognitive impairments are alleviated by switching Tau expression off despite the persistence of NFTs (Van der Jeugd et al., 2012).

This accumulating evidence shows that NFTs may be neither sufficient nor necessary for Tau toxicity and suggests a dichotomy between aggregating and toxic species of Tau. Indeed, like for amyloid plaques and although toxic *per se,* NFTs formation may be protective by sequestrating more toxic species. Indeed, **soluble Tau species**, in particular soluble oligomers, are assumed to be the most toxic Tau species in AD (Lasagna-Reeves et al., 2012a) by, for example, altering membrane integrity and reducing cell viability (Flach et al., 2012). However, toxic Tau oligomers remain quite elusive both in structure and toxicity.

In conclusion, the aggregation process seems to be responsible for Tau toxicity along with specific contributions of monomeric missorting and hyperphosphorylation of Tau. Mechanisms underlying such toxicities as well as the structure of the toxic species still remain to be fully elucidated.

1.8.2.5. Tau hypothesis for the physiopathology of Alzheimer's disease

Tau hypothesis is an alternative explanation to the amyloid cascade for AD physiopathology. Indeed, Tau conformational changes better correlates with neuronal loss and AD symptoms than Aβ (Ghoshal et al., 2002) and are virtually detected in all adult brains earlier in life than initially thought (Braak and Del Tredici, 2015). According to this hypothesis, Tau is the trigger of AD pathology and, as a result of neuronal death, oligomeric and fibrillar Tau forms are released to the extracellular space, contributing to microglial cell activation and stimulating a deleterious cycle leading to the spreading of neurodegeneration (Maccioni et al., 2010).

1.8.3. Neuroinflammation

Glial cells, such as **microglia** and **astrocytes**, are involved in cerebral inflammatory processes. Microglial cells are resident innate immune cells of the central nervous system and astrocytes are supporting cells with neuronal environment regulatory functions that can become reactive in case of injuries or pathologies. In AD, activated microglia and reactive astrocytes are associated to dense-core Aβ plaques (Vehmas et al., 2003) and both astrogliosis and microgliosis correlate with NFTs burden (Serrano-Pozo et al., 2011). Glial cells and neuroinflammation seem to be critical players in AD but it is unclear whether they contribute to the pathological process or have neuroprotective effects.

Regarding AD physiopathology, the **Aβ cascade/neuroinflammation hypothesis** has been proposed as a modified version of the amyloid cascade hypothesis (Streit et al., 2004). This hypothesis states that Aβ triggers microglial activation that produce neurotoxic substances inducing neurodegenerative changes such as NFTs formation and synapse loss (Akiyama et al., 2000). Clustering of activated microglial cells around Aβ plaques partly supports this hypothesis.

1.8.4. Vascular alterations

Patients with AD present with many vascular alterations. CAA is one of the most common vascular alterations. Also, **cerebral blood flow** is reduced, especially in temporal-parietal and posterior cingulate cortices (Mattsson et al., 2014) and **signs of cerebrovascular degeneration**, such as vascular injury and blood-brain barrier alterations, are often observed (Ryu and McLarnon, 2009; Zipser et al., 2007). These vascular alterations are predominantly observed in neocortical regions with Aβ pathology suggesting that they may be mostly related to Aβ pathology (Kalaria, 1997; Mattsson et al., 2014). Finally, **microhemorrhages** are common, especially in patients with CAA (Cordonnier and van der Flier, 2011).

The **vascular hypothesis** has proposed hypoperfusion as a central mechanism for the pathogenic evolution of AD (de la Torre, 2000). Under this assumption, aging and vascular risk factor lead to cerebral hypoperfusion affecting optimal brain function and leading to Aβ deposition, NFTs formation, and cognitive alterations. Recently, a complementary hypothesis suggests that alterations leading to cerebral microbleeds can link the vascular and Aβ hypotheses of AD (Cordonnier and van der Flier, 2011). Molecules developed upon this hypothesis are currently being tested in clinical trials (de la Torre, 2016).

1.8.5. Neuronal loss

AD is characterized by **neuronal degeneration** in several neurotransmitter-specific systems (Whitehouse, 1987) such as cholinergic neurons (Whitehouse et al., 1981). Indeed, AD is associated to massive neuronal loss with a pattern that differs from that of normal aging suggesting a specific process, mostly mediated by apoptosis although it may not be the only form of cell death (Mattson, 2004).

Causes of neuronal death in AD are not well understood but Tau is suspected to play a major role (Fukutani et al., 2000). Neuronal loss, especially in cerebral cortex and hippocampus, appears closely associated with NFTs. However, such correlation is not observed in some non-cortical nuclei, such as the locus coeruleus and nucleus basalis of Meynert (Bondareff et al., 1989). This suggests that neuronal death is linked to Tau and that Aβ may also play a role in this process.

1.8.6. Synaptic alterations

AD is also described as a "**synaptic failure**" (Selkoe, 2002) as synaptic density is the best correlate of cognitive decline in AD (Terry et al., 1991). Up to 45% of synaptic buttons are lost in the neocortex or hippocampus of AD patients as compared to control individuals (Pozueta et al., 2013).

Mechanisms for synaptic alterations in AD are still unclear. Synaptic loss is not only linked to neuronal loss as it precedes neurodegeneration (Selkoe, 2002) and is observed in living neurons (Coleman and Yao, 2003). Aβ toxicity may mostly be responsible for synaptic alterations as post-synaptic density (PSD) proteins of synaptic spines, such as PSD-95, and synaptic plasticity are altered in presence of misfolded Aβ (Selkoe, 2008; Shankar et al., 2007, 2008). In particular, soluble Aβ forms correlates with synaptic loss (Lue et al., 1999). Post-synaptic terminals are more vulnerable and degenerate before pre-synaptic ones and such effect is associated to Aβ rise and gliosis in regions that are not yet affected by AD lesions (Gylys et al., 2004). However, such effects are still debated and further research is needed to decipher synaptic alteration mechanisms in AD.

In summary, the characterization of AD pathology has led to several hypotheses to explain its physiopathology and has permitted the identification of potential therapeutic targets. However, AD physiopathology is still mostly unknown, in particular for the initial events and mechanisms leading to the pathological cascade.

1.9. Animal models of Alzheimer's disease

Animal models are critical for understanding AD physiopathology and evaluating therapy. As animals do not develop AD, various strategies were used to reproduce artificially AD endophenotypes (hallmarks). Here we will present an overview of mammal models of AD.

Ideally, an animal model should present with three levels of **validation** (Sams-Dodd, 2006): (1) a face validity, indicating a similarity between the model and human phenotypes; (2) a construct validity indicating that the etiology of the model's pathology is the same as in the human disease; (3) a predictive validity, indicating that the response to drug treatment and manipulations is similar to that observed clinically. An ideal animal model of AD should therefore embody all the hallmarks of human pathological phenotype, present with similar etiologies and respond to AD effective drugs. Since such a treatment has not yet been developed; the predictive validity will not be discussed here.

1.9.1. Transgenic models

The standard mammalian models used in biomedical research are rodents. From a practical perspective, there are many advantages to mice and rats in research. Indeed, their lifespan is relatively short, they are cost-effective, their breeding and biology are well-characterized and genetic manipulations on these species are quite easy. However, rodents are distantly related to humans as compared to non-human primate (NHP). For example, three aminoacids are different between mouse and human Aβ sequence (**Appendix 6**). It is generally admitted that rodents' Aβ is not prone to aggregation because Aβ deposits are not observed even in very aged animals although overexpression of murine Aβ has recently been shown to produce AD-like amyloid deposits (Xu et al., 2015). Therefore, to model AD, two types of transgenic mouse models were developed (www.alzforum.org) depending on the expression of mutated or wild-type proteins.

First, **transgenic mouse models overexpressing mutated forms of APP PS1, PS2 and/or Tau** were produced. Of note, some models were also developed with controlled and/or region-restricted expression of the transgenes.

- For **Tau** transgenic models, mutations from genetic tauopathies were used as no Tau mutation leads to AD in human. The most common are the P301S (expressing 4R/0N human Tau isoform with the P301S mutation) and the PS19 (P301L) (expressing 4R/1N human Tau with the P301L mutation). These Tau models do not present with construction validation and only partial face validity as Tau lesions are often important in the brainstem leading to motor disabilities and paralysis.
- For **APP**, some of the most common are Tg2576 (expressing the human APP gene with the double Swedish mutation) and APP23 (expressing the human APP gene with the double Swedish mutation).
- For **APP and PS**, various models were produced such as the $APP_{Swe}PS1_{\Delta E9}$ (expressing a chimeric humanized mouse/human mutant APP bearing the Swedish double mutation and a human PS1 lacking exon 9) or the PS2APP (expressing the PSEN2 gene with the N141I mutation and a human APP with the Swedish double mutation).
- For **PS**, models were also developed such as the PS1(M146L) (expressing the human PSEN1 with the M146L mutation) or the PS2(N141I) (expressing the human PSEN2 gene with the N141I mutation). APP and/or PS models present with only partial construct validity for the genetic cases, as proteins are very highly overexpressed, and a partial face validity as, although they present with cognitive deficits, Aβ overexpression is not associated with Tau pathology except for neuritic coronas.
- To overcome this absence of Tau pathology, a **triple mutant**, 3xTg, was generated with mutated human PSEN1 (M146V mutation), APP (double Swedish mutation) and MAPT (P30IL mutation). This model presents with a better face validity than the other models but not construct validity.

Some **transgenic rat models** were also developed, such as the APP21 (expressing the human APP bearing Swedish and Indiana mutations) and present similar construct and face validity as transgenic mouse models presented above.

Second, **models expressing human wild-type forms of APP or Tau proteins** were generated. For example, huTau mice (expressing all 6 isoforms of human Tau) develop age-

dependent Tau pathology but do not present with β-amyloidosis whereas huAPP mice (expressing the entire or fragments of the human wild-type APP) may develop amyloid plaques when proteins are overexpressed but do not develop Tau pathology. These models present with a better construction validity for sporadic AD cases although they generally overexpress these proteins and do not, or only partially, develop similar lesions to AD leading to poor face validity.

1.9.2. Inducible models

Various strategies for inducible model development have been proposed.

Virus-based gene transfer models are interesting because they allow controllable and localized expression of AD-related proteins (Audrain et al., 2016; Ubhi et al., 2009). However, they generally rely on a strong expression of mutated or wild-type proteins thus limiting their construct validity and present with the same limitations as transgenic models for face validity.

Other models, based on **stereotaxic injections** of streptozotocin (Kraska et al., 2012; Mayer et al., 1990), pro-inflammatory agents (White et al., 2016), Aβ and/or Aβ degrading enzyme inhibitors in rats (Iwata et al., 2000), rabbits (Newell et al., 2003) or macaques (Li et al., 2010) led to models with cognitive deficits, neurodegeneration and neuroinflammation. Also, injections of oligomeric forms of Aβ in mice (Brouillette et al., 2012; Epelbaum et al., 2015; Selenica et al., 2013) or macaques (Forny-Germano et al., 2014) mostly led to acute instead of progressive pathologies. Therefore, these models, however interesting, present with limited construct and face validities.

Finally, based on the prion-like hypothesis, various models of **experimental transmission** have been proposed (see **4.2** and **4.3**) and present with similar limitations regarding face and construct validity.

1.9.3. Spontaneous models

Animals do not develop AD but several species, such as dogs, goats, primates or bears, can spontaneously develop AD-like lesions and sometimes cognitive deficits while aging (Braak et al., 1994b; Cork et al., 1988; Giaccone et al., 1990; Nelson et al., 1994; Schultz et al., 2000; Walker et al., 1987).These models are of great interest although lesions are often found after

the animals have reached more than 75% of the species maximum lifespan (Baker et al., 1993).

1.9.3.1. Dogs

Dogs' Aβ sequence is similar to humans' (Johnstone et al., 1991). Naturally, dogs develop amyloid deposits, correlated to cognitive decline, but not NFTs or neuritic plaques (Cummings et al., 1996; Giaccone et al., 1990; Russell et al., 1996; Wisniewski et al., 1996). They also develop other AD endophenotypes such as cerebral atrophy and neuronal loss (Head, 2011). Therefore, aged dogs present with good construct and face validity for sporadic AD. Aged dogs have been used to evaluate AD treatments and in particular anti-Aβ immunotherapies (Cotman and Head, 2008). In particular, pet dogs are of interest, due to the care they receive, to evaluate anti-ageing drugs. For example, the Dog Aging Project (www.dogagingproject.com) aims to longitudinally characterize aging in dogs and probe rapamycin in an intervention trial to prevent disease and extend healthy longevity in middle-aged dogs (Check Hayden, 2014).

1.9.3.2. Non-human primates

Non-human primates (NHP) present advantages over rodents as they are phylogenetically closer to humans. Old NHP are also used as spontaneous models of AD as some animals spontaneously develop amyloid deposits and cognitive decline while aging and their Aβ and Tau sequences are very similar to humans.

In macaques, amyloid plaques can be detected in animals older than 20 years (Kimura et al., 2003; Struble et al., 1985). In Caribbean vervets, both parenchymal and vascular Aβ deposits have been shown after 15 years as well as plaque-associated gliosis (Lemere et al., 2008). Both species have been used to evaluate immunotherapies (Gandy et al., 2004; Lemere et al., 2004). Tau NFTs aggregates have been found in baboons but not in macaques (Kimura et al., 2003; Schultz et al., 2000). Therefore, although NHPs have good construct validity, they do not reproduce all AD endophenotypes.

Also, in aging-associated pathology studies, their long lifespan, low reproductive rate or relatively large body size represent a lot of constrains. Smaller shorter-lived species are very advantageous in terms of costs and research protocol span as they could develop AD-like pathologies more quickly and be a valuable alternative to evaluate therapies. Indeed, smaller

primates, such as the squirrel monkey or the mouse lemur, develop parenchymal and vascular β-amyloidosis while aging (Elfenbein et al., 2007; Mestre-Francés et al., 2000).

We will now focus on the mouse lemur, the primate used in this PhD thesis.

1.9.3.3. Mouse lemurs

Generalities on mouse lemurs

The mouse lemur, *Microcebus murinus* or gray mouse lemur (**Figure 12**), is a small prosimian primate endemic of Madagascar described first in 1777 by John Frederick Miller. Phylogenetically, it is part of the Primate order, in the infra-order of the Lemuriforms. It belongs to the Cheirogaleidae family along with other dwarf and mouse lemurs of the Strepsirrhini suborder. As the mouse lemur, this family is entirely endemic to Madagascar. It is composed of five genera, including the genus *Microcebus*, and 34 species (Mittermeier et al., 2008). In 1975, the mouse lemur was declared threatened with extinction by the Conventional on International Trade in Endangered Species (CITES) who prohibited its trade except for non-commercial use such as scientific research. Today, the mouse lemur is considered to be the most abundant small native mammal in Madagascar.

The mouse lemur is one of the largest of its genus. Its total length is 25 to 28 centimeters (cm), including a tail length of 13 to 14.5 cm. Quadrupeds, they have long bodies and short legs (Mittermeier et al., 2008). Like all mouse lemurs, *Microcebus murinus* is **nocturnal and arboreal**. During the day, they sleep in small **nests** of dead leaves or in tree holes. In the wild, its diet is varied and composed of insects, leaves, fruits, flowers and nectar. In captivity, it is approximated with fruits and a mixture of eggs, gingerbread, concentrated milk and banana. The mouse lemur is a **photoperiodic-dependent** animal. It expresses marked seasonal rhythms such as the variation of its body mass. In captivity, during long day photoperiod (summer; light > 12h), it weights around 75 grams and increases to 120 grams during short day photoperiod (winter; light < 12h). During winter, the mouse lemur can sometimes exhibit a form of dormancy (torpor), an unusual phenomenon in primates. The respect of photoperiod is very important for mouse lemurs as their lifespan can be artificially reduced by the acceleration of photoperiods (Perret, 1997). The mouse lemur also has a seasonal breeding with females having 3 estrus at most each summer lasting 1 to 5 days. Gestation latency is around 60 days and results in 1 to 4 young mouse lemurs weighting around 5 grams each.

Young mouse lemurs are quickly independent (breastfeeding lasts 6 to 8 weeks) and are considered adults when reaching their sexual maturity at 6 to 8 months (Perret, 1997).

Figure 12. **Adult mouse lemur**. From (Languille et al., 2012)

The mouse lemur has a **relatively short lifespan** for a primate but an exceptional longevity for a small mammal. In the wild, it averages 3 to 4 years because of high predation (owls, snakes and other endemic mammals) and environmental pressures (food privation and parasitism). In captivity, the maximum lifespan can reach 12 years (Perret, 1997). Adult life starts at 0.5 years and **animals are considered to be old at 6 years** (Languille et al., 2012). This increase of lifespan allows observing several age-related changes such as alterations of sensory functions (olfaction, hearing or visual acuity) as well as a decrease in motor activity (Beltran et al., 2007; Languille et al., 2012; Némoz-Bertholet and Aujard, 2003).

AD-like pathology while aging in the mouse lemur

Scientific interest in the mouse lemur began in 1953 when the first French colony was founded. Over the last decades, studies in various domains, including brain aging, have emerged. The mouse lemur could be a useful model for both physiological and pathological aging. AD-like pathological changes in the brain are thought to occur in about 20% old mouse lemurs (Bons et al., 1992).

- Amyloidosis

APP localization in the mouse lemur brain, performed by immunohistochemistry, is similar to its localization in the human brain. The sequence analysis of exons 16 and 17 (Aβ segment) of the APP gene has revealed that mouse lemur Aβ peptide is completely homologous with

human Aβ. No mutations involved in familial cases of AD have been detected. The aminoacid sequence of **PS1** and **PS2** are respectively 95.3% and 95.6% homologous to the human sequences and no mutation related to genetic AD was detected (Calenda et al., 1996, 1998). With respect to sporadic AD, genetics in the mouse lemur are poorly understood with the exception of **APOEε4**. The mouse lemur, as other monkeys, is homozygotous for APOEε4 with a sequence similarity of 92.4% between mouse lemur and human (Calenda et al., 1995).

Diffuse (**Figure 13**) and compact amyloid plaques have been described as well as vascular deposits, thought to be predominant (up to 60% of aged animals), and reported in some young mouse lemurs. Parenchymal plaques were reported in the cortex and occasionally in the hippocampus, amygdala, thalamus and brainstem. Three different plaque stages have been described: (1) early deposits (pre-amyloid stages); (2) diffuse plaques mainly composed of Aβ42; (3) compact plaques characterized by a dense core of $A\beta_{1-40}$ surrounded by a halo of $A\beta_{1-42}$. According to Bons *et al.,* early deposits are found in 66% of young animals and 36% of aged animals; diffuse plaques are detected in 33% of young mouse lemurs and 63% of aged ones; and compact plaques are not found in young animals and are detected in 15% of aged animals (Bons et al., 1992, 1994; Giannakopoulos et al., 1997; Mestre-Francés et al., 2000).

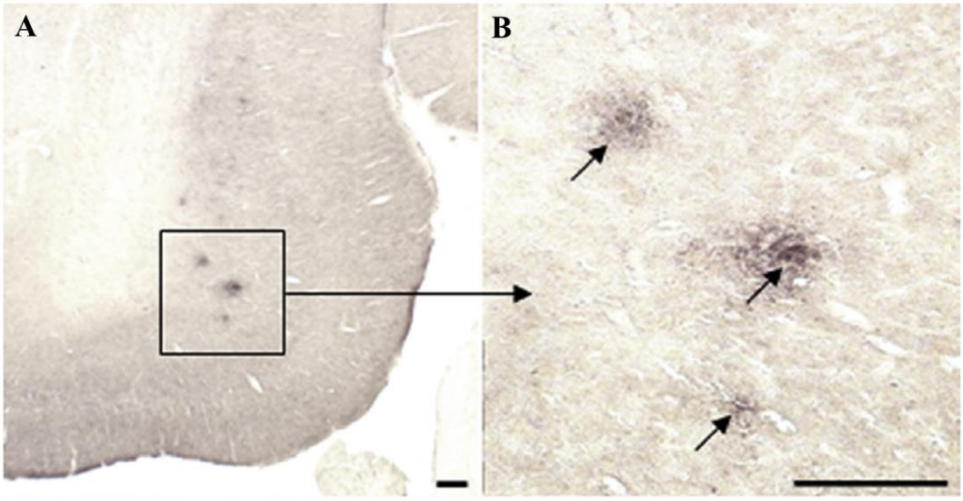

Figure 13. **Sparse cortical β-amyloidosis in aged mouse lemurs.** Scale bars : 200µm. Adapted from (Kraska et al., 2011).

- Tauopathy

Aged animals sometimes present a rare tauopathy (abnormal phosphorylation) and normal Tau accumulation has been detected in aged animals (Bons et al., 1995; Giannakopoulos et

al., 1997; Kraska et al., 2011) (**Figure 14**). Tau protein molecular weight increases with age suggesting a change of conformation and stabilization in the hyperphosphorylated state (Delacourte et al., 1995). No correlation was established between Aβ deposits and Tau accumulations and contrary to humans, a relative sparing of the hippocampus by Tau pathology seems to occur in the mouse lemur (Giannakopoulos et al., 1997).

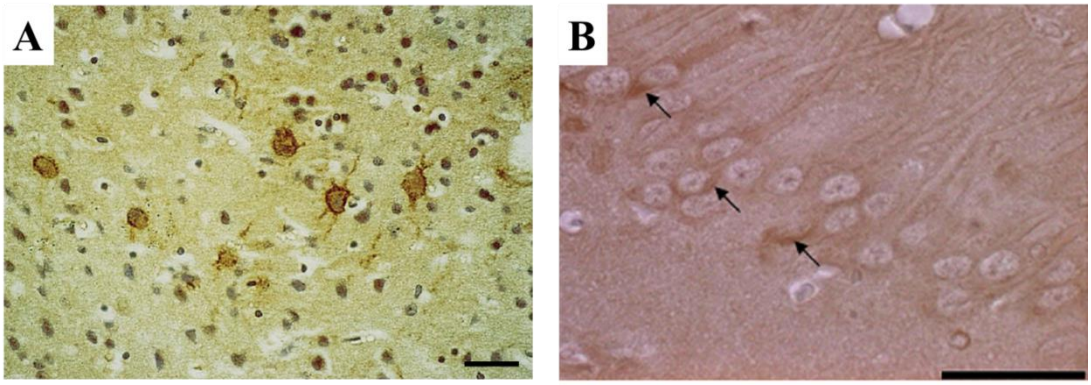

Figure 14. **Sparse Tau pathology in aged mouse lemurs.** A. Tau-immunoreactivity in the parietal cortex. B. CP13-immunoreactive neurons (arrows). Scale bars 400 and 50µm in A and B, respectively. Adapted from (Giannakopoulos et al., 1997; Kraska et al., 2011).

- Cerebral atrophy

MRI studies detected **cerebral atrophy** in aged mouse lemurs with an increased volume of CSF around the brain and in the ventricles (Dhenain et al., 2000). These atrophies seem to begin in the frontal region then the parietal and temporal regions and finally the occipital region (**Figure 15**). Cerebral atrophy in mouse lemurs is thought to occur in approximately 60% of middle aged or aged lemurs (Kraska et al., 2011) albeit with strong intensity variability.

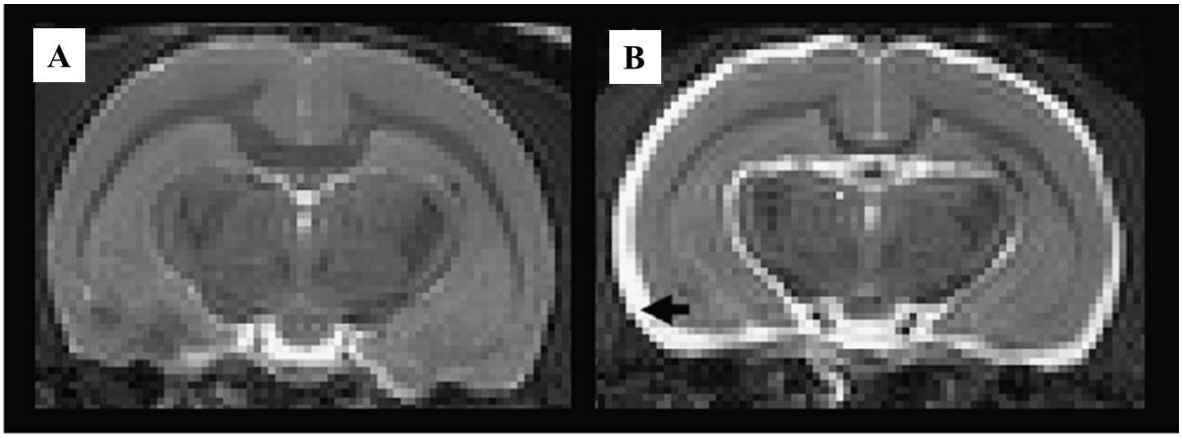

Figure 15. **Age-related cerebral atrophy.** Images of the brain of a 5.5 years non-atrophied (A) and a 8.8 years atrophied animal (B) where white CSF (arrow) surrounding cortical regions showing obvious cerebral atrophy. Adapted from (Kraska et al., 2011).

- Cognitive impairments

Cognitive functions as well as behavioral patterns (loss of social capacities, prostration, aggressiveness or circadian rhythm loss) are altered in a **subgroup of aged mouse lemurs** (Picq, 1995, 2007; Trouche et al., 2010). Moreover, cognitive impairments have been correlated to atrophies of the hippocampus and entorhinal cortex (Picq et al., 2012) (**Figure 16**). Importantly, only some of the aged individuals presented these impairments whereas other aged animals were as good as young lemurs in the cognitive tests, suggesting a specific pathological process (Picq, 2007; Picq et al., 2012, 2015).

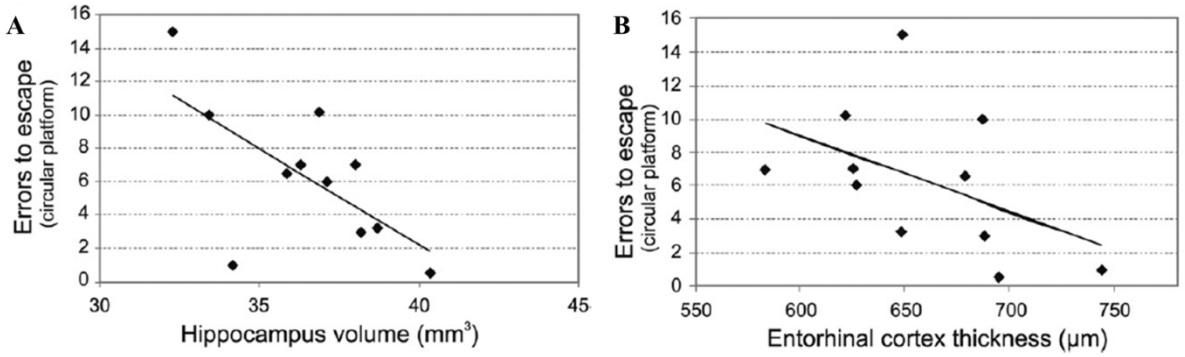

Figure 16. **Cognitive impairments are correlated to hippocampus and entorhinal cortex atrophies.** Adapted from (Picq et al., 2012).

Advantages and constraints of the mouse lemur model

Mouse lemurs can therefore present with AD-like endophenotypes while aging. Mouse lemurs as an AD model presents several **advantages**. First, this small-sized primate is phylogenetically close to humans, relatively easy to breed and cost-effective as compared to other primates. Then, its short lifespan allows longitudinal studies within a few years. Also, various methods such as electroencephalography, cognitive or MRI protocols are available in routine. Finally, its pathological aging reproduces many hallmarks of AD. In summary, aged mouse lemurs present with good construct validity and partial face validity. However, several **differences** with human can be noted. Indeed, if its brain structure is closer to humans' than mice's, it is still quite different by its size or its macroscopic organization (absence of sulci). Histopathological AD lesions are only partially reproduced in mouse lemurs. Indeed, the lesional pattern differs from AD as it mainly affects the cortex and relatively spares the hippocampus. Also, β-amyloidosis lesions are less pronounced and sparser and NFTs have never been reported in this model.

AD-like lesions have been mainly detected by one research group (Bons et al., 1992) and this pathological aging remains to be confirmed by a different research team. Also, the correlation and contribution of Aβ and Tau to cerebral atrophy and cognitive impairments still remains to be elucidated. Nowadays, it is not yet possible to identify which animals will develop the pathology as no predictive biomarker of pathological aging has been identified in the young or adult mouse lemur.

Alzheimer's disease (AD) is characterized by progressive cognitive impairments associated with a cerebral atrophy and various brain function alterations. The identification of the two cardinal lesions, respectively made of misfolded β-amyloid (Aβ) and Tau proteins, is still required for the definite diagnosis of AD.

The physiopathology of AD is still unclear although accumulating evidence suggests that endogenous assemblies of misfolded Aβ and Tau drive its pathogenesis through numerous mechanisms. In genetic cases, chronic Aβ overproduction or increased aggregation-prone propensity reproducibly leads to AD. However, sporadic AD etiology is still unknown although misfolded assembly formation seems to be critical in initiating pathological downstream events.

Current challenges for AD research are numerous. They comprise, among others, deciphering the etiology of sporadic AD, carrying on with the development of predictive biomarkers to achieve better early detection of the disease and identifying efficacy biomarkers to favor drug development in clinical trials. Despite extensive effort, more than 1,409 clinical studies referenced in total (www.clinicaltrials.gov) and 83 phase III trials between 2001 and 2012, no novel drugs have been approved since 2003 (Cummings et al., 2014). Such attrition rate (more than 99%) is not simply due to the tested drugs but rely on a combination of issues such as patients selection, lack of knowledge on AD physiopathology and lack of translational experimental models (Godyń et al., 2016).

Such observations highlight the need for fundamental and biomarker research as well as the development of more translational models for AD. Indeed, developing more valid and translational models would greatly favor breakthroughs in both basic and therapeutic AD research. Disease-modifying therapies are currently being developed and such approaches, along with prevention strategies, offer hopes to slow down or even prevent the onset of symptomatic AD. Indeed, patients' early care prior to symptomatic stages is likely to be an efficient strategy against this devastating disease.

Chapter II – Prion diseases

A **prion**, acronym for « PRoteinaceous Infection ONly particule » (Prusiner, 1982), is a proteinaceous pathogen constituted of a misfolded protein devoid of genetic material. Prions exist in organisms from yeasts to humans and, although primarily presented as pathogens, some can fulfill physiological functions.

Human prion diseases or transmissible spongiform encephalopathies (TSE) are a heterogenous group of subacute fatal neurodegenerative diseases. The prion protease-resistant protein (PrP) is responsible for fatal neurodegenerative diseases called transmissible spongiform encephalopathies (TSE) or prion diseases. At least five different human prion diseases have been described (Creutzfeldt-Jakob disease (CJD, including genetic, sporadic, iatrogenic and the new variant forms), Gerstmann-Sträussler-Scheinker syndrome, Fatal Familial Insomnia and Sporadic Fatal Insomnia) that are clinically characterized by a progressive dementia associated with various clinical signs. Neuropathologically, they are defined by spongiform change, neuronal loss and gliosis associated to misfolded PrP (PrP^{Sc}, Sc as in scrapie, as opposed to the cellular physiological conformation PrP^{C}) aggregates.

2.1. History of prion discovery

Prions became known to the public in 1990s at the onset of the "mad cow" crisis. This prion epidemic was not however the first in history. Indeed, scrapie, a prion disease affecting sheep and goats, was first described during the XVIIIth century. It is a fatal degenerative disorder characterized by behavioral changes (such as increased chewing movements), ataxia and chronic scratching. Diagnosed for the first time in 1732, the transmissible nature of scrapie was first demonstrated by two French veterinaries, Cuillé and Chelle, in 1936. They defined that scrapie was caused by a "**non-conventional transmissible agent**" present within the brain and spinal cord of ill animals (Liberski, 2012).

During the XXth century, various TSE, like CJD or Kuru, were described in humans and **experimentally transmitted to primates** (Gajdusek et al., 1967, 1968; Gibbs et al., 1968b). In 1967, **inactivation studies** of scrapie infectious agent suggested that it was devoid of nucleic acids (Alper et al., 1967; Pattison and Jones, 1967). Simultaneously, JS. Griffith proposed the hypothesis that scrapie infectious agent is a **misfolded protein**. This infectious agent propagation would rely on its ability to transmit its misfolded conformation to the host's

native proteins (Griffith, 1967). In 1982, further scrapie inactivation studies were performed by Prusiner's team. They confirmed that scrapie agent was devoid of nucleic acids and that **processes destroying or altering proteins led to an important inactivation of the agent** (Prusiner, 1982). Also in 1982, they identified a "Protease-resistant Protein" (PrP) correlating with the titer of the scrapie agent (Bolton et al., 1982) and proposed the term "prion" to define scrapie infectious agent (Prusiner, 1982). In 1991, they demonstrated that the PrP protein is an **endogenous protein** coded by the host genome and not by an infectious agent's (Stahl and Prusiner, 1991). In other words, scrapie is **transmitted by a protein of the donor to proteins of the recipient**.

In introducing the notion of "**proteinaceous infection only particle**", they challenged the medical paradigm of the three types of infectious agents (virus, parasites and microorganisms), all containing nucleic acids. This created a strong controversial debate in the scientific community which alleviated in 1997 when S. Prusiner received a Nobel Prize in Physiology or Medicine. This hypothesis was enforced in 1993 thanks to the development of mice **devoid of the PrP gene**. Indeed, in the absence of the endogenous protein, mice were resistant to scrapie (Büeler et al., 1993). Finally, in 2004, *de novo* **synthetic prions** from recombinant PrP were generated *in vitro* and transmitted a neurodegenerative disease when inoculated to PrP transgenic mice (Legname et al., 2004). These experiments gave additional proof that prions would only be constituted of misfolded proteins and that the misfolding is responsible for the development of the disease.

2.2. Etiology, epidemiology and clinical signs of human prion diseases

Unlike other neurodegenerative diseases, the etiology of human prion diseases can include **infectious or iatrogenic causes** resulting from human to human or cattle to human transmission. The annual incidence of all human prion diseases is thought to be around 1 to 2 case per million individuals (Chen and Dong, 2016). Human prion diseases are classified in three categories: genetic, sporadic and acquired. Although infectious forms are the most notorious, sporadic and genetic cases are much more frequent (Colby and Prusiner, 2011).

2.2.1. Genetic human prion diseases

Genetic cases represent about **10 to 15%** of all human prion disease cases (Mastrianni, 2010). More than 40 autosomal dominant mutations for the human gene encoding for PrP have been

linked to familial form of prion diseases including Gerstmann-Sträussler-Scheinker syndrome, genetic or familial CJD and Fatal Familial Insomnia. The age at onset of genetic prion diseases is often earlier than in sporadic diseases. Clinical symptoms of genetic TSE are very diverse and can include motor incoordination, dementia, ataxia, depression, and/or insomnia depending on the disease (Imran and Mahmood, 2011).

2.2.2. Sporadic human prion diseases

Sporadic CJD was described in 1920 by H. Creutzfeldt and in 1921 by A. Jakob, two German neuroscientists. It accounts for **85%** of human prion diseases cases with an incidence of 0.5 to 1.5 cases per million persons per year (Colby and Prusiner, 2011). Mean age of onset is around 65 years but this range is highly variable. Sporadic CJD is a rapidly evolving dementia associated with myoclonus (an involuntary twitching of one or a group of muscles) at a later stage. The mean duration of the pathology is 8 months and only 4% of cases survive more than 2 years after onset (WHO, 2003). Other sporadic forms of prion diseases, such as sporadic Fatal Familial Insomnia described in 1999, with clinical signs resembling the familial forms have been described (Imran and Mahmood, 2011).

2.2.3. Acquired human prion diseases

Acquired forms of human prion diseases comprise Kuru, iatrogenic CJD and the new variant of CJD. Acquired forms can be transmitted from human to human in particular situations such as cannibalism and iatrogenic transmission or from cattle to human.

Kuru is a TSE confined to the Fore linguistic groups of Papua New Guinea. Kuru, "shivering or trembling" in the Fore language, was transmitted by ritualistic cannibalism as a mark of respect and mourning for the dead (Norrby, 2011). At its peak, Kuru epidemic is thought to have killed 1 to 2% of the Fore population (Imran and Mahmood, 2011). Clinical symptoms are remarkably uniform with cerebellar symptoms evolving to incapacitation and death. Kuru is a quickly evolving disease as death occurs in 3 to 9 months after symptom onset (WHO, 2003). Since a ban on cannibalistic rituals has been imposed in the mid 1950's by Australian authorities, Kuru has gradually been disappearing although some cases are still reported due to the very variable incubation period from 4 to over 47 years (Collinge et al., 2006; WHO, 2003).

The first case of **iatrogenic transmission of CJD** between humans was reported in 1974 when a patient received a corneal transplant from an infected cadaver (Duffy et al., 1974). Afterwards, various sources of infection were identified including intracerebral EEG electrodes, neurosurgical instruments, dura mater or extracts of pituitary glands obtained from cadavers and, more recently, blood products in the case of the variant of CJD (Brown et al., 2012). Due to the very long incubation periods, varying from years to decades, recognition of some sporadic CJD cases as iatrogenic ones was difficult to obtain. The first epidemic of iatrogenic CJD was associated to cadaver-derived growth hormone treatments. Worldwide, 226 cases have been detected including 119 cases in France (Brown et al., 2012) with an average incubation time of 15 years. The second epidemic was associated to the heterologous grafts of contaminated cadaveric dura mater with 228 cases recorded, mostly in Japan (Brown et al., 2012; Norrby, 2011).

Finally, transmission from cattle to human has been the main focus of the last two decades. The Bovine Spongiform Encephalopathy or "**mad cow crisis**" began in the late 1980s and reached its peak in 1992 with more than 180 000 cow cases detected with a mean incubation time of five years. The source of this cow epidemic was the introduction of meat and bone meals prepared from cattle, sheep, pig and chicken (Norrby, 2011). In 1994, the first cases of bovine-related CJD were identified. They were described as "a **new variant of CJD**" as patients were generally younger with unique histopathological alterations and molecular characteristics of PrP were different from sporadic cases (Will et al., 1996). To date, 229 cases have been reported worldwide, mostly in the United Kingdom (Norrby, 2011).

2.3. Neuropathology of human prion diseases

Prion diseases are characterized by the degeneration of the central nervous system (CNS) whereas the whole body remains unharmed (Aguzzi and Heppner, 2000). Vacuole formation is observed in the encephalon giving to the brain a sponge-like appearance (**spongiform change**). This characteristic vacuole formation is associated to neuronal death, gliosis (astrocytic reactivity and microglial proliferation) and aggregates of misfolded PrP (PrP^{Sc}) in the parenchyma (Colby and Prusiner, 2011) (**Figure 17**).

Definite diagnosis of human prion diseases rely on histopathological assessment of brain tissues with the identification of a **typical triad** (spongiform change, neuronal loss and gliosis). As neuronal loss and gliosis are characteristic of other afflictions of the CNS, the

spongiform change is the most specific feature of prion diseases. Although PrP^{Sc} aggregates are specific to prion diseases, the amount and distribution of deposits do not always correlate with the type and severity of local tissue damage (Budka, 2003).

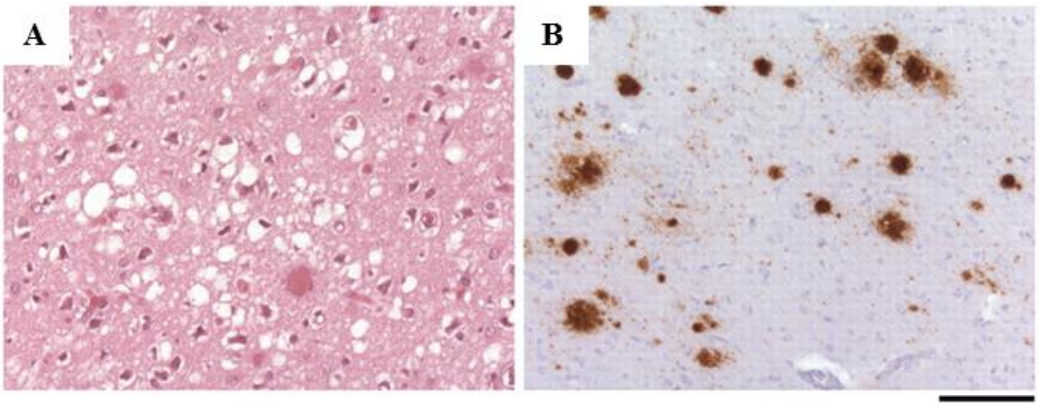

Figure 17. **Histopathological lesions in human prion diseases.** A. Spongiform change on haematoxylin and eosin stain of brain slices. B. PrP amyloid plaques detected by immunohistochemistry with anti-PrP antibody. Scale bar represents 100µm. Adapted from (Webb et al., 2008).

2.4. Prion protein

2.4.1. Physiological prion protein

PrP is a cell-surface glycoprotein encoded by the *Prnp* gene located on the chromosome 20 (Liao et al., 1986). Its expression is ubiquitous although it is higher in the CNS and in particular, in neurons (Kretzschmar et al., 1986). Its structure includes an N-ter flexibly disordered "tail" and a C-ter globular domain with three α-helices and a short anti-parallel β-sheet (Zahn et al., 2000).

PrP is not mandatory as *Prnp* knock-out mice can be generated and do not present with major abnormal phenotype (Büeler et al., 1992). However, PrP is highly conserved suggesting an important role. Nowadays, its functions still remain enigmatic and, in the brain, PrP has been proposed to have mainly a neuroprotective role. Indeed, PrP could intervene in many functions such as apoptotic and oxidative stress protection, copper ion metabolism, transmembrane signaling, synapse formation and maintenance or adhesion to the extracellular matrix (Westergard et al., 2007)

2.4.2. Pathological prion protein

Prion diseases result from **conversion** of the physiological PrP^{C} into a misfolded PrP^{Sc} isoform. Both proteins are encoded by the same gene (Basler et al., 1986), present with the same primary structure and the same post-translational modifications but differ by their secondary and tertiary structures (Riesner, 2003). Indeed, PrP^{Sc} is characterized by an enriched β-sheet secondary structure whereas PrP^{C}'s is mainly composed of α-helices (Caughey et al., 1991; Pan et al., 1993).

PrP^{Sc} present with specific characteristics. First, its conformation is **self-propagating**. Then, it is **highly resistant** to degradation and resists to formalin or heat inactivation. It can also be resistant to proteinase K treatment (PrP^{Res}) (Riesner, 2003). If PrP^{Res} is a biochemical marker of infectiousness, infectiousness and proteolysis resistance are not always correlated as shown in prion disease patients (Gambetti et al., 2008) or animal models (Lasmézas et al., 1997). Finally, in analogy to other infectious agents, PrP^{Sc} **strains** can be described as leading to pathologies with different phenotypes (Colby and Prusiner, 2011).

Strains are classically defined as a genetic variant of the infectious agent, but this concept cannot be extended to prions and was one of the strongest evidences against the protein-only hypothesis. Nowadays, it is commonly accepted that phenotypic differences between prion strains arise from alternative conformations of PrP^{Sc}. Such strains can be faithfully propagated as both the clinical and biochemical outcomes can be maintained through several passages of experimental transmission. However, the definitive proof for the structural nature of prion strains differences still has to be demonstrated. Prion strains can be classified by different **parameters** such as incubation periods, histopathological characteristics (vacuoles morphology, PrP deposits morphology, affected brain regions…), clinical signs, biochemical characteristics (electrophoretic mobility after proteinase K digestion, extent of proteinase K resistance, glycosylation pattern, binding affinity for copper, conformation-dependent immunoassays…) (Morales et al., 2007).

Since the discovery that prion diseases rely on misfolded endogenous proteins, various hypotheses about **transconformation** mechanisms have been proposed (Aguzzi and Heppner, 2000). The most commonly accepted model is the "**seeding**" model in which PrP^{C} and PrP^{Sc} are in equilibrium strongly favoring PrP^{C} and PrP^{Sc} is only stabilized when it polymerizes into a "seed". The seed formation is described as a very slow and stochastic process. Once formed,

this seed will then quickly recruit monomeric PrP^{Sc} in a nucleation-dependent polymerization process (Aguzzi and Heppner, 2000). The basis for this process will be described in Chapter III – Theoretical concepts for amyloid proteins.

Prion diseases are supposed to consist of two successive steps: the **seeding and spreading** (propagation of seeds within the brain) of misfolded proteins followed by extensive neurodegeneration.

Neurodegeneration does not necessarily correlates with the extent of PrP^{Sc} deposition. This suggests that infectious and neurotoxic forms could represent distinctive proteinaceous species (Cobb and Surewicz, 2009). Neurodegeneration also appears unrelated to a loss of PrP^{C} physiological functions. It is more and more commonly admitted by the scientific community that soluble species might be responsible for neurotoxicity (Cobb and Surewicz, 2009).

Prions, acronym for « PRoteinaceous Infection ONly particle », are proteinaceous pathogenic agents without genetic material.

Human prion diseases are a heterogeneous group of subacute fatal neurodegenerative diseases caused by the accumulation of a misfolded prion protein (Protease-resistant protein, PrP). They arise from genetic, sporadic as well as infectious etiologies. Clinically, they are characterized by progressive dementia associated with various clinical signs. Definite diagnosis of human prion diseases rely on histopathological assessment of brain tissues with the detection of spongiform change, neuronal loss and gliosis as well as PrP aggregates detection.

Prion diseases rely on the accumulation of misfolded endogenous proteins. Prion physiopathology is based on the transconformation and aggregation of endogenous proteins (seeding) followed by the propagation of proteopathic seeds within the brain (spreading) leading to extensive neurodegeneration and clinical signs.

Chapter III – Theoretical concepts for amyloid proteins

Aβ, Tau and PrP proteins are all part of the **amyloid family**. The critical role of amyloid proteins largely overtakes the single spectrum of neurodegenerative diseases as amyloid proteins are associated with more than 30 unrelated human or animal heterogeneous incurable diseases called "**amyloidoses**" (Sipe et al., 2014). During these diseases, the **deposition of autologous amyloid proteins** can occur in cells or tissues of different parts of the body. Some amyloidoses such as AD or type II diabetes are major threats to public health as they affect millions of patients worldwide.

3.1. Definitions of amyloids

As proposed by the "Nomenclature Committee of the International Society of Amyloidosis", an **amyloid protein** is "a protein that is deposited as insoluble fibrils, mainly in the extracellular spaces of organs and tissues as a result of sequential changes in protein folding that result in a condition known as amyloidosis. An amyloid fibril protein occurs in tissue deposits as rigid, non-branching fibrils of approximately 10nm in diameter. The fibrils bind the dye Congo red and exhibit green, yellow or orange birefringence when the stained deposits are viewed by polarization microscopy. When isolated from tissues and analyzed by X-ray diffraction, the fibrils exhibit a characteristic cross-β diffraction pattern".

Amyloid proteins constitute a **very diverse family** that are both essential to some biological functions and can lead to terminal diseases. For example, they can fulfill physiological roles such as the formation of biofilms (Curli proteins in E. coli) (Nizhnikov et al., 2015). Therefore, to integrate non-pathologic amyloids, biochemists and biophysicists proposed a larger definition of an amyloid protein as "**a protein that can form fibrillar polypeptide aggregates with cross-β conformation**" (Fändrich, 2007). Although mainly extracellular, intracellular protein inclusions can be considered as "intracellular" amyloid proteins like Tau protein (Sipe et al., 2014).

The term "**amyloid**" (starch-like, from the latin *amylum* or greek *amylon*) was introduced in 1838 by M. Schleiden to describe starch conglomerates in plant cells. This term was reused by R. Virchow in 1854 to describe inclusions in the liver that were, like starch, stained with iodine (Nizhnikov et al., 2015). Despite scientific controversy, amyloids were first shown to be of proteinaceous nature in 1859 (Kelly, 1987). The concept of amyloid was then applied to

various protein deposits exhibiting the same properties in light microscopy and the same tinctorial abilities (Sipe et al., 2014). Today, the **structural organization** of protein assemblies is the major criteria for their inclusion into the amyloid family.

3.2. Common structure of amyloid fibrils

Amyloid formation is the process leading from soluble proteins (native state) to insoluble protein deposits (amyloid state). The **amyloid state** of a protein is defined as the formation of thread-like fibrils (Otzen, 2013). The amyloid family is remarkable by the diversity of its aminoacid sequences and native structures (Chiti and Dobson, 2006) but present a common highly-ordered core structure, the cross-β molecular skeleton (Sunde et al., 1997). Indeed, all amyloid fibrils display a specific X-ray diffraction pattern, independent of the origin of the amyloid sample (Eanes and Glenner, 1968), called "**cross-β diffraction pattern**" (Sunde et al., 1997). The term "cross-β" corresponds to the observation of two sets of diffraction rings, one longitudinal and one transverse, forming a "cross" pattern (**Figure 18**). Such diffraction pattern indicates that the fibrils are composed of a "cross-β structure" composed of stacks of assembled proteins with β-sheet structures perpendicular to the fibril axis.

3.3. Overview of thermodynamic theory of the amyloid formation

In **theory**, a protein can fold in an almost infinite number of conformations between two extremes ranging from highly structured states to random denatured states. Each possible conformation of a protein corresponds to an energy level, called "**free energy level**". The free energy level of a conformation depends on relatively weak intra- or inter-molecular interactions (such as hydrogen bonds or electrostatic interactions) and interactions with the solvent, underlying the hydrophobic effect. In **reality**, a protein folds into secondary and tertiary structures that allow its conformation to reach the minimal free energy level. The functional native state is thus likely to be the conformation with the minimal free energy level under physiological conditions (Knowles et al., 2014).

In monomeric native states, interactions are mainly intra-molecular, with exception to its interactions with the solvent. In contrast, in the amyloid state, monomers mainly interact with the other monomers forming the polymer. As the free energy is dependent on intra-and inter-molecular interactions, **the free energy of the amyloid state is dependent on the concentration of monomers** contrarily to the native state (Knowles et al., 2014).

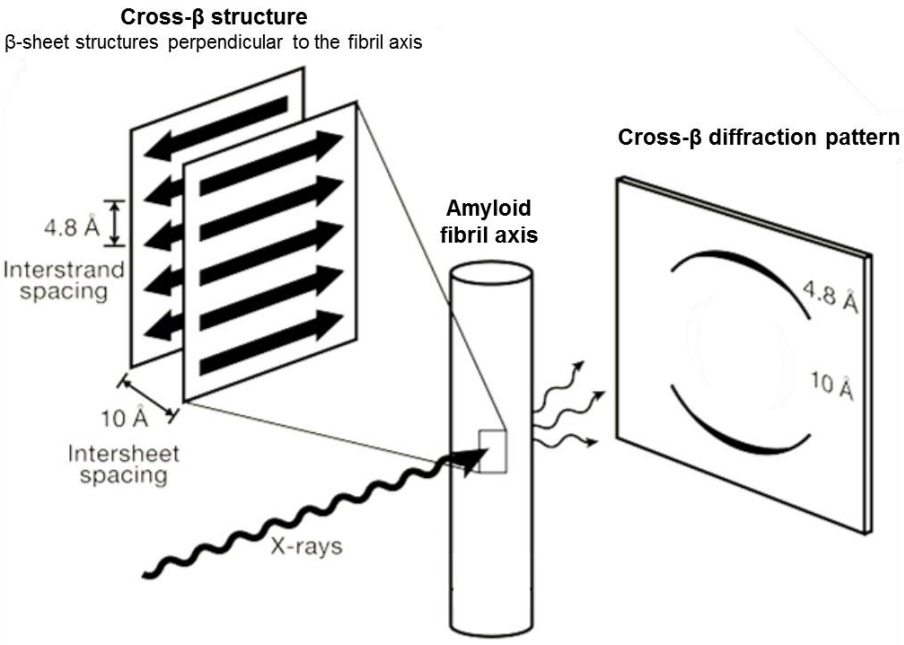

Figure 18. **Characteristic cross-β diffraction pattern of amyloid fibrils.** This specific pattern is observed when X-rays are directed on amyloid fibers. When the fibrils are mechanically oriented, the X-ray diffraction rings split in two diametrically opposed arcs. The first one (the 4.8Å diffraction ring) indicates the interstrand spacing that represents the distance between two hydrogen-bonded β-sheets. It corresponds to the value obtained for polypeptide chains with β-sheet configuration (Eanes and Glenner, 1968). In a fibril, two strands of β-sheets can interdigitate creating a compact dehydrated interval, called a steric zipper, relying on hydrophobic interactions. The second pattern (here 10 Å) is more variable as it shows the intersheet spacing (the packing distance between two juxtaposed β-sheets) that depends on the volume of the aminoacidic residues of the sequence of the amyloid protein (Fändrich, 2007). Adapted from (Eisenberg and Jucker, 2012).

Therefore, at a certain concentration of monomers, called the **critical concentration**, the amyloid state presents with the same free energy than the native state. At higher concentrations, the amyloid state becomes more stable than the native state. Conversion from the native state to the amyloid state requires the unfolding and the refolding and polymerization of monomeric proteins. These changes require additional energy and are called "**the free energy barrier**". At concentrations superior to the critical concentration, a protein can only remain in the native state if the free energy barrier is too high to allow the transition to the amyloid state (**Figure 19A**). Conversely, proteins cannot convert to the

amyloid state at concentrations lower to the critical concentration as the energy level would be too high (Knowles et al., 2014).

The native and the amyloid state represent the two free energy minima of an amyloid protein conformation. The conversion from the native state to the amyloid state is not linear. Between these two energetic extremes, various **intermediates**, for example partially folded states (alternative monomeric conformations) or oligomeric states (soluble assemblies of β-sheet enriched monomers), can reach local minima of free energy. In the cell, **chaperones** regulate the folding of amyloid proteins in order to favor the adoption of the native conformation (**Figure 19B**) (Kim et al., 2013).

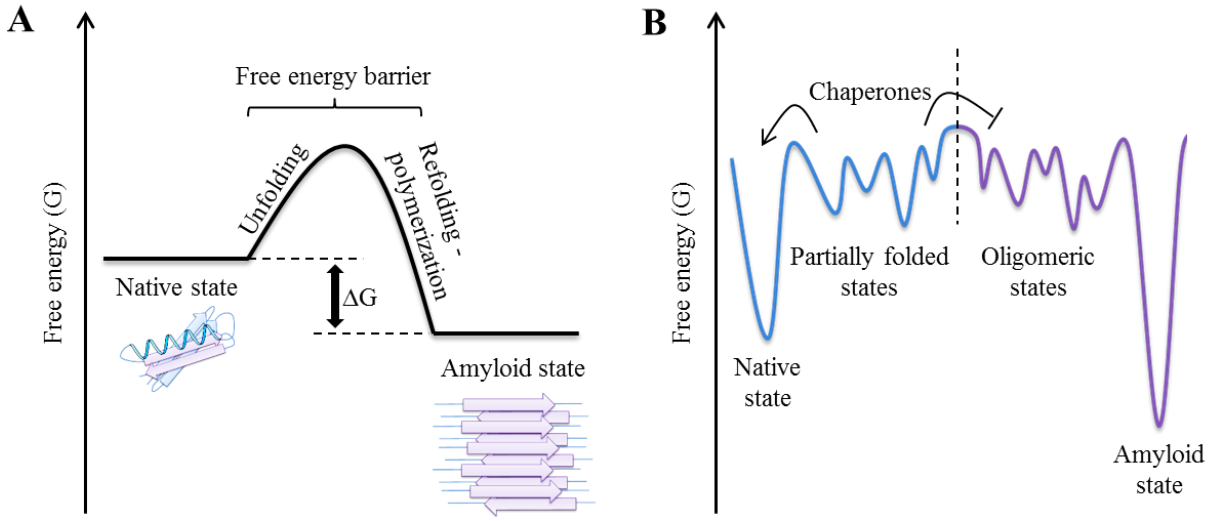

Figure 19. **Theoretical energy landscape maps representing the free energy levels of amyloid protein conformations and assemblies at concentrations exceeding the critical concentration.** A. Theoretical representation of the free energy barrier and the variation of the free energy (ΔG) between the native and the amyloid state adapted from (Knowles et al., 2014) and (Fändrich, 2007). B. Theoretical representation of the native, partially folded, oligomeric and amyloid state energy levels and the role of chaperones adapted from (Kim et al., 2013).

The various conformations of a monomeric protein are in equilibrium. These quick changes (**kinetic effects**) overcome the energy barrier between conformations. This equilibrium (K1) is unfavorable to misfolded proteins. However, in case of simultaneous unfolding exposing the amyloid-forming segment, misfolded proteins can assemble into a "**nucleus**". This unstable nucleus turns the kinetic equilibrium (K2) in favor of misfolded proteins as they are

incorporated into the growing nucleus (Harper and Lansbury, 1997). The nucleus **templates** the cross-β skeleton of the fibril that grows by incorporating monomers as they expose their amyloid-forming segment and bound at the ends of the fibril (**seeding**) (Eisenberg and Jucker, 2012) (**Figure 20A**).

It has been suggested that a nucleus requires three to four monomers to template the growth of the fibril (Nelson et al., 2005). For example, only Tau nuclei composed of more than three monomers can trigger seeding and fibril formation *in vitro* (Mirbaha et al., 2015). This suggests than three or four monomers must unfold and expose their amyloid-forming segments at the same time. Also, monomeric concentration should also be above the critical concentration for this elongation to happen (**Figure 20B**). The combination of those two requisites (simultaneous unfolding and concentration) makes the **nucleation process a rare event**.

Accordingly, the kinetics of amyloid formation are characterized by a long lag-time, corresponding to the nucleus formation, followed by a quicker formation of the fibril (seeded growth) (Jarrett and Lansbury, 1993) (**Figure 20B**). The fibril growth process is associated to the occurrence of several small to large intermediate assemblies between a nucleus and a full grown fibril. They are called oligomers and protofibrils (Lee et al., 2011b) (**Figure 20C**). It is interesting to outline that, in this model, **the formation of the nucleus is the determining step of the process**.

The fact that fibrils grow from their ends suggests that the fragmentation of these fibrils affects the kinetics of seeded fibrillar growth. For example, the fragmentation of one fibril multiplies the number of seeding ends accelerating the seeding process (Tanaka et al., 2006) and conversely, fibril stabilization reduces seeding activity by preventing fragmentation (Bieschke et al., 2011; Lam et al., 2016). Kinetic models for amyloid formation should therefore include rates of **nucleation, seeding growth as well as** (Eisenberg and Jucker, 2012).

Because of the critical role of monomer concentration for the native/amyloid state equilibrium, it has been proposed that **local abnormally high concentration**, due to increased synthesis or defect in degradation pathways, is a factor leading to amyloid formation (Eisenberg and Jucker, 2012; Nelson et al., 2005).

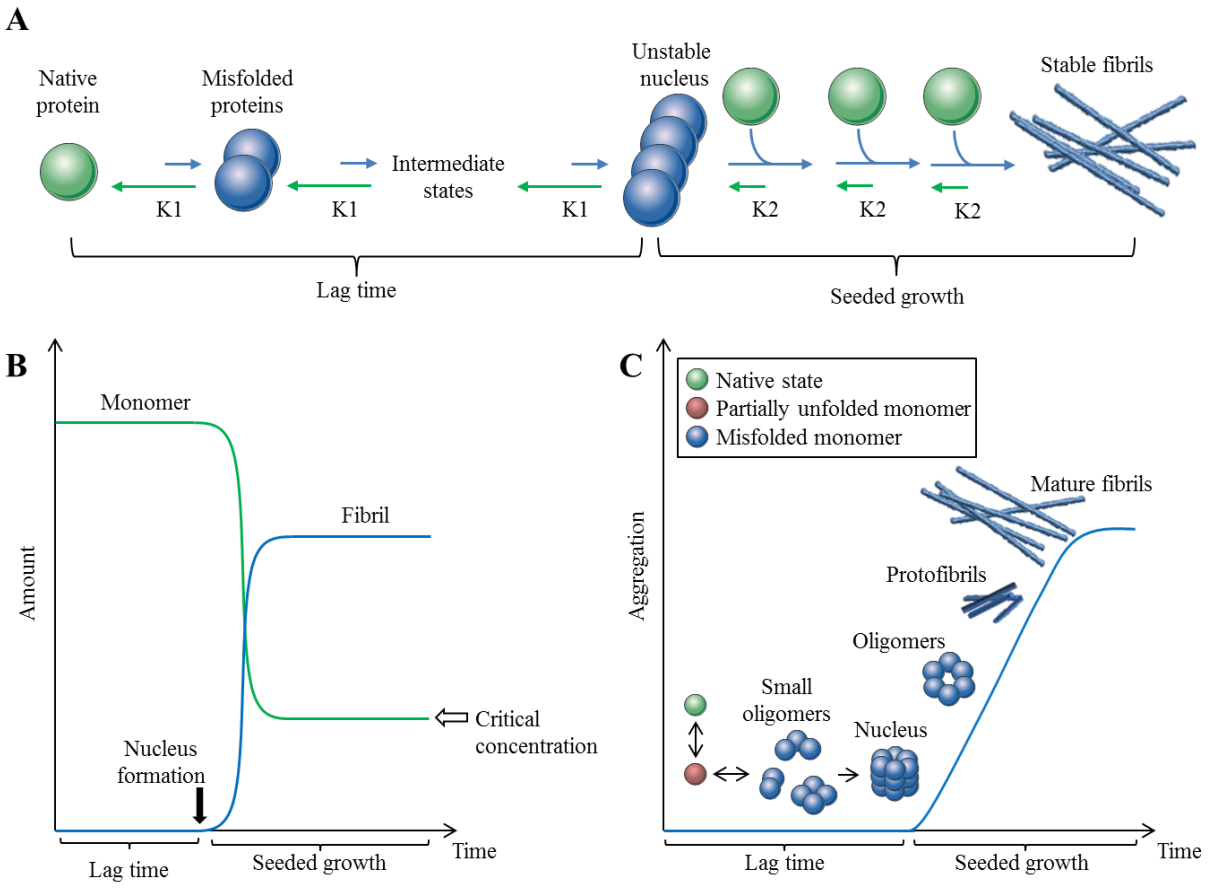

Figure 20. **Nucleation-dependent amyloid formation.** A. Theoretical representation of nucleation-dependent mechanism for amyloid formation. K1 indicates a kinetic equilibrium unfavorable to misfolded proteins and K2 a kinetic equilibrium unfavorable to native proteins. Adapted from (Harper and Lansbury, 1997). B. Simplified kinetic curves for amyloid formation at concentrations superior to the critical concentration neglecting intermediates between monomers and fibrils. Adapted from (Harper and Lansbury, 1997). C. Schematic of nucleation and fibril growth. Adapted from (Morriss-Andrews and Shea, 2015).

3.4. Amyloid polymorphism

Amyloid fibrils can present with structurally **distinct polymorphism**. Indeed, one polypeptidic sequence can adopt various secondary and tertiary structures (conformation). Therefore, different conformations of the same monomer may lead to different amyloid fibril phenotypes that can present with **distinctive properties** (Eisenberg and Jucker, 2012). This polymorphism is now admitted as a **common propriety of amyloid proteins** (Chiti and Dobson, 2006).

Amyloid proteins constitute a very diverse family that can lead to terminal diseases such as prion diseases or AD. Amyloids are defined as proteins able to form fibrillary assemblies in which the monomers present with a misfolded β-sheet enriched conformation and that display a characteristic cross-β diffraction pattern when analyzed by X-ray diffraction.

Amyloid formation is the process leading from soluble proteins (native state) to insoluble protein deposits (amyloid state). Native proteins need to cross an energy barrier in order to misfold and polymerize into the amyloid state. Once a nucleus or seed of misfolded proteins is formed, it serves as a facilitating template for the transconformation and incorporation of native proteins leading to the fibril formation.

Considering the mechanisms of amyloid formation, theoretically, all amyloids are transmissible as the introduction of a nucleus has been shown both *in vitro* and *in vivo* to induce the seeding of monomers (Eisenberg and Jucker, 2012). However, until now, only PrP has been demonstrated to present with infectious properties in humans (Prusiner, 1998).

Chapter IV– The prion-like hypothesis of Alzheimer's disease

Since the discovery of the transmissible character of prion diseases, other cerebral proteinopathies have been suspected to harbor similar transmissible properties. Among these diseases, growing evidence supports the concept that AD is initiated and sustained by the misfolding and aggregation of Aβ and Tau proteins.

4.1. Early history of the prion-like hypothesis of Alzheimer's disease

From the 1970s to the early 1990s, after the discovery of the infectious properties of various TSE, many researchers undertook experiments to determine if, like prions, AD was transmissible to various species of primates ranging from squirrel monkeys to chimpanzee using intracerebral and peripheral inoculation routes and long incubation times (up to 11 years) (Brown et al., 1994; Goudsmit et al., 1980). The overall results were inconclusive and at this time, only one study in marmosets (*Callithrix jacchus*) showed a sparse transmission of β-amyloidosis (Baker et al., 1993, 1994). Around the early 1990s, the prion-like hypothesis of AD was progressively abandoned in favor of the amyloid cascade hypothesis but interest grew back in the 2000s thanks to the development of transgenic mouse models of amyloidosis (Kane et al., 2000; Meyer-Luehmann et al., 2003, 2006; Walker et al., 2002). Nowadays, numerous experimental studies support the concept that AD-related proteins present with properties virtually similar to PrP.

4.2. Prion-like hypothesis for β-amyloidosis

4.2.1. β-amyloidosis seeding in humans

Several studies suggest that β-amyloidosis in humans can be the result of seeding processes. Although infectious etiology for AD has never been demonstrated by epidemiological studies (Beekes et al., 2014; Edgren et al., 2016; Schmidt et al., 2012), it has been recently suggested that **β-amyloidosis is, under specific conditions, transmissible to humans**. Indeed, neuropathological evidence for Aβ seeding was first reported in four young iatrogenic CJD cases related to treatment with cadaver-derived growth hormones (CGH) suggesting iatrogenic transmission (Jaunmuktane et al., 2015). β-amyloidosis iatrogenic transmission was also suspected in humans following grafting of dura mater obtained from cadavers. To date, 7 potential iatrogenic β-amyloidosis cases following dura mater graft have been described in

iatrogenic CJD cases (28 to 63 years-old) and reports suggested a causal link between dura mater grafting and Aβ pathology (Frontzek et al., 2016; Kovacs et al., 2016; Preusser et al., 2006). These studies raise the possibility that pathological Aβ could be seeded through contaminations. Such hypothesis deserves further investigation as it suggests that healthy recipients of CGH treatments or dura mater grafts may be at high risk of developing early-onset β-amyloidosis. Until now, no increase in the incidence of non-prion neurodegenerative diseases in CGH recipients has yet been reported (Irwin et al., 2013).

Suspicion of iatrogenic β-amyloidosis supports the relevance of seeding mechanisms for Aβ in AD. However, in these cases, β-amyloidosis was not associated with other typical lesions of AD such as NFTs. This suggests that the **full phenotype of AD may not be transmissible** although its development at longer incubation times cannot be excluded. Following non-CJD recipients may provide some further evidence of Aβ iatrogenic transmission and shed some light upon the possible development of AD.

4.2.2. Experimental β-amyloid seeding

Suspicion of Aβ seeding in humans follows of a long series of experiments that progressively shaped the concept that β-amyloidosis can be seeded in *in vitro* or animal models.

In vitro, fibril formation of Aβ occurs in supersaturated solutions (Spirig et al., 2014) and is accelerated by the addition of preformed Aβ aggregates in solution and cellular models (Friedrich et al., 2010; Harper and Lansbury, 1997; Paravastu et al., 2009; Petkova, 2005). In order to evaluate if β-amyloidosis can be seeded *in vivo* in a prion-like manner, one solution is to introduce preformed Aβ seeds into the organism of an animal model expressing Aβ with a similar sequence.

Three types of models have to be distinguished. The first one is composed of models that systematically develop β-amyloidosis (*i.e.* transgenic animal models, **Figure 21A**). In these models, introduction of Aβ preformed seeds should lead to the acceleration of β-amyloidosis development (**Figure 21B**). The second one is composed of models that can spontaneously develop β-amyloidosis but not in every animal (*i.e.* spontaneous animal models). In these models, introduction of Aβ preformed seeds should increase the number of animals developing β-amyloidosis or lead to an earlier onset of the pathology. Finally, the third type is composed of models that do not spontaneously develop β-amyloidosis in their lifetime (**Figure 21C)** but express Aβ peptides with an aminoacid sequence similar enough to

human's so that, when Aβ preformed seeds are introduced in their organism, they might trigger β-amyloidosis (**Figure 21D**).

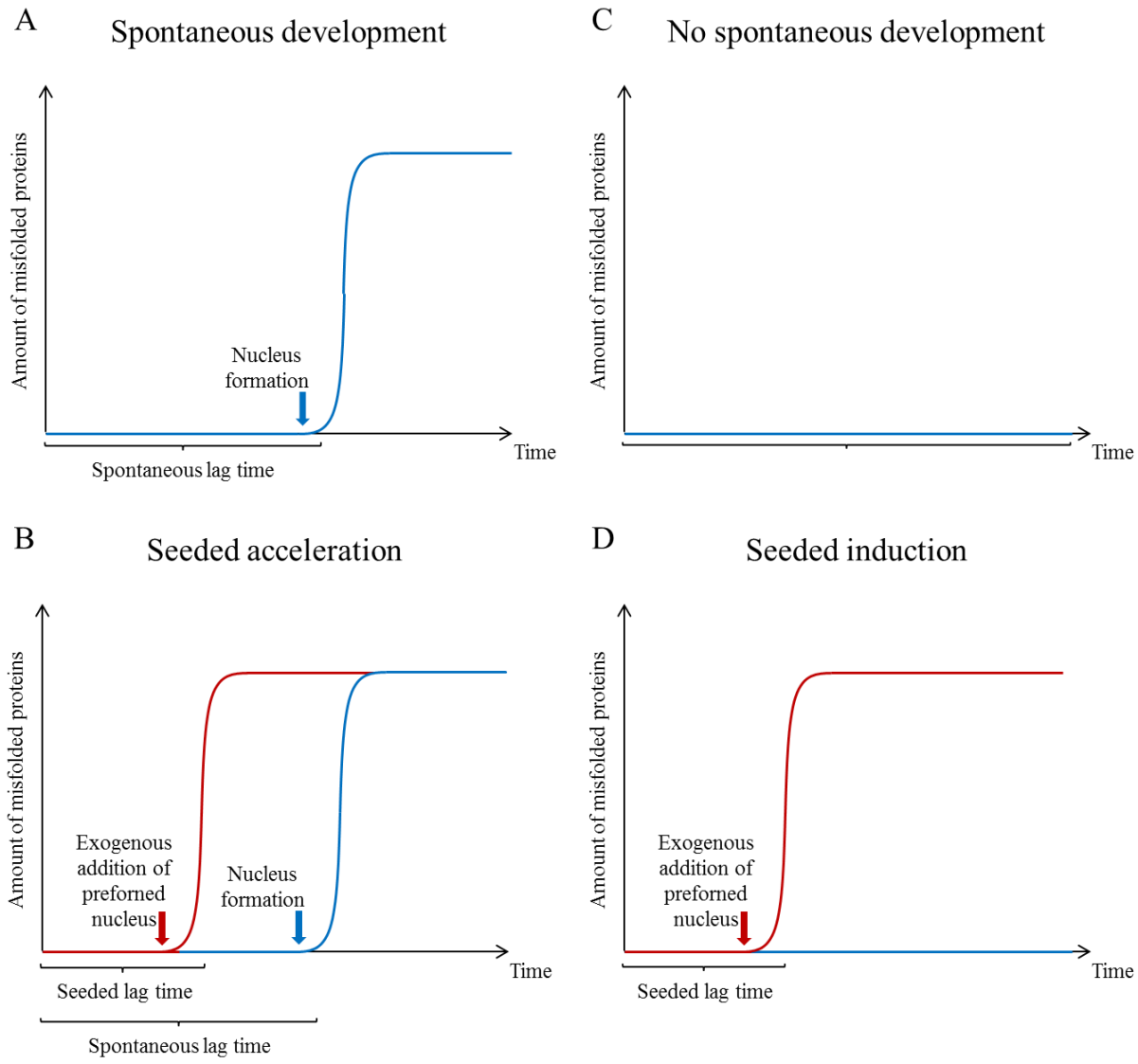

Figure 21. **Schematic representation of the kinetics of transconformation and seeding in animal models.** A. Transconformation in a spontaneous model (blue). B. Acceleration of transconformation (red) by the exogenous addition of preformed seeds in a spontaneous model (blue). C. Absence of transconformation in a susceptible model that do not spontaneously develop the pathology during its life time (blue). D. Induction of transconformation by the exogenous addition of preformed seeds (red) in a susceptible model (blue).

4.2.2.1. Acceleration of β-amyloidosis in transgenic models

Amyloid formation process requires the presence of a compatible aminoacid sequence for seeding. As murine Aβ is not analogous to human Aβ, the development of APP transgenic mouse models allowed evaluating Aβ seeding properties *in vivo* in the 2000s. These models show that high expression of Aβ peptides promotes Aβ aggregation and deposition in amyloid plaques and/or CAA.

The first seeding experiment was performed using **intracerebral inoculation** of AD patient brain homogenates into the brain of transgenic mice and non-transgenic littermates. The post-inoculation delays were defined before spontaneous β-amyloidosis development. Several months after inoculation, β-amyloidosis was accelerated in AD-inoculated transgenic mice in the inoculated structure and others to a lesser extent (**Figure 22**)(Kane et al., 2000). Similar results were obtained in numerous following experiments showing that intracerebral inoculation of either AD patient or aged transgenic mouse brain homogenates or extracts is able to accelerate β-amyloidosis in young transgenic mouse models of β-amyloidosis (Duran-Aniotz et al., 2013, 2014; Eisele et al., 2009; Fritschi et al., 2014a, 2014b; Langer et al., 2011; Marzesco et al., 2016; Meyer-Luehmann et al., 2006; Morales et al., 2015; Stöhr et al., 2012; Walker et al., 2002; Ye et al., 2015a, 2015b).

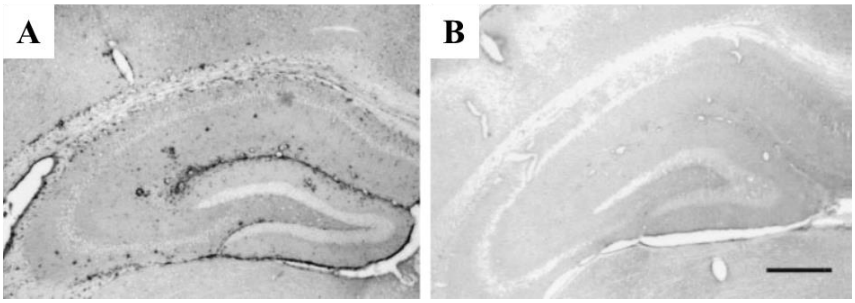

Figure 22. **AD brain homogenate inoculation accelerates β-amyloidosis in transgenic mice.** A. 8 months old Tg2576 mouse inoculated with AD brain homogenates. B. Aged-matched non-transgenic littermate mouse inoculated with AD brain homogenates. Scale bar, 500µm. Adapted from (Kane et al., 2000).

Other inoculation routes have been tested. If oral, intranasal, intraocular and intravenous inoculations failed to accelerate β-amyloidosis (Eisele et al., 2009), repeated **intraperitoneal inoculations** of old transgenic mouse brain extracts led to its acceleration in transgenic mice producing interestingly a different phenotype with a clustering of Aβ deposits in the blood

vessels and neighboring brain parenchyma (Eisele et al., 2010). Contrarily to PrP (Blättler et al., 1997; Mabbott and MacPherson, 2006), Aβ-related neuroinvasion did not require peripheral APP expression (Eisele et al., 2014) but the mechanisms still remain to be investigated.

4.2.2.2. Acceleration of β-amyloidosis in spontaneous animal models

Spontaneous animal models are models that develop late β-amyloidosis. They are typically models in which late Aβ deposits have been observed in some aged animals of the population. Several species can spontaneously develop β-amyloid lesions while aging and present with an Aβ sequence very similar to humans' (see **1.9.3**).

In one cohort of **marmosets** (*Callithrix jacchus*), sparse β-amyloidosis was observed 3.5 to 7 years after intracerebral inoculation with brain homogenates from AD cases or elderly patients with age-related Aβ pathology. No deposits were found in animals with inoculation time less than 2 years or inoculated with samples lacking Aβ pathology. Aβ lesion distribution did not show predilection for any particular region and was not related to the injection sites. Aβ deposits were sometimes Congo red or Thioflavin-S positive or associated to dystrophic neurites. Second passage (using 8 year-old marmosets previously inoculated for 6 years with a sporadic AD patient brain homogenate) was performed and all animals with incubation times superior to 3.5 years displayed similar sparse β-amyloidosis. No NFTs, reactive astrocytes or other inflammation signs were detected and it also has to be noted that marmosets were not clinically debilitated, although no behavioral testing was undertook (Baker et al., 1993, 1994; Maclean et al., 2000; Ridley et al., 2006). These results are similar to observations in suspected cases of iatrogenic β-amyloidosis and further suggest that **β-amyloidosis is transmissible without the development of the full spectrum of AD**.

4.2.2.3. Induction of β-amyloidosis in susceptible models

Susceptible models are models that do not spontaneously develop β-amyloidosis in their lifetime but express Aβ peptides with an aminoacid sequence analogous to humans'. In these models, transmission of β-amyloidosis after introduction of Aβ preformed seeds would further strengthen the seeding mechanism hypothesis.

To our knowledge, only two studies in transgenic mice for the human wild-type APP gene (HuAPPwt) and in APP21 rats reported such induction after AD brain homogenate

intracerebral inoculation (Morales et al., 2012; Rosen et al., 2012) (**Figure 23**). In mice, β-amyloidosis was associated with GFAP-immunoreactive astrocytes but no Tau pathology was observed (Morales et al., 2012).

Although very useful to detect "true" exogenous seeding, susceptible models are relatively resistant to β-amyloidosis. Indeed, a long lag time is required before the development of a sparse β-amyloidosis. Because of this long lag time and the age-associated attrition, these models present with limitations for prion-like mechanisms evaluation.

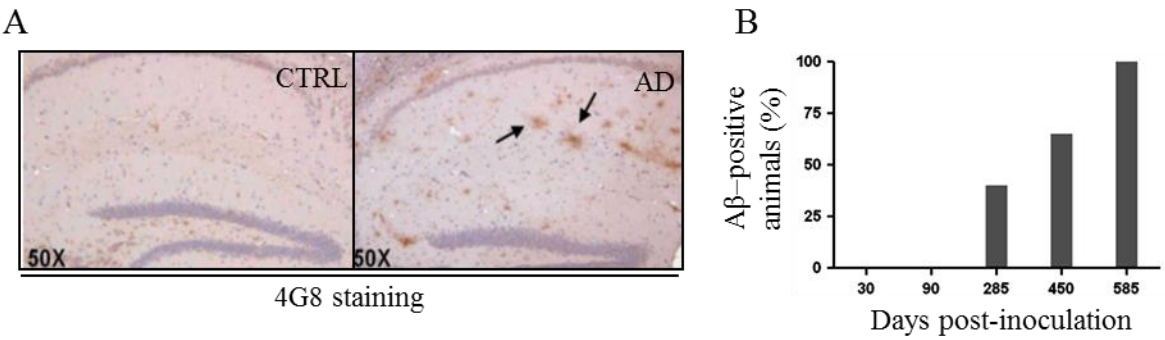

Figure 23.**Progressive β-amyloidosis is induced in AD-inoculated HuAPPwt mice.** A. Immunohistochemistry showing Aβ deposits in the hippocampus of AD-inoculated mice but not in CTRL-inoculated mice at 450 days post-inoculation. B. Percentage of AD-inoculated HuAPPwt mice exhibiting Aβ deposits in function of the incubation time. Adapted from (Morales et al., 2012).

4.2.3. Experimental evidence for β-amyloid seeds

In order to demonstrate that Aβ is the agent responsible for Aβ-laden brain homogenate-induced seeding, many experiments were performed.

First, several experiments have shown that **Aβ-free homogenates do not induce Aβdeposits** when administered intracerebrally (Hamaguchi et al., 2012; Kane et al., 2000; Meyer-Luehmann et al., 2006) or intraperitonally (Eisele et al., 2014) in various transgenic mouse strains. On the contrary, many types of **brain homogenates containing Aβ**, including transgenic mouse, AD, MCI or age-matched non-demented individuals presenting with diffuse Aβ deposits (Duran-Aniotz et al., 2013; Kane et al., 2000; Meyer-Luehmann et al., 2006) as well as brain-derived purified Aβ seeds (Stöhr et al., 2012) were shown to induce a time-dependent β-amyloidosis seeding.

Purified Aβ seeds from old transgenic mouse brain homogenates accelerated β-amyloidosis in transgenic mice (Stöhr et al., 2012).

Inactivation studies were also performed to prove that Aβ is the seeding agent contained in β-amyloidosis afflicted brain homogenates. Various inactivation methods were tested and protein denaturing treatments, such as formic acid treatment or plasma sterilization of Aβ-coated stainless steel wires, completely abolished the seeding (Eisele et al., 2009; Meyer-Luehmann et al., 2006).

Depletion studies were also initiated to demonstrate the nature of β-amyloidosis seeding agent. Removal of Aβ from brain extracts led to an attenuation of β-amyloidosis acceleration following AD brain homogenates intracerebral inoculation (Duran-Aniotz et al., 2014; Meyer-Luehmann et al., 2006) and abolished β-amyloidosis acceleration after peripheral inoculation (Eisele et al., 2014).

Finally, **passive or active immunization** of transgenic mice prior to inoculation led to an almost complete inhibition of Aβ acceleration following Aβ-containing brain extract inoculation (Meyer-Luehmann et al., 2006).

These observations show that **Aβ seeds are required for β-amyloidosis acceleration** and that **Aβ seeds are present even in the absence of symptomatic AD**. This suggests that, even in non-demented or pre-demented individuals, Aβ may present with a conformation that is permissive for seeding. It is however to note that the conformations of Aβ seeds still remains largely unknown (Eisele and Duyckaerts, 2016).

These results demonstrated that Aβ is essential for β-amyloidosis seeding and paved the way for **pure aggregated synthetic Aβ experiments**. Indeed, like in prion diseases, definite proof for the proteinaceous nature of the agent responsible for seeding can only be provided using synthetic Aβ preparations. Synthetic preparations of monomeric Aβ failed to accelerate β-amyloidosis in transgenic mouse models or marmosets although synthetic Aβ concentrations were 100 to 1000 times that of Aβ contained in inoculated brain extracts (Meyer-Luehmann et al., 2006; Ridley et al., 2006). As **monomeric Aβ *per se* is not responsible for seeding**, this suggested a role for misfolded/aggregated forms. Recently, *in vivo* Aβ seeding was obtained with synthetic preparations of wild-type or mutated Aβaggregates (Stöhr et al., 2014)showing that **misfolded Aβ peptides are sufficient seeding-competent agents for β-amyloidosis**.

Seeding experiments were more efficient with *in vivo* generated Aβ seeds than *in vitro* Aβ seeds (Eisele and Duyckaerts, 2016) and it has been observed that AD brain-derived *in vivo* structures are not easily generated *in vitro* (Alred et al., 2015). Indeed, injections of aged preparations of synthetic Aβ alone or mixed with wild-type brain extract, Aβ oligomers (homodimers, oligomers or globulomers) or Aβ complexed either with Cu/Zn or ApoE led to very limited seeding (Meyer-Luehmann et al., 2006). This observation suggests that either Aβ seeds present with a specific conformation or a panel of conformations *in vivo* favoring seeding, could be linked to the properties of Aβ seeds *in vivo* and/or the participation of cofactors as Aβ-enhancing agents. For example, it was observed that *in vivo* Aβ seeds are more resistant than *in vitro* Aβ seeds, for example to proteinase-K treatment (Langer et al., 2011; Stöhr et al., 2012; Xiao et al., 2015). These results suggests that the occurrence of **various Aβ conformations with partially distinct biological activities.** Such conformations could differentiate, for example, amyloid-positive non-demented individuals and AD patients (Piccini et al., 2005). Therefore, multimeric Aβ assemblies *in vivo* may be polymorphic and polyfunctional.

4.2.4. Properties of β-amyloid seeds

What are the characteristics of the brain-derived Aβ seeds? Brain extracts can be separated in insoluble and soluble fractions by ultracentrifugation to assess the size range of Aβ seeds in the brain. If most of Aβ is segregated in the pellet fraction (99.9%), the remaining Aβ of the soluble fraction (0.01%) present with significant seeding activity (30% of pellet seeding potency). This suggests that soluble Aβ seeds might be even more potent Aβ inducer than insoluble aggregates (Fritschi et al., 2014b; Langer et al., 2011). Also, considerable Aβ seeding activity in the pellet was found to be associated to membranes, even in the absence of detectable Aβ fibrils (Marzesco et al., 2016). These studies suggest that **Aβ seeds in the brain might be very diverse in nature**.

Properties that lead to improved seeding ability of Aβ may also come from their **resistance** to various agents. Indeed, like PrP^{Sc}, Aβ seeds resistance is remarkable. Aβ seeds resist to various treatments although their seeding properties are reduced. **Heating** reduces, without totally eliminating, β-amyloidosis acceleration by APP23 brain homogenates inoculation in APP23 mice (Meyer-Luehmann et al., 2006) or Aβ coated wires (Eisele et al., 2009) suggesting high persistence of Aβ seeds although lower than PrP^{Sc} seeds (Brown et al., 1990). Jucker's team showed that *in vivo* Aβ seeds segregated in the pellet fraction are resistant to

proteinase-K treatment although *in vivo* soluble Aβ seeds were largely proteinase-K sensitive and lost their seeding abilities (Langer et al., 2011). As PrP^{Sc} (Brown et al., 1990), Aβ seeds partly resist inactivation and structural modification by **formaldehyde** up to 2 years of fixation both *in vitro* and *in vivo*. Interestingly, diffuse Aβ staining, classically observed around amyloid plaques was lost after formaldehyde fixation suggesting that Aβ species might be differentially affected and present with different resistance properties (Fritschi et al., 2014a).

These results show that Aβ seeds have a remarkable resistance which may contribute to their **persistence** in the brain. Indeed, Aβ seeds can persist up to 6 months in *App*-null mice and, accelerate β-amyloidosis after a second passage in young APP23 transgenic mice (Ye et al., 2015a). These results suggest that Aβ seeds can persist and retain their seeding properties in the brain even in the absence of monomeric Aβ.

4.2.5. Modulation of β-amyloid seeding

Amyloid formation is a multistep process that may be modulated at various stages by factors that either promote or inhibit Aβ aggregation.

Role for the incubation time

As demonstrated in amyloids and prions, the kinetics of monomers assembly into fibrils present two phases, with first a long lag time followed by a rapid increase of the number of aggregates. Based on this model, the incubation time plays a role in the seeding process. Experimentally, β-amyloidosis acceleration increases with the **incubation time** (Hamaguchi et al., 2012; Meyer-Luehmann et al., 2006). Indeed, in transgenic rodents or marmosets, no deposits are observed at short incubation times (Baker et al., 1993; Eisele et al., 2009; Kane et al., 2000; Morales et al., 2012; Stöhr et al., 2012). Also, non-transgenic mice do not develop β-amyloidosis following human Aβ-containing extract inoculation. These results suggest that **β-amyloidosis development is not simply a reflection of the injected Aβ** (Kane et al., 2000; Meyer-Luehmann et al., 2006). In case of intraperitoneal inoculations, the lag time was increased as compared to intracerebral inoculations (Eisele et al., 2014). Finally, in susceptible models, the number of affected AD-inoculated animals increased with time (Morales et al., 2012). These results showed that the **lag time is a critical parameter** to take into account for Aβ seeding.

Role for the host

Acceleration of β-amyloidosis is also dependent on the "**host**". For example, the lag time depends on the transgenic mouse strain both after intracerebral (Meyer-Luehmann et al., 2006) and intraperitoneal inoculation (Eisele et al., 2014). This effect is presumably in accordance with the spontaneous lag time of each mouse strain and may rely on the basal expression of Aβ (Eisele et al., 2014). These results suggest that the **availability of native Aβ peptides in the brain plays a major role in seeding**.

On the contrary, **aging** might not contribute to the seeding effects. As age is the greatest risk factor for AD, the relationship between aging and seeding was investigated. Using late β-amyloidosis transgenic mice, seeding effectiveness in young and old animals was compared. While aging, human APP and Aβ levels in the brain of these mice do not increase and, following intracerebral inoculation, β-amyloidosis acceleration was similar in young and aged inoculate mice. This suggests that **aging does not provide a more favorable environment for Aβ seeding** although such an experiment should be replicated in very old animals to definitely conclude on the effect of aging (Hamaguchi et al., 2012).

Role for local environment

In accordance with theoretical seeding models, it has been suggested that regions with high availability of soluble Aβ would be the most effectively seeded regions (Eisele et al., 2014). For example, using the same brain extracts, seeding in the hippocampus of APP23 mice is quicker and more robust than in the thalamus, a region expressing lower quantities of the transgene and in which Aβ deposition does not occur spontaneously (Eisele et al., 2009). After seeding, Aβ deposits can present with various morphology depending on the affected regions (Ye et al., 2015b) showing that **local environment may play a strong role in Aβ seeding**.

Role for inoculation-induced inflammation

Considering the injection of crude human brain homogenates, immune responses and **inflammation** could trigger β-amyloidosis. However, in mouse to mouse experiments, the antigenicity of the brain homogenates as a factor for β-amyloidosis development can be ruled out (Meyer-Luehmann et al., 2006). Also, Tg(APP23:Gfap-luc) mice inoculated with murine or human brain homogenates did not show a peak of astrocyte-related inflammation

immediately following inoculation in Aβ-laden inoculates as compared to control inoculates (Stöhr et al., 2012; Watts et al., 2014). The possibility that **brain injury** is responsible for the acceleration is mitigated by the fact that control inoculation failed to accelerate β-amyloidosis (Meyer-Luehmann et al., 2006) whereas intraperitoneal inoculation succeeded (Eisele et al., 2010, 2014). In these experiments, systemic inflammation was triggered although mouse brain homogenates were used but β-amyloidosis acceleration was only observed in the presence of Aβ seeds (Eisele et al., 2010, 2014). Taken altogether, this suggests that **Aβ seeds, and not inflammation provoked by brain extracts or intracerebral injection, triggers β-amyloidosis acceleration**. Therefore, immune responses and inflammation are not to be considered as triggers although they could participate as facilitating cofactors.

Properties of the inoculate modulating β-amyloid seeding

Seed concentration as modulating factor for Aβ seeding was investigated in both intracerebral and intraperitoneal experiments (Eisele et al., 2014; Meyer-Luehmann et al., 2006; Morales et al., 2015). Similarly to infectious agents, titration of Aβ seeds can be achieved**. The more concentrated the extract, the more potent the acceleration** but highly diluted samples could still accelerate β-amyloidosis even after a million times dilution Indeed, 0.5% weight/volume (w/v) diluted brain extracts are less potent than when the same extracts were only diluted at 10%. However, after the same incubation time and despite a 20-fold difference in concentration, Aβ load in the 10% group is only 2-fold that of the 0.5% group (Meyer-Luehmann et al., 2006). **Sonication** increases Aβ seeding activity, probably by breakage of assemblies offering more ends for seeding (Langer et al., 2011). These results suggest that the **concentration of Aβ seeds is important but not critical for seeding processes and mainly modulates the extent of Aβ seeding** (Morales et al., 2015).

Role for cofactors and other modulators of β-amyloid seeding

It has been proposed that cofactors may be necessary for Aβ seeding (Kane et al., 2000; Kim et al., 2009; Walker et al., 2002). Evidence for and against a role for cofactors is presented here.

The **role of brain environment** as a cofactor is controversial. On one hand, synthetic Aβ mixed with wild-type brain extract inoculation did not facilitate seeding (Meyer-Luehmann et al., 2006). On the other hand, synthetic Aβ aggregates were reported to acquire some *in vivo* seeds properties such as proteinase-K resistance when incubated with an aged non-demented

individual brain homogenates (Xiao et al., 2015). However, in this study, suspicion that misfolded Aβ proteins were present in this aged brain homogenate cannot be excluded as seeding properties evaluation was not performed. **Membrane and proteins in the brain were suggested as cofactors** as AD brain-derived Aβ fibrils strongly resemble structures obtained *in vitro* in the presence of lipid vesicles (Alred et al., 2015). Also, a living cellular environment was shown to be required for synthetic Aβ to acquire *in vivo* seeding properties (Novotny et al., 2016). This last study strongly suggests that **cofactors present in living cells/tissues may allow synthetic Aβ to acquire *in vivo* seeding properties**.

Various other modulators for Aβ aggregation have been proposed in the literature (see McLaurin et al., 2000, for review). For example, **metal ions or ApoE** were proposed as cofactors for the polymerization of Aβ *in vivo* but results were inconclusive (Meyer-Luehmann et al., 2006). Also, some **post-translational modifications** could influence Aβ aggregation. For example, the oxidation of methionine-35 residue of Aβ modifies the secondary structure of the C-ter hydrophobic region and could potentially impede Aβ aggregation (Brown et al., 2014). This result suggests that **specific cofactors can enhance Aβ deposition** *in vivo* following the administration of monomeric synthetic Aβ.

In conclusion, if cofactors are not required for seeding, as synthetic Aβ seeds can accelerate β-amyloidosis *in vivo* (Stöhr et al., 2012, 2014), **cofactors might facilitate Aβ seeding *in vivo*.**

4.2.6. Evidence for β-amyloid strains

An important characteristic of prions is their abilities to propagate specific misconformations leading to specific biochemical and pathological properties as well as specific clinical features ("**strains**"). The misconformation encodes their properties as would do, for example, the genetic materials for viruses.

In vitro studies have also been very useful to highlight the concept that Aβfibrils can display a wide range of morphologies. These morphologies are related to different molecular structures with β-pleated sheet structures (Kodali et al., 2010; Petkova, 2005) and different toxicities in neuronal cell cultures (Petkova, 2005). Similarly to prions, both fibril morphologies and molecular structures were shown to self-propagate and their properties were retained across passages, even when original exogenous seeds were no more present, suggesting a template-

directed mechanism (Paravastu et al., 2009; Petkova, 2005; Spirig et al., 2014). These results support the hypothesis of a "**strain effect**" for Aβ seeds.

These strains can lead to different neuropathological changes *in vivo* with Aβ deposits presenting with specific morphology, distribution and composition. Aβ strains not only accelerated β-amyloidosis but also imposed a specific histopathological phenotype, presumably depending on their conformation and, following a second passage, they retained their biological properties (Stöhr et al., 2014). *In vivo,* Aβ deposits morphology and pattern (Kane et al., 2000; Meyer-Luehmann et al., 2006) as well as other characteristics can be transmitted from one transgenic line to the other suggesting a strain effect (Heilbronner et al., 2013). These results argue in favor of the existence of **Aβ strains encoded by different conformations**.

Little is known about Aβ strains in AD patients. One argument for the existence of strains in humans is the heterogeneity of AD presentation (Mayeux et al., 1985) although the morphology of Aβ deposits in humans seem to depend more on their maturation over time and localization than upon a strain effect (Eisele and Duyckaerts, 2016). Still, different conformations could account for intra- and inter-individual polymorphic presentation of AD, both in histopathological and clinical phenotypes (Heilbronner et al., 2013). Such a hypothesis is supported by the demonstration of conformational heterogeneity of $A\beta_{1-42}$ between rapidly and slowly evolving sporadic AD. Some conformers may be more susceptible to fragmentation leading to increased replication and to a more rapid disease progression (Cohen et al., 2015). This implies that **structural variability may account for different toxicity and propagation rates and could play a role in the polymorphic presentation of AD**.

To determine if AD patients could present with distinct Aβ strains, experimental transmission studies using two genetic (Arctic or Swedish mutations) and two sporadic AD cases were undertaken (Watts et al., 2014). Aβ aggregates of the different samples presented with distinct resistance to denaturation suggesting distinct Aβ conformations. Remarkably, only the Arctic sample induced a strain effect for CAA (**Figure 24**) but it is to note that parenchymal phenotype was quite similar to the one induced by other inocula. The APP Arctic mutation (E693G) is inside the Aβ sequence (E22G) and results in an atypical cotton wool plaques AD pathology (Philipson et al., 2012) whereas the APP Swedish mutation (K670M/N671L) is

outside the Aβ sequence and results in the overproduction of wild-type Aβ with a typical AD pathology (Lannfelt et al., 1994). The authors suggested that the Aβ residue 22 might be critical for Aβ conformation as Arctic (E22G), Dutch (E22Q) and Osaka (E22Δ) mutations) lead to specific β-amyloidosis phenotypes *in vitro* (Spirig et al., 2014). These results suggest that some AD mutations may lead to specific Aβ strains whereas others and sporadic cases may present with similar Aβ strains. Also, as the transgenic mouse line used in this study expressed a wild-type Aβ, **the conformation of Aβ encodes the strain properties** (Watts et al., 2014).

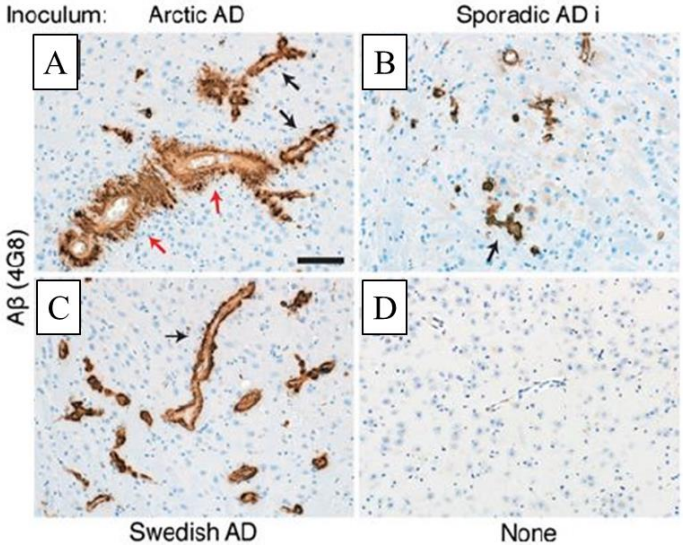

Figure 24. **Specific CAA phenotype induced after Arctic AD brain homogenate inoculation to transgenic mice.** CAA phenotype following Arctic AD patient (A), a sporadic AD patient (B), a Swedish AD patient (C) brain homogenate inoculation or without inoculation (D) in the thalamus of Tg(APP23:Gfap-luc) mice. Scale bar: 100µm. Adapted from (Watts et al., 2014).

Some Aβ strains might be dominant. *In vitro* seeding of $A\beta_{1\text{-}40}$ fibrils derived from multiple brain regions of two AD brains with distinct clinical history and neuropathology showed that each patient had developed one predominant fibrillar structure (Alred et al., 2015; Lu et al., 2013). However, polymorphism is an inherent property of Aβ fibril formation and the authors suggested that, although multiple strains may coexist, one dominant Aβ strain might be selected by the brain's environment, for example due to increased resistance to brain clearance mechanisms, and persist (Alred et al., 2015; Lu et al., 2013).

Further experiments are required to ascertain the existence of AD-related Aβ strains and to determine their consequences in term of physiopathology, diagnosis and therapy.

4.2.7. β-amyloid spreading properties

4.2.7.1. β-amyloid spreading in humans

Aβ seeding properties are critical to initiate a focal deposition in the brain. However, in AD, Aβ pathology affects the whole brain. Hypotheses for the development of Aβ are numerous and not exclusive. For example, Aβ deposits could form spontaneously at different sites of the brain (multifocal hypothesis) or propagate from one structure to another (focal hypothesis).

The term "**spreading**" or "**propagation**" suggests that a first locus is involved before, and usually with more intensity, than a second locus. It also implies that the pathological seeds travel or are transported from a first site to a second one (Eisele and Duyckaerts, 2016). This hypothesis is supported by *post-mortem* and recent PET studies that have shown that, in AD, the progression of Aβ deposition in the human cortex follows a stereotypical evolution (**Figure 25**, and Thal phases description in **1.4.1**) (Sepulcre et al., 2013; Thal et al., 2002a).

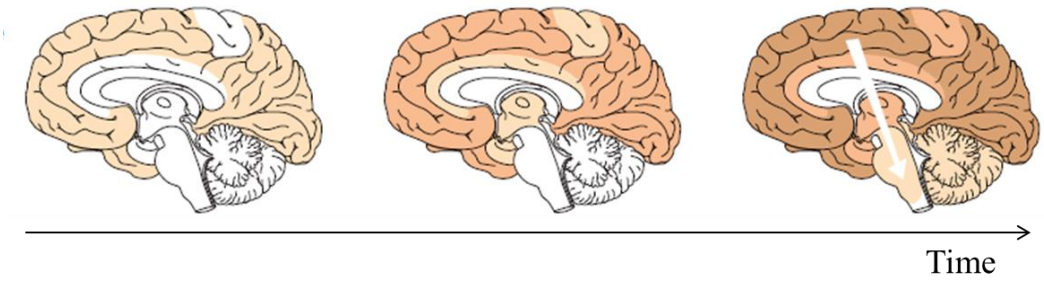

Figure 25. **Stereotypical progression of Aβ pathology in AD.** Adapted from (Jucker and Walker, 2013).

Aβ spreading in humans could occurs both by diffusion (in the parenchyma or by the blood) and along or through the neuroanatomical connections. Progression along neuroanatomical connections has been suggested by several studies and some arguments do not argue in favor of diffusion mechanisms for Aβ spreading. For example, the pallidum is spared when the neighboring putamen is largely affected by β-amyloidosis. However, some examples of non-involvement of neuroanatomical connections can be found such as the development of vascular β-amyloidosis (Eisele and Duyckaerts, 2016). Also, in the unique case of an AD

patient, a piece of the frontal cortex disconnected by a surgical lesion developed Aβ deposits in the absence of neuroanatomic connections (Duyckaerts et al., 1997b).

Differential selective vulnerability of some neuronal populations between brain regions could explain the spatiotemporal progression of pathology (Miller et al., 2013). The concept of **selective vulnerability** of specific neuron populations is based on the observation that all brain regions are not affected by β-amyloidosis at the same time. Indeed, some specific networks, like the "Default-mode Network", exhibit prominent amyloid plaque deposition. It has been suggested that metabolism and neuronal activity, that increases Aβ production, may underlie the selective vulnerability (Bero et al., 2011). Both hypotheses could explain β-amyloidosis evolution with the spreading of Aβ seeds accumulating only in the most vulnerable regions (Freer et al., 2016).

4.2.7.2. Mechanistic hypotheses for β-amyloid spreading

In animal models, following seeding experiments, time-dependent spreading of Aβ deposition from the injected structure to other regions was reported (Hamaguchi et al., 2012; Kane et al., 2000; Meyer-Luehmann et al., 2006; Stöhr et al., 2012; Walker et al., 2002). **Mechanisms of Aβ spreading** are not yet understood but several hypotheses have been proposed (**Appendix 7A-B**). The formation of Aβ seeds in various areas of the brain could occur independently (multifocal hypothesis). However, based on the stereotypical progression of Aβ lesions and the stochastic nature of Aβ seed formation, this random process hypothesis is not likely. Therefore, Aβ evolution in the brain should be linked to spreading processes and/or selective vulnerability of some neuronal populations (Eisele and Duyckaerts, 2016).

Directed diffusion along the neuroanatomic connections

Propagation of Aβ seeds along anterograde and/or retrograde neuronal connections implies a specific targeting of the secondary structures. The environment of neuroanatomic connections could provide with a favorable milieu for Aβ seeds propagation (Eisele and Duyckaerts, 2016). In some studies, β-amyloidosis was suggested to spread to interconnected regions following inoculation (Ye et al., 2015b) and lesions of such connections decreased β-amyloidosis in the anatomically connected structures (George et al., 2014; Rönnbäck et al., 2012). Taken together, these results suggest a **spreading mechanism along neuroanatomical connections** although it remains to be determined whether this spreading occurs by directed diffusion or neuronal transport (**Figure 26**).

Neuron-to-neuron spreading mechanism

Neuronal transport mechanisms may contribute to Aβ spreading from the injection site to connected regions (Eisele et al., 2009; Kane et al., 2000; Walker et al., 2002). This hypothesis is supported by the fact that, *in vitro,* ***v*arious Aβ assemblies can be uptaken and transferred from one cell to another** (Brahic et al., 2016; Domert et al., 2014; Hu et al., 2009). This cell-to-cell transfer precedes cytotoxicity (Brahic et al., 2016; Domert et al., 2014), providing evidence that seeds could propagate to new brain areas before the deterioration of the first cells. Also, it seems dependent upon the **clearance capacity** of the receiving cells (Domert et al., 2014) suggesting a relationship between neuron-to-neuron propagation and the selective vulnerability hypotheses. Also, Aβ seeds may interact with intracellular membranes as considerable Aβ seeding activity was found to be associated to membranes *in vivo* (Marzesco et al., 2016) and Aβ peptides have been found inside exosomes (Rajendran et al., 2006). Therefore, **neuron-to-neuron transmission mechanisms may play a role in the Aβ pathology spreading**.

This hypothesis should however be moderated by the fact that the brain contains numerous connection pathways that ultimately connects all the regions. Also, other mechanisms could be involved with for example transport by microglia and astrocytes as both are able to take up Aβ and have been shown to migrate along myelinated fiber tracts (Thal et al., 2015).

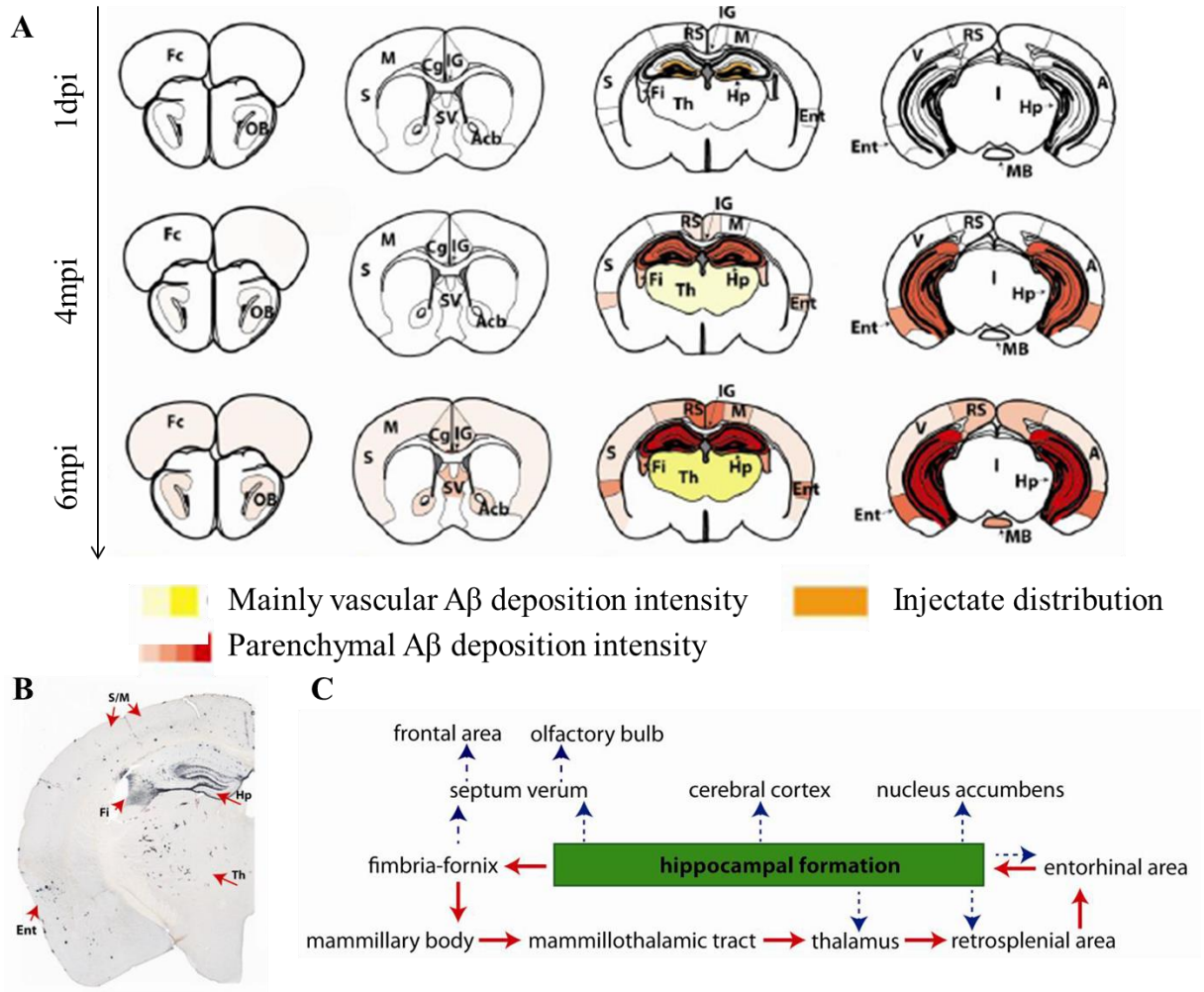

Figure 26. **β-amyloidosis may propagate along neuroanatomical connections.** A. Time-dependent spreading of Aβ lesions following bilateral Aβ-laden brain homogenate inoculation into the hippocampus of APP23 mice to connected regions (dpi: day post-inoculation, mpi: months post-inoculation; A: auditory cortex; Acb: nucleus accumbens; Cg: cingulate cortex; Ent: entorhinal cortex; Fc: frontal cortex; GrDG: granule cell layer of the dentate gyrus; Hp: hippocampal formation; IG: indusium griseum; M: motor cortex; MB: mammillary bodies; OB: olfactory bulb; PoDG: polymorphic cell layer of the dentate gyrus; RS: retrosplenial cortex; S: somatosensory cortex; SV: septum verum; Th: thalamus; V: visual cortex). B. Aβ deposition at 6mpi. C. Hypothesized spreading pathways following intrahippocampal inoculation. As the main affected structures belonged to Papez circuit, Aβ spreading might occur through or along antero- and retrograde anatomical connections because most of these structures are bi-directionally directed. In particular, the very strong reciprocal connections between the hippocampus and the entorhinal cortex further underline this hypothesis (red arrows: Papez circuit; blue arrows: direct output pathways from the hippocampus). Adapted from (Ye et al., 2015b).

Parenchymal diffusion

If passive diffusion was responsible for Aβ spreading, the consecutive affected regions would be contiguous and, as seen with Thal phases, it is not compatible with the evolution of Aβ pathology in the human brain. However, the facts that Aβ is secreted into the interstitial fluid, that amyloid plaques are extracellular, that small and soluble Aβ seeds are potent inducers of cerebral β-amyloidosis (Langer et al., 2011) and that Aβ oligomers can travel quickly and widely in the brain (Epelbaum et al., 2015) raise the possibility that such seeds may mediate the spreading of β-amyloidosis throughout the brain by **diffusion in the extracellular space**. Indeed, β-amyloidosis can propagate from transgenic mouse brain to embryonic wild-type neuronal cells grafts and as only few axons cross the border between the host tissue and the graft, diffusion mechanisms could mediate this spreading (Meyer-Luehmann et al., 2003). Finally, some brain regions could be more resistant than other to Aβ seeding. This selective vulnerability could explain the evolution gradient of affected structures (Eisele and Duyckaerts, 2016).

Diffusion through the vascular system

Finally, the vascular system could mediate Aβ propagation. Indeed, intracerebral administration of Aβ-containing brain extracts often induces CAA (Eisele et al., 2009; Kane et al., 2000; Meyer-Luehmann et al., 2006). Also, centering of Aβ deposition around blood vessels has been observed after intraperitoneal inoculation (Eisele et al., 2010, 2014). Moreover, elimination of Aβ occurs though the basement membrane of the capillaries and arteries of the brain serving as lymphatic drainage (Carare et al., 2013). Therefore, it has been suggested that **the vascular system and perivascular fluid drainage channels may intervene in Aβ spreading** (Eisele et al., 2009) and it has been proposed that parenchymal and vascular β-amyloidosis might arise from two different spreading mechanisms (Ye et al., 2015b).

In conclusion, it is likely that multiple mechanisms occur in Aβ pathology propagation. Taken together with selective vulnerability, these extra- and intracellular mechanisms could explain the propagation of Aβ pathology in the brain. It is noteworthy that the role of neuroanatomical connections seems to be less important for the spreading of Aβ pathology than for Tau (see **4.3.6.2**). However, **non-prion like mechanisms for the spreading of Aβ pathology** should also be considered (**Appendix 7C**). Indeed, neuronal toxicity on one part of the brain may

lead to a cellular response that could increase the secretion of Aβ at the synapse. Aβ aggregation being dependent on the concentration of monomers, this could lead indirectly to Aβ spontaneous seeding at a second locus of the network without requiring prion-like spreading mechanism. It should also be taken in consideration that Tau pathology may facilitate the development of Aβ pathology.

4.2.8. Does β-amyloidosis experimental transmission lead to functional alterations?

Whether the "pathogenic spread" of AD-related proteins causes AD symptom onset remains uncertain (Walsh and Selkoe, 2016) and very few studies explored the functional impact of β-amyloidosis experimental transmission. In one mouse study, long-term spatial memory was not impacted (Kane et al., 2000) and, in marmoset, no evidence for general cognitive impairment was described (Baker et al., 1993, 1994).

4.3. Prion-like hypothesis for Tau pathology in Alzheimer's disease

As Tau pathology was not the central object of this PhD thesis experiment, the presentation of the prion-like hypothesis of Tau will be brief.

4.3.1. Experimental Tau seeding

In vitro, Tau aggregation follows a nucleation–elongation mechanism associated with conformational changes (King et al., 1999) and seeding using exogenous PHFs seeds generated *in vitro* or isolated from AD brains accelerates Tau assembly (von Bergen et al., 2000; Friedhoff et al., 1998). In cellular models, various Tau assemblies are internalized and induce seeding by the recruitment (Guo and Lee, 2011; Takahashi et al., 2015), conformational change and aggregation of monomeric endogenous Tau (Falcon et al., 2015) through direct protein-protein contact (Kfoury et al., 2012).

As for Aβ, experimental transmission of tauopathy allows to study Tau seeding in animal models. The first experiment demonstrating the transmission of tauopathy was performed in a non-aggregation prone transgenic Tau mouse model. Following Tau-laden brain homogenates intracerebral inoculation, Tau pathology was triggered in the injected regions as well as the neighboring and distant areas (Clavaguera et al., 2009) (**Figure 27**). Similar results were obtained by numerous following experiments showing that intracerebral inoculation of either AD patients or aged transgenic mouse brain homogenates or extracts accelerate Tau

pathology in young transgenic mouse models of tauopathy (Ahmed et al., 2014; Boluda et al., 2015; Clavaguera et al., 2013) as well as in wild-type mice (Clavaguera et al., 2009; Lasagna-Reeves et al., 2012b).

Interestingly, Tau pathology can also be accelerated by intraperitoneal injection, although less efficiently than following intracerebral inoculation. No inclusions were found in peripheral organs and no signs of cerebral or peripheral inflammation were detected (Clavaguera et al., 2014). Other administration routes and underlying mechanisms of neuroinvasion remain to be identified.

Taken altogether, **these results suggest that seeding is highly plausible mechanism for NFTs formation *in vivo* although no evidence currently supports Tau seeding in humans**. Indeed, until now, no exogenous Tau pathology induction following contamination has ever been suggested in humans.

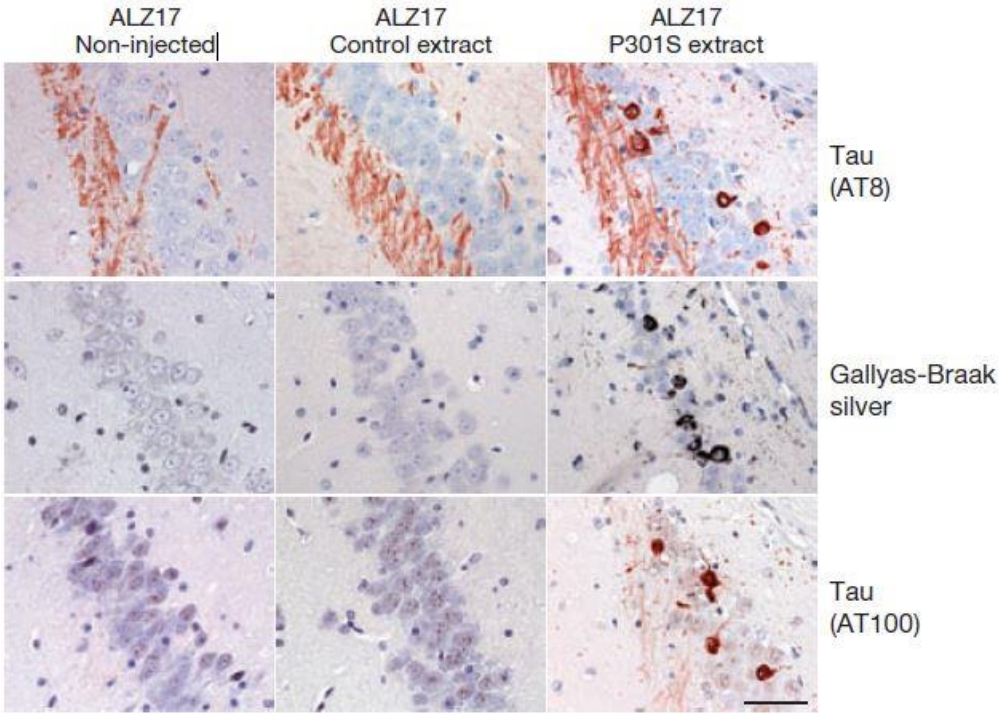

Figure 27. **Induction of Tau pathology by P301S brain extract inoculation.** Abnormal Tau is triggered in the CA3 region of 18 months old ALZ17 mice inoculated with P301S brain extract. Scale bar, 50 μm. From (Clavaguera et al., 2009).

4.3.2. Experimental evidence for Tau seeds

Experiments to prove that Tau seeds are responsible for the seeding properties of brain homogenates were based on the same paradigms as for Aβ seeds. Tau induction was only observed in transgenic mice after administration of **Tau-bearing homogenates** (Clavaguera et al., 2009, 2013, 2014) but not with Tau-free homogenates (Ahmed et al., 2014; Clavaguera et al., 2009). **Immunodepletion** abrogated Tau pathology acceleration (Clavaguera et al., 2009). **Purification studies** of Tau-laden brain homogenates showed that the seeding competent agent was exclusively related to the insoluble fraction (Clavaguera et al., 2009) suggesting that misfolded Tau seeds are the seeding agent in brain homogenates. Definite proof for the proteinaceous nature of the agent responsible for seeding was provided using **synthetic Tau seeds** (Clavaguera et al., 2013; Iba et al., 2013; Peeraer et al., 2015). However, like PrP and Aβ, brain-derived Tau seeds are more efficient than synthetics seeds (Falcon et al., 2015).

4.3.3. Properties of Tau seeds

In cellular models and *in vivo*, Tau-laden brain-derived sarkosyl-insoluble fraction are enriched in seed-competent Tau as compared to total brain lysate (Clavaguera et al., 2009; Falcon et al., 2015). In comparison, monomeric as well as sarkosyl-soluble Tau lacking aggregated Tau species were devoid of seeding activity *in vitro* (Falcon et al., 2015). This suggests that Tau seed-competent agents are mostly filamentous. Indeed, shorts fibrils of more than 10 monomers were shown as being the major seed-competent species both *in vitro* and *in vivo* (Jackson et al., 2016). However, AD-brain derived Tau oligomers can also induce the formation of silver-positive inclusions *in vivo* (Hu et al., 2016; Lasagna-Reeves et al., 2012b). This suggests that **Tau seeds are various and range from small oligomers to fibrils**.

4.3.4. Modulation of Tau seeding

As, for Aβ, several modulators of Tau seeding have been described. Tau seeding intensity is dependent on the **incubation time** (Clavaguera et al., 2009; Falcon et al., 2015; Iba et al., 2013) and the **number of seeds** as acceleration of Tau aggregation is dose-dependent (Iba et al., 2013) and is modulated by **sonication** (Falcon et al., 2015; Meyer et al., 2014). Seeding seems also to be dependent on the **availability of Tau soluble monomers** in the host as Tau

expression level was shown to modulate the lag time (Clavaguera et al., 2014). **Inflammation** may modulate Tau seeding (Maphis et al., 2015) but its impact has not yet been thoroughly investigated. Finally, some evidence argues for a role of **hyperphosphorylation** in Tau seeding modulation (Alonso et al., 2001; Falcon et al., 2015) as dephosphorylation of AD-derived Tau oligomers reduces Tau pathology acceleration *in vivo* (Hu et al., 2016). Hyperphosphorylation may also modulate Tau seeding by inducing an amyloidogenic shift of monomeric Tau conformation (Zhu et al., 2015) and increasing soluble Tau concentration in the cytosol (Hasegawa, 2016).

4.3.5. Evidence for Tau strains

Like Aβ and PrP, Tau may be able to form different conformers with "**strain**" properties (Wang and Mandelkow, 2016). Indeed, in seeding assays, Tau fibrils present with distinct secondary structures, properties, and morphologies that are maintained over multiple passages regardless of the primary structure (Frost et al., 2009). This shows that **wild-type Tau is capable of conformational diversity**.

In vivo, Tau seeds can lead to specific Tau aggregates morphology. These different morphologies are dependent on the origin and etiology of Tau pathology and are maintained after serial propagation (Clavaguera et al., 2009, 2013). *In vitro*, synthetic Tau repeat seeds can indefinitely propagate specific conformations and phenotypes through successive *in vitro*, *in vivo* and *in vitro* passages (Sanders et al., 2014). This suggests that **specific conformations determine Tau aggregate morphology and properties**, an observation reminiscent of prion strains.

In AD, Tau pathology is clinically more uniform than other tauopathies (Duyckaerts et al., 2009). One study showed that different types of Tau aggregates exists within one individual and across different tauopathies (**Figure 28**). Interestingly, Tau strains isolated from AD brains were shown to be far more homogeneous than other tauopathies both in and between individuals. This suggests that, **in AD, one Tau strain might be dominant** (Sanders et al., 2014).

In conclusion, **different Tau strains may underlie distinct phenotypes** and might explain the phenotypic diversity of tauopathies found between both individuals and pathologies.

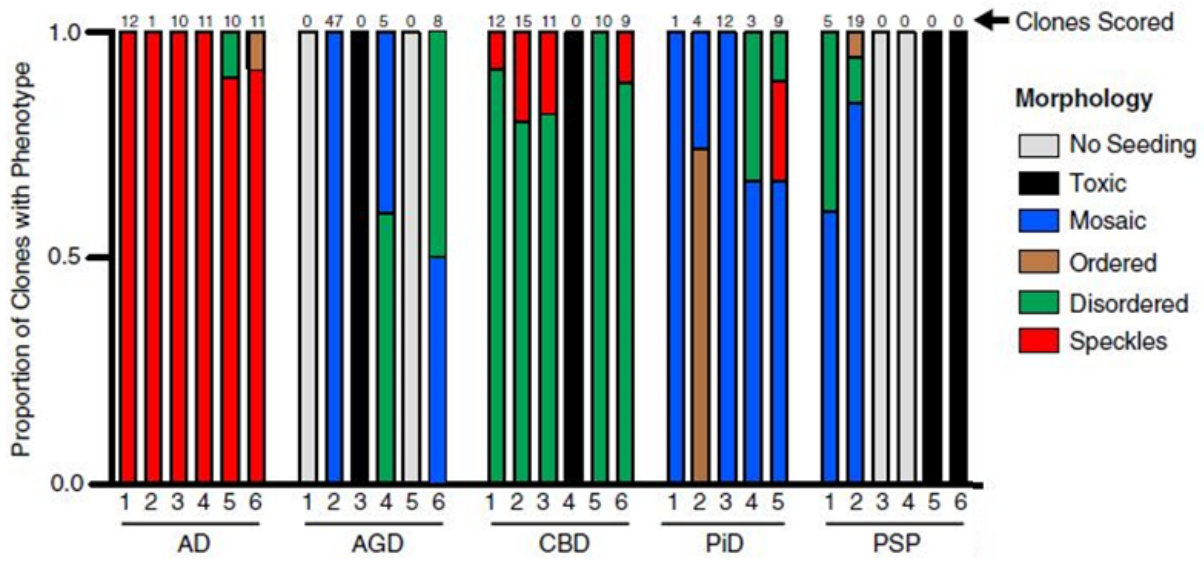

Figure 28. **Diversity of brain-derived Tau strains within patients and across diseases.** Tau proteins were purified by immunoprecipitation from 29 cortical samples of patients with AD, argyrophilic grain disease (AGD), corticobasal degeneration (CBD), Pick's disease (PiD) and progressive supranuclear palsy (PSP). Purified Tau was transduced into cells stably expressing Tau repeat domain fragment and morphological phenotypes (clones) were scored from (Sanders et al., 2014).

4.3.6. Spreading properties of Tau

4.3.6.1. Tau spreading in humans

Post-mortem and recent imaging studies have shown that Tau pathology propagation throughout the brain in AD follows a stereotypical pattern (**Figure 29**, and Braak stages description in **1.4.2**) (Braak et al., 2006; Schöll et al., 2016). Also, in the unique case of an AD patient, a piece of the frontal cortex had been disconnected by a surgical lesion and did not develop Tau lesions (Duyckaerts et al., 1997b). This argues for neuron-to-neuron spreading of Tau pathology.

Taken together, these observations strongly suggest that **spreading of Tau through neuroanatomic connections is a relevant mechanism for Tau pathology evolution in AD**. However, the spreading hypothesis cannot explain every step of the human progression. For example, the entorhinal cortex is one of the first structures affected in AD and, although it massively projects on the dentate gyrus through the perforant path, the dentate gyrus is not affected until the last stage of the pathology.

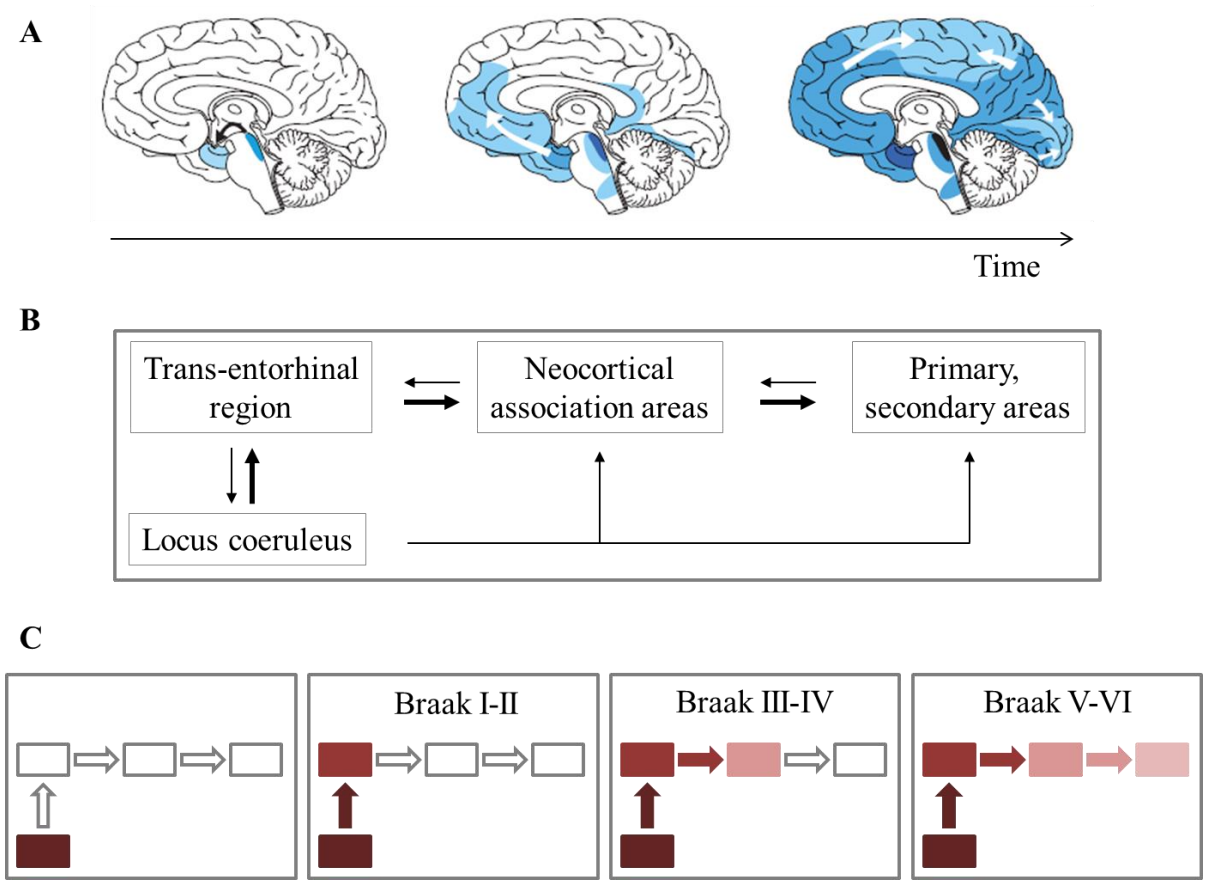

Figure 29. **Tau pathology propagation in AD.** A. Stereotypical progression of Tau pathology in AD adapted from (Jucker and Walker, 2013). B. Projections of subcortical structures (locus coeruleus), transentorhinal region, neocortical association and primary and secondary areas implicated in Tau pathology progression. Interestingly, all cortical regions that are affected in the progression of AD pathology are tightly connected with reciprocal connections. On the "return" pathway, connections are more diffuse and synaptic contact involves all cortical layers with the exception of layer IV that is usually devoid of Tau pathology in AD patients. C. Progression of Tau pathology in AD. Color-coded boxes indicates subcortical pretangle stages (dark red), temporal mesocortical NFT stages I–II (dark pink), neocortical association NFT stages III–IV (pink), and neocortical secondary and primary NFT stages V–VI (light pink). Adapted from (Braak and Del Tredici, 2011).

As for Aβ, additional parameters should be taken into account such as the "**selective vulnerability**" hypothesis (Braak et al., 2000). Very recently, it has been proposed that both hypotheses could participate in AD evolution with the spreading seeds affecting only the most vulnerable regions. Indeed, each region's vulnerability to AD pathology could be explained by its capacity to counteract protein aggregate accumulation. In healthy individuals, Braak

stages were superimposed with genome-wide transcriptome data from 500 cerebral regions. Vulnerability to AD (Braak staging) was found to correlate with aggregation-promoting genes expression (including APP and Tau) as well as with genes associated with inflammation expression (Freer et al., 2016).

4.3.6.2. Mechanistic hypotheses for Tau spreading

In animal models, following seeding experiments, time-dependent spreading of Tau pathology was reported to regions connected to the injection sites (Ahmed et al., 2014; Clavaguera et al., 2009, 2013, Iba et al., 2013, 2015; Peeraer et al., 2015; Sanders et al., 2014) and spreading along neural networks has been suggested in virus-based or transgenic models (de Calignon et al., 2012; Dujardin et al., 2014a; Liu et al., 2012). Surprisingly, *in vivo,* **endogenous Tau is not required for Tau propagation** that seems to rely on strong inter-neuronal transmission of Tau (Wegmann et al., 2015). Taken together, these observations provide evidence that **Tau can propagate along neuroanatomic connections,** depending on synaptic connectivity rather than spatial proximity.

However, Tau is a cytosolic protein lacking a signal peptide for the secretory pathway (Clavaguera et al., 2015). Therefore, **Tau secretion** could occur through unconventional pathways such as ectosomes (Mohamed et al., 2013) or exosomes (Dujardin et al., 2014b) independent from neuronal death (Karch et al., 2012; Saman et al., 2012). **Tau uptake** could occur by macropinocytosis or endocytosis (Guo and Lee, 2011; Holmes et al., 2013; Mirbaha et al., 2015) and recently, APP was proposed as a receptor for abnormal Tau fibrils (Takahashi et al., 2015). Internalization is dependent on the size of the assemblies (Wu et al., 2013) and Tau trimers were suggested as the minimal unit for Tau propagation (Mirbaha et al., 2015). Other mechanisms such as transfer through **nanotubes** connecting neurons or **passive release by membrane disruption** have been proposed (Walsh and Selkoe, 2016).

Tau spreading may be modulated by different factors such as Tau propensity to aggregate (Dujardin et al., 2014a), phosphorylation state (Dujardin et al., 2014a; Hu et al., 2016) and neuronal activity (Wu et al., 2016; Yamada et al., 2011, 2014).

Altogether, these results strongly suggest a spatio-temporal spreading of Tau through neuronal networks. Based on both human and experimental observations, a mechanism based on **neuron-to-neuron transmission** is plausible for Tau spreading. Spreading mechanisms

remain to be fully investigated. Indeed, identifying Tau assemblies responsible for Tau spreading and propagation modulators could open both diagnostic and therapeutic perspectives.

4.3.7. Does Tau experimental transmission lead to functional alterations?

Experimental transmission of Tau led to **inconsistent toxicity** (Boluda et al., 2015; Clavaguera et al., 2009, 2013; Iba et al., 2015; Peeraer et al., 2015). Only one experiment studied functional outcomes *in vivo*. Inoculation of preformed synthetic Tau fibrils into the entorhinal cortex of Tau transgenic mice accelerated synaptic plasticity impairments and cognitive deficits in the object recognition test whereas inoculation in the basal ganglia accelerated motor deficits. The authors suggested that oligomeric forms of Tau may be responsible for the observed deficits rather than NFTs (Stancu et al., 2015).

To conclude, Aβ and Tau seeds present with properties similar to PrP seeds except for infectivity (Table 1). Indeed, the greatest discrepancy between PrP and AD-related seeds is the fact that, until now, transmission of an AD clinical phenotype by the inoculation of misfolded proteins has not yet been demonstrated in animals or humans.

	PrP	Aβ	Tau
Structure			
β-sheet enriched conformation	+	+	+
Aggregation	+	+	+
Amyloid characteristics	+	+	+
Strain phenomenon	+	+	+
Seeding proprieties			
Acceleration	+	+	+
De novo induction	+	+	+
Purified and synthetic seeds	+	+	+
Resistance and persistence			
Resistance to proteinase K digestion	+	+	+
Resistance to high temperatures	+	+	+
Resistance to formaldehyde fixation	+	+	+
Persistence in brain tissues without replication	+	+	+
Spreading			
Within the brain	+	+	+
To the brain	+	+	+
Infectivity			
Transmission of a clinical phenotype	+	-	+
Transmissibility to humans	+	*	-

* suspicion

Table 1. **Properties of PrP, Aβ and Tau seeds**. Adapted from (Walker et al., 2016).

AD is characterized by a long clinically silent period of intracerebral protein aggregation that precedes dementia by decades. Since the discovery that prion diseases can be transmitted by afflicted brain tissue inoculation, AD has been speculated to also harbor transmissible agents. Growing evidence suggests that prion-like mechanisms might play a role in AD physiopathology.

There is no evidence that AD is transmissible to humans and current knowledge favor endogenous generation of Aβ and Tau seeds in the brain. Indeed, prion-like mechanisms for Aβ and Tau pathologies provide compelling evidence for the role of seeds in the instigation and progression of AD and reinforces the interest of targeting proteopathic seeds preferably early in the pathology.

Fully developed AD pathology has not yet been induced in animal models. Until now, very few studies evaluated the impact of AD experimental transmission on brain functions. Also, most models mimic separately Aβ or Tau pathologies. The development of experimental models is still needed in order to provide a better understanding of Aβ and Tau synergy in AD. Such models might help proposing a more accurate modeling of AD pathogenesis and understanding Aβ and Tau separate and synergistic contributions to AD symptoms.

In conclusion, the study of the "prion-like hypothesis of AD" offers interesting mechanistic and therapeutic options for AD. Several questions still need to be answered such as understanding what triggers the first seed formation, characterizing propagation mechanisms, identifying the more detrimental species, and how to counteract them. Answering to these questions will allow making progress toward effective therapeutic strategies for AD.

Objectives

Nowadays, growing evidence suggests that prion-like mechanisms play a part in the instigation and progression of AD. Indeed, misfolded Aβ and Tau protein assemblies in AD have been shown to present with prion-like properties (Soto, 2003). Experimental transmission is a useful tool to evaluate prion-like mechanisms of β-amyloidosis and tauopathy and their impacts in animal models. It requires the inoculation of proteopathic seeds obtained *in vitro* or from pathologic brains homogenization. Here we evaluated experimental transmission of AD endophenotypes to mice and mouse lemur primates.

Our **first objective** was to assess the transmission of β-amyloidosis to mouse models of early widespread or late focal β-amyloidosis (Chapter V – Experimental transmission of β-amyloidosis to mice). We used human AD brain homogenates intracerebral inoculation as a mean to introduce Aβ seeds into the brain of young animals. We evaluated their seeding and spreading properties as well as the impact of the host and local environment on β-amyloidosis seeding modulation.

Our **second objective** was to describe the physiological and pathological aging processes of mouse lemurs (Chapter VI – Mouse lemur model characterization). Some aged animals have been reported to develop spontaneously some of AD endophenotypes while aging such cerebral atrophy, amyloid plaques or cognitive alterations. Here, we aimed to characterize the physiological age-related cerebral atrophy and AD-like lesions in mouse lemurs. These studies also provided the opportunity to develop new cognitive testing, MRI processing and immunohistochemical protocols in order to prepare our last study.

Finally, our **third objective** was to evaluate the impacts of experimental transmission of AD on functional, morphological and histopathological endophenotypes in mouse lemur primates (Chapter VII – Experimental transmission of Alzheimer's disease endophenotypes to primates). Until now, very few studies evaluated if AD experimental transmission could lead to a clinical phenotype and it has been proposed that, if Aβ and Tau pathologies may be transmissible, AD clinical signs may not. We evaluated whether human AD brain homogenate intracerebral inoculation induced cognitive impairments and other brain disruptions such as cerebral atrophy and alterations of neuronal activity in primates as well as AD neuropathological lesions.

In conclusion, we aimed to complement recent evidence regarding the relevance of prion-like hypothesis for AD. Also, if Aβ and Tau species responsible for β-amyloidosis and tauopathy may be transmissible, no argument supports the transmission of AD clinical phenotype. Here, we intended to investigate this crucial question. Finally, preclinical research is primordial to decipher pathologic mechanisms. As animals do not develop AD, developing more translational models may be beneficial for a better understanding of AD physiopathology.

Part II – Experimental studies

Chapter V – Experimental transmission of β-amyloidosis to mice

5.1. Introduction

In the literature, AD-related misfolded Aβ and Tau protein assemblies have been shown to present with prion-like properties. If the prion-like seeding and spreading hypothesis is correct, AD β-amyloidosis and Tau pathology should be experimentally transmissible. Indeed, in case of exogenous addition of preformed Aβ and Tau seeds, the nucleation-dependent polymerization process should be triggered (Soto, 2003).

Experimental transmission can be used for exogenous induction of β-amyloidosis and Tau pathology. It requires the inoculation of proteopathic seeds obtained *in vitro* or from pathologic brain sample homogenization. In particular, intracerebral inoculation of AD brain homogenates lead to β-amyloidosis acceleration in symptomatic (Duran-Aniotz et al., 2013; Kane et al., 2000; Meyer-Luehmann et al., 2006) or non-symptomatic (Morales et al., 2012) transgenic mouse models of β-amyloidosis.

Here we aimed to evaluate the impacts of experimental transmission on β-amyloidosis in two different murine models presenting with early, strong and widespread β-amyloidosis ($APP_{Swe}PS1_{\Delta E9}$) or late, sparse and focal β-amyloidosis (AAV-$APP_{SweLon}PS1_{M146L}$). We studied seeding and spreading effects following human AD brain homogenate intracerebral inoculation in these models and evaluated the influence of the host.

5.2. Materials and methods

5.2.1. Human samples

Frozen brain tissue samples (parietal cortex) from two AD patients (Braak stage VI, Thal stages 5 and 4, respectively) and from one age-matched control individual (Braak and Thal stages 0) were obtained from brains collected in a Brain Donation Program of the Brain Bank "GIE NeuroCEB" run by a consortium of Patients Associations: ARSEP (association for research on multiple sclerosis), CSC (cerebellar ataxias), France Alzheimer and France Parkinson, with the support of Fondation Plan Alzheimer and IHU A-ICM. The consents were signed by the patients themselves or their next of kin in their name, in accordance with the French Bioethical Laws. The Brain Bank GIE NeuroCEB has been declared at the Ministry of

Higher Education and Research and has received approval to distribute samples (agreement AC-2007-5).

5.2.1.1. Immunohistopathological characterization of the human samples

Immunostaining was performed on 4-µm-thick paraffin sections. Sections were de-paraffinized in xylene, rehydrated through ethanol (100%, 90%, and 70%) and finally brought to running tap water for 10 min. They were then incubated in 99% formic acid for 5 min, washed again under running tap water, quenched for endogenous peroxidase with 3% hydrogen peroxide and 20% methanol, and finally washed in water. Sections were then blocked by incubating the sections for 30 min in 4% bovine serum albumin (BSA) in 0.05M Tris Buffered Saline, with 0.05% Tween 20, pH=8 (TBS-Tween) (Sigma Aldrich, MO, USA). Then they were incubated overnight at +4°C with the 6F3D anti-Aβ antibody (Dako, Glostrup, Denmark) or polyclonal anti-tau antibody (Dako, Glostrup, Denmark), routinely used for the detection of amyloid deposits and tau accumulation. The sections were further incubated with a biotinylated secondary antibody (25 min). The presence of the secondary antibody was revealed by streptavidin–horseradish peroxidase conjugate using diaminobenzidine as chromogen (Dako, Glostrup, Denmark). The sections were counterstained with Harris haematoxylin.

5.2.1.2. Homogenate preparation

Parietal cortex samples were individually homogenized at 20% (weight/volume) in sterile Dulbecco's phosphate-buffered saline PBS (Gibco, ThermoFisher Scientific, France) in a Ribolyser sample homogenizer (Hybaid, ThermoFisher Scientific, France). Brain homogenates were aliquoted in polypropylene tubes and stored at -80°C until use.

5.2.1.3. Biochemical characterization of the homogenates

Brain homogenates were further characterized by biochemistry.

ELISA immunoquantification of β-amyloid peptides

Brains homogenates were diluted in 6.8M guanidine; 68mM TrisHCl to obtain a 5M guanidine final concentration with protease inhibitor (Complete Mini, Sigma Aldrich, MO, USA) and vortexed for 3 hours at room temperature. Aβ immunoquantification was

performed with human $A\beta_{1-42}$ and $A\beta_{1-40}$ (Invitrogen, Carlsbad, CA, USA) ELISA kits according to the manufacturer recommendations.

Tau characterization

Brain homogenates were sonicated on ice for 5 minutes, centrifuged for 5min at 3000g at 4°C, diluted in Tris 20mM/SDS 2% and sonicated on ice for 5 minutes. Samples were normalized to 1µg/µL, diluted in 2X LDS buffer with reducers and heated at 100°C for 10 minutes. 10µg of samples were loaded on Criterion gels (Biorad, Hercules, CA, USA) and migrated on MOPS buffer during 90 minutes at 165V on ice. After membrane transfer, pS396 (Life technologies, Carlsbad, CA, USA) or Tau C-ter (Papegaey et al., 2016) antibodies were incubated overnight at +4°C. Secondary anti-rabbit antibody (reference 23817-2, Biovalley, Nanterre, France) was then applied for 45 minutes at ambient temperature before ECL revelation.

5.2.2. Ethic statement and breeding conditions

All animal experiments were conducted in accordance with the European Communities Council Directive (2010/63/UE). Animal care was in accordance with institutional guidelines and experimental procedures were approved by local ethic committees (authorizations 12-089; ethic committee CETEA-CEA DSV IdF).

Mice were born and bred in our facilities (Commissariat à l'Energie Atomique, centre de Fontenay-aux-roses; European Institutions Agreement #B92-032-02). Conditions of captivity were maintained under constant temperature of 22°C and circadian cycle (12h of light/12h of dark). Animals were housed in group (5mice/cage) inside ventilated cages with nesting enrichment. Animals had free access to food and tap water. Housing conditions were in accordance with annex III of 2010/63/EU directive. None of the animals has been previously involved in pharmacological trials or invasive studies. General examination was performed every day and weight was monitored once a month. Critical ethic limit points were defined as one or more of the following observations: important weight loss (>20%), suffering signs, prostration signs or general state degradation approved by the local veterinary.

5.2.3. Mouse models of β-amyloidosis

5.2.3.1. $APP_{Swe}PS1_{\Delta E9}$ model

These transgenic mice were produced by co-injecting two vectors. The first encoded a chimeric mouse/human mutant APP that was "humanized" by modifying three amino acids and bearing the Swedish double mutation K670M/N671L and the second encoded a human presenilin-1 (PS1) lacking exon 9 (ΔE9). Both genes were directed to the central nervous system with the murine prion protein promoter (Jankowsky et al., 2004). Mice were kept on a C57Bl/6 J background and bred in our facility as heterozygous.

In the literature, $APP_{Swe}PS1_{\Delta E9}$ mice are described to develop Aβ deposits by six months of age, with abundant plaques in the hippocampus and cortex by nine months (Jankowsky et al., 2004) that continue to increase up to 12 months of age (Garcia-Alloza et al., 2006) without tangle development. In our colony, $APP_{Swe}PS1_{\Delta E9}$ mice start to develop parenchymal and vascular amyloidosis as soon as 3 months of age.

5.2.3.2. AAV-APP/PS1 model

Contrary to transgenic models, Adeno-associated virus (AAV)-based gene transfer allows avoiding transgene expression *in utero* and during youth. Here, we used an AAV-based mouse model of AD developed by Nathalie Cartier's team (Audrain et al., 2016). As a means to mimic *in vivo* APP processing, this model uses two AAV-based gene transfer of human mutant APP bearing the double Swedish K670M/N671L and London mutations and presenilin 1 (PS1) bearing the M146L mutation. AAV-APP and AAV-PS1 were co-injected in the hippocampus to 8 weeks old C57Bl/6 J mice (AAV-APP/PS1). This strategy allows the expression of mutated human APP and PS1 without significant overexpression. At 4 weeks post-injection, human APP, Aβ and PS1 are expressed in the hippocampus of wild-type mice. At 12 weeks post-injection, mutated human APP expression and $A\beta_{1\text{-}42/1\text{-}40}$ ratio is similar to sporadic AD patients' hippocampal tissues (Audrain et al., 2016).

This model allowed to evaluate β-amyloidosis acceleration in a wild-type mouse model expressing focally mutated human APP and PS1 (Audrain et al., 2016). Its particular interest is that, contrarily to $APP_{Swe}PS1_{\Delta E9}$, it presents with a restricted human Aβ expression at physiological levels in the injected brain region only (dorsal hippocampus).

5.2.4. Experimental designs

5.2.4.1. $APP_{Swe}PS1_{\Delta E9}$ experiment

At 8 weeks of age, mice received 10% w/v brain homogenates from a control individual (CTRL-inoculated group) that was age-matched to two AD patients (AD1- or AD2-inoculated group) or PBS (**Figure 30**). We evaluated 3 time-points: 4, 8 and 16 weeks post-inoculation (wpi). At 4 and 8wpi, only CTRL and AD homogenates were inoculated for the evaluation of callosal β-amyloidosis.

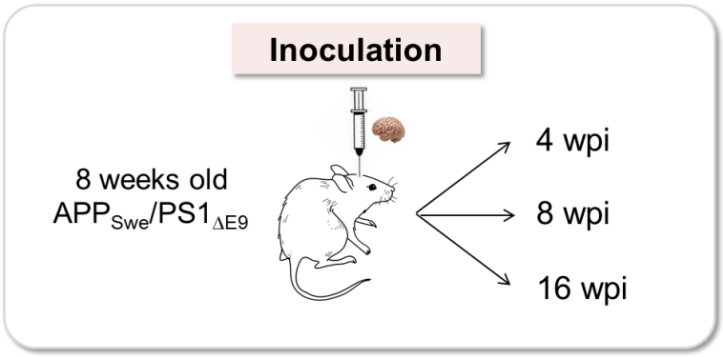

Figure 30. **Design of the $APP_{Swe}PS1_{\Delta E9}$ experiment.** wpi: weeks post-inoculation.

5.2.4.2. AAV-APP/PS1 experiment

Two studies were performed (**Figure 31**). We first characterized our AAV-based model at a long time-point (80 wpi) as no β-amyloidosis was observed at 4 and 12 weeks post-injection (Audrain et al., 2016). For the time-point at 80 weeks post-injection, two groups AAV-APP+AAV-PS1 (AAV-APP/PS1) and AAV-PS1 (as a control virus) were investigated (**Figure 31A**). Then, we investigated the impact of human brain homogenate inoculation in this model using the same human homogenates as for the $APP_{Swe}PS1_{\Delta E9}$ experiment (**Figure 31B**). At 8 weeks of age, mice received viral preparation injections of AAV-APP and AAV-PS1. At 12 weeks of age, 10% w/v brain homogenates from control individual (CTRL-inoculated group), two AD patients (AD-inoculated group) or PBS were inoculated at the same coordinates. We evaluated 2 time-points (8 and 48 wpi). Four groups were investigated:

1. AAV-APP_{SweLon}+ AAV-$PS1_{M146L}$ + PBS: AAV-APP/PS1 + PBS
2. AAV-APP_{SweLon} + AAV-$PS1_{M146L}$ + CTRL homogenate: AAV-APP/PS1 + CTRL
3. AAV-APP_{SweLon} + AAV-$PS1_{M146L}$ + AD1 homogenate: AAV-APP/PS1 + AD1
4. AAV-APP_{SweLon} + AAV-$PS1_{M146L}$ + AD2 homogenate: AAV-APP/PS1 + AD2.

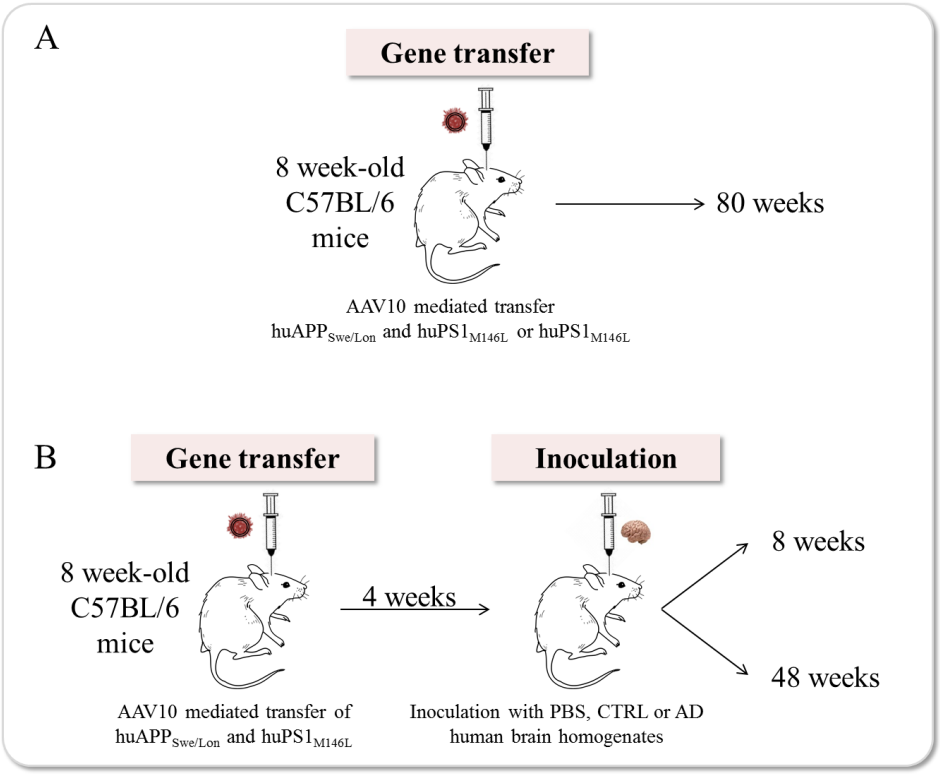

Figure 31. **Design of the AAV-APP/PS1 experiment.** A. Evaluation of β-amyloidosis development in AAV-APP/PS1 mice. B. Evaluation of β-amyloidosis experimental transmission in AAV-APP/PS1 mice. AAV10: Adeno-Associated Virus serotype 10; CTRL: aged control individual; AD: AD patient.

5.2.5. Viral vector production

To generate the vector, human double-mutant APP751 cDNA with Swedish and London mutations, and human mutated PS1 cDNA containing the M146L mutation (GeneArt, Life Technologies, Saint Aubin, France) were cloned in an AAV2 plasmid with the CAG promoter. AAV2-CAG-APP_{SweLon} or AAV-CAG-$PS1_{M146L}$ vectors were produced using an AAV packaging plasmid containing the rep gene of AAV2 and the cap gene of AAVrh10 (Audrain et al., 2016).

5.2.6. Stereotaxic injections

Brain homogenates, PBS (Gibco, ThermoFisher Scientific, Waltham, MA, USA) and/or viral preparations (5.10^8vg/site for AAV-PS1 and 10^9vg/site for AAV-APP vector) were injected bilaterally in the dorsal hippocampus (AP-2mm, DV-2mm, L+/-1mm, **Figure 32**) of 8 week-old female $APP_{Swe}PS1_{\Delta E9}$ and male wild-type C57BL/6 mice by stereotaxic surgery.

Anesthesia was obtained by intraperitoneal injection of 0.1mL/10g of a mixture of ketamine (Imalgene® 1000, Merial, Lyon, France) and xylazine (Rompun® 2%, Bayer Healthcare, Leverkusen, Germany). Animals were then placed in a stereotaxic frame (Phymep, Paris, France). Local analgesia was performed by subcutaneous injection of lidocaine/bupivacaine before incision. For $APP_{Swe}PS1_{\Delta E9}$ mice, burr holes were drilled in the appropriate location and bilateral injections of 2µL with 26-gauge needle for the brain homogenates and PBS. For AAV mice, burr holes were drilled in the appropriate location and bilateral injections of 2µL 34-gauge needle for the viral injections were performed in the dorsal hippocampus and, 4 weeks later, with 26-gauge needle for the brain homogenates and PBS. The injection speed was 1µL/min for the homogenates and PBS and 0.2µL/min for viral preparations. Needles were kept in place for an additional 2 minutes before they were slowly moved into the subjacent parietal cortex where needles were kept in place for an additional 5 minutes before being slowly removed. Respiration rate was monitored during the whole experiment and body temperature was maintained at 37±0.5°C with a heating blanket during surgery. The surgical area was cleaned (Vetedine®, Vetoquinol, Lure, France), the incision was sutured and subcutaneous injection of a solution of 0.9% NaCl was performed to favor rehydration.

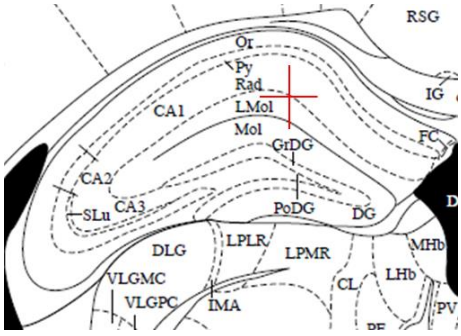

Figure 32. **Sites for bilateral injections in the dorsal CA1 for homogenates, PBS and AAVs.** From (Paxinos and Franklin, 2004)

Animals were placed in an incubator (temperature 25°C) and monitored until recovery from anesthesia. Paracetamol syrup solution (Doliprane®, Sanofi, Paris, France) was added to drinking water (1,45mL/20mL tap water) and jellified water placed in the housing cage to favor rehydration after surgery.

5.2.7. Histology and quantifications

Mice were euthanized with an overdose of sodium pentobarbital (100 mg/kg intraperitoneally) and perfused intracardiacally with 4% paraformaldehyde in PBS. After overnight post-fixation with 4% paraformaldehyde in PBS, brains were cryoprotected using overnight 15% and 30% sucrose solutions. 40µm-thick coronal brain sections were cut on a microtome (SM2400, Leica Microsytem, Wetzlar, Germany) and free-floating histological serial sections were preserved in a storage solution (glycerol 30%, ethylene glycol 30%, distilled water 30% and phosphate buffer 10%) until use.

$APP_{Swe}PS1_{\Delta E9}$experiment

Serial brain sections were used for β-amyloid immunohistochemistry. Free-floating sections were rinsed in PBS 0.1M and then incubated with hydrogen peroxide 0.3% for 20min. Pretreatment with PBS-Triton 0.5% (Triton X-100, Sigma Aldrich, MO, USA) and 4.5% of normal goat serum (Sigma Aldrich, Saint-Louis, MO, USA) blocking was performed before a 2-day incubation at +4°C with Bam10 antibody (Sigma Aldrich, MO, USA 1/10 000). Secondary biotinylated anti-mouse antibodies (Vector Laboratories, Burlingame, CA, USA) were incubated before revelation. Negative controls were performed for each group by the omission of the primary or secondary antibody. ABC Vectastain kit (Vector Laboratories, Burlingame, CA, USA) was used to amplify DAB revelation (DAB SK4100 kit, Vector Laboratories, Burlingame, CA, USA).

Stained sections were blindly analyzed. Images were acquired on Axio scan.Z1 (Zeiss, Oberkochen, Germany) at 10x magnification. Analysis was performed on ImageJ software. For β-amyloidosis analysis, region of interest for each structure (CA1, subiculum, entorhinal cortex, corpus callosum, retrosplenial cortex) were manually defined and analysis was performed bilaterally on three consecutive slices. All selected sections represented the same levels along the anteroposterior axis. Parenchymal β-amyloidosis (measured as amyloid load, amyloid plaque number/mm^2 and amyloid plaque mean size) was evaluated after threshold application and manual exclusion of stained vessels. Vascular β-amyloidosis was measured manually as the number of Bam10-immunoreactive vessels/mm^2.

For neuroinflammation evaluation, immunofluorescence was performed. Free-floating sections were rinsed in PBS 0.1M and then pretreated with PBS-Triton 0.2% and normal goat serum (Sigma Aldrich, Saint-Louis, MO, USA). Sections were incubated overnight with

Bam10 antibody (Sigma Aldrich, MO, USA 1/10 000). After washing, they were incubated with anti-mouse IgG-FITC (Life Technologies, Carlsbad, CA, USA, 1/500) for one hour and washed. They were then incubated with Iba-1 (Wako, Neuss, Germany, 1/500) or GFAP-Streptavidin Cy3 (Sigma Aldrich, Saint-Louis, MO, USA, 1/500) antibodies overnight. Iba1 sections were finally incubated with anti-rabbit IgG-Streptavidin Cy3 (Sigma Aldrich, Saint-Louis, MO, USA, 1/1000). Negative controls were performed for each group by the omission of the primary or secondary antibody. Finally, after washing, 4',6-diamidino-2-phenylindole (Vector Laboratories, Burlingame, CA, USA) aqueous medium was used to stain nuclei. Sections were mounted in Fluoromount (Sigma Aldrich, Saint-Louis, MO, USA), sealed, and dried overnight at +4°C. Every section was observed and representative photographs were taken with a Leica fluorescence microscope.

AAV-APP/PS1 experiment

Free-floating sections were rinsed in PBS 0.1M and then incubated with hydrogen peroxide 0.3% for 20min. Pretreatment with PBS-Triton 0.5% (Triton X-100, Sigma Aldrich, MO, USA) and 4.5% of normal goat serum (Sigma Aldrich, Saint-Louis, MO, USA) blocking was performed before a 2-day incubation at +4°C with 4G8 (Covance, Princeton, NJ, USA 1/500) or $A\beta_{1-40}$ or $A\beta_{1-42}$ (Life Technologies, Carlsbad, CA, USA, 1/1000) antibodies. Secondary biotinylated anti-rabbit antibodies (Vector Laboratories, Burlingame, CA, USA) were incubated before revelation for $A\beta_{1-40}$ or $A\beta_{1-42}$ staining. Negative controls were performed for each group by the omission of the primary or secondary antibody. ABC Vectastain kit (Vector Laboratories, Burlingame, CA, USA) was used to amplify DAB revelation (DAB SK4100 kit, Vector Laboratories, Burlingame, CA, USA). Stained sections were blindly analyzed.

5.2.8. Statistical analysis

Statistical analyses were performed using GraphPad Prism software (San Diego, CA, USA). Data are expressed as means ± standard error of the mean (SEM). Normality of the data was assessed by Shapiro-Wilk's test. For $APP_{Swe}PS1_{\Delta E9}$ experiments, Mann-Whitney U tests were used to compare between groups and Kruskal-Wallis tests with Dunn's multiple comparison tests were used to compare between groups and post-inoculation times. At 8wpi, no differences were seen between AD1 and AD2 groups and mice were pooled as one AD group. At 16wpi, experimental groups comprised non-inoculated, PBS, CTRL, AD1 and AD2. As no differences were found between non-inoculated, PBS and CTRL-inoculated mice, these three

groups were regrouped as one CTRL group. Similarly, no differences were found between AD1- and AD2-inoculated mice and these mice were pooled as one AD group. Spearman's test was used for correlations. For AAV experiments, Chi 2 test was performed to evaluate the differences in percentage of Aβ-positive animals between groups. As no differences were found between AD1- and AD2-inoculated mice and these mice were pooled as one AD group.

5.3. Results

5.3.1. Human sample characterization

Post-mortem staging and immunohistopathological characterization was performed by Charles Duyckaerts' team.

Braak stages and Thal phases of our three donors were determined. The control individual (CTRL), aged 69 year-old, was determined as Braak stage 0 and Thal phase 0. The first AD patient (AD1), aged 76 year-old, was evaluated as Braak stage VI and Thal phase 5. The second AD patient (AD2), aged 83 year-old, was assessed as Braak stage VI and Thal phase 4. Assessment of the CERAD neuritic score was not performed however, as both AD patients presented with Braak stage VI and Thal phases 4 or 5, they met the NIAAA criteria for "Intermediate" or "High" AD neuropathologic changes whereas the control individual did not meet the criteria (**Table 2**).

Patient	Braak stage	Thal stage	Associated pathology	Age (years)	*Post-mortem* delay (hours)
CTRL	0	0	None	69	6
AD 1	VI	5	CAA	76	10
AD 2	VI	4	None	83	21

Table 2. **Anatomopathological examination of human samples and associated informations.** CAA: cerebral amyloid angiopathy.

Parietal cortex samples from these individuals were used to prepare the homogenates for this study. Immunohistochemistry was performed in order to evaluate the extent and the morphology of Aβ and Tau lesions in these samples (**Figure 33**). The CTRL individual did not present with any Aβ or Tau lesions. AD patients were positive for both pathologies and

some morphological differences were observed between AD1 (CAA-positive) and AD2 (extensive diffuse Aβ deposition in the parenchyma).

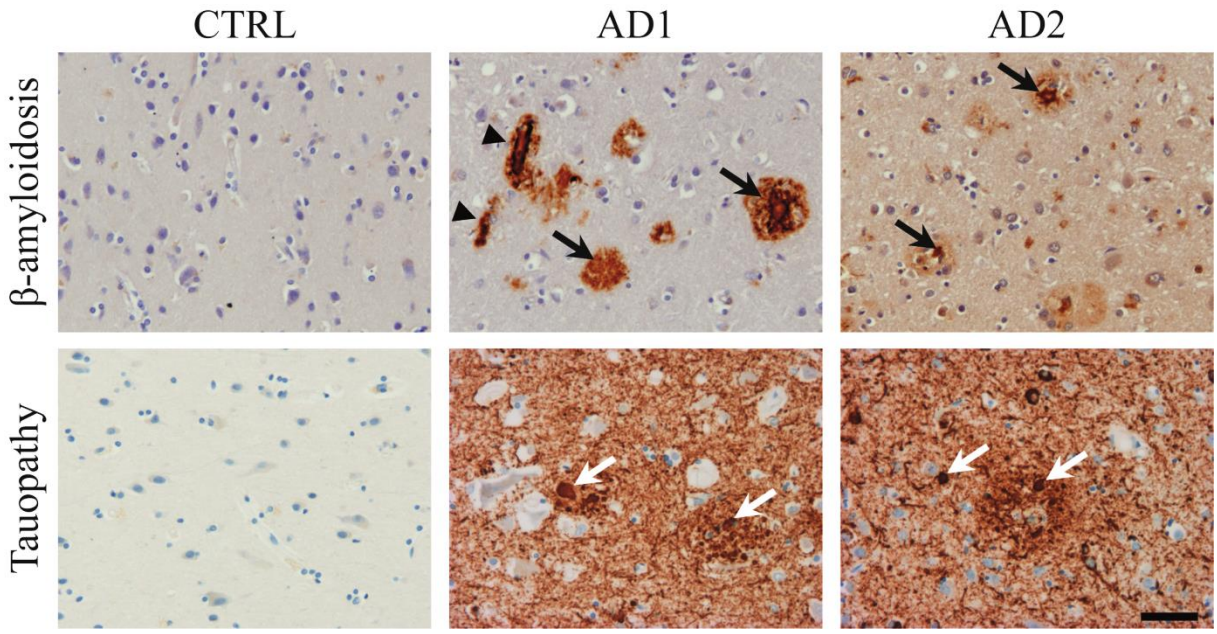

Figure 33. **Immunohistopathological characterization of the human samples.** Immunohistological Aβ staining revealed amyloid plaques (black arrows) in the two AD samples but not in the CTRL individual. Arrow heads correspond to CAA that was only detected in AD1. Extracellular diffuse Aβ deposits (apparent brown background) were detected in AD2 but not in AD1 or CTRL. Immunohistological Tau staining revealed NFTs (white arrows) in the two AD samples but not in the CTRL sample. Intensive neuropil threads (apparent brown background) and dystrophic neurites were only detected in AD patients. Scale bar indicates 50µm.

5.3.2. Biochemical characterization of the human homogenates

Characterization of β-amyloid peptides levels

ELISA immunoquantification was performed to measure Aβ peptide levels in the three homogenates (**Figure 34A-B**). Aβ levels in the CTRL individual were always below the detection threshold. Both AD1 and AD2 presented with similar high $A\beta_{1-42}$ levels (**Figure 34A**). However, AD1 exhibited very high level of $A\beta_{1-40}$ as compared to AD2 (**Figure 34B**). This observation is coherent with the observation of CAA only in the AD1 patient as $A\beta_{1-40}$ is known as being the main Aβ peptide accumulating in blood vessels (Güntert et al., 2006).

Characterization of pathological Tau

Presence or absence of pathological Tau in the homogenates was assessed by Western-blots analysis (**Figure 34C-D**). Using an anti-C-ter Tau antibody, we observed the typical AD shift in apparent molecular weights of Tau triplet in the AD patients but not in the CTRL individual (**Figure 34C**). Such Tau triplet display and shift is characteristic of Type I tauopathies that include AD and has been suggested to result from Tau hyperphosphorylation (Sergeant et al., 2005). To further evaluate the phosphorylation state of Tau in our homogenates, we used an anti-phosphoserine396 (pS396) Tau antibody (**Figure 34D**). Serine 396 is a physiological site for Tau phosphorylation that is hyperphosphorylated in AD (Martin et al., 2011). It revealed the presence of hyperphosphorylated Tau in both AD patients but not in the CTRL individual. These results showed that AD brain homogenates bore the biochemical signature of AD pathological Tau, thus confirming its presence in AD homogenates and its absence in CTRL homogenate.

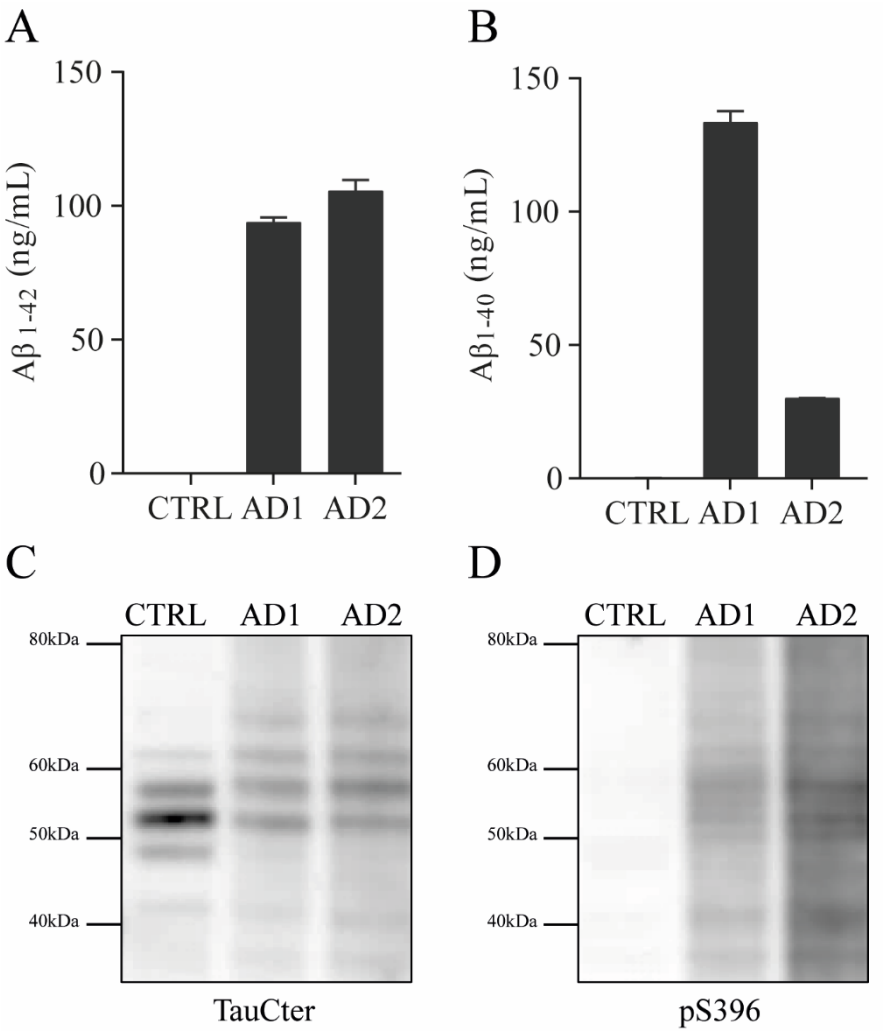

Figure 34. **Biochemical characterization of the human brain homogenates.** A-B. Aβ peptide levels in the three homogenates determined by ELISA. A. $Aβ_{1-42}$. B. $Aβ_{1-40}$. C-D. Identification of pathological Tau in CTRL and AD patient homogenates by Western-blot. A. Total Tau is revealed by anti-C-terminal Tau antibody. B. Phosphorylated Tau is detected by anti-phosphoSerine396 (pS396) Tau antibody.

5.3.3. Acceleration of β-amyloidosis in $APP_{Swe}PS1_{\Delta E9}$ mice

First, we used $APP_{Swe}PS1_{\Delta E9}$ mice as an early and quickly evolving model of β-amyloidosis. $APP_{Swe}PS1_{\Delta E9}$ were inoculated in the CA1 region of the hippocampus at 8 weeks of age. Parenchymal and vascular β-amyloidosis were quantified at 8 and 16wpi in the inoculated (CA1) and connected structures (retrosplenial cortex (RS), subiculum (S) and entorhinal cortex (EC), **Figure 35**) as well as in the corpus callosum.

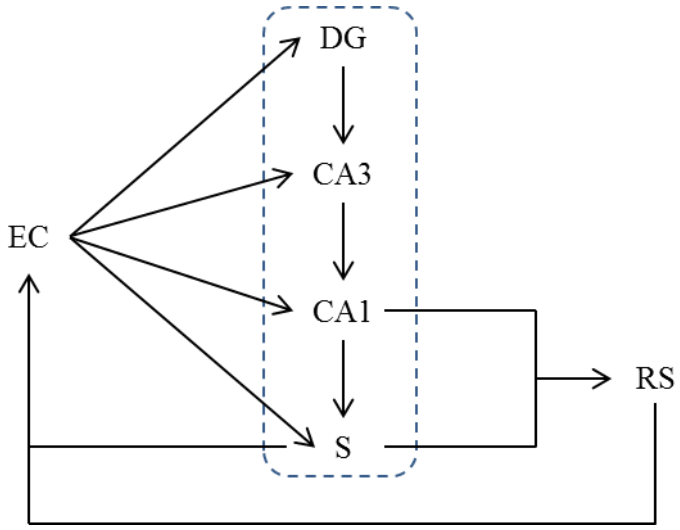

Figure 35. **Connected regions of the CA1.** Dotted blue rectangle indicates regions spatially close. Dark arrows indicate connections. DG: dentate gyrus, S: subiculum, EC: entorhinal cortex, RS: retrosplenial cortex. Adapted from (Bird and Burgess, 2008; Tannenholz et al., 2014; Ye et al., 2015b).

5.3.3.1. Parenchymal and vascular β-amyloidosis

Sections of the entire brain were stained for β-amyloidosis (**Figure 36**). We observed parenchymal and vascular β-amyloidosis as soon as 12 weeks of age (4 weeks post-inoculation, wpi) and its progressive development up to 28 weeks of age (16wpi).

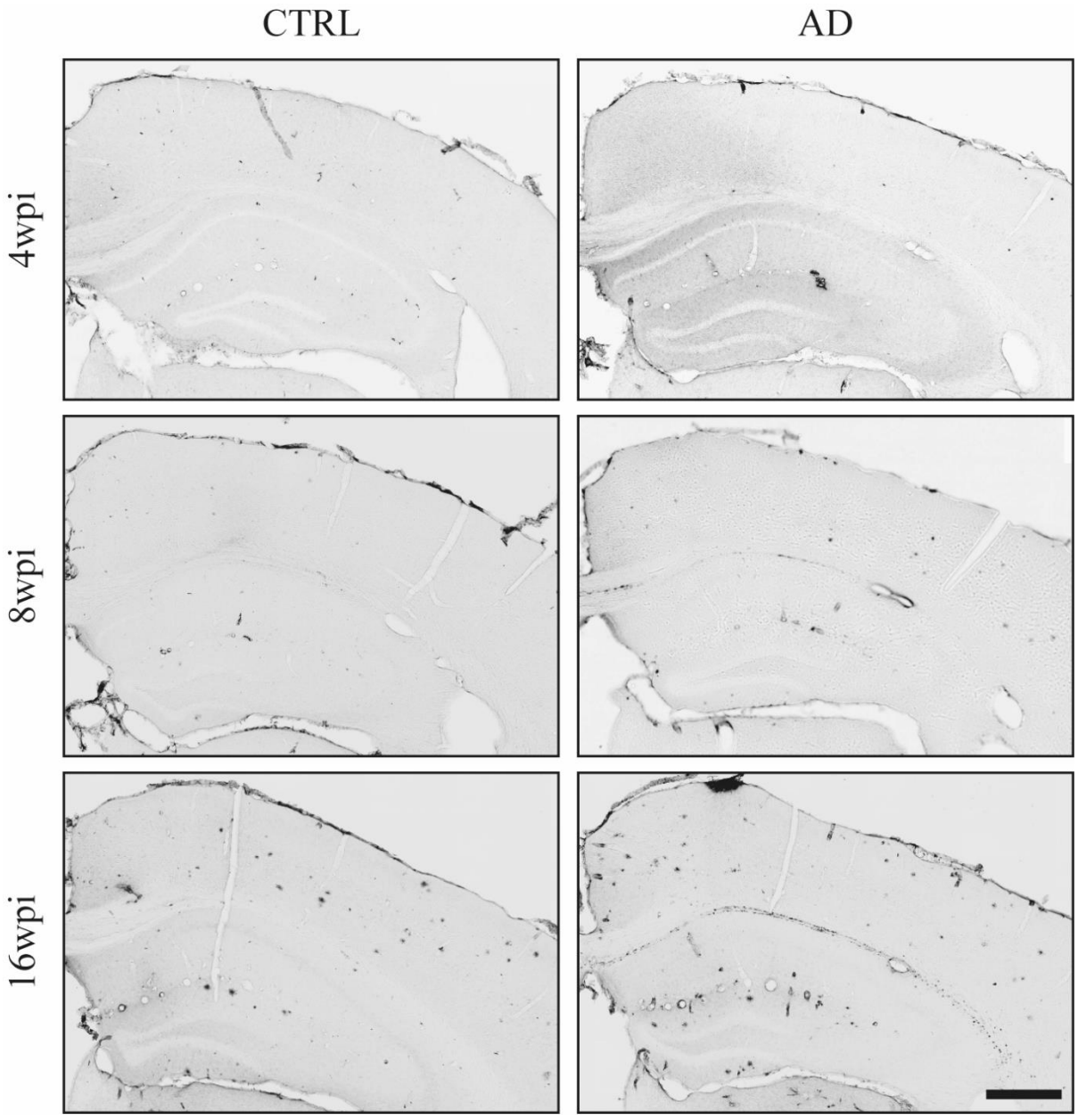

Figure 36. **Time-dependant β-amyloidosis in CTRL- and AD-inoculated $APP_{Swe}PS1_{\Delta E9}$ mice.** Representative slices stained with Bam10 antibody. wpi: weeks post-inoculation. Scale bar: 500µm.

Parenchymal β-amyloidosis was neither increased in the inoculated CA1 nor any connected structure at 8wpi (**Figure 37A**). Parenchymal β-amyloidosis increased in the CA1 but spreading to hippocampal connected structures was not observed at 16wpi (**Figure 37B**).

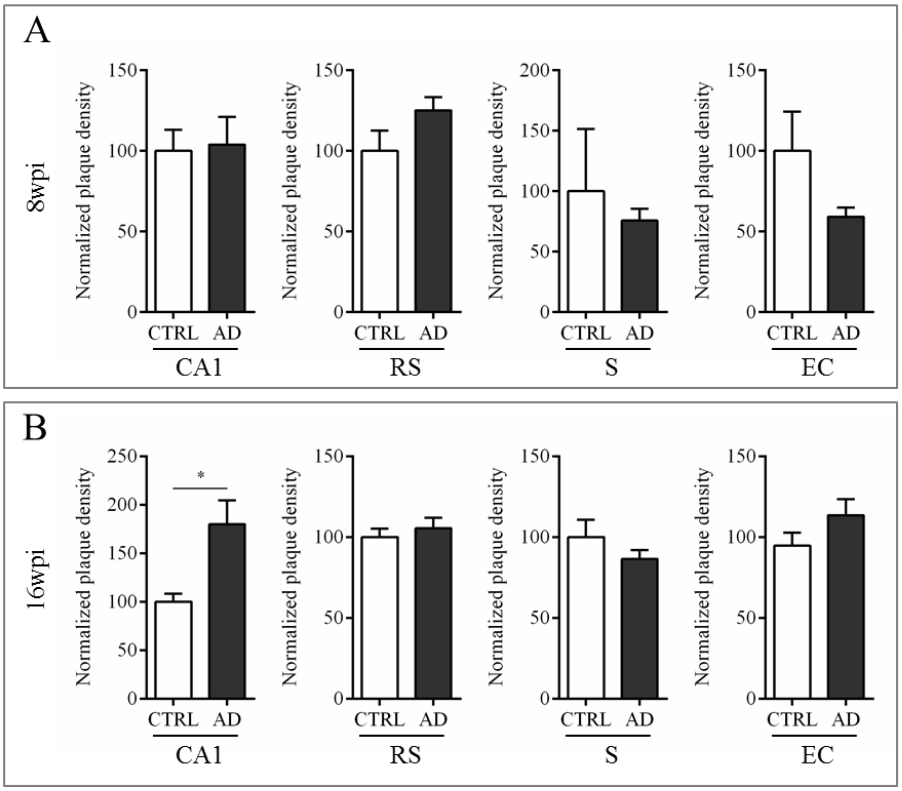

Figure 37. **AD brain homogenate inoculation accelerates β-amyloidosis at 16wpi in the inoculated CA1 but does not spread to connected structures.** Number of amyloid plaques per mm^2 normalized to the CTRL group in the CA1, retrosplenial cortex (RS), subiculum (S) and entorhinal cortex (EC) at 8wpi (A, n>5/group) or 16 wpi (B, n>16/group). Mann-Whitney U test, * $p<0.05$, wpi: weeks post-inoculation.

$APP_{Swe}PS1_{\Delta E9}$ spontaneously develop cerebral amyloid angiopathy (CAA, **Figure 36**). We also investigated if AD brain homogenates inoculation accelerates CAA. Amyloid-positive vessels were counted in the inoculated and hippocampal connected structures. No differences were found between CTRL and AD groups at 8wpi (**Figure 38A**) and 16wpi (**Figure 38B**).

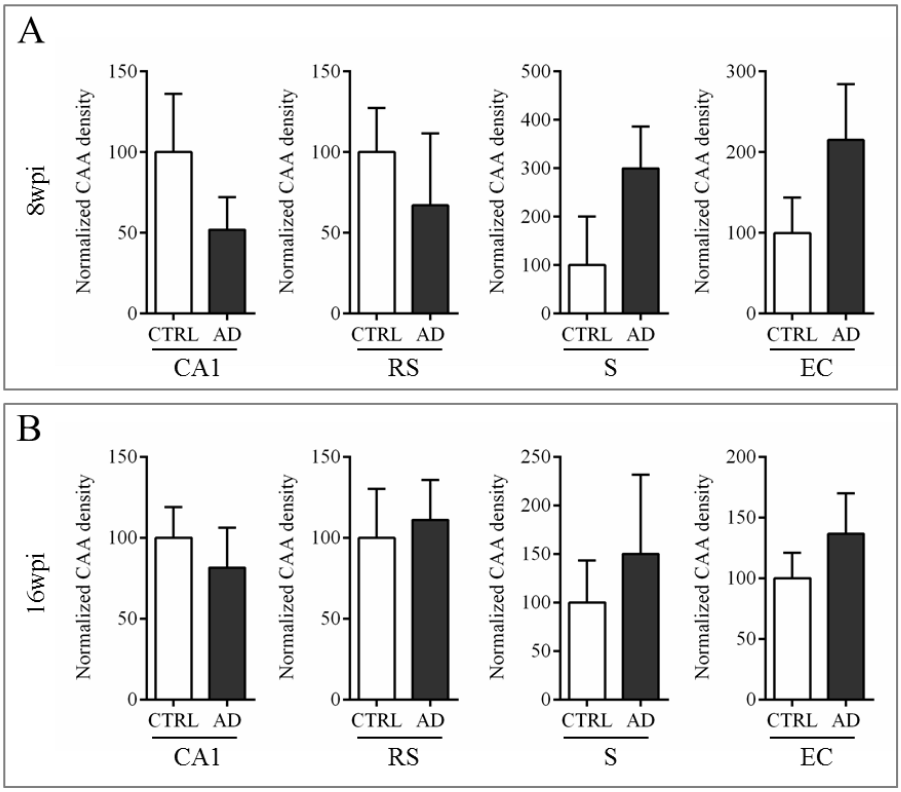

Figure 38. **AD brain homogenate inoculation does not impact cerebral amyloid angiopathy.** Number of amyloid positive vessels per mm^2 normalized to the CTRL group in the CA1, retrosplenial cortex (RS), subiculum (S) and entorhinal cortex (EC) at 8wpi (A, n>5/group) or 16 wpi (B, n>16/group). Mann-Whitney U test, wpi: weeks-post-inoculation.

5.3.3.2. Callosal β-amyloidosis

AD brain homogenate inoculation induces a specific callosal β-amyloidosis

We observed the development of a typical callosal β-amyloidosis in the AD-inoculated group (**Figure 39**). Although β-amyloidosis does not affect the white matter in humans, many APP over-expressing transgenic mouse strains develop an age-related callosal β-amyloidosis. In aged $APP_{Swe}PS1_{\Delta E9}$, spontaneous callosal β-amyloidosis is characterized by large round Aβ deposits generally well-defined in the entire corpus callosum. Here, AD-induced Aβ deposits are smaller and often contiguous. They mostly formed a dotted line between the corpus callosum and the alveus but are also observed in the lower part of the corpus callosum. This callosal acceleration phenotypically differs from normal callosal β-amyloidosis development in this transgenic mouse strain. This suggests a specific and progressive seeding process related to AD brain homogenate inoculation in the hippocampus.

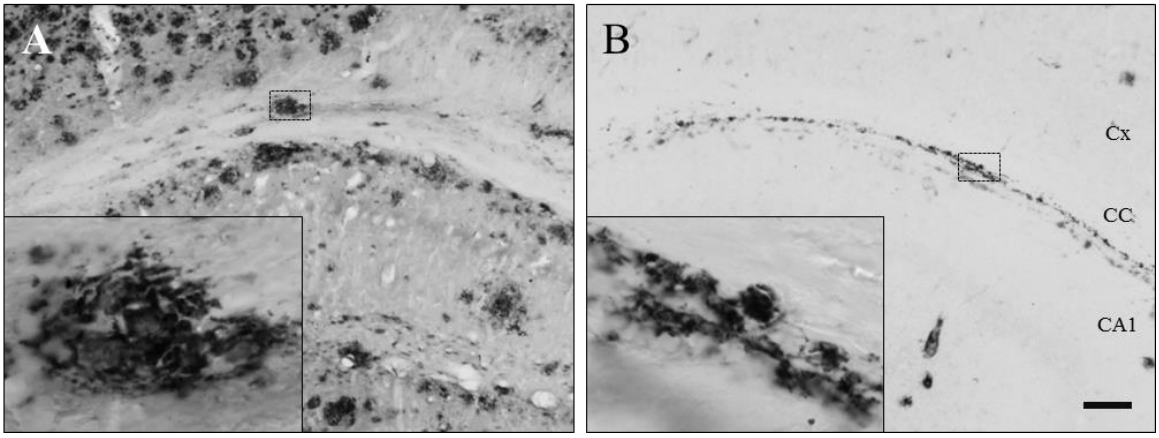

Figure 39. **AD-induced callosal β-amyloidosis pattern differs from normal aging.** Bam10 immunostaining A. 80 weeks old non- inoculated $APP_{Swe}PS1_{\Delta E9}$ mouse. B. 24 weeks old AD-inoculated $APP_{Swe}PS1_{\Delta E9}$ mouse (16 wpi). Scale bar: 100µm.

AD-induced callosal β-amyloidosis is associated to astrocytes and microglia

Similarly to parenchymal amyloid plaques, we found Aβ deposits in the corpus callosum to be associated to both microglia and astrocytes in AD-inoculated mice (**Figure 40**).

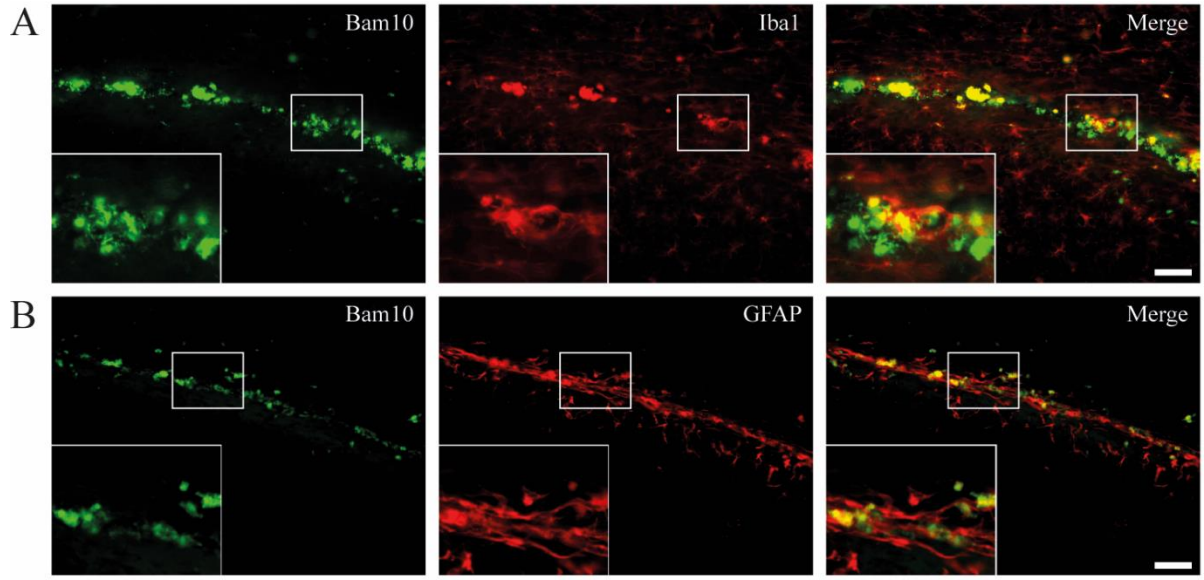

Figure 40. **AD-induced callosal β-amyloidosis is associated to microglia and astrocytes.** A. Co-immunofluorescence of Aβ-deposits (Bam10) and microglia (Iba-1) in the corpus callosum of AD-inoculated $APP_{Swe}PS1_{\Delta E9}$ mice shows that Aβ deposits are surrounded by activated microglia. B. Co-immunofluorescence of Aβ-deposits (Bam10) and astrocytes (GFAP) in the corpus callosum of AD-inoculated $APP_{Swe}PS1_{\Delta E9}$ mice shows that Aβ deposits are surrounded by reactive astrocytes. Scale bars: 50µm.

AD-induced callosal β-amyloidosis is time-dependent

At 4wpi, no Aβ deposits were detected in the corpus callosum of CTRL and AD-inoculated mice (**Figure 41**). This suggests that callosal β-amyloidosis is not an accumulation of the inoculated material.

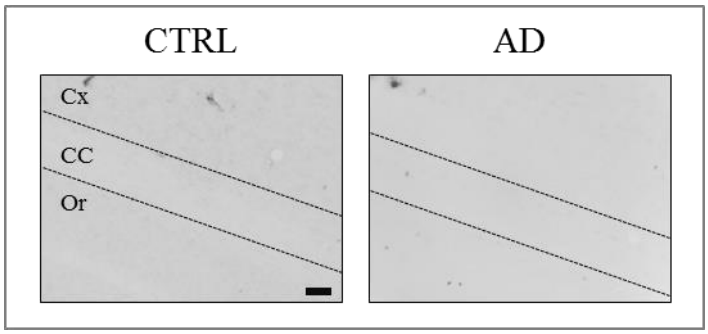

Figure 41. **Absence of Aβ deposits in the corpus callosum at 4wpi.**Bam10 immunostaining in CTRL and AD-inoculated $APP_{Swe}PS1_{\Delta E9}$ mice (n>3/group). Cx: cortex, CC: Corpus callosum, Or: stratum oriens. Dotted lines indicate the CC. Scale bar: 50µm.

At 8wpi, callosal Aβ deposits were detected in the AD-inoculated group. Such deposits increased at 16wpi whereas no similar deposits were found in the CTRL-inoculated group (**Figure 42A**). Quantification of amyloid load (% of stained area) in the corpus callosum showed the progressive development of β-amyloidosis in the AD-inoculated group (**Figure 42B**).

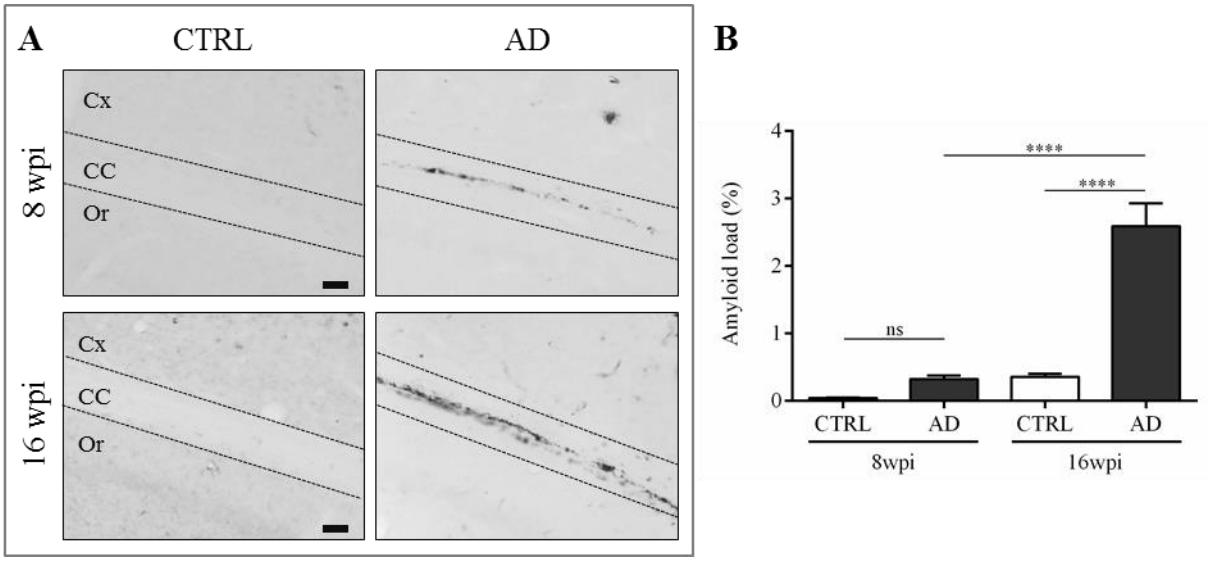

Figure 42. A**D brain homogenate inoculation leads to a progressive callosal β-amyloidosis.** A. Bam10 immunostaining in CTRL or AD-inoculated mice at 8wpi (n>5/group) or 16 wpi (n>16/group). Dotted lines indicate the CC. Scale bar: 50µm. B. Quantification of the amyloid load of the corpus callosum. Kruskal-Wallis test with Dunn's multiple comparisons test (ns: p>0.05; ****: p<0.0001).

5.3.3.3. Decreased amyloid plaque size in neighboring regions of the CA1 and corpus callosum

We also measured Aβ plaque size in the CA1 and hippocampal connected regions. Surprisingly, we observed a decrease of amyloid plaque size in the retrosplenial cortex and the subiculum, two neighboring regions of the corpus callosum (**Figure 43A-B**) whereas the number of amyloid plaques was not affected (**Figure 37**). Amyloid plaque size in the retrosplenial cortex and subiculum correlated with β-amyloidosis increase in the CA1 (**Figure 43C-D**) and corpus callosum (**Figure 43E-F**).

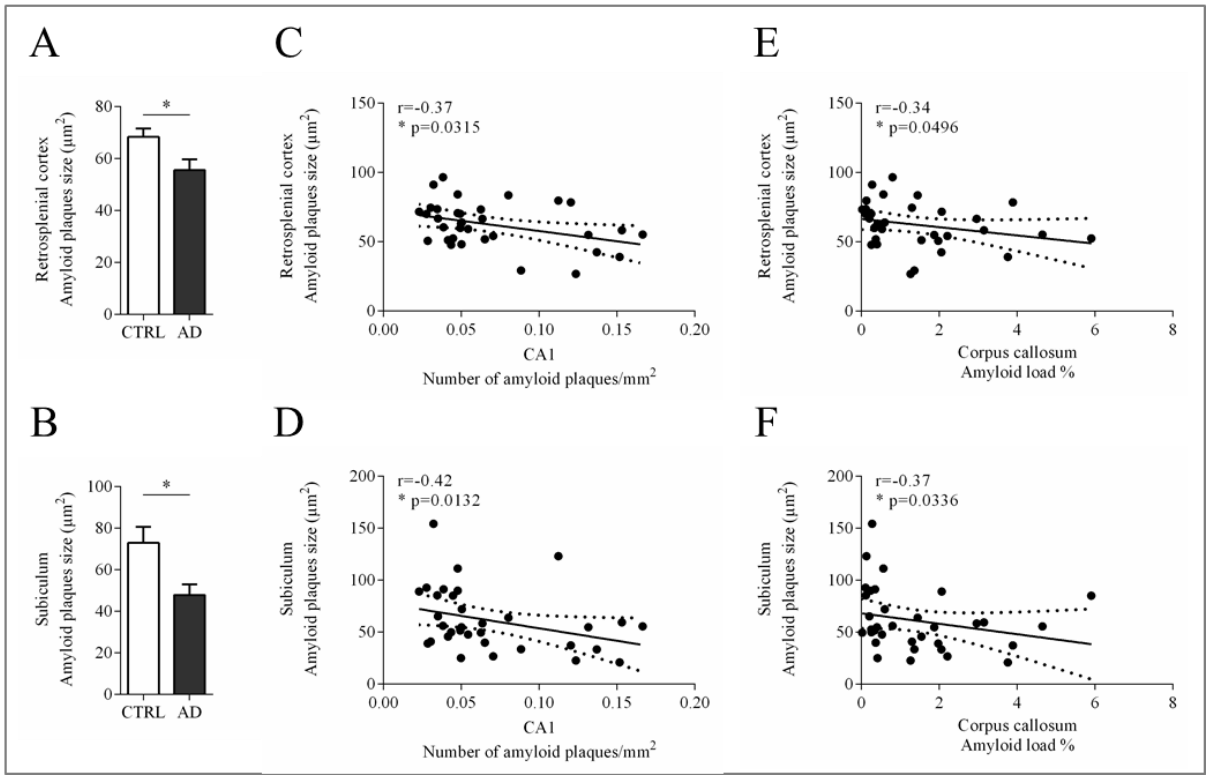

Figure 43. **β-amyloidosis acceleration in CA1 and corpus callosum is associated to a decrease in amyloid plaque size in neighboring regions.** A-B. Amyloid plaque size decrease in the retrosplenial cortex (A) and the subiculum (B).C-D. Amyloid plaque size decrease in the retrosplenial cortex (C) and the subiculum (D) is correlated to amyloid plaque density in the CA1. E-F. Amyloid plaque size decrease in the retrosplenial cortex (E) and the subiculum (F) is correlated to amyloid load in the corpus callosum. A-B: Mann-Whitney U test, * $p<0.05$ ** $p<0.01$; C-F. Spearman correlation test, * $p<0.05$.

5.3.4. Acceleration of β-amyloidosis in AAV-APP/PS1 mice

5.3.4.1. Characterization of β-amyloidosis development

Wild-type AAV-APP/PS1 mice focally express mutated forms of human APP and PS proteins in the dorsal hippocampus. In the literature, this model was studied up to 12 weeks post-injection. At 4 and 12 weeks post-injection of AAV, β-amyloidosis was not detected in co-injected mice (Audrain et al., 2016). Here, we studied AAV-PS1 and AAV-APP/PS1 mice up to 80 weeks post-injection. Human PS1 expression alone did not lead to β-amyloidosis development. Co-expression of human mutated APP and PS1 induced a sparse β-amyloidosis (2 out of 3 mice, AAV-APP/PS1) in the dorsal CA1 and subiculum (**Figure 44A**). They mainly consisted of $A\beta_{1-42}$ proteins (**Figure 44B**) although some rare amyloid plaques could

also contain $A\beta_{1-40}$. Therefore, β-amyloidosis in AAV-APP/PS1 mice was a late and sparse event restricted, as expected, to the dorsal hippocampus.

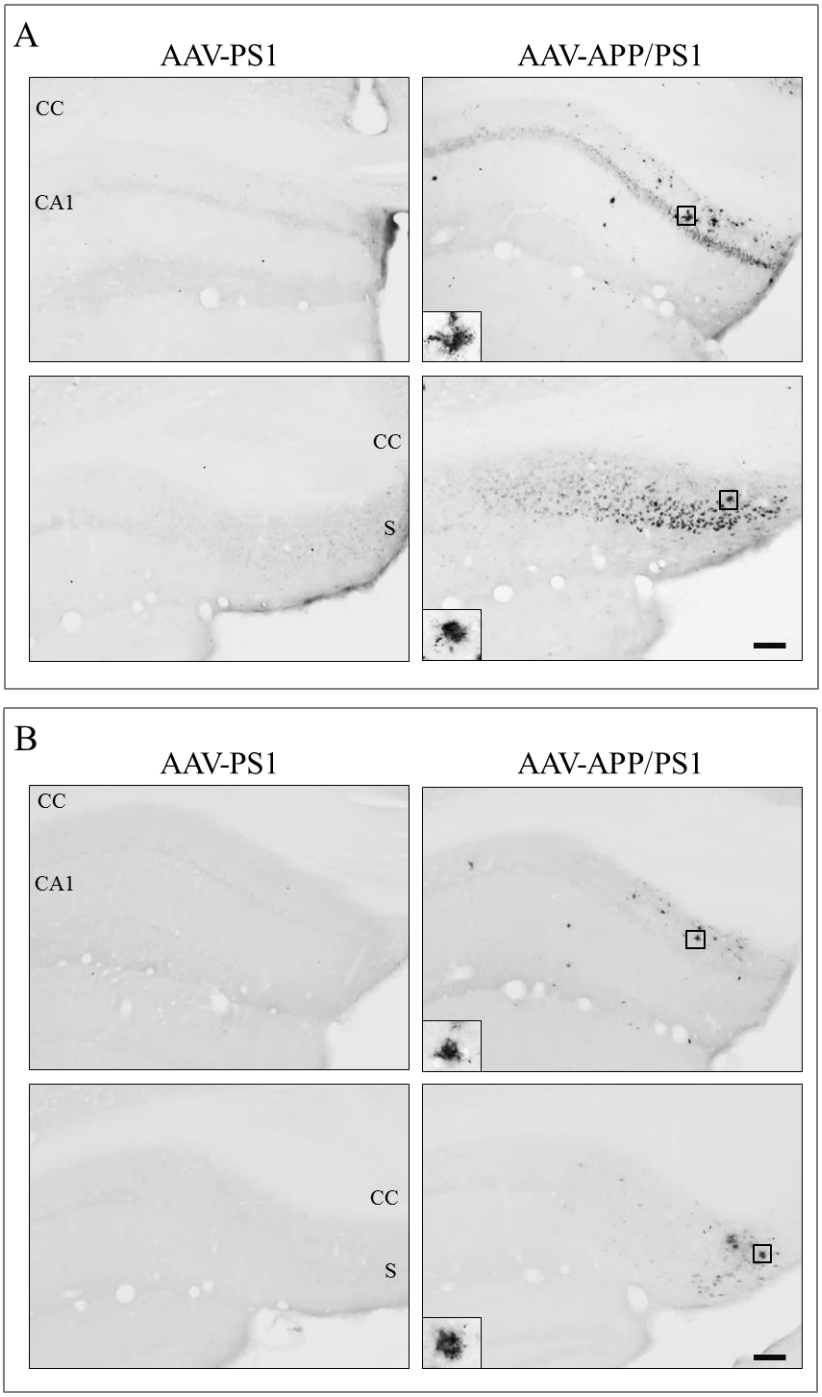

Figure 44. **Sparse parenchymal β-amyloidosis is only detected in AAV-APP/PS1 mice at 80 weeks after AAV-APP and AAV-PS1 co-injection.** A. 4G8 immunostaining of AAV-PS1 or AAV-APP/PS1 injected mice at 80 weeks after AAV injection. B. $A\beta_{1-42}$ immunostaining of AAV-PS1 or AAV-APP/PS1 injected mice at 80 weeks after AAV injection. CC: Corpus callosum, S: Subiculum. Scale bars: 100µm.

5.3.4.2. β-amyloidosis acceleration

4 weeks after co-injection of AAV-APP and AAV-PS1, we inoculated CTRL or AD brain homogenates at the same coordinates. PBS was injected as a control for repeated intracerebral injection. We evaluated two time-points: 8 and 48wpi. At 8wpi, no Aβ deposits were found in any structures of PBS-, CTRL- or AD-inoculated mice (**Figure 45**).

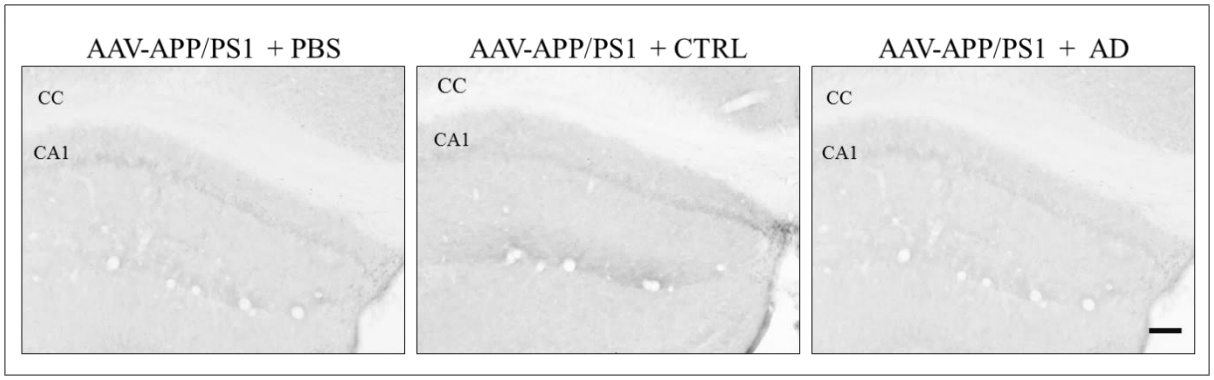

Figure 45. **β-amyloidosis is not detected at 8wpi in PBS-, CTRL- or AD- inoculated AAV-APP/PS1 groups.** $A\beta_{1-42}$ immunostaining; CC: Corpus callosum. n=4-5/group.

At 48wpi, Aβ deposition was observed in AAV-APP/PS1 (**Figure 46A**). Indeed, very rare Aβ deposition was only found in the subiculum of one the PBS group (1/8 animals, 12.5%) and one of the CTRL-inoculated mice (1/6 animals, 16.7%) but none in the CA1. These two groups were pooled as one CTRL group (2/14 animals, 14.3%). In contrast, numerous Aβ deposits were found in the CA1 and the subiculum of the AD1- (5/7 animals, 71.4%) and AD2-inoculated mice (6/8 animals, 75%). Sparse deposits could also be detected in or in between the alveus and the corpus callosum similarly to AD-inoculated $APP_{Swe}PS1_{\Delta E9}$ mice but less prominently. No qualitative differences in morphology, distribution or number of Aβ-positive animals between AD1 (5/7 animals, 71.4%) and AD2 (6/8 animals, 75%) were observed and both groups were pooled in one AD group (11/15 animals, 73.3%).

At 48wpi, the number of affected animals in the AD-inoculated group was higher than in the CTRL-inoculated group (** p=0.001; Chi 2=10.21; df=1). In contrast, the number of affected animals in the AD-inoculated group was similar to the one observed in 80 weeks post-injection animals (p>0.95; Chi 2=0.06; df=2) (**Figure 46B**). Although accelerated β-amyloidosis was sparse, Aβ deposits seemed qualitatively more numerous in 52 weeks (48wpi) AD-inoculated AAV-APP/PS1 mice (**Figure 46A)** than in 80 weeks AAV-APP/PS1 mice (**Figure 44**).

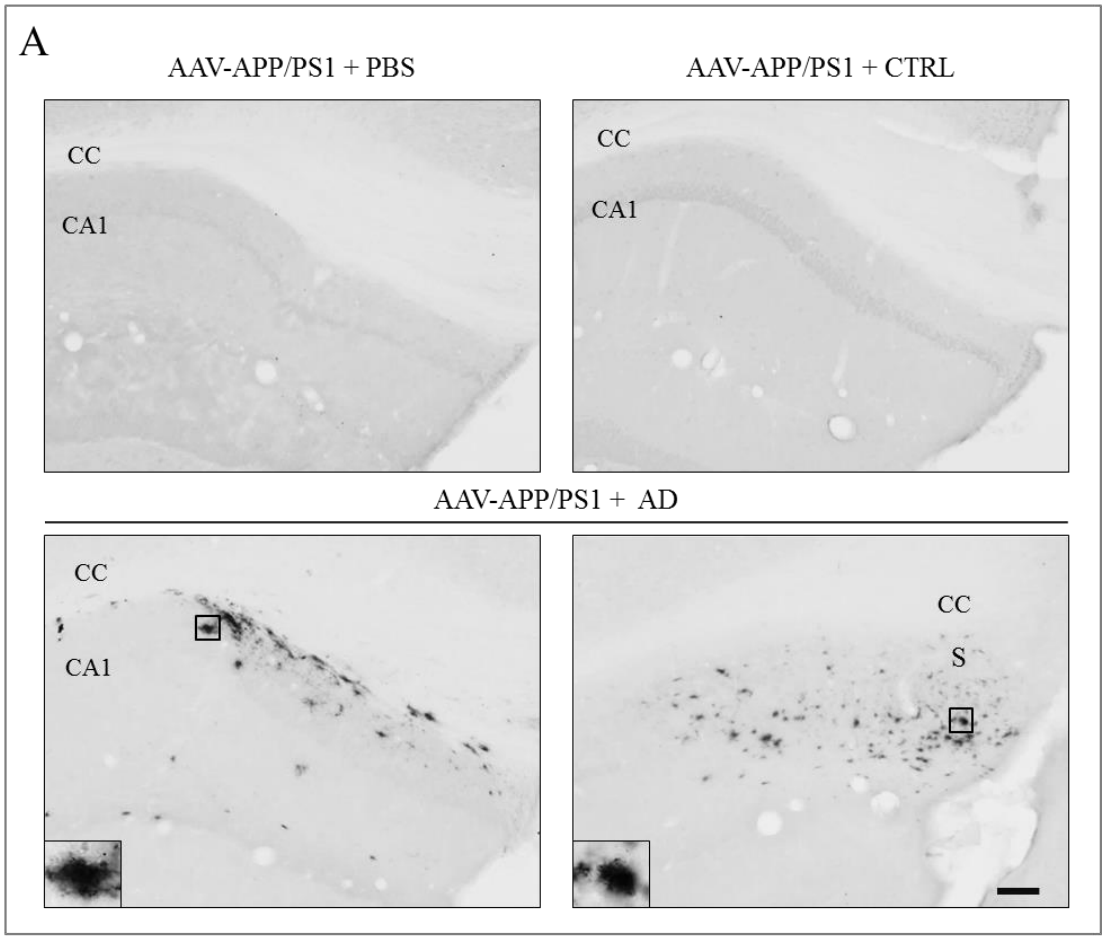

Figure 46. **AD brain homogenates inoculation accelerates β-amyloidosis in AAV-APP/PS1 mice at 48wpi.** A. $A\beta_{1-42}$ immunostaining reveals Aβ plaques in the CA1 and subiculum of AD-inoculated AAV-APP/PS1. B. Percentage of animals presenting with Aβ lesions in the CTRL-, AD-inoculated AAV-APP/PS1 (n=14 and 15 for CTRL and AD, respectively) mice as well as 80 weeks post-injection of AAV non-inoculated AAV-APP/PS1 mice (Aged, n=3).

We finally investigated β-amyloidosis spreading from the injection site (CA1) to other cortical structures. Interestingly, we found Aβ accumulation only in the dorsal hippocampus (dorsal CA1, subiculum and dentate gyrus, **Figure 47A**) but not in the ventral hippocampus of AD-inoculated mice. Also, no deposits were found in other structures such as the cortex, the amygdala or the thalamus (**Figure 47B**). The subiculum and dentate gyrus are both proximal and connected to the CA1. As acceleration in these structures by spontaneous dissemination of the inoculate cannot be ruled out in this experiment, we cannot consider their affection as spreading from the injected CA1.

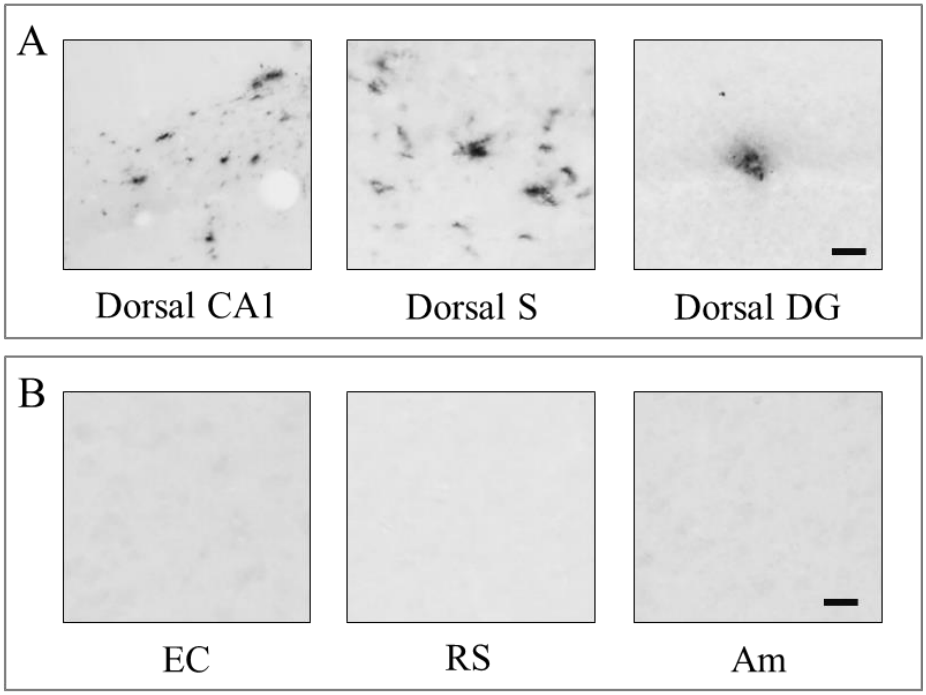

Figure 47. **β-amyloidosis acceleration depends on human APP expression in inoculated AAV mice.** A. Acceleration of $A\beta_{1-42}$ deposition in the dorsal hippocampus where human APP is expressed 48 weeks after AD brain homogenate inoculation. B. Absence of $A\beta_{1-42}$ deposition in regions that do not express human APP 48 weeks after AD brain homogenate inoculation despite their connection to the inoculation site. S: subiculum; DG: dentate gyrus; EC: entorhinal cortex; RS: retrosplenial cortex; Am: amygdala; scale bars: 20µm.

5.4. Discussion

In order to evaluate β-amyloidosis prion-like transmission, we inoculated two complementary murine models of β-amyloidosis with AD brain homogenates. First, we used $APP_{Swe}PS1_{\Delta E9}$transgenic mice that highly express Aβ peptides. Spontaneous Aβ aggregation and deposition in amyloid plaques and/or cerebral amyloid angiopathy (CAA) is systematic, early (as soon as 12 weeks of life in our breeding colony) and robust (**Figure 36**). Then, we explored β-amyloidosis transmission in an AAV-based mouse model of AD that expresses human mutant APP and PS1 proteins. This model presents with late, sparse and non-systematic β-amyloidosis (**Figure 44**). It allowed us to evaluate β-amyloidosis acceleration in a wild-type mouse model expressing focally low levels of human Aβ (Audrain et al., 2016).

5.4.1. β-amyloidosis experimental transmission in mice

Using intracerebral inoculation of AD brain homogenates, we observed seeding effects in both models in the inoculated hippocampus, at 16 and 48 weeks post-inoculation, respectively (**Figure 37** and **Figure 46**). In our two models, no acceleration were observed at short incubation times (8 weeks, **Figure 37** and **Figure 45** respectively) indicating that seeding effects were not linked to the deposition of the Aβ contained in the AD-homogenates. These results are in accordance with the literature showing that seeded Aβ deposits require time to develop (Baker et al., 1993; Eisele et al., 2009; Kane et al., 2000; Morales et al., 2012; Stöhr et al., 2012).

Inoculation of an aged-matched individual (CTRL) brain sample lacking Aβ deposits (**Figure 33**) and in which Aβ levels were below detection limits (**Figure 34A-B**) did not accelerate β-amyloidosis (**Figure 37**, **Figure 42**, **Figure 46**). In the literature, β-amyloidosis seeding was reported following AD brain homogenates inoculation but also following MCI or age-matched non-demented individuals presenting with diffuse Aβ deposits (Duran-Aniotz et al., 2013; Kane et al., 2000; Meyer-Luehmann et al., 2006). However, Aβ-free homogenates from young individuals or old wild-type mice did not induce any Aβ deposit in various transgenic mouse strains (Eisele et al., 2014; Hamaguchi et al., 2012; Kane et al., 2000; Meyer-Luehmann et al., 2006). Thus our results, along with previous ones, show that transmission-induced β-amyloidosis requires a donor brain extract with Aβ seeds. These results are consistent with the long list of publications showing that Aβ assemblies are the seeding agents

that can induce cerebral amyloid deposition in mice (Duran-Aniotz et al., 2014; Eisele et al., 2009, 2014; Meyer-Luehmann et al., 2006; Stöhr et al., 2012, 2014).

Considering that we inoculated unpurified human AD brain homogenates, immune responses and inflammation could be responsible for β-amyloidosis acceleration. However, such effects were not observed using a human CTRL brain homogenate and inflammation and immune responses have never been reported to trigger β-amyloidosis following brain homogenates inoculations (Meyer-Luehmann et al., 2006; Stöhr et al., 2012; Watts et al., 2014). Also, the possibility that brain injury is responsible for the acceleration is mitigated by the fact that both PBS and CTRL inoculation failed to accelerate β-amyloidosis (**Figure 37**, **Figure 42**, **Figure 46**) as reported previously (Meyer-Luehmann et al., 2006). Taken altogether, this suggests that Aβ seeds, and not inflammation or brain injury, are responsible for our observed β-amyloidosis acceleration.

Our results, along with numerous others, suggest that transmission-induced β-amyloidosis is a progressive process requiring a lag time for Aβ assemblies to accumulate into insoluble amyloid plaques.

5.4.2. The host is a modulator of β-amyloidosis transmission

Here, we used two different models to investigate the effect of the receiving "host" animals upon β-amyloidosis experimental transmission. We observed different seeding effects in our two models.

$APP_{Swe}PS1_{\Delta E9}$ mice develop β-amyloidosis very early in life as soon as 12 weeks of life. The mice were inoculated at 8 weeks of age, letting only a very small lag time before the initiation of the spontaneous aggregation at 12 weeks. At short delays (4 and 8 weeks post-inoculation, **Figure 36**, **Figure 37**, **Figure 38**), we did not observed any differences in β-amyloidosis development, except for the corpus callosum in which Aβ deposition started at 8 weeks post-inoculation (**Figure 42**). However, at 16 weeks post-inoculation, β-amyloidosis was increased in the AD-inoculated mice (**Figure 37**). These results suggest that in mice in which the spontaneous amyloid deposition has already started, AD brain homogenate inoculation can further increase the pathology intensity. In previous studies from the literature, homogenate inoculation experiments were often performed in mice with a long spontaneous lag time, *i.e.* in models such as the APP23 or R1.40 mice that spontaneously develop amyloid at 40 and 60

weeks of life, respectively (Meyer-Luehmann et al., 2006; Ye et al., 2015b). Here, we show that models with such long spontaneous lag times are not necessary to detect seeding effects.

In AAV-APP/PS1 mice, we showed that β-amyloidosis develops spontaneously very late (**Figure 44**) and we detected an acceleration of the pathology following AD brain homogenate inoculation with an increase in both affected animal number and pathology intensity (**Figure 46**).

It has been reported in the literature that the lag time before accelerated Aβ deposition depends on the transgenic mouse strain (Eisele et al., 2014; Meyer-Luehmann et al., 2006). Here we confirmed that the "host" effect is presumably in accordance with the spontaneous lag time of each mouse strain and may rely on the basal expression of Aβ (Eisele et al., 2014). Indeed, in the hippocampus, Aβ is over-expressed in $APP_{Swe}PS1_{\Delta E9}$ whereas it is almost physiological in the AAV model (Audrain et al., 2016). Our results, along with others, suggest that the availability of native Aβ peptides in the brain plays a major role in seeding.

5.4.3. Callosal β-amyloidosis: a signature of intracerebral inoculation?

In both our models, we observed the development of a very specific callosal β-amyloidosis after AD brain homogenate inoculation (**Figure 39**, **Figure 40**, **Figure 41** and **Figure 42**). Similar results were reported in previous experimental transmission studies (**Table 3**) using intracerebral inoculation of either human or murine brain homogenates containing misfolded Aβ (Duran-Aniotz et al., 2013; Hamaguchi et al., 2012; Kane et al., 2000; Meyer-Luehmann et al., 2006) or synthetic Aβ peptides (Stöhr et al., 2012, 2014). This callosal β-amyloidosis is a progressive phenomenon that was not detected at 4 weeks post-injection (**Figure 41**) and others have shown that no such deposits could be detected at 1 day, 5 days and 2 weeks after inoculation (Kane et al., 2000; Meyer-Luehmann et al., 2006). This suggests that the inoculum is resorbed and that Aβ seeds may be trapped leading to the development of callosal β-amyloidosis. Also, we found that accumulation of Aβ peptides at the edge and in the corpus callosum recapitulate features of parenchymal Aβ plaques. Indeed, we have shown that these deposits are surrounded by astrocytes and microglia (**Figure 40**) and they have been shown to bind amyloid dye (Duran-Aniotz et al., 2013, 2014; Stöhr et al., 2014).

Aβ seeds source	Mouse model	Injected structure	Callosal β-amyloidosis	Other observations	Reference
AD	Tg2576	CA1	+	-	Kane et al., 2000
AD, APP23 and APPPS1	APP23 and APPPS1	CA1 and cortex	+	-	Meyer-Luehman et al., 2006
APP23	APP23:Gfap-luc	CA1 and cortex	+	GFAP	Watts et al., 2011
APP23	R1.40	CA1 and cortex	+	-	Hamaguchi et al., 2012
APP23, CRND8 and synthetic $A\beta_{1-40\ or\ S26C}$	APP23:Gfap-luc	IC	+	GFAP	Stöhr et al., 2012
AD	$APP_{Swe}/PS1_{\Delta E9}$	CA1	+	ThS positive	Duran-Aniotz et al., 2013
Synthetic $A\beta_{1-40\ or\ 1-42}$	APP23:Gfap-luc	IC	+	ThS positive	Stöhr et al., 2014

Table 3. **Studies in which callosal β-amyloidosis can be observed following intracerebral experimental transmission.** AD: human AD brain homogenate; APP23: old APP23 brain homogenate; APPPS1: old APPPS1 brain homogenate; CNRD8: old CNRD8 brain homogenate; IC: intracerebral; GFAP: observation of reactive astrocytes overexpressing GFAP around the callosal β-amyloidosis; ThS: Thioflavin S.

This callosal β-amyloidosis resembles observations in prion experiments. Indeed, following intracerebral inoculation with PrP^{Sc}-contaminated homogenates, similar PrP deposition on the inferior surface of or in the corpus callosum was observed (Manson et al., 1999; Piccardo et al., 2007; Scott et al., 1989). Interestingly, callosal PrP amyloidosis seems specific of intracerebral inoculation as it does not develop after intraperitoneal inoculation (Gibson, 1986). Similarly, callosal β-amyloidosis does not seem to develop after Aβ-laden brain homogenate intraperitoneal inoculation (Eisele et al., 2014). Callosal amyloidosis could therefore be a hallmark of prion and prion-like intracerebral transmission in rodents. It has been suggested that, since this hallmark was not observed after intraperitoneal inoculation, it could be due to a physical dissemination of the inoculum from the injection site. In addition, the localization of plaques in the corpus callosum suggests that the inoculum may spread towards the lateral ventricles after injection (Gibson, 1986). Indeed, the orientated disposition of white matter fibers may provide an efficient path for diffusion. Therefore, retention of the inoculum in this region may be responsible for callosal amyloidosis following intracerebral inoculation (Manson et al., 1999). Indeed, as β-pleated assemblies are more hydrophobic than native proteins, the hydrophobic environment of white matter may thus favor their retention in the corpus callosum.

However, human APP is not produced in the corpus callosum in our models. We observed that plaque size was reduced in regions adjacent to the corpus callosum and inversely

correlated with callosal β-amyloidosis and β-amyloidosis acceleration in the CA1, the inoculated structure (**Figure 43**). This could suggest that monomeric Aβ diffused from their production site towards the corpus callosum. The current view for Aβ prion-like mechanisms is that Aβ seeds propagate into the brain leading to seeding in remote regions. Here, we hypothesize that soluble Aβ may be attracted to regions where seeding effects are higher, leading to a decrease in amyloid plaque size in the regions of origin. Also, based on the theoretical models for amyloid plaque formation, in particular the critical concentration parameter (Burgold et al., 2014), we hypothesize that such local reorganization (decreased plaque size) could be linked to a leak of monomeric Aβ leading to a decrease of local Aβ concentration limiting amyloid plaque growth.

5.4.4. β-amyloid strain effect

An important characteristic of prions is their ability to propagate specific misconformations leading to specific clinical presentations ("strain" phenomenon). It has been proposed that Aβ might also present in different strains (Petkova, 2005). Little is known about Aβ strains in AD patients and Aβ deposit morphology in humans seems to depend more on their maturation over time and regional localization than upon a strain effect (Eisele and Duyckaerts, 2016). Still, different Aβ conformations could account for intra- and inter-individual polymorphic presentation of AD, both in histopathological and clinical phenotypes (Heilbronner et al., 2013). To investigate this question, we inoculated homogenates from two different AD patients (**Figure 33** and **Figure 34**). One presented with CAA and the other did not (**Table 2**) and, accordingly, they differed in terms of $A\beta_{1\text{-}40}$ levels **(Figure 34A)**. In $APP_{Swe}PS1_{\Delta E9}$ inoculated mice, we did not observe any difference in Aβ deposit distribution and morphology nor in the amount of amyloid plaques or CAA between mice inoculated with one AD patient or the other. Similarly, no differences were seen between AD-inoculated AAV-APP/PS1 mice as similar localization, morphology and incidence were observed.

Our observations do not support a strain effect between our two samples despite the difference in $A\beta_{1\text{-}40}$ levels and Aβ lesion morphology of the human samples. In the literature, to our knowledge, only Arctic AD patient homogenates led to a specific CAA endophenotype in mice whereas sporadic and Swedish AD patient homogenates induced similar lesions (Watts et al., 2014). As the APP Arctic mutation (E693G) is inside the Aβ sequence (E22G) and results in an atypical AD pathology (Philipson et al., 2012), this may suggest that Aβ strains in AD patients rely more on mutated Aβ peptides with an alternative folding able to

self-propagate to wild-type peptides. Compared to PrP, wild-type Aβ may present with less conformational flexibility and thus less strain effect.

The observed diminution in plaque size observed in the retrosplenial cortex and the subiculum in AD- as compared to CTRL- inoculated $APP_{Swe}PS1_{\Delta E9}$ may reflect a strain effect common to both AD patients and different from $APP_{Swe}PS1_{\Delta E9}$ mice (**Figure 43 A-B**). This reduced size could be linked to the contraction of plaques in these regions leading to more mature compact plaques. However, the fact that CA1 was less impacted (non-significant decrease) than remote regions is inconsistent with this hypothesis. One proposition could be that spontaneous β-amyloidosis is less important in the CA1 than in the subiculum and retrosplenial cortex and therefore, compaction of amyloid plaques could be slower. This strain hypothesis will require further evaluation.

5.4.5. β-amyloid spreading

Finally, following seeding experiments *in vivo*, time-dependent spreading of Aβ deposition from the injected structure to other regions was reported in various transgenic mouse strains (Hamaguchi et al., 2012; Kane et al., 2000; Meyer-Luehmann et al., 2006; Stöhr et al., 2012; Walker et al., 2002). Aβ spreading has been proposed to occur by various mechanisms including dissemination along neuroanatomic connections.

In our two models, we investigated the spreading from the inoculated structure to anatomically connected regions. In $APP_{Swe}PS1_{\Delta E9}$ no spreading was detected (**Figure 37**). Two hypotheses can be proposed to explain this lack of spreading. (1) Spreading has been described to be a time-dependent process. Here, we only detected seeding in the inoculated structure at 16 weeks post-inoculation (**Figure 37B**). As spreading is only observed after a robust acceleration in the inoculated structure, performing longer time-points may allow observing spreading in $APP_{Swe}PS1_{\Delta E9}$. (2) $APP_{Swe}PS1_{\Delta E9}$ is an early-depositing model and spontaneous aggregation may therefore be already too robust in the receiving structures for additional Aβ seeds to spread β-amyloidosis acceleration. Further experiments will be needed to conclude on Aβ spreading in this model. In the AAV model, no spreading was observed. Indeed, Aβ deposition was only observed in the dorsal hippocampus. Two hypotheses can also be proposed. (1) First, like in $APP_{Swe}PS1_{\Delta E9}$ mice, spreading should be investigated at later time-points. (2) Second, as APP is only expressed in the dorsal hippocampus in this model (Audrain et al., 2016), it suggests that APP expression is mandatory for Aβ spreading.

It has been recently shown that Tau can spread from neuron-to-neuron even in the absence of Tau expression in the receiving region (Wegmann et al., 2015). Here, our results suggest that Aβ cannot spread without human APP being expressed in the receiving structure (**Figure 47**).

In conclusion, our results, along with previous ones, show that β-amyloidosis can be transmitted *in vivo* in a prion-like manner. Such transmission is achieved by the introduction of Aβ seeds in a susceptible model expressing a similar aminoacid sequence of Aβ, as human APP expression seems to be required for both Aβ seeding and spreading. Overall, our results support the prion-like hypothesis of Aβ.

In these experiments, we evaluated if β-amyloidosis could be transmitted in vivo in a prion-like manner. We performed experimental transmission of β-amyloidosis in two different amyloidogenic models.

First, we showed that intracerebral inoculation of AD brain homogenates leads to Aβ seeding in both models whereas inoculation of an aged-matched control individual homogenate failed to accelerate β-amyloidosis. Then, we demonstrated that the "host" was a determinant modulator for β-amyloidosis experimental transmission as we observed difference in seeding in our two models. Furthermore, we observed intracallosal Aβ deposition and suggest that it could be a specific pathologic signature for Aβ intracerebral seeding in mice. Additionally, we did not find any phenotypic differences between our two AD patients, suggesting that they do not present with different Aβ strains. Finally, we suggest that APP expression is mandatory for Aβ spreading contrary to Tau protein. Overall, we conclude that our experiments support the prion-like hypothesis of Aβ.

Several questions remain to be answered for the prion-like hypothesis of Aβ. There is no evidence that AD is transmissible to humans and the origin of the formation of the first Aβ seeds remains to be investigated. Additionally, very little is known about Aβ spreading mechanisms although many hypotheses have been proposed. The identification of Aβ seed structures is also necessary to better understand these mechanisms and decipher their impacts on various brain functions. Finally, until now, very few studies evaluated the impact of AD experimental transmission on brain functions.

Chapter VI – Mouse lemur model characterization

6.1. Introduction

Aging is a natural process modifying organism's structure and functions. It ineluctably leads to functional decline of different systems such as the nervous system. In humans, normal cerebral aging is associated with atrophy (Chui et al., 1984; Lowes-Hummel et al., 1989; Petersen et al., 2000; Salat et al., 2004).

Cerebral atrophy is more prominent in AD than in normal aging, especially in temporal regions such as the hippocampus or the entorhinal cortex (Jack et al., 1998) or the central cholinergic system (Teipel et al., 2005). Rodent models are most commonly used for physiological and pathological aging research. These models generally do not display cerebral atrophy while aging, and even show cerebral growth. For example, classical rodent AD models mostly do not reproduce the typical pattern of cerebral atrophy observed in patients (Maheswaran et al., 2009).

Non-human primates (NHP) present with cerebral age-related changes (Andersen et al., 1999; Dhenain et al., 2000). The mouse lemur is a useful model of age-related cerebral atrophy as it is the only primate in which a link between cerebral atrophy and cognitive alterations has been found (Picq et al., 2012). Several studies were performed to characterize cerebral atrophy in mouse lemurs using manual segmentation, scoring or automatized analysis of MR images (Dhenain et al., 2000, 2003; Kraska et al., 2011; Picq et al., 2012; Sawiak et al., 2014). Here, we further characterized the effect of age on cerebral atrophy using MR images acquired on a 7 Tesla scanner, offering a better spatial resolution, and voxel-based morphometry (VBM) automated processing.

In humans, aging is also the most important risk-factor for neurodegenerative diseases such as AD. AD is characterized by the accumulation of abnormal Aβ and Tau proteins in the brain. Old NHP are used as spontaneous models of AD. In mouse lemurs, abnormal accumulations of Aβ and hyperphosphorylated Tau proteins while aging have been reported in some animals. Most studies of AD-related lesions in mouse lemurs were performed on paraffin-embedded tissues (Giannakopoulos et al., 1997; Kraska et al., 2011), here we developed free-floating immunohistochemistry protocols to further characterize Aβ and Tau pathologies related to

aging. Indeed, this technic is more permissive, notably for stereological analysis, and allows a cost-effective evaluation of the entire brain.

6.2. Materials and methods

6.2.1. Ethic statement

All animal experiments were conducted in accordance with the European Communities Council Directive (2010/63/UE). Animal care was in accordance with institutional guidelines and experimental procedures were approved by local ethic committees (authorizations 12-089; ethic committee CETEA-CEA DSV IdF). Critical ethic limit points were defined as one or more of the following observations: suffering signs, prostration signs or general state degradation approved by the local veterinary. Weight loss was not considered as reliable criterion as mouse lemur's weight varies a lot both between weeks and seasons.

6.2.2. MRI study

6.2.2.1. Animals

24 male and female mouse lemurs aged from 1 to 9 year-old were included in this study (6.35±2.4 years). They were all born in a laboratory breeding colony (UMR 7179 CNRS/MNHN, France; European Institutions Agreement #962773) and bred in our laboratory (Commissariat à l'Energie Atomique, centre de Fontenay-aux-roses; European Institutions Agreement #B92-032-02). Conditions of captivity were maintained under constant temperature of 24–26°C and relative humidity of 55%. Animals were housed in individual cages with jumping and hiding enrichment. Seasonal enlightenment (summer: 14 hours of light/10 hours of dark; winter: 10 hours of light/14 hours of dark) was applied with respect to the seasonal rhythm of the animals. Food consisted of fresh apple and a homemade mixture of banana, cereals, eggs and milk. Animals had free access to tap water. None of the animals has been previously involved in pharmacological trials or invasive studies.

6.2.2.2. Anatomic Magnetic Resonance Imaging

Principles of Magnetic Resonance Imaging

MRI is based on the phenomenon of nuclear magnetic resonance. The atom nucleus is made of nucleons (neutrons and protons) animated by axial rotation movements or "spin". A

rotating load induces a local magnetic field around it, named the magnetic moment, which is linked to the spin. Protons and neutrons magnetic moments can cancel each other by pairing. Therefore, only atoms with impaired nucleons, such as hydrogen, have magnetic properties. As hydrogen represents the majority of an organism's atoms, its properties are exploited in structural MRI. In the absence of external magnetic field, magnetic moments are randomly oriented leading to a null sum of these moments. However, when an external magnetic field is applied, magnetic moments of atoms are oriented parallel or anti-parallel to the magnetic field. The difference between parallel and anti-parallel magnetic moments creates a macroscopic magnetization that depends on the external magnetic field. However, this magnetization *per se* is not detectable directly as it is aligned with the external magnetic field. To detect it, it is mandatory to induce a modification of its orientation that allows detecting its return to equilibrium. Such modification can be achieved by stimulation by a radiofrequency wave. When the radiofrequency is applied, it leads to a modification of the orientation of the macroscopic magnetization. When its stops, the macroscopic magnetization returns to its initial orientation, aligned with the external magnetic field, and relaxation phenomena occur (namely T1 and T2). These relaxation phenomena are responsible for the signal detected in MRI and are dependent on the properties of the different tissues allowing for example to differentiate fat- and water-enriched tissues.

Depending on the weight of each relaxation phenomenon in an anatomical MRI sequence, it allows to visualize differently the tissues differing on its water and fat proportions. For example, in T1-weighted images, fat is light-colored (hyper-intense) and water is dark-colored (hypo-intense). Distinctively, T2-weighted contrast allows water to appear hyper-intense whereas fat appears a little bit darker. Therefore, T2-weighted contrast leads to CSF to appear in light-white, gray matter in light-gray and white matter in dark gray. Such contrast is very interesting for atrophy studies as CSF is very easily visualized.

Magnetic Resonance Imaging in mouse lemurs

Anatomical MRI was performed using T2-weighted spin-echo images recorded on a 7T spectrometer (Agilent, USA; TR=10000ms, TE=17.4ms, slice thickness=230µm, field of view=29.4x29.4mm^2, matrix=128x128, resolution=230x230µm^2 zero-filled to 115x115µm^2). Animals were fasted the day before MRI. Pre-anesthesia (atropine, 0.025mg/kg, subcutaneous injection) was performed 30 minutes before anesthesia (Isoflurane,Vetflurane,4.5% for

induction and 1–2% for maintenance)(Dhenain et al., 2003). Respiration rate was monitored and body temperature was maintained at 37±0.5°C with an air-heating system during all MRI.

Voxel-based morphometry

Voxel-based morphometry (VBM) is an unbiased whole-brain technique for the analysis of anatomic MR images. In this study, we assessed the evolution of gray matter in the brain as a function of age in a statistical manner. MR images were analyzed using VBM thanks to SPM8 (Wellcome Trust Institute of Neurology, University College London, UK, (http://www.fil.ion.ucl.ac.uk/spm) software with the SPMMouse toolbox (http://spmmouse.org) as described previously (Sawiak et al., 2014). Briefly, brain images were segmented into gray (GM) and white matter (WM) tissue probability maps using in-house developed priors, then spatially transformed to the standard space using a GM mouse-lemur template. Affine regularization was set for an average-sized template, with a bias non-uniformity cut-off at a full width at half maximum (FWHM) of 10mm, a 5mm basis-function cut-off and a sampling distance of 0.3mm. The resulting GM and WM portions were output in rigid template space and DARTEL (Ashburner, 2007) was used to create non-linearly registered maps for each subject and common templates for the cohort of animals. The warped GM portions for each subject were modulated with the Jacobian determinant from the DARTEL registration fields to preserve tissue amounts (‘optimized VBM’) (Good et al., 2001) and smoothed with a Gaussian kernel of 600µm to produce maps for analysis (Sawiak et al., 2014). A general linear model was designed based on multiple regressions to evaluate relative changes in GM values as a function of age. Total intracranial volumes and sex were taken as covariates of no interest. To control for multiple comparisons, an adjusted p-value was calculated using the voxel-wise false discovery rate (FDR) $q<0.05$ with extent threshold values of 10 voxels (Genovese et al., 2002). Voxels with a modulated GM value below 0.2 were not considered for statistical analysis.

6.2.3. Histology

Another cohort of 25 male and female mouse lemurs aged from 1 to 11 (7.2±2.9 years) were euthanized with an overdose of sodium pentobarbital (100 mg/kg intraperitoneally). After overnight post-fixation with 4% paraformaldehyde in PBS, brains were cryoprotected using overnight 15% and 30% sucrose solutions. 40µm-thick coronal sections of brains were cut on a microtome (SM2400, Leica Microsytem, Wetzlar, Germany) and floating histological serial

sections were preserved in a storage solution (glycerol 30%, ethylene glycol 30%, distilled water 30% and phosphate buffer 10%) until use.

Serial sections of the entire brains were used for β-amyloid (4G8) and Tau (AT8 and AT100) immunohistochemistry. AT8 antibody binds to a phospho-epitope of Tau that is phosphorylated in physiological conditions and hyperphosphorylated in pathological conditions such as AD. AT100 antibody is supposed to bind to another phospho-epitope more specific of PHFs. Free-floating sections were rinsed in PBS 0.1M and then incubated with hydrogen peroxide 0.3% for 20min. Human sections were used as positive controls. Negative controls were performed for each group by the omission of the primary or secondary antibody. For 4G8 staining, 80% formic acid pretreatment was applied for 2 min. Pretreatment with PBS-Triton 0.5% (Triton X-100, Sigma Aldrich, MO, USA) and 3% Bovine Serum Albumin (BSA) blocking was performed before a 2-day incubation at +4°C with either biotinylated 4G8 (Covance, NJ, USA, 1/250), $A\beta_{1-42}$ (Life Technologies, Carlsbad, CA, USA, 1/500), AT8 (Pierce endogen, IL, USA, 1/100), or AT100 (Pierce endogen, IL, USA, 1/100). Secondary antibodies, biotinylated anti-mouse or anti-rabbit IgG (Vector Laboratories, Burlingame, CA, USA), were incubated for 1 hour at +4°C before revelation. ABC Vectastain kit (Vector Laboratories, Burlingame, CA, USA) was used to amplify DAB revelation (DAB SK4100 kit, Vector Laboratories, Burlingame, CA, USA). Stained sections were analyzed by two operators blinded to the age of the animals.

6.3. Results

6.3.1. Age-related cerebral atrophy

MR images were acquired in 24 mouse lemurs aged from 1 to 9 year-old (6.35±2.4 years). VBM morphometry analysis was performed in order to extract the global effect of age upon GM evolution (**Figure 48A**). As it neglects individual effects in favor of global evolution, we can suggest that this analysis reflects the physiological evolution of GM during aging. GM decrease as a function of age massively affected cortical areas belonging to the parietal lobe, the posterior cingulate cortex and non-cortical structures (the basal nucleus of Meynert and the anterior hypothalamus) (**Figure 48B-C**, black). The retrosplenial cortex as well as the frontal lobe were only partially affected (**Figure 48B-C**, dark gray). The temporal and occipital lobes (**Figure 48B-C**, light gray) were mostly preserved as well as other non-cortical structures such as the hippocampus or the caudate nucleus.

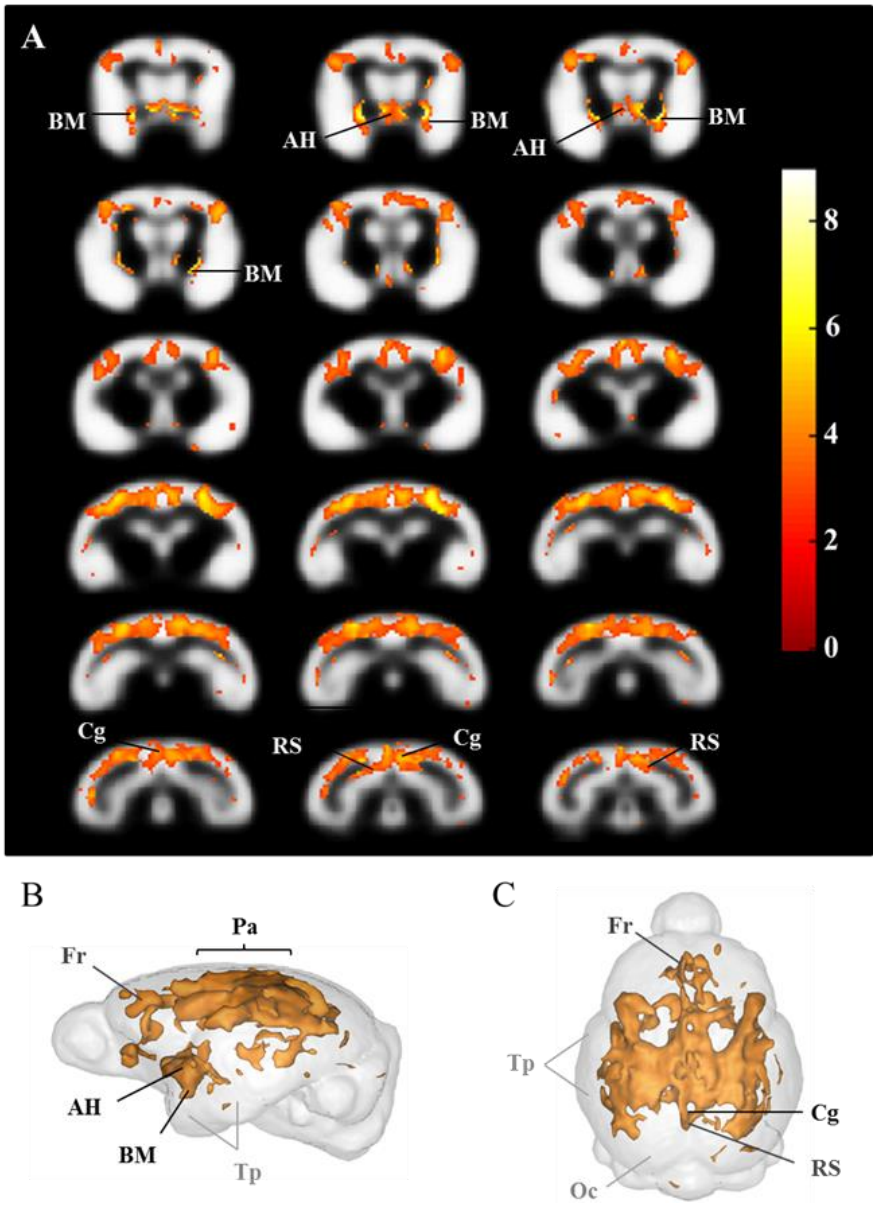

Figure 48. **Physiological aging does not induce gray matter loss in the temporal lobe.** A. Statistical heatmap of T values indicating the significant clusters in which GM probability diminishes as a function of age (FDR correction p-value=0.05, Voxel threshold k extent=10). BM: nucleus basalis of Meynert, AH: anterior hypothalamus, Cg: posterior cingulate cortex, RS: retrosplenial cortex. B. 3D side view of the significant clusters (A) showing a massive age-related diminution of GM probability in the parietal (Pa) lobe, the AH and BM (black) whereas the frontal (Fr) lobe is partially affected (dark gray) and the temporal (Tp) lobe (light gray) is mostly preserved. C. 3D upper view of the significant clusters (A) showing an important age-related diminution of GM probability in the Cg (black) whereas the RS is only affected in its dorsal part and the Tp and occipital (Oc) lobes are mainly preserved.

6.3.2. Aβ and Tau pathologies in aged mouse lemurs

We developed free-floating immunohistochemistry for Aβ and Tau staining in mouse lemurs to characterize the incidence of Aβ and Tau pathologies in the mouse lemur.

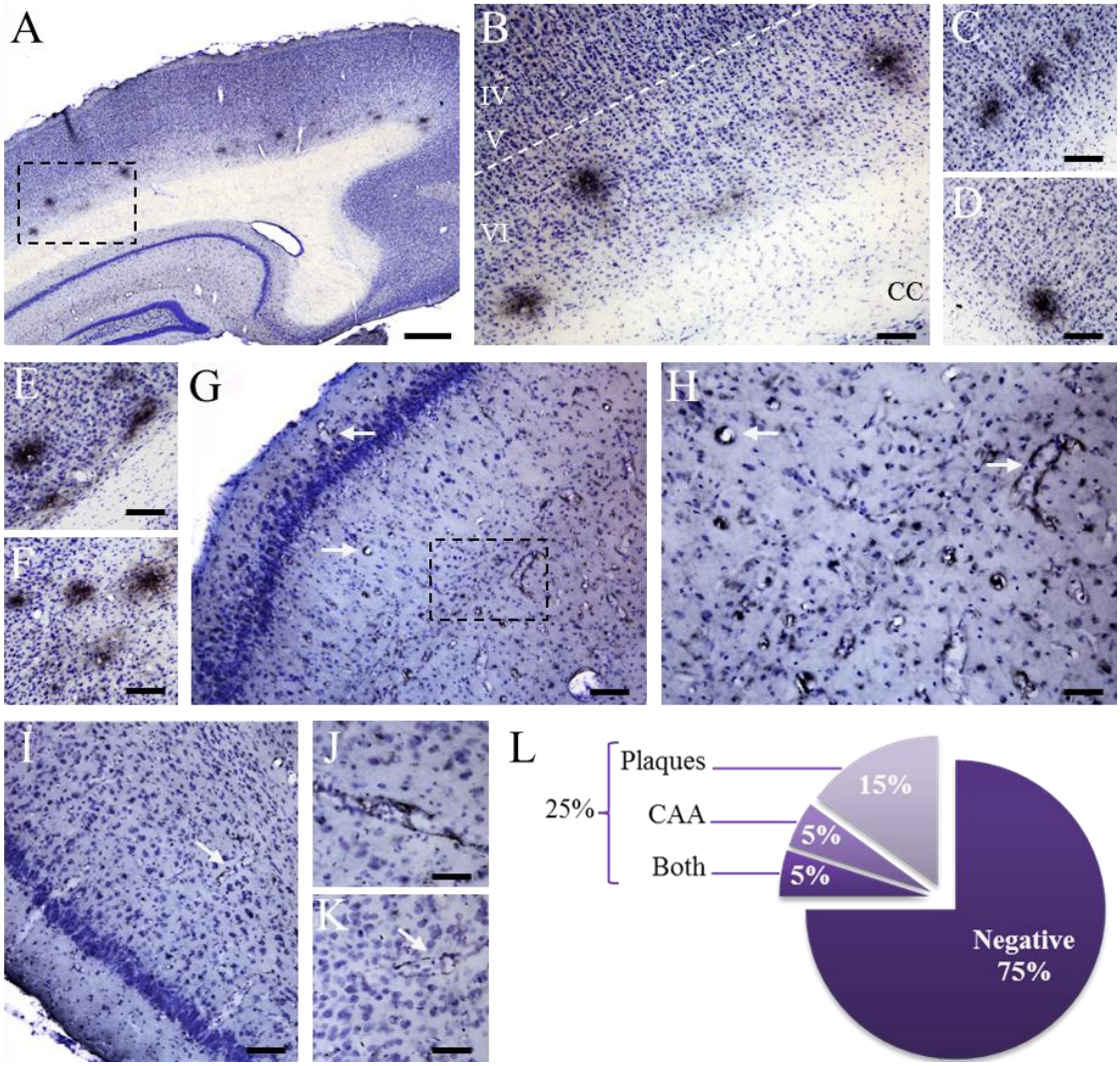

Figure 49. **β-amyloidosis in aged mouse lemurs (>6 years-old).** A. Amyloid plaques in the parietal and superior temporal cortex. B. High-magnification photomicrograph of the boxed area in panel A showing amyloid plaques in the layer VI of the superior temporal cortex. C-D. Amyloid plaques in the parietal cortex. E-F. Amyloid plaques in the occipital cortex. G. CAA in the ventral hippocampus. H. High-magnification photomicrograph of the boxed area in panel G showing CAA in the small vessels. I. CAA in the inferior temporal cortex. J. Small vessel CAA in the amygdala. K. Small vessel CAA in the parietal cortex. L. Proportion of aged lemurs (>6year-old) with amyloid plaques and/or CAA. White arrows indicate 4G8-immunoreactive vessels. Scale bars: 500µm (A); 100µm (B-G; I); 50µm (H-J; K).

We evaluated Aβ lesions presence, morphology and localization in 5 young (1 to 3 years) and 20 old (6 to 11 years) mouse lemurs. We did not observe any Aβ lesions in any of the young animals. We detected amyloid plaques in the frontal, parietal, temporal superior and/or occipital cortices of 4 out of 20 mouse lemurs older than 6 years (**Table 4**). Interestingly, amyloid plaques were always diffuse and localized in deep cortical layers (**Figure 49A-F**). We also detected CAA, mostly in the small vessels, in the cortex, the hippocampus and/or the amygdala of 2 out of 20 aged mouse lemurs (**Figure 49G-K**, **Table 4**). Only one aged mouse lemur presented with both types of Aβ lesions. In summary, 5 out of 20 aged mouse lemurs (25%) exhibited parenchymal and/or vascular Aβ lesions (**Figure 49L**).

Age	CAA	Amyloid plaque localization
7	-	Parietal, temporal superior and occipital cortex
7	+	-
8	-	Temporal superior cortex
8	-	Fronto-parietal cortex
9.5	+	Parietal, temporal superior and occipital cortex

Table 4. **Localization of amyloid plaques and presence of cerebral amyloid angiopathy in the brain of aged mouse lemurs.** CAA: cerebral amyloid angiopathy. Age is indicated in years. Presence is marked +, absence is marked -.

We then analyzed Tau pathology using AT8 and AT100 antibodies in 3 young (1 to 2 years old) and 14 aged (6 to 9.75 years old) mouse lemurs. We did not detect any Tau lesions in any of the 3 young animals. In 4 out of 14 mouse lemurs older than 6 years old (28.6%), AT8-immunoreactive Tau missorting to the soma and dendrites of neurons was observed in the frontal, parietal, temporal, including the entorhinal, and occipital cortices (**Figure 50C-E**, **Table 5**). In one animal, specific cortical and subcortical regions were spared as compared to the other positive animals (**Table 5**). Interestingly, in all animals, AT8-immunoreactive somas were mostly detected in the outer layers of the cortex (II-IV) and almost never in the inner layers (V-VI). Also, AT8-immunoreactive Tau missorting was detected in the hippocampus (**Figure 50A-B**), the amygdala (**Figure 50C**), septal nuclei, medial thalamus and/or hypothalamus. However, no staining was observed with AT100 antibody either in young or old animals and no neuritic plaques were observed.

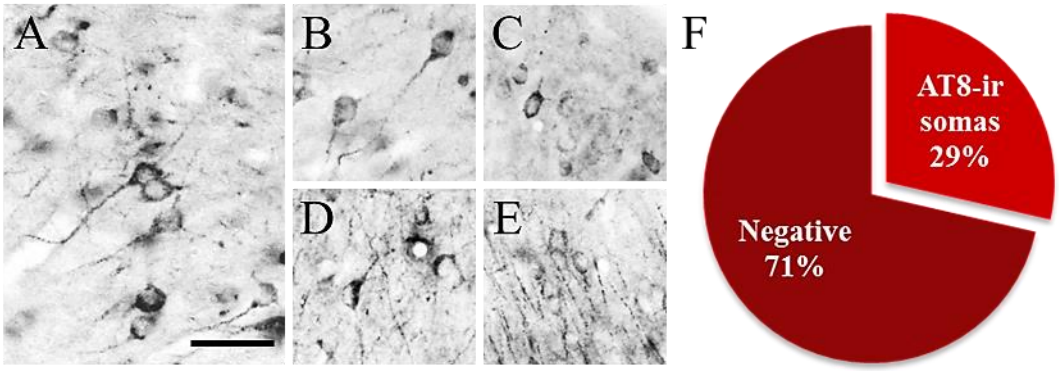

Figure 50. **Tau pathology in aged mouse lemurs (>6 years-old).** A-E. Examples of AT8-immunoreactive somas in the hippocampus (A-B), temporal superior cortex (C), amygdala (D) and entorhinal cortex (E). F. Percentage of animals presenting with AT8-immunoreactive somas. Scale bar: 50µm.

Age	AC	PC	RS	EC	CA	DG	S	NS	Am
7	+	+	+	+	-	+	-	+	+
8	+	+	+	+	-	+	-	+	+
9	-	-	-	+	-	+	-	-	-
9.5	+	+	+	+	+	+	+	+	+

Table 5. **Differential localization of AT8-immunoreactive somas in aged mouse lemurs.** AT8-immunoreactive somas were detected in every lobe of the brain but some specific cortices (cingulate and retrosplenial) as well as subcortical structures could be affected differentially in aged mouse lemurs. Presence of AT8-immunoreactive somas is marked +, absence is marked -. AC: Anterior Cingulate cortex; PC: Posterior Cingulate cortex; RS: Retrosplenial cortex; EC: Entorhinal Cortex; CA: Ammon's Horn; DG: dentate gyrus; S: subiculum; NS: nuclei septali; Am: Amygdala.

Finally, only two aged animal presented with Aβ and hyperphosphorylated Tau pathologies representing 14.3% of all aged animals and 28.6% of animals affected by Aβ and/or Tau pathologies.

6.4. Discussion

In this study, we aimed to investigate both physiological and pathological aging in mouse lemurs focusing on the characterization of physiological cerebral atrophy and pathological deposition of Aβ and Tau proteins.

6.4.1. Aging is associated to physiological cerebral atrophy in mouse lemurs

First, we evaluated cerebral atrophy in a cohort of 24 mouse lemurs aged from 1 to 9 year-old (6.35±2.4 years) using VBM analysis to highlight the pattern of cerebral physiological aging of mouse lemurs.

In humans, aging leads to a global loss of cerebral volume (Fjell et al., 2009). Age-related cortical atrophy mostly involves the frontal and parietal lobes (Driscoll et al., 2009; Salat et al., 2004). In our study, we observe an age-related atrophy involving mainly the parietal whereas the frontal lobe was only partially affected (**Figure 48**). However, the anterior cingulate cortex, one of the most impacted cortices in humans (Salat et al., 2004), was also impacted in mouse lemurs during aging. Concerning subcortical structures, the basal nucleus of Meynert was impacted by age-related atrophy in mouse lemurs. The basal nucleus of Meynert is a cholinergic structure of the basal forebrain that is affected by atrophy in both normal and pathological (MCI and AD) aging (Grothe et al., 2014; Wolf et al., 2014) as well as in macaques during aging (Smith et al., 2004).

Our results are mostly consistent with a previous study using VBM in mouse lemurs (Sawiak et al., 2014). GM loss was more widespread in this previous study and differences in the involvement of the prefrontal, superior temporal and occipital cortices as well as the caudate nucleus were observed. Most aged mouse lemurs do not display excessive atrophy while aging whereas others present with an abnormal pattern of cerebral atrophy indicative of a pathological process (Kraska et al., 2011). In the present study, no aged mouse lemur presented with high cerebral atrophy. The observed discrepancy between the two VBM studies may rely on the number and population of mouse lemurs used in the two studies as well as on MRI acquisition and processing. The atrophy pattern presented here confirmed most of the cortical and subcortical regions previously detected as being part of the physiological cerebral aging.

Atrophy of the temporal lobe has been described in a subset of aged mouse lemurs (Kraska et al., 2011) and, in particular, atrophy of the entorhinal cortex correlates with spatial memory impairments (Picq et al., 2012). In comparison to pathological aging, the temporal cortex is preserved during aging, as observed in both VBM studies carried out on mouse lemurs by our team. Such preservation is similar to what had been observed in human physiological aging

(Driscoll et al., 2009; Salat et al., 2004). Here, we further confirmed that the temporal lobe is not affected by atrophy during the physiological aging process in mouse lemurs.

With respect to the hippocampus, atrophy also correlates with spatial memory impairments (Picq et al., 2012). Here, during physiological aging, no atrophy was detected in this structure. Our results are also consistent with other primate studies in which hippocampal atrophy is not associated with physiological aging (Shamy et al., 2006). Although impacted by atrophy during aging (Golomb et al., 1993; Jack et al., 1997), the hippocampus is relatively spared in human normal aging as compared to other regions (Hsu et al., 2002). Our results further suggest that both the temporal lobe and the hippocampus are preserved during physiological aging in mouse lemurs.

Here we described the atrophy pattern of physiological aging of mouse lemurs. With respect to cerebral atrophy during human aging, mouse lemurs present with good face and construct validity thus representing interesting models for human cerebral aging and testing interventional strategies (Pifferi et al., 2016). Characterizing physiological aging is also crucial for deciphering and understanding the impacts of pathological processes on cerebral atrophy. For example, most mouse lemurs do not present cognitive alterations while aging and physiological aging mostly spares the temporal lobe and the hippocampus. Along with previous studies, our results suggest a major role for atrophy of these structures in pathological aging processes.

6.4.2. Aging leads to AD-related neuropathological lesions in mouse lemurs

There has been longstanding interest as to whether AD-related pathology could develop in the brain of aged animals. In this project, we aimed to evaluate pathological aging focusing on the identification of AD-related histopathological lesions in another cohort of mouse lemurs.

Although Aβ and Tau pathologies have been described in mouse lemurs before, almost all studies were performed in separated cohorts. Such AD-like pathological changes have been reported to affect about 20% of old mouse lemurs (Bons et al., 1992). Here we determined that Aβ and Tau lesions can be detected in 25 to 29%, respectively (**Figure 49L**, **Figure 50F**), of mouse lemurs older than 6 years and we also showed that these pathologies are not usually concomitant (28.6%).

Contrary to previous studies (Bons et al., 1992, 1994; Giannakopoulos et al., 1997; Mestre-Francés et al., 2000), we detected only diffuse amyloid plaques in the cortex of aged mouse lemurs (**Figure 49**). With the exception of the inferior temporal cortex, all cortices were involved with predominance for parietal, temporal superior and occipital cortices. Interestingly, amyloid plaques were restricted to the deep cortical layers. CAA was less frequent than previously described affecting only 10% of aged mouse lemurs (**Figure 49L**). It mostly involved small vessels with large vessels being generally spared. This is consistent with the observation that, in humans, small vessel CAA is associated with ApoEε4 as mouse lemurs are homozygous for ApoEε4.

It has been suggested that old mouse lemurs' is similar to humans' β-amyloidosis (Bons and Mestre, 1993). Here, we did not confirm this result as we found parenchymal β-amyloidosis in mouse lemurs to be sparse and only present as diffuse deposits. Also, we found CAA to be less frequent than in humans and to present mostly in small vessels (**Figure 49F**).

Our results will have to be confirmed in a larger cohort that is currently undertaken. Other markers will be examined to identify Aβ peptides proportions and amyloid dye binding properties of Aβ deposits in aged mouse lemurs. Also, a larger cohort may allow deciphering the pattern of Aβ deposition in the brain.

Aged mouse lemurs were sometimes reported to present a rare tauopathy (Giannakopoulos et al., 1997; Kraska et al., 2011). Here, we found AT8-positive neurons only in aged animals (29%) and never in young animals (**Figure 50**). AT8-positive somas were detected in all cortices with predominance in the temporal lobe and in particular the entorhinal cortex. The hippocampal formation was mostly spared with the exception of the dentate gyrus. This observation is in accordance with the spreading hypothesis of Tau along neuroanatomic connections as AT8-positive somas were predominantly found in the layer II and III of the entorhinal cortex that are heavily connected to the dentate gyrus (**Table 5**).

Interestingly, as in humans, Tau pathology distribution (**Table 5**) seems to match the pathological atrophy reported in mouse lemurs (Picq et al., 2012). Indeed, atrophy of the entorhinal cortex is not observed during physiological aging (**Figure 48**) but correlates with cognitive deficits suggesting a pathological process specific of some mouse lemurs (Picq et al., 2012). Therefore, as the entorhinal cortex is strongly affected by Tau pathology in some aged mouse lemurs, spared by Aβ pathology and seems to be atrophied only during

pathological aging, we hypothesize that atrophy might be related to Tau pathology in lemurs. Based on this hypothesis, we are currently performing a study aiming to evaluate the relationship between cerebral atrophy, cognitive alterations and Aβ and Tau lesion distribution. In particular, 3D immunohistology is being performed in order to spatially correlate Aβ and Tau lesions with atrophy occurrence.

Tau pathology in mouse lemurs does not seem to involve neuritic plaques and NFTs (**Figure 50**). Also, we observed that AT8-positive hyperphosphorylated Tau was not stained by AT100 antibodies suggesting that accumulated Tau is not hyperphosphorylated at the AT100 epitope contrary to human pathology. Further evaluation will be necessary to fully characterize Tau pathology in mouse lemurs including the use of conformational antibodies and amyloid dyes.

AT8-positive somas were predominantly detected in the temporal lobe that was not affected by amyloid plaques. Also, this pathology was mostly found in the superficial layers of the cortex whereas amyloid plaques were restricted to the deep layers. This result suggests that Aβ and Tau pathology do not overlap in mouse lemurs. This observation is further reinforced by the fact that these pathologies are only concomitant in 28.6% of affected aged lemurs and, similarly to previous studies (Giannakopoulos et al., 1997), no correlation was established between β-amyloidosis and Tau pathology in aged mouse lemurs.

Differential selective vulnerability of neuronal populations has been proposed to explain the spatiotemporal distribution of Aβ and Tau pathology (Miller et al., 2013). Very recently, it was proposed that regional vulnerability to AD pathology could be explained by the differential expression of pro- or anti-aggregation genes (Freer et al., 2016). Investigating such gene expression profiles in mouse lemurs could provide some insights on both distribution and relative resistance of mouse lemurs to Aβ and Tau pathologies, as compared to humans.

The lack of animal models closely reproducing the endophenotypes of AD is a major obstacle to the understanding of the pathogenesis of the disease. If animals have never been shown to develop AD, Aβ deposits have been found in aged animals from various species including dogs and nonhuman primates (Cummings et al., 1996; Elfenbein et al., 2007; Kimura et al., 2003; Lemere et al., 2008; Maclean et al., 2000; Mestre-Francés et al., 2000; Struble et al., 1985).

With age, nonhuman primates develop parenchymal and/or vascular Aβ lesions but this β-amyloidosis is generally sparser than the one observed in humans. Also, NFTs, as found in humans, are unusual in primates including mouse lemurs. It has been suggested that insoluble aggregates of Tau may occur specifically in human neurons but do not form in the neurons of nonhuman primates (Selkoe et al., 1987). Until now, NFTs have only been found in baboons and gorillas and were not yet observed in other primate species (Kimura et al., 2003; Perez et al., 2016; Schultz et al., 2000) suggesting that nonhuman primates may present a relative resistance to Tau pathology (Heuer et al., 2012).

Mouse lemur aging can be separated into physiological and pathological aging. Here, we characterized the pattern of physiological age-related cerebral atrophy that, contrary to pathological aging, does not involve the temporal lobe.

We also further characterized AD-related histopathological lesions in mouse lemurs. A subset of aged mouse lemurs presents with parenchymal and vascular Aβ lesions and/or hyperphosphorylated Tau lesions. However, as other primates, they show a relative resistance to both pathologies that do not resemble the massive lesions observed in humans.

As a conclusion, our data, along with others, suggest that mouse lemurs are interesting models for cerebral aging and AD pathology although, as all nonhuman primates, they present with limitations as far as the intensity of the pathology is concerned. Further evaluation of the differences between afflicted aged primates and AD patients could help better understanding why AD is a human specific disease.

Chapter VII – Experimental transmission of Alzheimer's disease endophenotypes to primates

7.1. Introduction

There has been longstanding interest as to whether Alzheimer's disease (AD) might be transmissible (Goudsmit et al., 1980). In humans, patients exposed to cadaver-derived hormones or dura mater grafts presumably contaminated with Aβ have higher risk to develop early-onset Aβ pathology than non-exposed subjects (Frontzek et al., 2016; Jaunmuktane et al., 2015; Kovacs et al., 2016; Preusser et al., 2006).

Experimental transmission of β-amyloidosis or tauopathy has been described in rodents after intracerebral, and even peripheral, inoculation with AD brain homogenates suggesting prion-like mechanisms (Clavaguera et al., 2009, 2014, Eisele et al., 2009, 2010; Meyer-Luehmann et al., 2006). Although non-human aged primates can naturally develop Aβ lesions (Heuer et al., 2012), experimental transmission of AD to various primate species ranging from chimpanzee to marmoset was inconclusive (Brown et al., 1994; Goudsmit et al., 1980). Only one long term study in marmosets revealed the induction of sparse amyloidosis 3.5 to 7 years after intracerebral inoculation with AD brain homogenates but no Tau lesions were reported (Baker et al., 1993, 1994; Maclean et al., 2000; Ridley et al., 2006).

Also, whether the "pathogenic spread" of AD-related proteins causes AD symptom onset remains uncertain (Walsh and Selkoe, 2016). None of the transmission studies with Aβ or Tau inocula provided evidence for pronounced cognitive decline or neurodegeneration (Beekes et al., 2014) although only very few experiments studied the functional impact of experimental transmission. In prion diseases, experimental transmission is achieved in primates and leads to clinical symptoms (Brown et al., 1994; Gajdusek et al., 1967, 1968; Gibbs et al., 1968a). Such questions remain to be answered for AD.

As for prion diseases, experimental transmission of AD can only be performed in susceptible models. Aged mouse lemurs can develop most of AD endophenotypes including β-amyloidosis, Tau hyperphosphorylation, cerebral atrophy, and, cognitive deficits. Also, only a very small subset of aged (>6 year-old) mouse lemurs have been shown to present with these alterations contrarily to transgenic models that systematically develop AD-related lesions. Therefore, mouse lemur characteristics (for example, complete homology of Aβ sequence

with human's sequence) allow the study of experimental transmission in a context closer to sporadic human pathology than in transgenic mice.

Therefore, the mouse lemur seems to be a relevant model to perform such studies. Here we aimed to investigate the impacts of AD experimental transmission in mouse lemurs focusing on functional and morphological endophenotypes of AD.

7.2. Materials and methods

In our study, we evaluated the impact of human AD brain homogenates inoculation on both brain function and integrity in 12 adult mouse lemur primates (males, age=3.5±0.2years) using a behavioral and biomarker-based approach. Before entering the study, all animals were checked for health and given an ophthalmologic examination. None of the animals has been previously involved in pharmacological trials or invasive studies.

These small-sized primates have a maximal lifespan of 11.0±0.2 years and start to be considered as old after 6 years (Languille et al., 2012). After this age, some animals can spontaneously develop cognitive impairments, cerebral atrophy, and/or histopathological hallmarks (β-amyloidosis (25%, **Figure 49)** or tauopathy (29%, **Figure 50**)) whereas younger animal never present these alterations (see **6.3.2** and **7.2.5.2**; Kraska et al., 2011; Picq et al., 2012, 2015). To ensure the detection of inoculation-related changes without spontaneous aging interference, inoculated mouse lemurs were euthanized before 6 year-old (5.0±0.2years).

7.2.1. Ethic statement

All animal experiments were conducted in accordance with the European Communities Council Directive (2010/63/UE). Animal care was in accordance with institutional guidelines and experimental procedures were approved by local ethic committees (authorizations 12-089; ethic committee CETEA-CEA DSV IdF). They were all born and bred in a laboratory breeding colony (UMR 7179 CNRS/MNHN, France; European Institutions Agreement #962773) and bred in our laboratory (Commissariat à l'Energie Atomique, centre de Fontenay-aux-roses; European Institutions Agreement #B92-032-02). Conditions of captivity were maintained as described previously.

Critical ethic limit points were defined as one or more of the following observations: suffering signs, prostration signs or general state degradation approved by the local veterinary. Weight loss was not considered as a relevant criterion as mouse lemur's weight varies a lot both between weeks and seasons. Two control animals were euthanized for ethical reasons at 12 months post-inoculation because of abdominal infection from self-removal of abdominal sutures after implant removal. Therefore, these animals were not evaluated by MRI at 12, 15 and 18 months post-inoculation or behavioral studies at 18 months.

7.2.2. Experimental design

The experiment (**Table 6**) was based on the inoculation of human brain homogenates from AD patients (AD group) or CTRL age-matched subject (CTRL group) in the hippocampus and subjacent cortex of mouse lemurs (n=6 animals per group). Group assignment of the animals was performed on their scores on a jumping stand-based discrimination learning task before the inoculation in order to obtain similar learning scores. Longitudinal cognitive, electroencephalography (EEG) and anatomical MRI studies were performed up to 18 months post-inoculation followed by immunohistopathological examinations of brain tissues.

Experimental protocol	0mpi	3mpi	6mpi	9mpi	12mpi	15mpi	18mpi
Rotarod test	X		X		X		X
Learning tasks	X		X		X		X
Long-term memory tasks			X		X		X
Electroencephalography	X		X		X		
MRI	X	X	X	X	X	X	X
Inoculation	X						
Immunohistochemistry							X

Table 6. **Design of the mouse lemur experiment.** n=6 animals/group. Inoculation at 3.5±0.2years. Euthanasia and immunohistochemistry at 5.0±0.2years. mpi: months post-inoculation; MRI: Magnetic Imaging Resonance.

7.2.3. Human samples and homogenate preparation

The human samples and the homogenates used in this study were the same as used and characterized our previous study (see **5.2.1**, **5.3.1** and **5.3.2**).

7.2.4. Stereotaxic injections

Brain homogenates were injected bilaterally in the dorsal hippocampus (AP 1.25mm, DV 8.25mm, L +/- 2.5 mm) and subjacent parietal cortex (AP 1.25mm, DV 10.25mm, L +/- 2.5 mm) by stereotaxic surgery (Bons et al., 1998). Animals were fasted the day before surgery with free access to water. Pre-anesthesia (atropine, 0.025mg/kg, subcutaneous injection) was performed 30 minutes before anesthesia (Isoflurane,Vetflurane,4.5% for induction and 1–2% for maintenance) as described previously (Dhenain et al., 2003). Animals were then placed in a stereotaxic frame (Phymep, France). Burr holes were drilled in the appropriate location and bilateral injections of 6.5µL of 10% weight/volume brain homogenates with 26-gauge needle were performed in the dorsal hippocampus (injection speed: 1µL/min). Needles were kept in place for an additional 2 minutes before they were slowly moved into the subjacent parietal cortex where bilateral injections were also performed (same volume and injection speed as described above). Needles were kept in place for an additional 5 minutes before being slowly removed. Respiration rate was monitored during the whole experiment and body temperature was maintained at 37±0.5°C with a heating blanket during surgery. Six animals received brain extract from the control patient (CTRL-inoculated group) and 6 animals received brain extract from AD patients (n=3/patient, AD-inoculated group). The surgical area was cleaned (iodinate povidone, Vetedine, Vetoquinol, France), the incision was sutured and animals were placed in an incubator (temperature 25°C) and monitored until recovery from anesthesia.

7.2.5. Behavioral studies

7.2.5.1. Rotarod test

Mouse lemurs were evaluated with the accelerating rotarod task (model 7750, Ugo Basile, Italy) before inoculation and every 6 months after inoculation. The rod was a plastic drum, 5 cm in diameter, which was machined to provide traction. Animals were placed on the rotating cylinder at 20 rotations per minute (rpm). The rod then accelerated steadily up to 40 rpm until the end of the test which was reached when the animal fell or gripped on the rod during at least three consecutive turns without stabilizing its balance. Latency to fall or grip on the rod was recorded for each trial. Animals underwent 5 consecutive trials and the best result was recorded. Values are expressed in seconds. The system was cleaned between each trial and each animal.

7.2.5.2. Jumping-stand visual discrimination tasks

Cognitive test development

In association with this PhD thesis, we developed a **new cognitive testing protocol** based on pairwise visual discriminations in a jumping stand apparatus (see Publications, Picq et al., 2015).

This test was performed in an apparatus adapted from Lashley jumping stand apparatus which is a vertical cage made of plywood walls except the front panel that is a one-way mirror allowing observation (**Figure 51**).

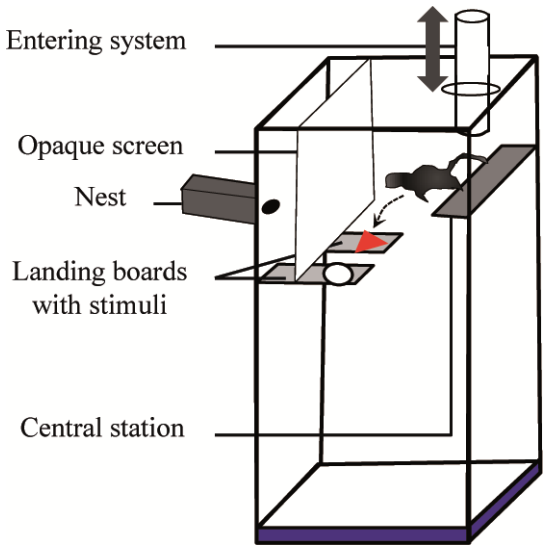

Figure 51. **Jumping-stand apparatus for visual discrimination tasks.** (Picq et al., 2015).

Our **first objective** was to develop a fast, efficient and reliable test for cognitive evaluation in this species. Indeed, previously developed testing procedures were very tedious and time-consuming and could be subject to motivation issues resulting in high attrition rates (Joly et al., 2006, 2014; Picq, 2007). Here we developed a time-effective testing procedure without motivational issues particularly appropriate to mouse lemurs' biology as this test was designed for arboreal lifestyle animals. Indeed, only 20 to 40 trials to reach the success criterion of the test were needed whereas, in earlier studies, 120 to 570 trials were required in a touchscreen device (Joly et al., 2014) and 24 to 93 in a corridor device (Picq, 2007). Also, in our testing procedure, the attrition rate was zero and inter-individual variability was not excessive. This is important since the number of mouse lemurs available for experimental studies is relatively limited as compared to rodents.

Our **second objective** was to evaluate further age-related cognitive alterations in mouse lemurs. We showed that some aged animals (> 6 years old) can present with long-term memory impairments but not learning deficits and that young animals (<4.5 years old) do not present with any cognitive impairments (see Publications, Picq et al., 2015). As, during this study, this test was validated as a powerful tool to evaluate cognition in mouse lemurs, it will be used for cognitive testing in our study.

Cognitive testing

Two discrimination tests were performed: a learning task and a long term memory task. These tests consisted in a succession of visual discriminations during which the mouse lemur had to jump from a central station heightened to one of two lateral boards allowing the access to a reinforcing chamber containing a positive reward (*i.e.* the possibility to reach a safe nestbox for a 2 minutes rest). Indeed, mouse lemurs prefer confined spaces therefore reaching their nest when placed in an open space is a strong motivator for behavioral testing. The central station can be progressively tilted downwardly causing a slippery slope pushing gently mouse lemurs to jump if no jump is performed within one minute. Boards can be covered with removable easily-discriminable patches of varied shape, texture and pattern (*i.e.* visual discrimination clues). Each board can be locked in a stable position or unlocked to become unstable and fall if a lemur jumps on it. For a pair of patches, the first patch is always associated to a stable board giving access to the nest (positive stimulus). The second patch is always associated to an unstable board that falls when a lemur jumps on it (negative stimulus). During a discrimination task, the mouse lemur had to identify, the positive stimulus giving access to the nest. Left/right locations of the stimuli were randomly alternated during the attempts with the restriction of no more than three consecutive trials in the same configuration. Testing continued until a success criterion, defined as at least 8 correct choices out of 10 successive attempts, was reached.

Before the first test, lemurs were submitted to a habituation session composed of seven trials. For the first four trials, only one fixed central board was attached just below the nestbox opening. On trial 1, a cylindrical rod connected the central station to the board so that no jump was required to reach the nestbox. On trial 2, the rod was removed so that the mouse lemur had to jump onto the central board to access its nestbox. On trials 3 and 4, an opaque vertical screen was added above the middle of the board masking the nestbox opening. The mouse lemur had to jump onto the board then walk under the screen to access its nestbox. For the last

three trials, the fixed landing platform was placed alternatively to the left or to the right of the nestbox opening which was masked by the opaque screen.

After the habituation session, mouse lemurs were tested for the first discrimination learning task. They had to learn a discrimination task (*i.e.* a pair of patches) to test their learning abilities. This task was first performed before inoculation. It was also performed 6, 12, and 18 months post-inoculation with, each time, a new discrimination task (*i.e.* a new pair of patches). At each post-inoculation time-point, long-time retention was also evaluated as recall testing of the discrimination task previously learnt 6 months before (**Figure 52**).

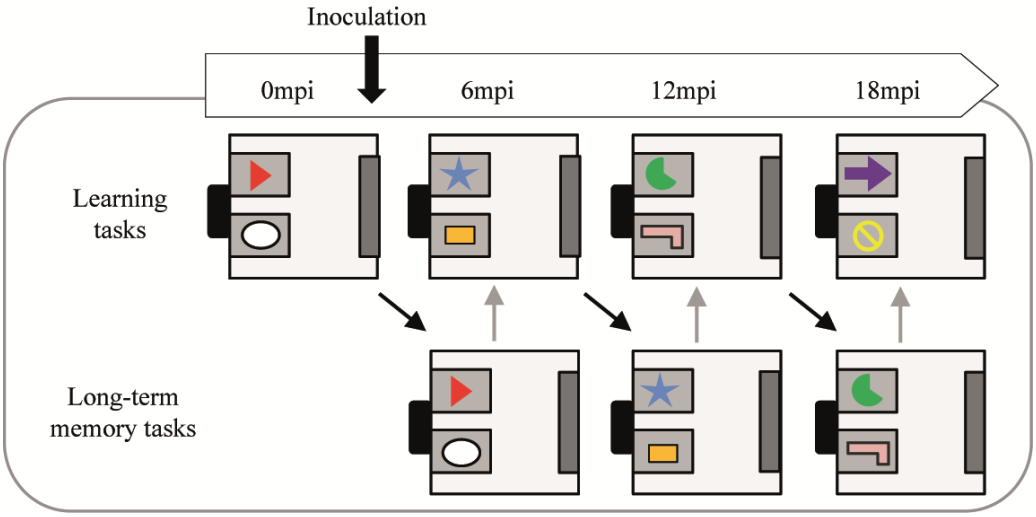

Figure 52. **Overview of the cognitive testing design.** Arrows indicate the sequence of the different testing with black arrows designating a 6-month gap and gray arrows a one-day gap between experiments. Symbols are not representative. mpi: months post-inoculation.

7.2.6. EEG study

7.2.6.1. EEG acquisition

EEG studies were conducted in mouse lemurs using telemetric devices (Infarinato et al., 2015; Rahman et al., 2013). EEGs were performed before inoculation, 6, and 12 months after inoculation. Briefly, animals received a pre-anesthesia (Diazepam 5mg/mL, Roche, France; intramuscular injection of 200µL/100g animal) and were anaesthetized with isoflurane. A wireless telemetry transmitter (2.5g; PhysioTel F20-EET; Data Science, St Paul, MN, USA), equipped with the simultaneous recording for one EEG and one electromyogram (EMG) channel (1–500 Hz sampling rate), was implanted in the abdominal cavity. The electrode

leads were threaded subcutaneously from the abdomen to the skull. Electrodes were skull-mounted and hold in place using dental cement on the dura-mater of the anterior frontal cortex according to a stereotaxic atlas of the mouse lemur brain (Bons et al., 1998). For EMG recording, bipolar electrodes were stitched into the neck muscles with non-absorbable polyamide suture. Animals were monitored for respiration rate and body temperature during surgery and monitored until anesthesia recovery. Animals were allowed to recover from surgery for one week before recording. EEG and EMG data were continuously collected using PC running Dataquest software (Data Science International, St Paul, MN, USA) thanks to a receiver base (RPC-1, Data Science, St Paul, MN, USA) placed on the floor of the home cage inhabited by the implanted animals. Electrodes and telemetry transmitter were then removed using same experimental conditions after one week of recording.

7.2.6.2. EEG analysis

The EEG data was analyzed by Neuroscore v2.1.0 (Data Science International, St Paul, MN, USA). Analysis was performed on multiple artefact-free 10 seconds periods of the awake active state determined with locomotor activity recording (included in the telemetry data of EMG recordings). We focused on delta (0.5-4 Hz), theta (4-8 Hz), alpha (8-12 Hz), sigma (12-16 Hz), and beta (16-24 Hz) frequency waves. At each time point, each frequency power was normalized according to mean values in the CTRL-inoculated animals.

7.2.7. MRI study

Morphological MRI was performed as described previously. MR images were recorded for each animal before inoculation, 15 days after inoculation and then every 3mpi until 18mpi. MR Images were analyzed using voxel-based morphometry as described previously (see **6.2.2.2**). Fifteen days post-inoculation images were not included in this analysis. A general linear model was designed based on multiple regressions to evaluate relative changes in GM values as a function of time between the CTRL- and AD-inoculated groups. Longitudinal follow-up of each animal was taken into account in the design matrix and total intracranial volumes were taken as covariate of no interest. Two-tailed t-test contrast was performed to compare the slope of GM evolution in the two groups. To control for multiple comparisons, an adjusted p-value was calculated using the voxel-wise FDR $q<0.05$ with extent threshold values of 10 voxels (Genovese et al., 2002). Voxels with a modulated GM value below 0.2 were not considered for statistical analysis.

7.2.8. Histology

Mouse lemurs were euthanized with an overdose of sodium pentobarbital (100 mg/kg intraperitoneally) and perfused intracardiacally with 4% paraformaldehyde in PBS. After overnight post-fixation, brains were cryoprotected using overnight 15% and 30% sucrose solutions. Brains were then frozen in isopentane and stored at -20°C. 40µm-thick coronal brains sections were cut on a microtome (SM2400, Leica Microsytem, Wetzlar, Germany) and free-floating histological serial sections were preserved in a storage solution (glycerol 30%, ethylene glycol 30%, distilled water 30% and phosphate buffer 10%) until use.

7.2.8.1. Immunohistochemistry

Serial sections of the entire brains were used for β-amyloid (4G8), tau (AT8 and AT100) and neuronal (NeuN) immunohistochemistry. Free-floating sections were rinsed in PBS 0.1M and then incubated with hydrogen peroxide 0.3% for 20min. Human sections were used as positive controls. Negative controls were obtained as the omission of primary or secondary antibodies for each group. For 4G8 staining, 80% formic acid pretreatment was applied for 2 min. Pretreatment with PBS-Triton 0.5% (Triton X-100, Sigma Aldrich, MO, USA) and 3% Bovine Serum Albumin (BSA) blocking was performed before a 2-day incubation at +4°C with either biotinylated 4G8 (Covance, NJ, USA, 1/250), AT8 (Pierce endogen, IL, USA, 1/100), AT100 (Pierce endogen, IL, USA, 1/100), and NeuN (Abcam, Cambridge, UK, 1/2000) antibodies. Secondary antibodies, biotinylated anti-mouse or anti-rabbit IgG (Vector Laboratories, Burlingame, CA, USA), were incubated for 1 hour at +4°C before revelation. ABC Vectastain kit (Vector Laboratories, Burlingame, CA, USA) was used to amplify DAB revelation (DAB SK4100 kit, Vector Laboratories, Burlingame, CA, USA). Stained sections were analyzed by two operators blinded to the group attribution.

7.2.8.2. Layer thickness evaluation

NeuN-stained sections were used to evaluate the thickness of the CA1 and CA3 pyramidal layers, dentate gyrus granular layer, retrosplenial cortex and layer II of the entorhinal cortex. CA1, CA3 and DG regions were assessed from ten measurements per section, for 3 consecutive sections. The thickness of the anterior retrosplenial cortex (layer I to VI) was measured on two consecutive sections as a mean of five measurements per section. Thickness of the layer II of the entorhinal cortex was measured as the mean of five measurements per

sections for six consecutive sections. All sections selected for each layer represented the same levels along the anteroposterior axis.

7.2.9. Statistical analysis

Statistical analyses were performed using GraphPad Prism software (San Diego, CA, USA). Data are expressed as means ± standard error of the mean (SEM). Data normality and variance homogeneity were evaluated using Shapiro-Wilk and Cochran C tests, respectively. Data from behavior experiments were transformed as reciprocal in order to obtain normality and variance homogeneity. As values within CTRL-inoculated animals were very homogeneous at each time post-inoculation, we replaced 18 mpi missing data from the two CTRL animals that died by the worst values in the CTRL group at 18 mpi. EEG and neuronal layer thickness data were evaluated by Mann Whitney's tests. Spearman's rank correlations were performed to examine relationships between EEG, neuronal layer thickness and behavioral data. The proportion of animals presenting with amyloid lesion in the CTRL and AD groups was compared with the Chi-square test. No statistical methods were used to predetermine sample size.

7.3. Results

7.3.1. Macroscopic impacts of experimental transmission

7.3.1.1. Cognitive deficits

Motor function was assessed using a rotarod test before all cognitive evaluations and, as expected, was not impacted by surgery or brain homogenate inoculation (**Figure 53A**).

Cognitive evaluation was performed every 6 months in a jumping-stand apparatus (Picq et al., 2015). Before brain homogenate inoculation, discrimination acquisition abilities were similar in the animals assigned to the AD- and CTRL-inoculated groups. AD- and CTRL-inoculated groups similarly improved their learning abilities 6mpi. The CTRL-inoculated animals continued to improve at 12mpi until reaching the best possible scores (dotted gray line), thus showing learning set acquisition. On the contrary, animals from the AD-inoculated group progressively worsened at 12 and 18mpi (**Figure 53B**).

For long-term memory performance, the CTRL-inoculated group always performed within the best possible scores (dotted gray line). The AD-inoculated group was impaired as soon as

6 months in the AD-inoculated group compared to the CTRL group and worsened at 18 months post-inoculation (**Figure 53C**).

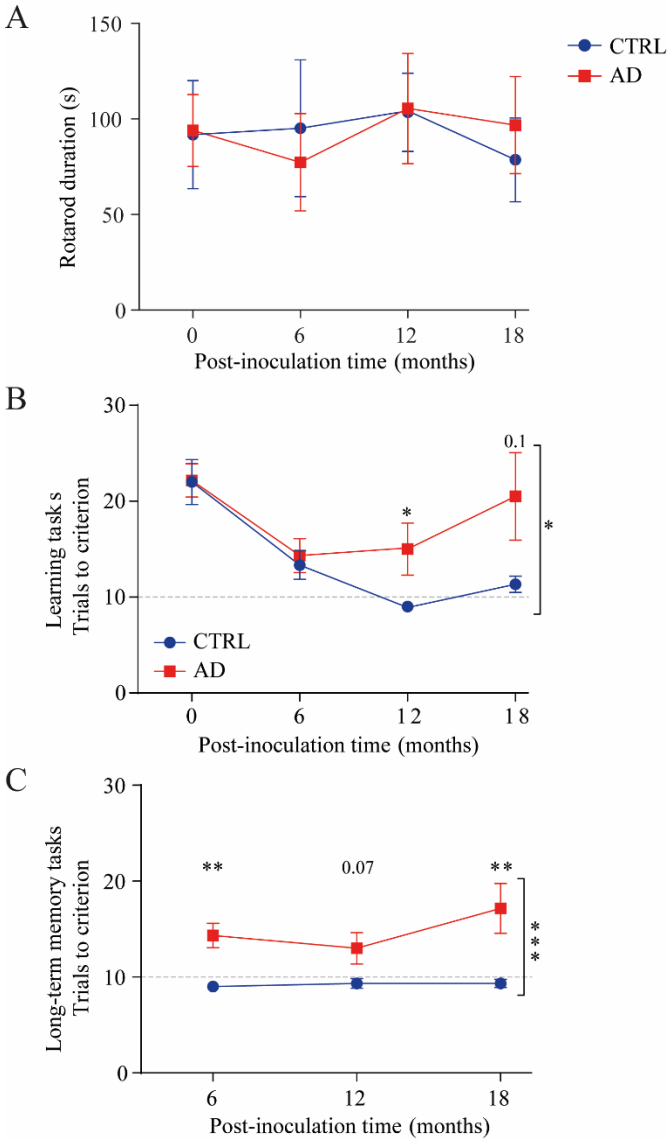

Figure 53. **AD brain homogenate inoculation leads to cognitive impairments in primates without motor deficiency.** A. Absence of motor impairments during the rotarod task ($p>0.05$, two-way ANOVA with Bonferroni post-hoc test). B. Learning discrimination tasks. Increase in the number of trials in function of the post-inoculation time ($p<0.05$, two-way ANOVA with Bonferroni post-hoc test) shows learning deficits in the AD-inoculated (AD) as compared to the CTRL-inoculated (CTRL) group. C. Long term memory tasks. Increase in the number of trials in function of the post-inoculation time ($p<0.001$, two-way ANOVA with Bonferroni post-hoc test) shows long-term memory deficits in the AD-inoculated (AD) as compared to the CTRL-inoculated (CTRL) group. * $p<0.05$; ** $p<0.01$; *** $p<0.001$.

7.3.1.2. Quantitative EEG alterations

To evaluate neuronal activity, we performed longitudinal studies of the active state EEG profile in the frontal cortex (**Figure 54A**). EEG wave power densities of the AD- and CTRL-inoculated groups were perfectly similar before inoculation (**Figure 54B**). Following inoculation, the EEG wave power densities of the AD- were altered as compared to the CTRL-inoculated group. Slow EEG wave (delta and theta frequency bands) were altered at 6 and 12mpi, with delta frequency band decrease and theta frequency band increase in the AD-inoculated mouse lemurs compared to the CTRL-inoculated animals (**Figure 54C-D**). At 12mpi, fast waves (alpha, sigma, and beta frequencies) were increased in AD-inoculated animals compared to CTRL-inoculated lemurs (**Figure 54D**). As the EEG electrodes were placed on the frontal cortex distant from the injection sites, our results suggest that inoculation of AD brain homogenates remotely altered neuronal activity.

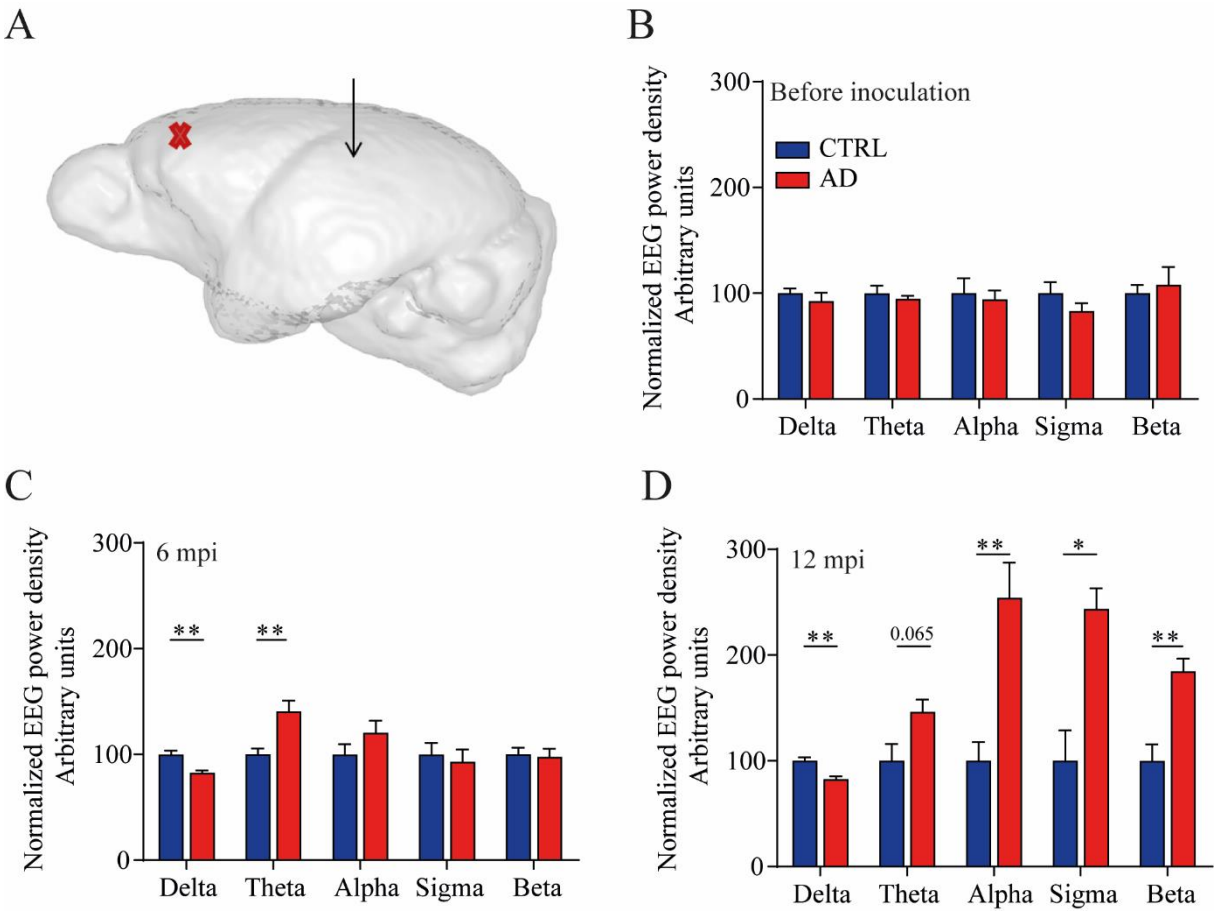

Figure 54. **AD brain homogenate inoculation alters neuronal activity.** A. Lateral 3D representation of the left hemisphere of a generic mouse lemur brain indicating the EEG implantation sites (red cross) in the frontal cortex and injection sites (black arrow) in the dorsal hippocampus and overlying cortex. EEG power density normalized to arbitrary units before inoculation (B), at 6mpi (C) and 12mpi (D) in function of delta (0.5-4Hz), theta (4-8Hz), alpha (8-12Hz), sigma (12-16Hz) and beta (16-24Hz) frequencies; Mann-Whitney U test; *p<0.05; **p<0.01; ***p<0.001; mpi: months post-inoculation.

Interestingly, long-term memory performance was correlated with the reduction of delta (p=0.004, **Figure 55A**), increase of theta (p=0.056, **Figure 55B**) and increase of alpha (p=0.02, **Figure 55C**) frequency power densities. This result suggests a relationship between cognitive and neuronal activity alterations.

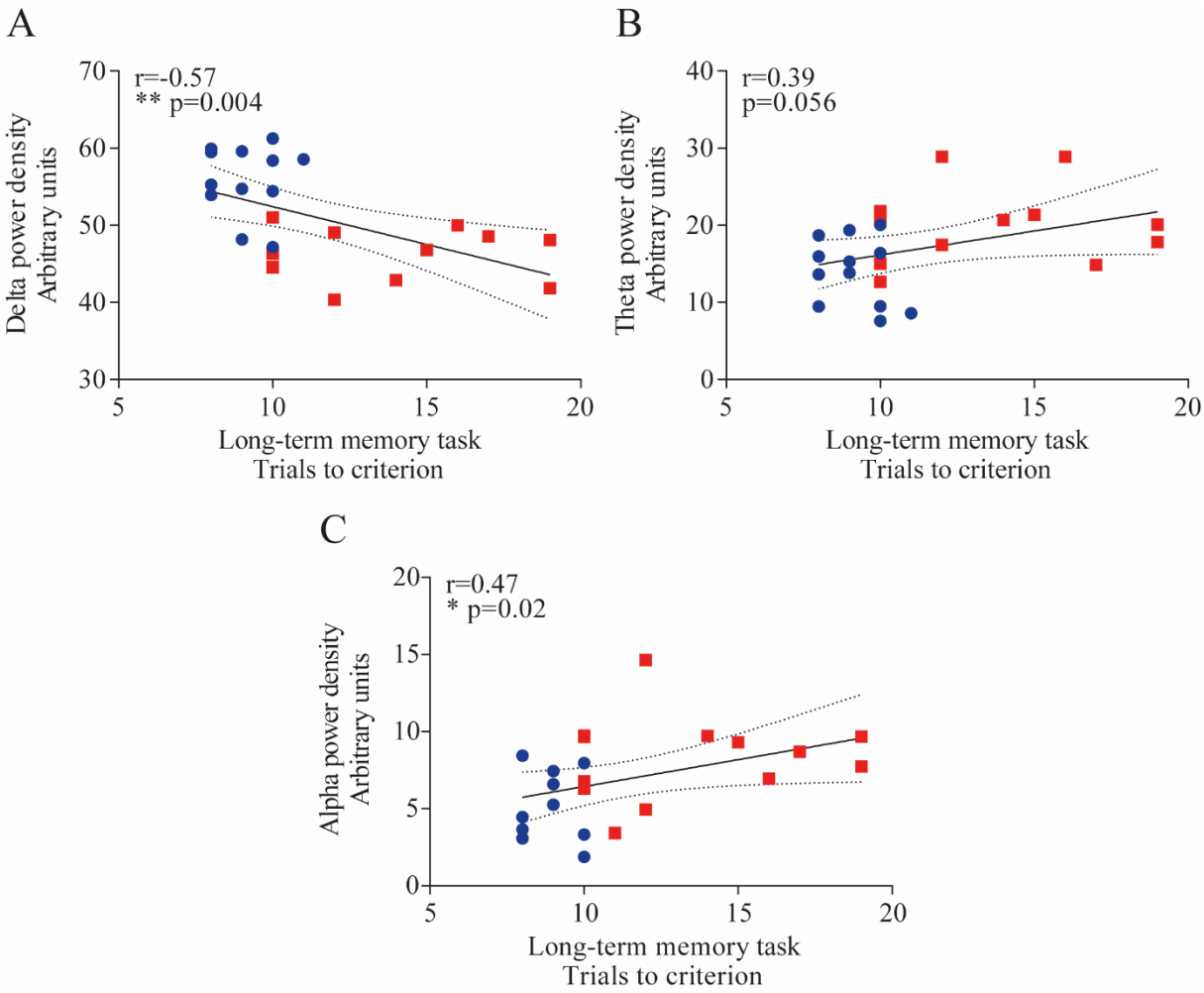

Figure 55. **Correlation of long-term memory impairments and neuronal activity alterations in inoculated lemurs.** Correlations between long-term memory performance and delta (A), theta (B) and alpha (C) frequency power densities. Spearman correlation test; *p<0.05; **p<0.01.

7.3.1.3. Cerebral atrophy

MR images were acquired before, 15 days after and every three months after inoculation up to 18mpi. We observed the progressive development of cerebral atrophies in the AD- as compared to the CTRL-inoculated group (**Figure 56**).

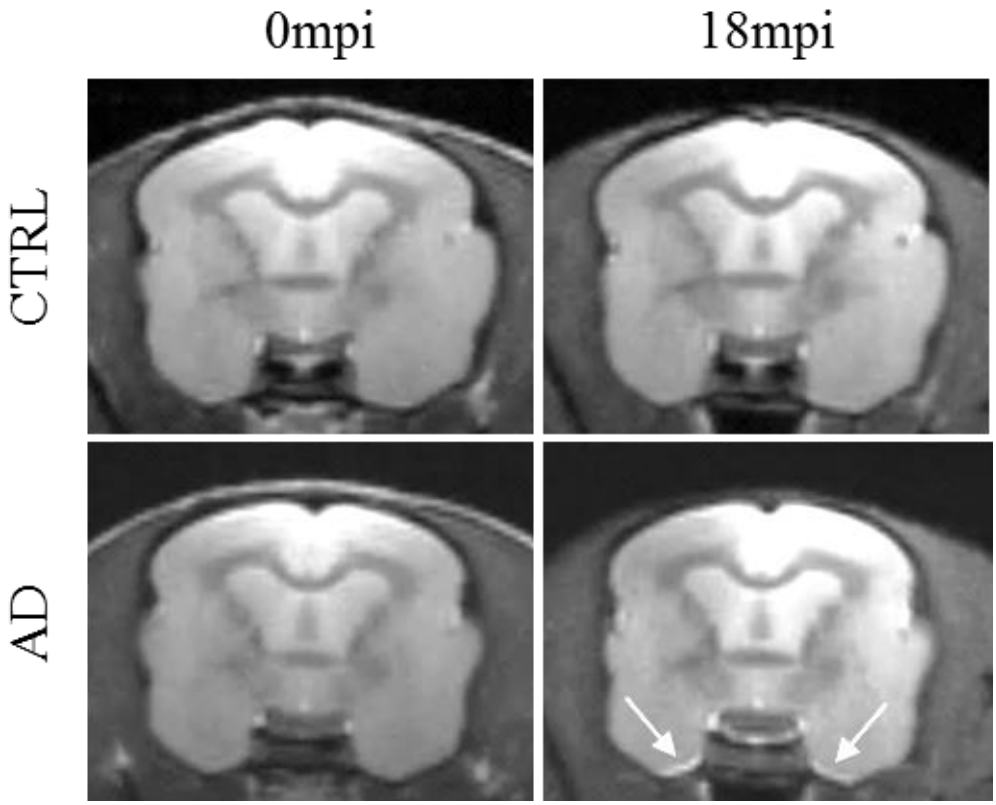

Figure 56. **Development of cerebral atrophy in AD-inoculated mouse lemurs.** MR images from two CTRL- or AD-inoculated animals before (left) and at 18mpi (right) showing the development of cerebral atrophy with white CSF (white arrows) appearing in the temporal lobe. mpi: months post-inoculation.

To evaluate and map this apparent cerebral atrophy, VBM analysis was performed. First, we extracted the global effect of inoculation upon GM in each group as a function of time. As expected, we did not detect any increase in GM over time in any group. We detected several clusters indicating GM loss in both groups as a function of time (**Figure 57A-B**). However, some structures, such as the inferior temporal lobe, were only affected in the AD-inoculated group (**Figure 57B**). Indeed, GM loss in the entorhinal cortex, the amygdala, the ventral hippocampus as well as the posterior cingulate and the retrosplenial cortices was specific of the AD-inoculated group.

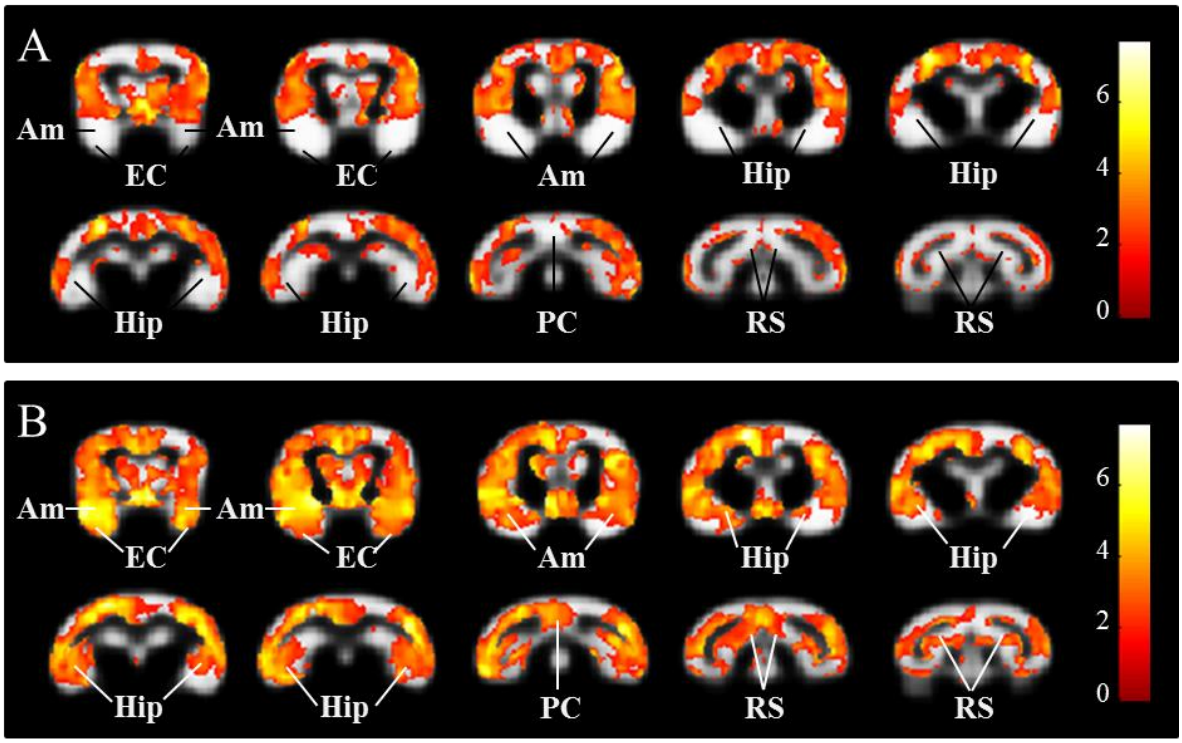

Figure 57. **Time-related gray matter loss.** Statistical heatmaps of T values indicating the significant clusters in which GM probability diminished as a function of time (FDR correction p-value=0.05, Voxel threshold k extent=10) in the CTRL- (A) and the AD-inoculated (B) groups. EC: entorhinal cortex, Am: amygdala; Hipp: hippocampal formation; PC: posterior cingulate cortex; RS: retrosplenial cortex.

Then, we compared both groups in order to determine the regions differentially affected by atrophy as a function of time. In the CTRL- group, no regions were found to be more atrophied than the AD-inoculated group as a function of time (**Figure 58**).

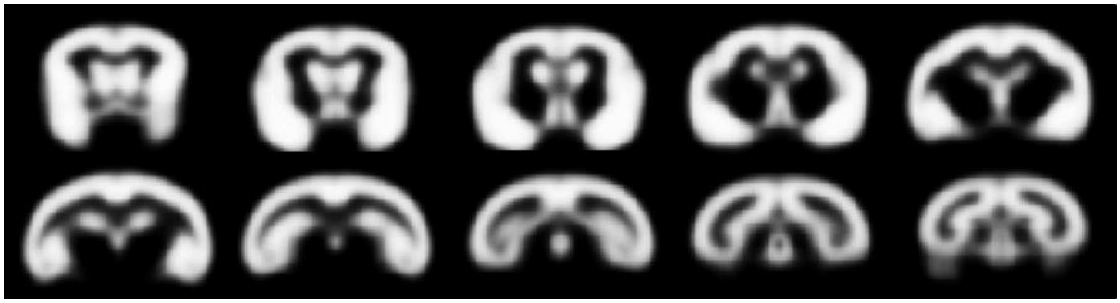

Figure 58. **Absence of time-related gray matter loss in the CTRL- as compared to the AD-inoculated group.** Absence of significant clusters in which GM probability diminished as a function of time (FDR correction p-value=0.05, Voxel threshold k extent=10) in the CTRL as compared to the AD group.

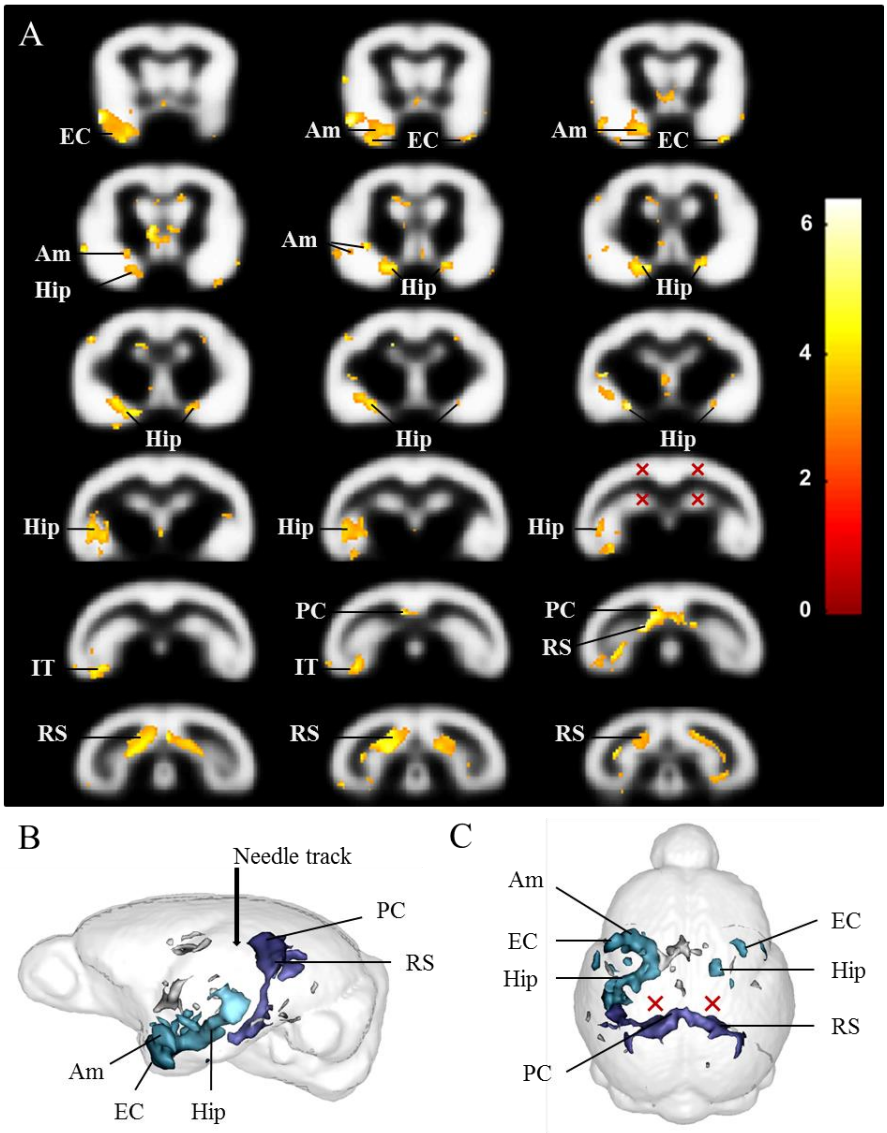

Figure 59. **Time-related gray matter loss in the AD group as compared to the CTRL group.** A. Statistical heatmap of T values indicating the significant clusters in which GM probability diminished as a function of age (FDR correction p-value=0.05, Voxel threshold k extent=10) in the AD- as compared to the CTRL-inoculated group. EC: entorhinal cortex, Am: amygdala, Hip: hippocampal formation, IT: inferior temporal, PC: posterior cingulate cortex, RS: retrosplenial cortex. B. 3D lateral view of the significant clusters (A) showing the time-dependent diminution of GM probability in the AD- as compared to the CTRL-inoculated group in the PC and RS (dark blue) and the temporal lobe (light blue). C. 3D upper view of the significant clusters (A) showing the time-dependent diminution of GM probability in the AD- as compared to the CTRL-inoculated group is mostly bilateral for the PC and RS (dark blue) whereas lateralization is observed for the temporal lobe (light blue). Red crosses indicate the injection sites.

On the contrary, many regions were more affected by atrophy in the AD group as compared to the CTRL group as a function of time (**Figure 59A**). No statistical difference was detected at the injection sites (red crosses). This atrophy involved mainly the entorhinal cortex, the amygdala, the ventral hippocampus, the posterior cingulate cortex and the retrosplenial cortex (**Figure 59B**, **Table 7**). Interestingly, all these regions are part of the limbic system and distant from the injection sites (**Table 7**). Although atrophy in the AD group involved both hemispheres (**Figure 59A**), the comparison between the AD and the CTRL group revealed a lateralization with the left hemisphere being more affected than the right (**Figure 59C**). The two regions closer to the inoculation sites displayed a strong bilateral atrophy (retrosplenial and posterior cingulate cortices, dark blue clusters) whereas the left temporal lobe was more affected than the right one (entorhinal cortex, amygdala, ventral hippocampus, light blue clusters). Atrophy was also found in other regions such as the parietal cortex and the caudate nucleus (gray clusters; **Table 7**). No atrophy was detected in frontal or occipital regions.

Brain region involved in voxelwise clusters	Cluster size (voxels)	Peak p-value FDR-corrected		Peak T value
Entorhinal cortex, amygdala, ventral hippocampus and inferior temporal cortex	1562	***	0.0004	6.3952
Cingulate and retrosplenial cortices	1342	***	0.0004	6.3777
Diagonal band of Broca, fornix and nucleus and stria terminalis	184	**	0.0013	5.7422
Ventral hippocampus	103	*	0.0109	4.2790
Caudate nucleus	70	**	0.0059	4.8479
Entorhinal cortex	59	*	0.0117	4.2231
Lateral temporal cortex	55	**	0.0062	4.7998
Peri-third ventricule area	52	*	0.0112	4.2488
Inferior temporal cortex	47	*	0.0175	3.8968
Fornix and stria terminalis	33	**	0.0061	4.8140
Parietal cortex	31	**	0.0045	5.0162
Amygdala	30	*	0.0102	4.4005
Lateral temporal cortex	23	*	0.0221	3.6795
Amygdala	22	*	0.0267	3.4984
Parietal cortex	18	*	0.0227	3.6538
Amygdala	18	*	0.0255	3.5305
Inferior temporal cortex	17	*	0.0221	3.6785
Caudate nucleus	16	**	0.0067	4.7113
Fornix	15	*	0.0172	3.9105
Inferior temporal cortex	15	*	0.0193	3.7971
Caudate nucleus	14	*	0.0233	3.6270
Inferior temporal cortex	13	*	0.0234	3.6142
Inferior temporal cortex	13	*	0.0140	4.0705
Entorhinal cortex	11	*	0.0135	4.1200
Parietal cortex	10	*	0.0108	4.3009
Amygdala	10	*	0.0255	3.5285

Table 7. **Regions affected by the time-related gray matter loss in the AD- as compared to the CTRL-inoculated group.*** $p<0.05$; ** $p<0.01$; *** $p<0.001$.

7.3.2. Microscopic impacts of experimental transmission

7.3.2.1. Neuronal layer thickness

To evaluate the impacts of human brain homogenate inoculation on neurons, we measured neuronal layer thickness in the hippocampal formation (CA1, CA3 and DG) as well as in the entorhinal and retrosplenial cortices. Here, we observed that neuronal layer thickness was decreased in the CA3 (-9.7%; * p=0.04; Mann-Whitney U test) and CA1 (-8.6%; p=0.13; Mann-Whitney U test) pyramidal layers in the AD- as compared to the CTRL-inoculated group. Thicknesses of dentate gyrus granular layer and the layer II of the entorhinal cortex were not impacted by AD brain homogenate inoculation (**Figure 60**).

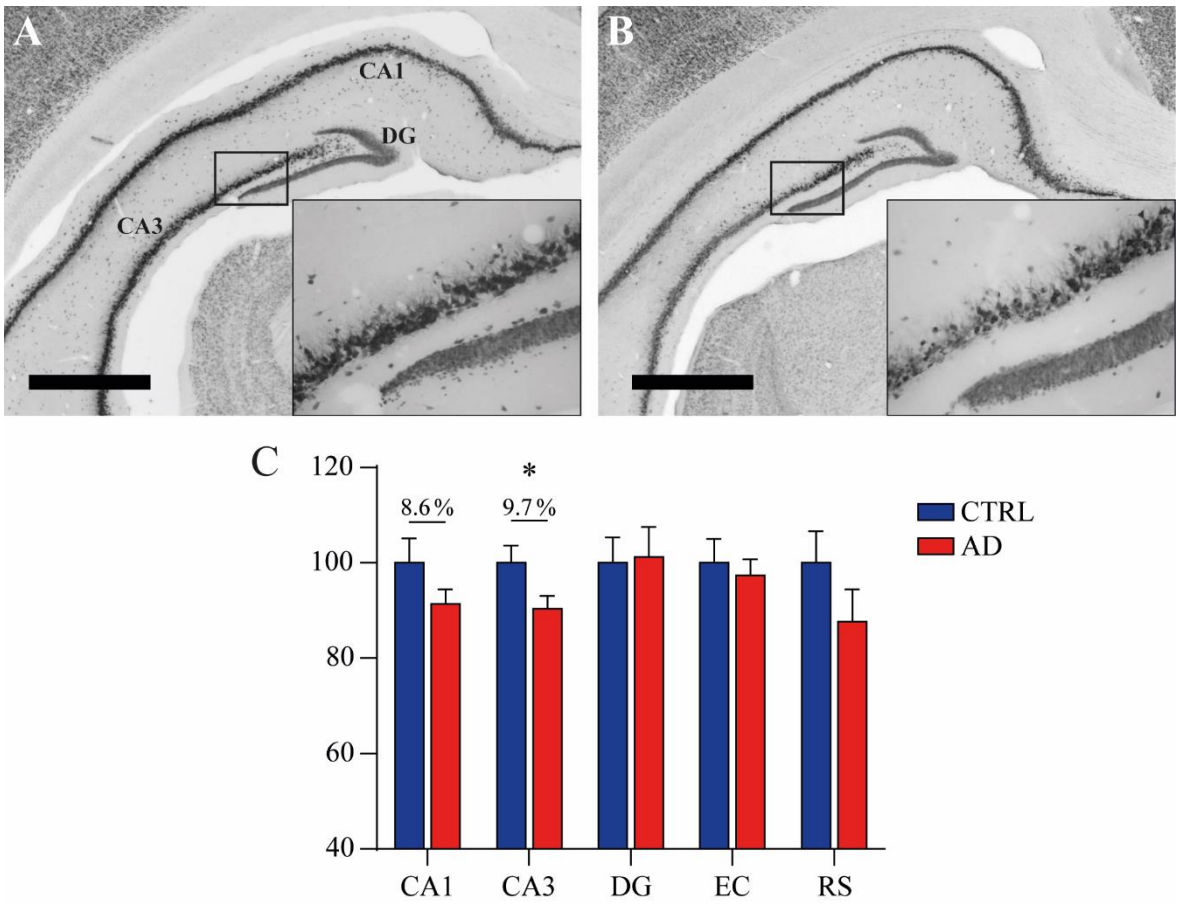

Figure 60. **Reduced neuronal layer thickness in the CA3 layer of the AD- as compared to the CTRL-inoculated group.** A. Representative CTRL animal stained with NeuN antibodies. B. Representative AD animal stained with NeuN antibodies. C. Layer thickness measurement normalized to mean CTRL values. DG: dentate gyrus; EC: entorhinal cortex; RS: retrosplenial cortex; Mann-Whitney U test; scale bars: 1mm.

7.3.2.2. β-amyloidosis

We then assessed β-amyloidosis. We performed 4G8 immunohistochemistry and evaluated the presence, type and location of Aβ lesions. We only detected sparse Aβ lesions in AD-inoculated mouse lemurs and none in the CTRL group (**Figure 61**). In one animal, we detected sparse diffuse amyloid plaques in the inferior frontal cortex. Theses plaques were located in the deep layers of the cortex, similarly to the ones observed in aged mouse lemurs (**Figure 61B**). It is to note that they were distant from the EEG electrodes localization. In this animal and two other AD-inoculated lemurs, we also detected sparse CAA in both large and small vessels of various brain regions such as the cortex or the hippocampus (**Figure 61C**). Overall, sparse Aβ lesions were detected in 50% of AD-inoculated lemurs and in 0% CTRL-inoculated (*p=0.045, Chi 2=4.00, df=1).

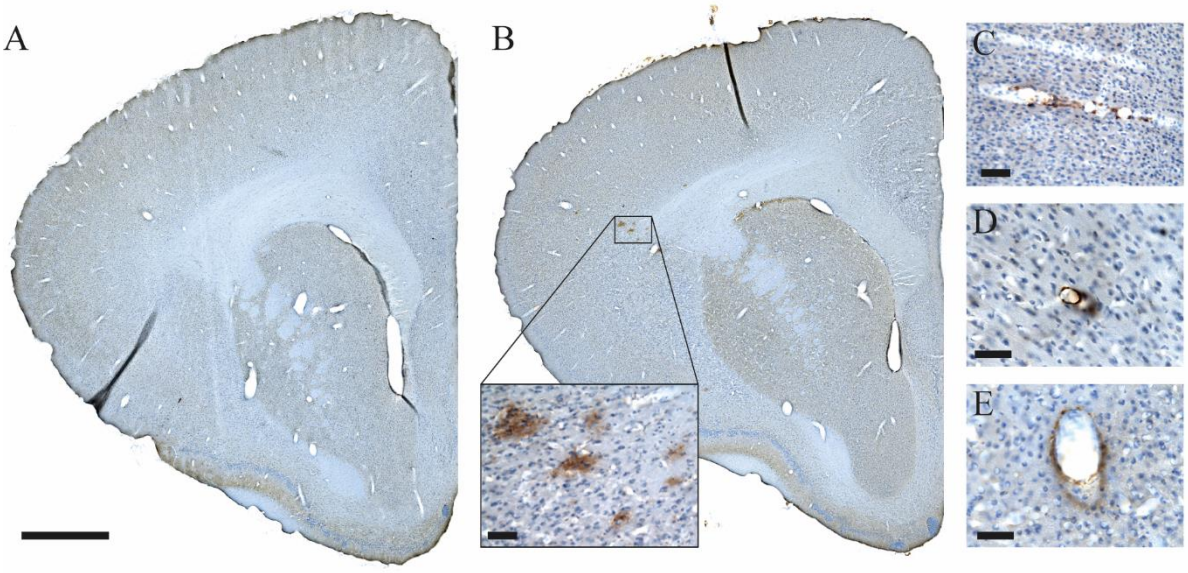

Figure 61. **Sparse β-amyloidosis in the AD-inoculated animals.** A. CTRL-inoculated mouse lemur with no Aβ lesions. B. AD-inoculated animal with sparse amyloid plaques (insert). C-E. Examples of large and small 4G8-immunoreactive vessels. Scale bars indicate 1mm (A-B) and 50µm for insert in B and C-E.

7.3.2.3. Tau pathology

For the evaluation of Tau pathology, we performed immunohistochemistry using AT8 and AT100 antibodies. We did not detect any Tau lesion in any of the animals from the CTRL- and AD-inoculated groups either at the injection sites or any other brain region (**Figure 62**).

This absence of Tau pathology was not related to a technical problem as it was detected in positive controls (AD and aged transgenic mouse tissues).

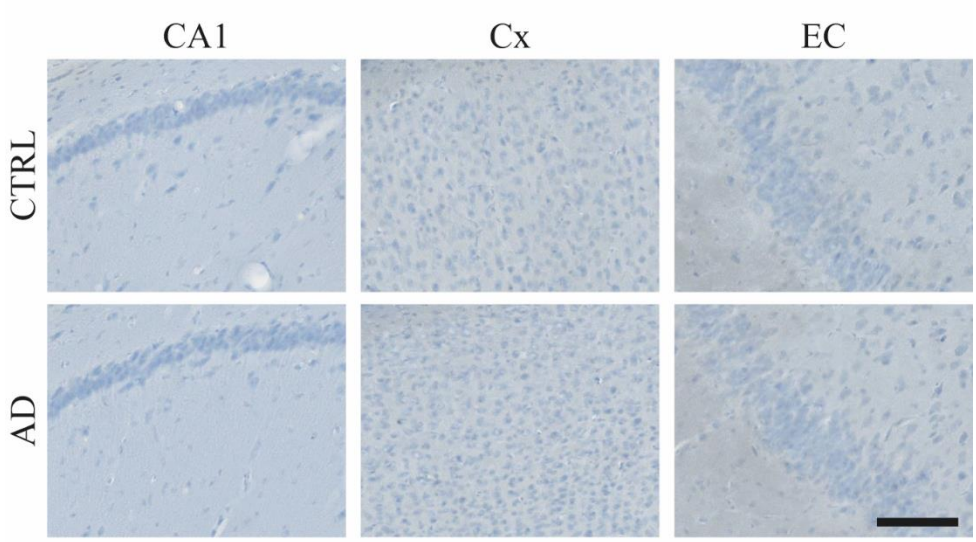

Figure 62. **Absence of Tau pathology.** Immunohistochemistry using AT8 antibodies in the CTRL- and AD-inoculated animals. Representative images from the CA1, subjacent parietal cortex (Cx) and the entorhinal cortex (EC). Scale bar: 100µm.

7.3.2.4. Astrocytic reactivity

Neuroinflammation has been proposed as a cofactor for seeding and is a hallmark of AD. We performed immunohistochemistry using Glial Fibrillary Acidic Protein (GFAP) antibody that recognizes an intermediate filament protein mostly specific of astrocytes. In case of inflammation, astrocyte somas and primary processes are hypertrophied. This change in morphology, from bushy to well-defined star-shape, is accompanied with the over-expression of GFAP. As astrocyte basal morphology and density is very different from one region to another, all brain regions were evaluated separately. No morphological difference could be found between the two groups. Some regions are represented as examples (**Figure 63**).

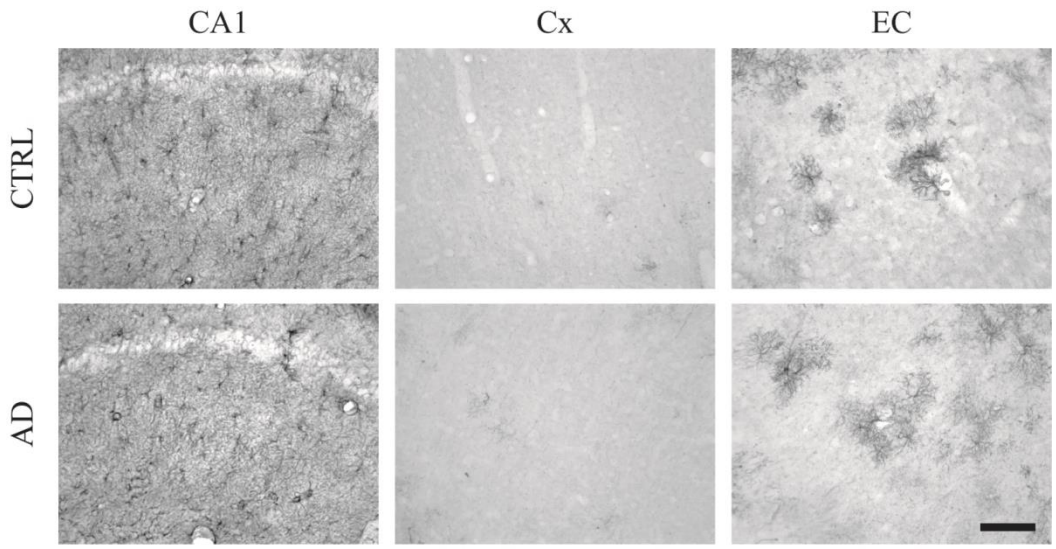

Figure 63. **Absence of astrocytic reactivity.** GFAP immunohistochemistry showing astrocyte morphology in the CTRL- and AD-inoculated groups in the CA1 region of the hippocampus, the subjacent parietal cortex (Cx) and the entorhinal cortex. Scale bar=100µm.

7.4. Discussion

Since the discovery that prion diseases can be transmitted by afflicted brain tissue inoculation, AD has been speculated to also harbor transmissible agents. Growing evidence suggests that prion-like mechanisms might play a role in AD physiopathology. Indeed, similarly to PrP, Aβ and Tau pathologies are experimentally transmissible to animal models. However, such transmission occurs seemingly without the development of the full spectrum of AD in mice and primates (Baker et al., 1994; Kane et al., 2000; Ridley et al., 2006). This is in opposition with prion diseases in which experimental transmission leads to clinical symptoms.

Until now, the induction of a clinical symptomatic phenotype by AD experimental transmission remains uncertain, especially in primate models (Beekes et al., 2014; Stancu et al., 2015; Walsh and Selkoe, 2016). In this study, we aimed to answer to these questions. We investigated the impacts of AD experimental transmission in mouse lemur primates focusing on functional and morphological endophenotypes of AD.

Mouse lemur's characteristics allow evaluating AD experimental transmission in a context closer to human sporadic pathology than transgenic mice. Here, we used adult mouse lemurs (age=3.5±0.2years). Human brain homogenates (10% weight/volume) from AD patients or control (CTRL) age-matched subjects were inoculated in the dorsal hippocampus and

subjacent cortex of 12 adult mouse lemurs (n=6 animals per group). Human brain tissue samples were issued from two AD patients (Braak stage VI and Thal stages 5 and 4, respectively) and one control subject (**Table 2** in **5.3.1**). AD samples were characterized by immunohistochemistry (**Figure 33** in **5.3.1**) and biochemistry (**Figure 34** in **5.3.2**). Longitudinal cognitive assessments, EEG and morphological MRI studies were performed up to 18mpi and followed by immunohistopathological examination of brain tissues.

7.4.1. Experimental transmission leads to cognitive alterations

Cognitive abilities were evaluated every 6 months by pairwise discrimination tasks in a jumping-stand apparatus (**Figure 51**). Two tasks were performed for each animal (**Figure 52**). The first one was a learning task that rated visual discrimination acquisition abilities; the second one was a long-term memory task that assessed retention of the discrimination problem learned 6 months before. Before inoculation, discrimination acquisition abilities were similar in both groups but learning performance and long-term memory were progressively altered in the AD group following AD brain homogenate inoculation (**Figure 53B-C**). Motor function was not altered by inoculation (**Figure 53A**) showing that motor deficits were not responsible for diminished cognitive performance.

In the literature, only very few experiments studied the impact of AD experimental transmission on cognitive abilities. In marmosets, cognitive decline was not reported but no specific test was performed (Baker et al., 1993, 1994; Maclean et al., 2000; Ridley et al., 2006). In transgenic mice, AD brain homogenates inoculation did not impact long-term spatial memory in a β-amyloidosis model (Kane et al., 2000) but preformed synthetic Tau fibrils inoculation was shown to impair object recognition in a tauopathy model (Stancu et al., 2015). As these mice spontaneously develop deficits in this task, at the same age, Tau fibrils inoculation worsened but did not induced these alterations.

Here, we showed that AD brain homogenate inoculation induced long-term memory impairments at younger age than normally detected in some aged animals (**Figure 53B-C**). Also, in aged animals, we have shown that learning abilities are not impaired, even at very old ages, up to 10 years-old (see Publications, Picq et al., 2015 and **7.2.5.2**). In our study, AD brain homogenate induced alterations of cognitive functions (learning) that are preserved even in cognitively impaired old animals. This is relevant to human pathology in the sense that

aged individuals can present with mild cognitive deficits but specific alterations are only observed in AD (McKhann et al., 2011).

In conclusion, we showed that experimental transmission to mouse lemurs led to a specific clinical phenotype similar to AD.

7.4.2. Experimental transmission leads to functional alterations

To evaluate neuronal activity, we performed longitudinal quantitative EEG studies of the awake active state in the frontal cortex. AD brain homogenate inoculation progressively altered EEG frequency power densities (**Figure 54B-D**). The functional role of specific EEG frequency bands is still a matter of intense research (Roux and Uhlhaas, 2014). Comparable EEG experiments were performed in a triple mutant transgenic mouse model. Similar alterations were observed (Jyoti et al., 2015) before the development of subtle Aβ and Tau pathologies (Koss et al., 2013) suggesting that soluble Aβ or Tau assemblies may be responsible for neuronal activity alterations in AD-inoculated lemurs.

Interestingly, evolution of long-term memory performance was correlated with the evolution of the lowest EEG frequencies (delta, theta and alpha frequency bands) in the AD group (**Figure 55**). In AD patients, alterations of these frequency bands are observed (Giannitrapani et al., 1991; Huang et al., 2000; Mattia et al., 2003) and correlate with the severity of cognitive impairments (Dierks et al., 1991; van der Hiele et al., 2007a, 2007b; Koenig et al., 2005). These results suggest that neuronal activity alterations may play a part in long-term memory impairment in mouse lemurs. In our study, cognitive testing and EEG recordings were performed at an interval of two weeks. Performing EEG recordings during and right after cognitive testing could allow us to further evaluate the relationship between neuronal activity and cognitive alterations as their association remains elusive (Roux and Uhlhaas, 2014).

Finally, as EEG electrodes were placed on the frontal cortex distant from the injection sites (**Figure 54A**), our results suggest that AD brain homogenates inoculation remotely altered neuronal activity, suggesting a spreading mechanism from the injection sites to the frontal cortex (local effect). As neuronal activity functions in networks, these alterations could also reflect a network-wide impact (network effect). Such hypothesis calls for further experiments using for example several EEG electrodes or functional MRI in order to evaluate network synchrony.

7.4.3. Experimental transmission leads to cerebral atrophy

Morphologically, AD is characterized by a progressive cerebral atrophy affecting the hippocampus and various cortices. We recorded MR images of the brains of AD- and CTRL-inoculated animals every three months and automatically evaluated GM evolution. Compared to CTRL-, AD-inoculated animals displayed an atrophy of the retrosplenial and posterior cingulate cortices, two areas close to the inoculation sites (**Figure 59B-C**, dark blue clusters). Atrophy involved also further regions in the temporal lobe including the ventral hippocampus, entorhinal cortex, amygdala, and the lateral and inferior temporal cortices (**Figure 59B-C**, light blue clusters). These results show that AD brain homogenate inoculation decreases GM in remote structures of the brain, suggesting a spreading mechanism.

In AD, atrophy starts in the temporal lobe and the most atrophied structures are the entorhinal cortex, the amygdala and the hippocampus (de la Monte, 1989). In AD-inoculated lemurs, atrophy mostly involves the temporal lobe suggesting a similar pattern of early atrophy. Interestingly, similar damage to temporal regions is only observed during pathological aging processes in mouse lemurs (Picq et al., 2012) and these regions are not atrophied during normal aging (**Figure 48** in **6.3.1** and Sawiak et al., 2014). Our results therefore suggest that AD brain homogenate inoculation alters the cerebral atrophy pattern in mouse lemurs.

As atrophy of the entorhinal cortex and hippocampus is associated to cognitive impairments in aged mouse lemurs (Picq et al., 2012), we propose that temporal atrophy in AD-inoculated lemurs may play a part in the observed cognitive alterations.

7.4.4. Experimental transmission leads to sparse β-amyloidosis

Finally, we detected a reduction of neuronal layer thickness in some hippocampal regions (**Figure 60**). Further examination will be required to determine if such atrophy could be linked to neuronal loss. Nevertheless, this observation further confirmed an alteration of neuronal integrity following AD brain homogenate inoculation in mouse lemurs.

Brain sections were evaluated for Aβ and Tau pathologies. To ensure the detection of inoculation-related changes without spontaneous aging interference, inoculated mouse lemurs were euthanized before reaching 6 years (5.0±0.2years) as we showed that some animals can spontaneously develop β-amyloidosis and/or Tau pathology after this age (**Figure 49** and **Figure 50** in **6.3.2**).

We detected very few cortical amyloid plaques (**Figure 61B**, 1 animal out of 6) and sparse cortical amyloid angiopathy (**Figure 61C**, 3 animals out of 6) in 50% of the AD-inoculated group. No lesions were found in the CTRL-inoculated group. As discussed previously (see **5.4.1**), Aβ seeds are the agents responsible for β-amyloidosis transmission contained in AD brain homogenates. Our results further suggest a seeding phenomenon due to the introduction of Aβ seeds in the brain of mouse lemur primates.

In the AD-inoculated animals, β-amyloidosis was never localized at the injection sites. This is consistent with previous marmosets studies, a primate with a similar lifespan in which sparse β-amyloidosis was observed after at least 3.5 years post-inoculation (Baker et al., 1993, 1994; Maclean et al., 2000; Ridley et al., 2006). In transgenic mice, seeding effects were predominantly seen at the level of the injection site (see **Figure 37** and discussed in **5.4.1**) before spreading to other regions (Kane et al., 2000; Meyer-Luehmann et al., 2006; Ye et al., 2015b). As lesions were not observed at the injection site but in various brain regions, this suggests that Aβ seeds diffused widely into the brain of AD-inoculated lemurs. This diffusion may be favored in the primate brain as compared to transgenic mouse brain by the fact that primate Aβ is less expressed and therefore provides a less aggregation-prone environment. Indeed, inoculated Aβ seeds in transgenic mice may be segregated to the injection site by involvement with the host's overexpressed Aβ. This hypothesis would explain why lesions in primates are not preferentially localized in the inoculated structures.

We demonstrated previously that sparse β-amyloidosis only affects 25% of animals aged more than 6 years (**Figure 49** in Chapter VI – Mouse lemur model characterization). Here, in younger animals that do not normally present with Aβ lesions (5±0.2 years-old at euthanasia), the percentage of Aβ-positive animals was doubled as compared to aged ones suggesting an induction of the pathology. Indeed, if Aβ lesions had only been accelerated in animals who would have spontaneously developed lesions while aging, the proportion of affected animals should be similar in AD-inoculated and aged animals.

Taken altogether, our results show that β-amyloidosis was induced by experimental transmission in mouse lemurs suggesting a seeding mechanism.

Aβ lesions were light as compared to what occurs in the brain of AD patients and transgenic mouse models of AD. We demonstrated previously the seeding abilities of our AD homogenates in two murine models of β-amyloidosis including a late and sparse β-

amyloidosis model (**Figure 37** and **Figure 46** in Chapter V – Experimental transmission of β-amyloidosis to mice). In these experiments and accordingly to the literature (see **4.2.5**), we observed that the host was a critical parameter for Aβ seeding. Aged non-human primates (Kimura et al., 2003; Lemere et al., 2008; Struble et al., 1985), including mouse lemurs (**Figure 49** in Chapter VI – Mouse lemur model characterization), can develop parenchymal and/or vascular Aβ lesions but these lesions are sparser than in humans. In AD-inoculated lemurs, β-amyloidosis induction was sparse, resembling spontaneous β-amyloidosis development. This result further emphasizes the role of the host in Aβ prion-like mechanisms and could be responsible for this absence of severe Aβ lesions following AD brain homogenate inoculation.

Also, we did not detect any Tau lesions. This result is consistent with previous marmoset studies (Baker et al., 1993, 1994; Maclean et al., 2000; Ridley et al., 2006) and the fact that, in suspected cases of human-to-human transmission, Aβ deposition occurred without Tau pathology (Frontzek et al., 2016; Jaunmuktane et al., 2015; Kovacs et al., 2016; Preusser et al., 2006). In addition, Tau pathology, as found in humans, is unusual in non-human primates, including mouse lemurs (**Figure 50** in Chapter VI – Mouse lemur model characterization) suggesting a relative resistance to tauopathy (Heuer et al., 2012). Therefore, similarly to Aβ, host effects may explain why Tau seeding was not observed in AD-inoculated lemurs. However, to ensure that the lack of Tau pathology in AD-inoculated mouse lemurs is not linked to an absence of seeding effects of our homogenates, we are currently evaluating their seeding properties in a mouse model of tauopathy. Also, further experiments will be required at longer incubation time to conclude on Tau prion-like mechanisms in mouse lemurs as Aβ and Tau lag time may be different.

The animals presenting Aβ lesions were inoculated with one or the other AD patient. Consistently with our results in transgenic mouse models of β-amyloidosis, we did not observe any strain effect relative to the inoculated homogenate (see **5.4.4**). Moreover, in accordance with marmoset studies, amyloid plaques and CAA did not differ in morphology or localization as compared to aged animals following inoculation (Baker et al., 1993, 1994; Maclean et al., 2000; Ridley et al., 2006). This suggests that AD brain homogenate inoculation did not modify Aβ deposition in primates. It has been proposed that, in humans, Aβ deposit morphology depends more on their maturation over time and localization than upon a strain effect (Eisele and Duyckaerts, 2016). Taken altogether, β-amyloidosis

transmission in mouse lemurs did not seem to present with a strain effect. However, in AD-inoculated lemurs, 50% of animals presented with CAA affecting mostly cortical areas whereas only 1 animal out of 6 developed amyloid plaques. Interestingly, we observed that CAA is only present in 10% of aged mouse lemurs (**Figure 49** in Chapter VI – Mouse lemur model characterization). Similarly, in suspected cases of human-to human transmission, CAA was systematically reported (Frontzek et al., 2016; Jaunmuktane et al., 2015; Kovacs et al., 2016; Preusser et al., 2006). These observations suggest that CAA may be a typical hallmark of β-amyloidosis transmission.

Finally, we did not detect any obvious signs of astrocytic reactivity in any mouse lemurs. Astrocyte and microglia reactivity is mostly observed around Aβ and Tau lesions in AD patients and transgenic models (Duyckaerts et al., 2009; Vehmas et al., 2003). As Aβ lesions were sparse and no Tau pathology was observed, this could explain the absence of astrocytic reactivity in AD- and CTRL-inoculated lemurs.

7.4.5. Mechanistic hypotheses

Our study demonstrates for the first time that cognitive, functional and morphological alterations can be induced by AD experimental transmission in primates. These alterations developed progressively and some were not detected at 6mpi but became obvious at 12 or 18mpi. These observations rule out an immediate effect of the homogenates and suggest an evolving mechanism.

The fact that the brain structure and function alterations occurred in the absence of severe neuropathological lesions is striking. Indeed, the induction of clinical symptoms after inoculation of pathologic brains in the absence of detectable pathological protein accumulation has already been reported for classical prion diseases (Lasmézas et al., 1997) but never in the context of AD-pathology. Indeed, in prion diseases, amyloid seeding can be dissociated from disease transmission. Symptomatic spongiform encephalopathy can be transmitted without PrP deposition in the brain (Lasmézas et al., 1997; Piccardo et al., 2013) and, conversely, PrP deposition can be transmitted without producing a symptomatic outcome (Barron et al., 2016; Piccardo et al., 2007). For AD, such dissociation may also be observed as behavioral outcomes are almost never worsened although protein deposition is accelerated (Kane et al., 2000; Stancu et al., 2015). Conversely, in mouse lemurs, we observed disease

transmission without protein deposition in the brain. These results suggest dissociation between agents leading to toxicity and agents leading to non-symptomatic deposition.

Such hypothesis is supported by observations in humans. Indeed, non-symptomatic individuals can present with protein deposition. Also, cases have been reported as presenting with functional deficits and atrophy without Aβ pathology ("suspected non-Alzheimer's/amyloid pathophysiology", SNAP) (Chételat et al., 2016; Jack, 2014). Recently, a classification of the major AD biomarkers into 3 categories for Aβ, Tau or neuronal injury biomarkers emphasized the possibility to detect AD-related neurodegeneration in the absence of strong Aβ and/or Tau lesions (Jack et al., 2016). Finally, in AD patients, the severity of the disease does not correlate or exceeds deposited lesions (Gómez-Isla et al., 1997).

Our results suggest that neuropathological lesions cannot be held responsible for the deficits observed. This is consistent with accumulating evidence that deposited aggregates are not the most toxic species and that soluble assemblies may drive the toxicity. Therefore, the prion-like hypothesis of AD should not be restrained to the identification of deposited Aβ and Tau lesions. It has been proposed that seeding processes should not be restrained to the identification of Aβ plaques as other species might be seeded and lead to stronger functional impacts without deposition (Barghorn et al., 2005). Indeed, *in vitro*, Aβ oligomers self-propagate in a prion-like manner (Kumar et al., 2014) and are responsible for neuronal death (Dean et al., 2016). However, whether soluble Aβ assemblies, thought to be the most toxic species, can also be seeded *in vivo* remains to be determined (Meyer-Luehmann et al., 2006).

It is more and more commonly admitted by the scientific community that soluble species are responsible for neurotoxicity (Cobb and Surewicz, 2009) and that deposition may represent a way to segregate toxic assemblies.

Soluble assemblies of Aβ and Tau can lead to cognitive deficits. Also, in animal models, cognitive impairments can develop before β-amyloidosis (Hsia et al., 1999) and injection of oligomeric Aβ assemblies lead to cognitive deficits (Gandy et al., 2010). Small and soluble Aβ seeds are potent inducers of cerebral β-amyloidosis (Langer et al., 2011). Also, in the only experiment showing worsened cognition after preformed synthetic Tau fibrils inoculation in a tauopathy model, an increase in Tau oligomers was detected. The authors suggested that early pathological forms of Tau may be responsible for the observed deficits rather than NFTs

(Stancu et al., 2015). Induction of cognitive deficits in mouse lemurs following AD brain homogenate inoculation may therefore rely on soluble Aβ and/or Tau assemblies.

In transgenic mice, EEG frequency alterations were shown to precede deposition and soluble Aβ and Tau species were suggested to play a major role in generating these alterations (Jyoti et al., 2015). The mechanisms leading to EEG alterations are not yet well understood (Palop and Mucke, 2010) and may be linked to Aβ pathology in AD patients (Mander et al., 2015). Therefore, EEG alterations in mouse lemurs following experimental transmission may be induced directly by soluble Aβ and/or Tau assemblies or indirectly through neuronal death or network alterations (Palop and Mucke, 2010).

On the contrary, cerebral atrophy may rely more on Tau assemblies. Indeed, it correlates with neuronal loss (Zarow et al., 2005) and Braak stages (Jack et al., 2002; Vemuri et al., 2008; Whitwell et al., 2008) but not well with Aβ load (Josephs et al., 2008). In addition, neuronal loss have been shown to correlate with but exceed the number of NFTs (Gómez-Isla et al., 1997) suggesting that non-deposited assemblies may underlie cerebral atrophy. In our study, we observed that atrophy mainly involved the temporal lobe of AD-inoculated lemurs (**Figure 57B** and **Figure 59**). In aged lemurs, we showed that AT8-positive Tau species preferentially accumulate in the temporal lobe where Aβ plaques were never found (**Figure 49**, **Figure 50**, **Table 4** and **Table 5** in Chapter VI – Mouse lemur model characterization). One hypothesis may be that soluble Tau assemblies could potentially play a part in the development of cerebral atrophy both in aged and AD-inoculated lemurs.

We hypothesize that the alterations of brain structure and function observed after AD experimental transmission may rely on soluble Aβ and Tau assemblies. Indeed, our results are coherent with the hypothesis of the self-propagation of non-deposition-prone Aβ and/or Tau assemblies as strong functional and morphological outcomes progressively developed in the absence of proteinaceous deposition. Indeed, the progression of the endophenotypes seems to exclude a toxicity resulting only from the injection of soluble species and suggest a progressive replication of these species in the brain.

In accordance with our hypothesis, soluble forms of Aβ or Tau can initiate a self-replicating process both *in vitro* (Dean et al., 2016; Kumar et al., 2014) and *in vivo* (Clavaguera et al., 2009; Langer et al., 2011). Very recently, it has been shown that oligomeric forms of Tau could be seeded without NFTs formation in a non-symptomatic model of tauopathy, ALZ17

(Baker et al., 2016). Also, Aβ oligomers can travel quickly and widely in the brain (Epelbaum et al., 2015) raising the possibility that such soluble seeds may mediate the spread of toxic assemblies in the brain. As soluble assemblies usually escape detection by immunohistochemistry (Thal et al., 2015), other experiments will have to be performed to demonstrate our hypothesis and to identify the relative contribution of soluble species to the observed toxicities.

Absence of available models with fully developed AD pathology strongly limits AD research in particular for the evaluation of Aβ and Tau relationship. Similarly to Aβ and Tau, their relationship could also rely on prion-like mechanisms. Indeed, experimentally, Aβ seeds have been shown to accelerate Tau pathology whereas the reciprocal has never been observed. In humans, Tau pathology precedes Aβ's in many systems such as the entorhino-dentate circuit. If Aβ pathology seems to be necessary to promote Tau pathology in the cortex, the role of Tau in Aβ pathology remains to be understood. Experimental transmission of purified Aβ and/or Tau seeds to mouse lemur could represent an interesting model to decipher both Aβ and Tau seeding and spreading mechanism and evaluate the relationship between Aβ and Tau in the context of AD.

As a conclusion, our results complement recent evidence supporting the involvement of prion-like mechanisms in AD as well as β-amyloidosis iatrogenic transmission in humans (Frontzek et al., 2016; Jaunmuktane et al., 2015; Kovacs et al., 2016; Preusser et al., 2006). However, our results are in contradiction with the current view that AD-related lesions rather than AD may be subject to prion-like mechanisms (propagons *vs* prions) (Eisele and Duyckaerts, 2016; Kovacs et al., 2016). Indeed, we demonstrated than an AD-like pathology can be transmitted from humans to primates. Our study provides strong arguments to further evaluate functional outcomes in potentially contaminated individuals. Such study is currently being performed by M. Jucker's team on a cohort of 700 epileptic patients who have gone through brain surgery over the last 25 years. For this cohort, both histopathological features and cognitive status, that was recorded before surgery and at regular intervals after surgery, will be examined. This study will provide evidence for or against the transmissibility of Aβ and Tau pathologies as well as their functional consequence in a context free of concomitant CJD (Abbott, 2016).

Apart from specific iatrogenic conditions, there is no evidence that AD is transmissible between humans (Beekes et al., 2014; Edgren et al., 2016; Schmidt et al., 2012) and current

knowledge favor endogenous generation of Aβ and Tau seeds in the brain. Identifying the origin of the formation of these first seeds will be critical to understand the physiopathology of AD. We proposed that self-propagating soluble assemblies may be responsible for the development of clinical alterations. Demonstrating this hypothesis will be crucial to understand their relative toxicity and relationship regarding the observed symptomatic pathology. Such identification could represent a critical step for the understanding of AD and the development of disease-relieving strategies.

Alzheimer's disease (AD) is characterized by the accumulation of misfolded and aggregated β-amyloid (Aβ) and tau proteins. Iatrogenic induction of amyloidosis has recently been suggested in patients who received pituitary-derived hormone treatment or dural grafts presumably contaminated with Aβ. Induction of Aβ and/or Tau lesions by experimental transmission has been demonstrated in various models but almost no functional consequences were observed.

Here we demonstrate for the first time that AD experimental transmission progressively leads to cognitive impairments, neuronal activity modifications, and cerebral atrophy in primates. These clinical outcomes are dissociated from severe immunohistopathologically detectable Aβ or Tau lesions. Our results support the hypothesis that non-deposited toxic Aβ and/or Tau assemblies may self-propagate within the brain leading to a pathological AD-like phenotype.

This new paradigm provide compelling evidence for the role of Aβ and Tau seeds in the instigation and progression of AD and reinforces the interest of targeting proteopathic seeds, preferably early in the pathology.

Part III – Conclusions and Perspectives

Since the discovery of the transmissible character of prion diseases, other cerebral proteopathies have been suspected to harbor similar transmissible properties. Among these diseases, growing evidence supports the concept that AD is initiated and sustained by the misfolding and aggregation of Aβ and Tau proteins. This "prion-like" mechanism is virtually identical to that of PrP in prion diseases (Prusiner, 1998). Experimental transmission is a useful tool to evaluate the "prion-like hypothesis of AD" in animal models. It requires the inoculation of proteopathic Aβ and/or Tau seeds obtained *in vitro* or from pathologic brains homogenization. Here we evaluated experimental transmission of AD endophenotypes to mice and mouse lemur primates.

First, we showed that β-amyloidosis is transmissible to mice by intracerebral AD brain homogenates inoculation. We showed that the host is a modulator of β-amyloidosis transmission using early and late amyloidogenic mouse models. We identified a typical hallmark of β-amyloidosis transmission (callosal amyloidosis) and suggest that it could be an inoculation-dependent signature of both prion and prion-like transmission in rodents. We also showed the absence of "strain phenomenon" in two sporadic AD patients and suggest that AD Aβ strains may rely more on primary aminoacidic sequence than PrP strains and present with less conformational flexibility (Watts et al., 2014). Finally, we investigated Aβ spreading in our two models and we propose that Aβ spreading is dependent on APP expression and spontaneous aggregation.

Then, we characterized the physiological and pathological aging processes of mouse lemurs. Physiological aging in mouse lemurs is accompanied by an age-related cerebral atrophy that, contrary to pathological aging, does not involve the inferior temporal lobe and hippocampus. We characterized the proportion of mouse lemurs AD-related histopathological lesions and we showed that, like other non-human primates, they present with a relative resistance to both pathologies that do not resemble the massive lesions observed in humans.

Several questions remain to be answered such as deciphering the impacts of β-amyloidosis transmission. Indeed, it has been suggested that, if β-amyloidosis might be transmissible between humans, AD clinical phenotype is not reproduced, contrasting with prion diseases (Kovacs et al., 2016). Indeed, whether the "pathogenic spread" of AD-related proteins causes

AD symptom onset remains uncertain (Walsh and Selkoe, 2016). In prion diseases, experimental transmission is achieved in primates and leads to clinical symptoms.

Here, we investigated these questions in mouse lemurs and demonstrated for the first time that AD experimental transmission progressively leads to cognitive impairments, neuronal activity modifications, and cerebral atrophy in primates. These clinical outcomes are dissociated from severe immunohistopathologically detectable Aβ or Tau lesions. Our results are consistent with accumulating evidence that deposited aggregates are not the most toxic species and that soluble assemblies may drive the toxicity. Such dissociation has already been reported for prion diseases (Lasmézas et al., 1997) but never in the context of AD.

Our results support the hypothesis that non-deposited toxic Aβ and/or Tau assemblies may self-propagate within the brain leading to a pathological AD-like phenotype. Such hypothesis is supported by SNAP cases (Chételat et al., 2016; Jack, 2014). We propose that the prion-like hypothesis of AD should not be restrained to the identification of Aβ and Tau deposited lesions and that non-deposition prone Aβ and/or Tau assemblies may propagate and lead to strong functional and morphological outcomes. Our results provide evidence for the role of Aβ and Tau seeds in the instigation and progression of AD and reinforces the interest of targeting proteopathic seeds, preferably early in the pathology.

Self-propagation of soluble species may explain the relative resistance of mouse lemurs to Aβ and Tau lesions and the development of AD-like cerebral atrophy and cognitive deficits while aging or after AD experimental transmission. Further experiments will be needed to confirm the hypothesis but this model may allow the evaluation of Aβ and Tau prion-like and toxic mechanisms as well as their interaction. It could also provide an interesting model for the evaluation of therapies targeting soluble assemblies.

As a conclusion, our results complement recent evidence supporting the involvement of prion-like mechanisms in AD as well as the suspicion of iatrogenic induction of β-amyloidosis in humans (Frontzek et al., 2016; Jaunmuktane et al., 2015; Kovacs et al., 2016; Preusser et al., 2006). Contrary to the current view that AD *per se* is not transmissible, we demonstrate that an AD-like pathology can be transmitted from human to primate. Our results provide strong arguments to further evaluate functional outcomes in potentially contaminated individuals. Current knowledge suggest the endogenous generation of Aβ and Tau seeds in the brain. Identifying the origin of the formation of these first seeds and their self-propagation mechanisms will be critical to understand the physiopathology of AD. It will also favor the development of disease-relieving strategies as patients' early care, prior to symptomatic stages, is likely to be an efficient strategy against this devastating disease.

Scientific production

- **Scientific publications**

Gary C., Koch J., Petit F., Eddarkaoui S., Sawiak SJ., Hérard AS., Aujard F., Deslys JP., French Neuropathology Network, Brouillet E., Buée L., Picq JL., Pifferi F., Comoy E., Dhenain M. Experimental transmission of Alzheimer's disease to a non-human primate. (Submitted).

Gary C., Petit F., Pifferi F., Dhenain M. Occurrence of Alzheimer's disease pathology in aged mouse lemur primates. (In prep.).

Gary C., Audrain M., Petit F., Bemelmans AP., French Neuropathology Network, Cartier N., Braudeau J., Dhenain M. Amyloid deposition is triggered by AD brain homogenates inoculation in wild-type mice with focal AD-like pathology. (In prep.).

Gary C., Hanss Z., Ciaptacz L., Petit F., French Neuropathology Network, Dhenain M. Dissociation of amyloid distribution patterns during normal aging and following of AD brain homogenates inoculation in transgenic mice. (In prep.).

Gary C., Hanss Z., Dhenain M. Plasmatic amyloid is regulated by seasonal rhythms in mouse lemur primates. (In prep.).

Picq JL., Villain N., **Gary C.**, Pifferi F., Dhenain M. Jumping Stand Apparatus Reveals Rapidly Specific Age-Related Cognitive Impairments in Mouse Lemur Primates. PLoS One. 2015 Dec 30;10(12):e0146238.

- **Proceedings**

Gary C.,, Koch J., Petit F., Hanss Z., Rahman Palash A., Eddarkaoui S., Sawiak S., Herard AS., Deslys JP., Buee L., Comoy E., Picq JL., Pifferi F., Dhenain M., French Neuropathology Network. First demonstration of functional and morphological alterations in primates after alzheimer brain homogenates inoculation. Alzheimer's & Dementia: The Journal of the Alzheimer's Association, Vol. 12, Issue 7, P360–P361

Gary C.,, Hanss Z., Ciaptacz L., Petit P., Dhenain M., French Neuropathology Network. Dissociation of amyloid distribution patterns during normal aging and following of alzheimer's disease brain homogenates inoculation in transgenic mice. Alzheimer's & Dementia: The Journal of the Alzheimer's Association, Vol. 12, Issue 7, P445–P446

Gary C.,, Audrain M., Petit F., Bemelmans AP., Cartier N., Braudeau J., Dhenain M., French Neuropathology Network. Amyloid deposition is triggered by alzheimer's disease brain homogenates inoculation in wild-type mice with focal ad-like pathology. Alzheimer's & Dementia: The Journal of the Alzheimer's Association, Vol. 12, Issue 7, P841

Gary C., Pifferi F., Koch J., Petit F., Comoy E., Picq JL., Dhenain M. Experimental transmissibility of Alzheimer pathology in a non-human primate. Symposium 22: Seeding, Spreading and prion-like mechanisms. Neurodegener Dis 2015;15(suppl 1): 8-158 - P74-75

- **Oral scientific communications**

Gary C., Koch J., Petit F., Hanss Z., Rahman A., Chikar A., Dehen C., Deslys JP., Hérard AS., Eddarkaoui S., Buée L., Picq JL., Pifferi F., Comoy E., Dhenain M. First demonstration of functional and morphological alterations in primates after Alzheimer brain homogenates inoculation. International AAIC congress Toronto 2016

Gary C., Koch J., Petit F., Hanss Z., Rahman A., Chikar A., Dehen C., Deslys JP., Hérard AS., Eddarkaoui S., Buée L., Picq JL., Pifferi F., Comoy E., Dhenain M. First demonstration of functional and morphological alterations in primates after Alzheimer brain homogenates inoculation. Conférence Jacques Monod. Mépliement des protéines – Vers une agrégation toxique des protéines au cours du vieillissement et des maladies liées à l'âge : de la structure à la pathologie et sa propagation Roscoff 2016.

Dhenain M., **Gary C.**, Comoy E., Pifferi F., Picq JL. Prions, nucléons, propagons, toxons agrégons et autre maux en "on". Réunion Francophone sur la maladie d'Alzheimer et les syndromes apparentés Lyon 2016.

Gary C., Pifferi F., Koch J., Petit F., Comoy E., Picq JL., Dhenain M. Experimental transmissibility of Alzheimer pathology in a non-human primate. International AD/PD congress Nice 2015.

- **Posters**

Gary C., Audrain M., Petit F., Bemelmans AP., French Neuropathology Network, Cartier N., Braudeau J., Dhenain M. Amyloid deposition is triggered by AD brain homogenates inoculation in wild-type mice with focal AD-like pathology. International AAIC congress Toronto 2016.

Gary C., Hanss Z., Ciaptacz L., Petit F., French Neuropathology Network, Dhenain M. Dissociation of amyloid distribution patterns during normal aging and following of AD brain homogenates inoculation in transgenic mice. International AAIC congress Toronto 2016.

Flament J., **Gary C.**, Koch J., Pifferi F., Comoy E., Picq JL., Valette J., Dhenain M. GluCEST imaging in a primate model of Alzheimer's disease. International ISMRM congress Toronto 2015.

- **Distinctions and Awards**

Invited chairman for the "Development of New Models and Analysis Methods: Insights from Animals Models" oral session at the International AAIC congress Toronto 2016.

Travel fellowship laureate AAIC International congress Toronto 2016.

Publications

Alzheimer brain inoculation induces functional and morphological alterations in primates

Charlotte Gary[1,2], James E. Koch[1,2,3], Fanny Petit[1,2], Sabiha Eddarkaoui[4], Stephen J. Sawiak[5,6], Anne-Sophie Herard[1,2], Fabienne Aujard[7], Jean-Philippe Deslys[8], French Neuropathology Network[9,§], Emmanuel Brouillet[1,2], Luc Buée[4], Emmanuel E. Comoy[8], Jean-Luc Picq[1,2,10,*], Fabien Pifferi[7,*], Marc Dhenain[1,2]

[1] Centre National de la Recherche Scientifique (CNRS), Université Paris-Sud, Université Paris-Saclay UMR 9199, Neurodegenerative Diseases Laboratory, 18 Route du Panorama, F-92265 Fontenay-aux-Roses, France

[2] Commissariat à l'Energie Atomique et aux Energies Alternatives (CEA), Direction de la Recherche Fondamentale (DRF), Institut d'Imagerie Biomédicale (I2BM), MIRCen, 18 Route du Panorama, F-92265 Fontenay-aux-Roses, France

[3] University of Wisconsin Oshkosh, 800 Algoma Boulevard, Oshkosh, WI 54901, USA

[4] Université de Lille, Inserm, CHU-Lille, UMR-S1172, Alzheimer & Tauopathies, Lille, France

[5] Wolfson Brain Imaging Centre, University of Cambridge, Addenbrooke's Hospital, Cambridge, UK

[6] Behavioural and Clinical Neuroscience Institute, University of Cambridge, Cambridge, UK

[7] UMR7179 CNRS-MNHN, MECADEV (Adaptive Mechanisms and Evolution), 1 Avenue du petit château, 91800 Brunoy, France

[8] Commissariat à l'Energie Atomique et aux Energies Alternatives (CEA), Direction de la Recherche Fondamentale (DRF), Institut des Maladies Emergentes et des Therapies Innovantes (IMETI), SEPIA, 18 Route du Panorama, F-92265 Fontenay-aux-Roses, France

[9] GIE Neuro-CEB/Neuropathologist Network: Plate-Forme de Ressources Biologiques, Bâtiment Roger Baillet, Hôpital de la Pitié-Salpétrière, 47-83 boulevard de l'Hôpital, 75651 Paris Cedex 13.

[10] Laboratoire de psychopathologie et de neuropsychologie, EA, 2027, Université Paris 8, St-Denis, France

[§] GIE Neuro-CEB: Charles Duyckaerts, Sabrina Leclère-Turbant, and Marie-Claire Artaud-Botté; The national network includes the following neuropathologists: Anne Vital (Bordeaux), Françoise Chapon (Caen), Jean-Louis Kemeny (Clermont-Ferrand), Claude-Alain Maurage & Vincent Deramecourt (Lille), David Meyronet & Nathalie Streichenberger (Lyon), André Maues de Paula (Marseille), Valérie Rigau (Montpellier), Fanny Vandenbos-Burel (Nice), Charles Duyckaerts, Danielle Seilhean (Paris), Serge Milin (Poitiers), Dan Christian Chiforeanu (Rennes), Annie Laquerrière (Rouen), Béatrice Lannes (Strasbourg), Marie-Bernadette Delisle & Emmanuelle Uro-Coste (Toulouse).

[*] These authors contributed equally to this work

Abstract

Alzheimer's disease (AD) is characterized by the accumulation of misfolded and aggregated β-amyloid (Aβ) and tau proteins. Iatrogenic induction of amyloidosis has recently been suspected in patients who received pituitary-derived hormone treatment or dural grafts presumably contaminated with Aβ[1,2]. Induction of Aβ and tau lesions was demonstrated in transgenic mouse models after contamination with AD brain homogenates[3,4] despite very limited functional consequences[5]. Here we show for the first time in a primate (*Microcebus murinus*) that intracerebral inoculation of human AD brain homogenates induces substantial functional and morphological changes. After several months, these include progressive cognitive impairments, modifications of neuronal activity, widespread cerebral atrophy, and reduction of hippocampal neuronal layer thickness. This demonstrates that agents inducing a clinical outcome can be transmitted experimentally. However, strikingly, the clinical signs were observed in absence of severe parenchymal or vascular amyloid deposition or aggregated tau lesions. The toxic species leading to the pathological phenotype are thus probably soluble and are aggressive enough to induce a neurodegenerative process. More importantly, the progressive occurrence of widespread morphological defects suggests that the toxic species propagate to the whole brain, which supports their ability to induce a self-replicating process. This new paradigm opens avenues for further exploration of the physiopathology of Alzheimer's disease.

There has been longstanding interest as to whether Alzheimer's disease (AD) might be transmissible[6]. In humans, patients exposed to cadaver-derived hormones or dural grafts presumably contaminated with β-amyloid peptide (Aβ) have a higher risk of developing early-onset Aβ pathology than non-exposed subjects[1,2]. Experimental induction of amyloidosis or tauopathy has been described in rodents after intracerebral and even peripheral contamination with AD brain homogenates[7,8]. However none of the transmission studies with Aβ or tau inocula provided evidence for pronounced cognitive decline or neurodegeneration[9]. Aged non-human primates can naturally develop amyloid lesions[10], but most studies of AD brain homogenate inoculation in primate species ranging from chimpanzees to marmosets have not revealed AD-specific histopathological hallmarks[11]. A single long-term study in marmosets did reveal the induction of sparse amyloidosis 3.5 to 7 years post-inoculation, but there was no evidence of cognitive decline, neurodegeneration, functional AD hallmarks, or other clinical signs[12]. This calls for more clinical analysis in primates after inoculation of AD brain homogenates.

In this study, we used a multimodal approach including non-invasive methods to evaluate the impact of inoculation of human AD brain homogenates on both brain function and integrity in mouse lemur primates (*Microcebus murinus*). These small-sized primates (body length: 12cm; weight: 60-120g) have a maximal lifespan of 12 years and are considered "old" after 6 years[13], after which up to 25% of animals can spontaneously develop cognitive impairments, cerebral atrophy, and/or histopathological lesions such as amyloidosis or tauopathy[14-16]. Human brain homogenates (10% weight/volume) from AD patients or control (CTRL) age-matched subjects were inoculated into the dorsal hippocampus and adjacent cortex of 12 adult mouse lemurs (n=6 animals per group, age=3.5±0.2 years). Longitudinal cognitive assessments, electroencephalography (EEG) and morphological MRI studies were performed up to 18 months post-inoculation (mpi) and followed by immunohistopathological examination of brain tissues (age=5.0±0.2 years, Supplementary Table 1).

Human brain tissue samples were from two AD patients (Braak stage VI and Thal phases 5 and 4, respectively) and one control subject (Supplementary Table 2). Immunohistochemistry revealed typical amyloid plaques and tau lesions in the AD patients but not in the control subject (Extended Data Fig. 1a-f). Biochemical analysis detected $A\beta_{1-42}$ only in AD brain homogenates. Western blotting showed a typical shift of AD tau-Cter triplet[17] and pathological pS396 positive tau only in AD samples (Extended Data Fig. 1g-i).

Cognitive evaluation was performed every 6 months in a jumping-stand apparatus[18] (Fig. 1a) and consisted of two tasks (Fig. 1b). The first was a learning task that rated visual discrimination acquisition abilities, while the second was a long-term memory task that assessed retention of the discrimination problem learned 6 months before. In the learning task, before brain homogenate inoculation, animals assigned to AD- and CTRL-inoculated groups performed similarly (Fig. 1c). Animals from both groups showed similar improvement in their learning abilities 6 months after inoculation (Fig. 1c). However, performance then diverged with CTRL-inoculated animals further improving at 12 mpi until reaching the best possible scores (thus demonstrating learning set acquisition) while the AD group instead progressively worsened at 12 and 18 mpi, with overall performance significantly lower than that of CTRL-animals (Fig. 1c). In the long-term memory task, the overall performance of the AD-inoculated group and their performances at 6 and 18 mpi were significantly lower than those of CTRL-animals (Fig. 1d). Motor function was assessed using a rotarod test prior to cognitive evaluations and did not reveal any significant difference between groups (Fig. 1e).

To evaluate neuronal activity, we performed longitudinal EEG studies in the frontal cortex during the active state. At 6 mpi, slow wave EEG frequencies were altered, with a decrease in delta frequency and an increase in theta frequency in the AD-inoculated lemurs compared to the CTRL animals (Fig. 2b). Also, delta frequency was correlated with long-term memory abilities ($p=0.009$, Extended Data Fig. 2a). This result is consistent with the reported relationship between slow-wave oscillations and memory consolidation in humans[19]. At 12 mpi, AD-inoculated lemurs still displayed a significant decrease in delta frequency and their fast waves (alpha, sigma, and beta) were significantly increased (Fig. 2c).

Our results suggest that inoculation with AD brain homogenates alters neuronal activity. This is consistent with data in humans showing that Aβ-pathology is linked to alterations of slow-wave generators[20]. Interestingly, the EEG electrodes were placed on the frontal cortex distant from the injection sites. This suggests a remote impact of pathologic brain inocula. Taken together, behavioral and EEG results show that inoculation of AD-brain homogenates leads to progressive cognitive and functional impairments in mouse lemurs.

Morphologically, AD is characterized by progressive cerebral atrophy affecting the hippocampus and the cortex. We recorded MR images of the brains of AD- and CTRL-inoculated animals every 3 months. Automated voxel-based analysis was performed to study gray matter atrophy. Compared to CTRL-inoculated, AD animals displayed a strong bilateral

atrophy of the retrosplenial and posterior cingulate cortices, two areas close to the inoculation sites (Fig. 3a-c, dark blue clusters in b-c; Supplementary Table 3). Atrophy also involved temporal regions including the hippocampus, entorhinal cortex, amygdala, and the inferior temporal cortex (Fig. 3a-c, light blue clusters in b-c). For these structures, the left hemisphere was more affected than the right one. Atrophy was also identified in the diagonal band of Broca, fornix, stria terminalis, parietal cortex and caudate nucleus (Fig. 3a-c, gray clusters in b-c; Supplementary Table 3). The widespread morphological defects suggest a propagation of the toxicity to the whole brain resulting from the focal administration of AD brain homogenates. Interestingly, in lemurs, atrophy of temporal and hippocampal regions, similar to that reported in the current study, is associated with pathological aging processes[15], while these regions are not atrophied during normal aging[21].

The animals were euthanized 18 mpi, at 5 years of age. Brain sections were stained with NeuN antibody and neuronal layer thickness was evaluated in the hippocampus and in regions directly communicating with it (Fig. 4a-c). The thickness of CA1, CA3 pyramidal layers and dentate gyrus granular layer were positively correlated with each other (all $p<0.05$). The thicknesses of CA1 and CA3 pyramidal layers were respectively 8.6% and 9.7% lower in AD-inoculated animals than in CTRL ($p=0.13$ and $p=0.04$, respectively, Fig. 4c). The thickness of CA1 was negatively correlated with learning abilities of the animals ($p=0.04$, Extended Data Fig. 2b). The thickness of the dentate gyrus granular layer, layer II of the entorhinal cortex and retrosplenial cortex was not impacted by inoculation with AD brain homogenates (Fig. 4c).

Brain sections were then evaluated for Aβ and tau pathologies. As expected, CTRL-inoculated animals did not show any amyloid deposits. Surprisingly, we detected very few cortical amyloid plaques (Fig. 4d-e) or amyloid angiopathy (Fig. 4d-h) in AD-inoculated animals. However, the proportion of mouse lemurs harboring amyloid positive lesions was increased in the AD-inoculated animals as compared to CTRL-inoculated ones (3/6 versus 0/6, Chi-square=4.00, df=1, $p=0.045$). In the AD-inoculated animals, amyloidosis was never localized close to the injection sites, and no tau lesions were detected with AT8 or AT100 staining. We also did not detect obvious signs of glial reactivity in any mouse lemurs (Extended Data Fig. 3).

Our results support the transmission of AD pathology by brain inocula in primates and complement recent evidence supporting iatrogenic induction of amyloidosis in humans[1,2].

Contrary to previously published data, we demonstrate for the first time a clinical impact of the inoculation of AD brain homogenates as they resulted in pronounced cognitive, functional and morphological alterations. Most alterations were not detected 6 mpi but became obvious at 12 mpi ruling out an immediate toxicity of the homogenates. These results provide strong arguments for further evaluating functional outcomes in humans potentially contaminated with amyloid-positive tissues.

The ability to induce a neurodegenerative process in AD-inoculated mouse lemurs despite the absence of severe neuropathological lesions is striking. The induction of clinical symptoms in the absence of detectable pathological protein accumulation after inoculation of brain homogenates was previously reported for classical prion diseases[22] but never in the context of AD. The functional deficits accompanied by atrophy without tau or Aβ pathology bear some similarity to cases of "suspected non-Alzheimer's pathophysiology (SNAP)" meaning individuals with imaging evidence of AD-like neurodegeneration without β-amyloidosis (reported to be 9 to 21% of subjects clinically diagnosed with AD[23]). The recent "Amyloid/Tau/Neurodegeneration" classification of AD biomarkers has further emphasized the possibility of detecting AD-related neurodegeneration in the absence of strong amyloid or tau lesions[24].

Studies in humans have shown that neuronal loss contributing to cognitive alterations is not correlated with amyloid deposits and exceeds substantially the number of neurons with pathological tau lesions[25]. Conversely, soluble forms of Aβ or tau are highly toxic[26,27] and can initiate a self-replicating process[28]. Our results, in a non-human primate less prone to developing amyloid plaques or tau lesions than humans or transgenic mice[29], strongly suggest the following: 1) agents inducing toxic species, not detected by immunohistology, can be transmitted experimentally; 2) these toxic species are aggressive enough to induce a neurodegenerative process; and 3) the widespread morphological defects provide evidence for a propagation of these species to the whole brain. Our conclusion is that these transmissible toxic species are a critical target for future therapeutic strategies against Alzheimer's disease.

References

1 Jaunmuktane, Z. *et al.* Evidence for human transmission of amyloid-beta pathology and cerebral amyloid angiopathy. *Nature* **525**, 247-250 (2015).

2 Kovacs, G. G. *et al.* Dura mater is a potential source of Abeta seeds. *Acta Neuropathol.* **131**, 911-923 (2016).

3 Meyer-Luehmann, M. *et al.* Exogenous induction of cerebral beta-amyloidogenesis is governed by agent and host. *Science* **313**, 1781-1784 (2006).

4 Clavaguera, F. *et al.* Transmission and spreading of tauopathy in transgenic mouse brain. *Nat. Cell. Biol.* **11**, 909-913 (2009).

5 Walsh, D. M. & Selkoe, D. J. A critical appraisal of the pathogenic protein spread hypothesis of neurodegeneration. *Nat. Rev. Neurosci.* **17**, 251-260 (2016).

6 Gajdusek, D. C. Transmissible and non-transmissible amyloidoses: autocatalytic post-translational conversion of host precursor proteins to beta-pleated sheet configurations. *J. Neuroimmunol.* **20**, 95-110 (1988).

7 Eisele, Y. S. *et al.* Multiple factors contribute to the peripheral induction of cerebral beta-amyloidosis. *J. Neurosci.* **34**, 10264-10273 (2014).

8 Clavaguera, F. *et al.* Peripheral administration of tau aggregates triggers intracerebral tauopathy in transgenic mice. *Acta Neuropathol.* **127**, 299-301 (2014).

9 Beekes, M., Thomzig, A., Schulz-Schaeffer, W. J. & Burger, R. Is there a risk of prion-like disease transmission by Alzheimer- or Parkinson-associated protein particles? *Acta Neuropathol.* **128**, 463-476 (2014).

10 Heuer, E., Rosen, R. F., Cintron, A. & Walker, L. C. Nonhuman primate models of Alzheimer-like cerebral proteopathy. *Curr. Pharm. Des.* **18**, 1159-1169 (2012).

11 Brown, P. *et al.* Human spongiform encephalopathy: the National Institutes of Health series of 300 cases of experimentally transmitted disease. *Ann. Neurol.* **35**, 513-529 (1994).

12 Ridley, R. M., Baker, H. F., Windle, C. P. & Cummings, R. M. Very long term studies of the seeding of beta-amyloidosis in primates. *J. Neural. Transm.* **113**, 1243-1251 (2006).

13 Languille, S. *et al.* The grey mouse lemur: A non-human primate model for ageing studies. *Ageing Res. Rev.* **11**, 150-162 (2012).

14 Bons, N., Mestre, N. & Petter, A. Senile plaques and neurofibrillary changes in the brain of an aged lemurian primate, *Microcebus murinus*. *Neurobiol. Aging* **13**, 99-105 (1991).

15 Picq, J. L., Aujard, F., Volk, A. & Dhenain, M. Age-related cerebral atrophy in nonhuman primates predicts cognitive impairments. *Neurobiol. Aging* **33**, 1096–1109 (2012).

16 Giannakopoulos, P. *et al.* Quantitative analysis of tau protein-immunoreactive accumulations and beta amyloid protein deposits in the cerebral cortex of the mouse lemur, *Microcebus murinus*. *Acta Neuropathol.* **94**, 131-139 (1997).

17 Papegaey, A. *et al.* Reduced Tau protein expression is associated with frontotemporal degeneration with progranulin mutation. *Acta Neuropathol. Commun.* **4**, 74 (2016).

18 Picq, J. L., Villain, N., Gary, C., Pifferi, F. & Dhenain, M. Jumping stand apparatus reveals rapidly specific age-related cognitive impairments in mouse lemur primates. *PLoS ONE* **10**, e0146238 (2015).

19 Hoffman, K. L. *et al.* The upshot of up states in the neocortex: from slow oscillations to memory formation. *J. Neurosci.* **27**, 11838-11841 (2007).

20 Mander, B. A. *et al.* Beta-amyloid disrupts human NREM slow waves and related hippocampus-dependent memory consolidation. *Nat. Neurosci.* **18**, 1051-1057 (2015).

21 Sawiak, S. J., Picq, J. L. & Dhenain, M. Voxel-based morphometry analyses of *in vivo* MRI in the aging mouse lemur primate. *Front. Aging Neurosci.* **6**, 82 (2014).

22 Lasmezas, C. I. *et al.* Transmission of the BSE agent to mice in the absence of detectable abnormal prion protein. *Science* **275**, 402-405 (1997).

23 Chetelat, G. *et al.* Atrophy, hypometabolism and clinical trajectories in patients with amyloid-negative Alzheimer's disease. *Brain* **139**, 2528-2539 (2016).

24 Jack, C. R., Jr. *et al.* A/T/N: An unbiased descriptive classification scheme for Alzheimer disease biomarkers. *Neurology* **87**, 539-547 (2016).

25 Gomez-Isla, T. *et al.* Neuronal loss correlates with but exceeds neurofibrillary tangles in Alzheimer's disease. *Ann. Neurol.* **41**, 17-24 (1997).

26 Haass, C. & Selkoe, D. J. Soluble protein oligomers in neurodegeneration: lessons from the Alzheimer's amyloid beta-peptide. *Nat. Rev. Mol. Cell. Biol.* **8**, 101-112 (2007).

27 Lasagna-Reeves, C. A. *et al.* Identification of oligomers at early stages of tau aggregation in Alzheimer's disease. *Faseb J.* **26**, 1946-1959 (2012).

28 Langer, F. *et al.* Soluble Abeta seeds are potent inducers of cerebral beta-amyloid deposition. *J. Neurosci.* **31**, 14488-14495 (2011).

29 Rosen, R. F. *et al.* Comparative pathobiology of beta-amyloid and the unique susceptibility of humans to Alzheimer's disease. *Neurobiol. Aging* **44**, 185-196 (2016).

30 Bons, N., Sihol, S., Barbier, V., Mestre-Frances, N. & Albe-Fessard, D. A stereotaxic atlas of the grey lesser mouse lemur brain (*Microcebus murinus*). *Brain Res. Bull.* **46**, 1-173 (1998).

31 Dhenain, M., Chenu, E., Hisley, C. K., Aujard, F. & Volk, A. Regional atrophy in the brain of lissencephalic mouse lemur primates: measurement by automatic histogram-based segmentation of MR images. *Magn. Reson. Med.* **50**, 984-992 (2003).

32 Infarinato, F. *et al.* On-going frontal alpha rhythms are dominant in passive state and desynchronize in active state in adult gray mouse lemurs. *PLoS ONE* **10**, e0143719 (2015).

33 Rahman, A. *et al.* Sleep deprivation impairs spatial retrieval but not spatial learning in the non-human primate grey mouse lemur. *PLoS ONE* **8**, e64493 (2013).

34 Ashburner, J. A fast diffeomorphic image registration algorithm. *Neuroimage* **38**, 95-113 (2007).

35 Good, C. D. *et al.* A voxel-based morphometric study of ageing in 465 normal adult human brains. *Neuroimage* **14**, 21-36 (2001).

36 Genovese, C. R., Lazar, N. A. & Nichols, T. Thresholding of statistical maps in functional neuroimaging using the false discovery rate. *Neuroimage* **15**, 870-878 (2002).

Acknowledgements

We thank the France-Alzheimer Association for funding this study. We thank V. Buee-Scherrer for tau biochemical evaluation. We thank the Brain Donation Program of the Brain Bank "GIE NeuroCEB" run by a consortium of Patients Associations: ARSEP (association for research on multiple sclerosis), CSC (cerebellar ataxias), France Alzheimer and France Parkinson, with the support of Fondation Plan Alzheimer and IHU A-ICM for providing the brain samples used in this study.

Author Contributions

C.G, J.K., E.E.C., J.L.P., F.Pi., M.D. designed the study. M.D. coordinated the study. F.N.N. provided the human brain samples. L.B., S.E., F.N.N., A.S.H and C.G characterized brain samples. C.G., M.D. and J.K. performed the inoculations and the MRI study. C.G., S.J.S., J.L.P., M.D., designed the MRI analysis. F.A. and F.Pi. raised mouse lemurs and conducted EEG evaluations. J.L.P. was in charge of cognitive evaluation. F.Pe., and C.G. performed immunohistological studies. C.G. and M.D. were responsible for statistical analysis and wrote the manuscript. J.K., L.B., C.D., A.S.H, J.P.D., E.E.C., J.L.P. and F.Pi. revised the manuscript.

Competing financial interests

The authors declare no competing financial interests.

Author Information

Reprints and permissions information is available at www.nature.com/reprints. The authors declare no competing financial interests. Readers are welcome to comment on the online version of the paper. Correspondence and requests for materials should be addressed to M.D. (Marc.Dhenain@cea.fr).

Methods

Animals and overall experimental plan

Experiments were conducted on 12 adult gray mouse lemurs (*Microcebus murinus*) (males, age=3.5±0.2 years). They were all born and bred in a laboratory breeding colony (UMR 7179 CNRS/MNHN, France; European Institutions Agreement #962773). Animals were maintained under a constant temperature of 24–26°C and relative humidity of 55% and were housed in individual cages with jumping and hiding enrichment. Seasonal lighting (summer: 14 hours of light/10 hours of dark; winter: 10 hours of light/14 hours of dark) was applied so as to coincide with the seasonal rhythm of the animals. Food consisted of fresh apple and a homemade mixture of banana, cereals, eggs and milk, and animals had free access to tap water. Before entering the study, all animals were checked for health and given an ophthalmologic examination. None of the animals were previously involved in pharmacological trials or invasive studies. The experiment was based on the inoculation of human brain homogenates from AD patients (AD group) or CTRL age-matched subject (CTRL group) in the hippocampus and adjacent cortex of mouse lemurs (n=6 animals per group). Group assignments of the animals to the two groups were performed in order to obtain two homogeneous groups with respect to learning abilities before the inoculation. Longitudinal behavioral, EEG and morphological MRI studies were performed up to 18 mpi followed by immunohistopathological examinations of brain tissues (age of death=5.0±0.2years, Supplementary Table 1). The investigators were blinded to the group allocation when assessing these outcomes. Two control animals were euthanized for ethical reasons at 12 mpi due to an abdominal infection following self-removal of abdominal sutures after wireless telemetry transmitter explantation. Therefore, these animals were not evaluated by MRI at 12, 15 or 18 mpi or for behavioral studies at 18 mpi.

Ethical statement

All animal experiments were conducted in accordance with the European Community Council Directive 2010/63/UE. Animal care was in accordance with institutional guidelines and experimental procedures were approved by local ethics committees (authorizations 12-089; ethics committee CEtEA-CEA DSV IdF).

Brain tissue homogenates

Frozen brain tissue samples (parietal cortex) from two AD patients (Braak stage VI, Thal stages 5 and 4, respectively) and from one age-matched control individual (Braak and Thal stages 0) were obtained from brains collected in a brain donation program of the Brain Bank GIE NeuroCEB run by a consortium of Patients Associations: ARSEP (French association for research on multiple sclerosis), CSC (cerebellar ataxias), France Alzheimer and France Parkinson, with the support of Fondation Plan Alzheimer and IHU A-ICM (Supplementary Table 2, Extended Data Fig. 1). The consent forms were signed by either the patients themselves or their next of kin in their name, in accordance with French bioethical laws. The Brain Bank GIE NeuroCEB has been declared at the Ministry of Higher Education and Research and has received approval to distribute samples (agreement AC-2013-1887). Parietal cortex samples were individually homogenized at 20% weight/volume (w/v) in sterile Dulbecco's phosphate-buffered saline (PBS, Gibco, ThermoFisher Scientific, France) in a ribolyser sample homogenizer (Hybaid). Brain homogenates were then aliquoted into sterile polypropylene tubes and stored at -80°C until use.

Characterization of brain homogenates

The inoculated brain tissues were first assessed by immunohistochemistry. Immunostaining was performed on 4-µm-thick paraffin sections. Sections were deparaffinized in xylene, rehydrated through ethanol (100%, 90%, and 70%) and finally rinsed under running tap water for 10 minutes. They were then incubated in 99% formic acid for 5 minutes, washed again under running tap water, quenched for endogenous peroxidase with 3% hydrogen peroxide and 20% methanol, and finally washed in water. Sections were then blocked by incubating the sections at room temperature for 30 minutes in 4% bovine serum albumin (BSA) in 0.05 M tris-buffered saline, with 0.05% Tween 20, pH=8 (TBS-Tween, Sigma). They were then incubated overnight at +4°C with the 6F3D anti-Aβ antibody (Dako, Glostrup, Denmark) or polyclonal anti-tau antibody (Dako, Glostrup, Denmark), routinely used for the detection of amyloid deposits and tau accumulation. The sections were further incubated with a biotinylated secondary antibody (25 minutes at room temperature), and the presence of the secondary antibody was revealed by streptavidin–horseradish peroxidase conjugate using diaminobenzidine as chromogen (Dako, Glostrup, Denmark) after which they were counterstained with Harris haematoxylin.

Brain homogenates were further characterized by biochemistry. For Aβ, brain homogenates were diluted in 6.8 M guanidine and 68 mM TrisHCl to obtain a 5 M guanidine final concentration with protease inhibitor (Complete Mini, Sigma Aldrich, MO, USA) and vortexed for 3 hours at room temperature. Aβ immunoquantification was performed in duplicates with human Aβ1-42 ELISA kits (Invitrogen, Carlsbad, CA, USA) according to the manufacturer's instructions. For tau characterization, brain homogenates were sonicated on ice for 5 minutes, centrifuged for 5 minutes at 3000g at +4°C, diluted in Tris 20 mM/SDS 2% and sonicated on ice for 5 minutes. Samples were normalized to 1 µg/µL, diluted in 2X LDS buffer with reducers and heated at +100°C for 10 minutes. Ten µg of samples were loaded on Criterion gels (Biorad, Hercules, CA, USA) and migrated in MOPS buffer for 90 minutes at 165V on ice. After membrane transfer, pS396 (Life technologies, Carlsbad, CA, USA) or tau-Cter antibodies[17] were incubated overnight at +4°C. Secondary anti-rabbit antibody (ref-23817-2, Biovalley, Nanterre, France) was then applied for 45 minutes at room temperature before ECL revelation. Operators were blinded to the status of the patients.

Stereotaxic injections in mouse lemurs

Brain homogenates were injected bilaterally in the dorsal hippocampus (AP 1.25 mm, DV 8.25 mm, L +/- 2.5 mm) and adjacent parietal cortex (AP 1.25 mm, DV 10.25 mm, L +/- 2.5 mm) during a stereotaxic surgery[30]. Animals were fasted the day before surgery. Pre-anesthesia (atropine, 0.025mg/kg, subcutaneous injection) was performed 30 minutes before anesthesia (Isoflurane, Vetflurane, 4.5% for induction and 1–2% for maintenance) as described previously[31]. Animals were then placed in a stereotaxic frame (Phymep, France). Burr holes were drilled in the appropriate location. Using 26-gauge needles, 6.5 µL of 10% w/v brain homogenates were injected bilaterally in the dorsal hippocampus at 1 µL/min. Needles were kept in place for an additional 2 minutes before they were slowly moved into the adjacent parietal cortex where bilateral injections were also performed (same volume and injection speed as described above). Needles were kept in place for an additional 5 minutes before being slowly removed. Respiration rate was monitored during the whole procedure and body temperature was maintained at 37±0.5°C with a heating blanket or air-heating system. Six animals received brain extract from the control patient (CTRL-inoculated group) and 6 animals received brain extract from AD patients (n=3 per patient, AD-inoculated group). The surgical area was cleaned (iodinate povidone, Vetedine, Vetoquinol, France), the incision was sutured and animals were placed in an incubator at 25°C and monitored until recovery from anesthesia.

Accelerating rotarod task

Mouse lemurs were evaluated with the accelerating rotarod task (model 7750, Ugo Basile, Italy) before inoculation and every 6 mpi. Animals were placed on a 5-cm-diameter rotating cylinder turning at 20 rotations per minute (rpm). The rod then accelerated steadily up to 40 rpm until the end of the test which was reached when the animal fell or gripped onto the rod during at least three consecutive turns without stabilizing its balance. Latency to fall or grip on the rod was recorded for each trial. Animals underwent 5 consecutive trials and the best result was recorded with values expressed in seconds. The system was cleaned with ethanol between each trial and each animal.

Visual discrimination test

The cognition of mouse lemurs was evaluated in an apparatus (Fig. 1a) adapted from the Lashley jumping stand apparatus[18] which is a vertical cage made of plywood walls except for the front panel which is a one-way mirror allowing observation. Two discrimination tasks were performed: a learning task and a long-term memory task. These tests involved a succession of visual discriminations during which the mouse lemur had to jump from a heightened central platform to one of two lateral boards allowing access to a reinforcing chamber containing a positive reward (the possibility of reaching a safe nestbox for a 2 minutes rest). Mouse lemurs prefer confined spaces, therefore reaching a nest when placed in an open space is a strong motivator for behavioral testing. If no jump is performed within one minute, the central station can be progressively and gently tilted downwards creating a slippery slope encouraging the mouse lemur to jump. Boards can be covered with removable easily-discriminable patches of varied shape, texture and pattern (*i.e.* visual discrimination clues). Each board can be locked in a stable position or unlocked to become unstable and fall if a lemur jumps on it. For a pair of patches, one patch is always associated with the stable board giving access to the nest (positive result). The other patch is always associated with the unstable board that falls when the lemur jumps on it (negative result). During a discrimination task, the mouse lemur had to identify the positive stimulus giving access to the nest. Left/right locations of the stimuli were randomly alternated during the attempts with the restriction of no more than three consecutive trials in the same configuration. Testing continued until a success criterion - defined as 8 correct choices out of 10 successive attempts - was achieved. Before the first test, lemurs underwent a habituation session composed of seven trials. For the first four trials, only one fixed central board was attached just below the nestbox opening. In trial

1, a cylindrical rod connected the central station to the board so that no jump was required to reach the nestbox. In trial 2, the rod was removed so that the mouse lemur had to jump onto the central board to access its nestbox. In trials 3 and 4, an opaque vertical screen was added above the middle of the board masking the nestbox opening. The mouse lemur had to jump onto the board and then walk under the screen to access its nestbox. For the final three trials, the fixed landing platform was placed alternately to the left or to the right of the nestbox opening which was masked by the opaque screen. After the habituation session, mouse lemurs underwent the first discrimination learning task – distinguishing between a pair of patches – to test their learning abilities. This task was first performed before inoculation and then at 6, 12, and 18 mpi with, each time, a new set of discrimination task stimuli (*i.e.* a new pair of patches). At the three post-inoculation time points, long-time retention was also evaluated through recall of the discrimination task from 6 months before (Fig 1b).

Electroencephalography (EEG)

EEG studies were conducted in mouse lemurs using telemetric devices as described before[32,33]. Briefly, animals received pre-anesthesia (Diazepam 5 mg/mL, Roche, France; intramuscular injection of 200 µL/100g animal) and were then anesthetized with isoflurane. A wireless telemetry transmitter (2.5g; PhysioTel F20-EET; Data Science, St Paul, MN, USA), equipped with simultaneous recording for one EEG and one electromyogram (EMG) channel (1–500 Hz sampling rate), was implanted in the abdominal cavity. The electrode leads were threaded subcutaneously from the abdomen to the skull. Using dental cement, electrodes were placed on the dura mater of the anterior frontal cortex according to a stereotaxic atlas of the mouse lemur brain[30]. For EMG recording, bipolar electrodes were sutured into the neck muscles with non-absorbable polyamide suture. Animals were monitored for respiration rate and body temperature during surgery, observed until anesthesia recovery, and allowed to recover from surgery for one week before recording. EEG and EMG data were continuously collected using a PC running Dataquest software (Data Science International, St Paul, MN, USA) linked to a receiver base (RPC-1, Data Science, St Paul, MN, USA) placed on the floor of the home cage inhabited by the implanted animals. Electrodes and the telemetry transmitter were removed after one week of recording using the same surgical conditions as for implantation. The EEG data were analyzed with Neuroscore v2.1.0 (Data Science International, St Paul, MN, USA). Analysis focused on the active state determined by locomotor activity recording (included in the telemetry data of EMG recordings). EEGs were performed before inoculation, plus 6, and 12 mpi. We focused on delta (0.5-4 Hz), theta (4-8

Hz), alpha (8-12 Hz), sigma (12-16 Hz), and beta (16-24 Hz) frequency waves. At each time point, each wave was normalized according to mean values in the CTRL-inoculated animals. The operator was blinded to the group attribution during EEG signal processing.

Morphological MRI

Morphological MRI was performed using T2-weighted spin-echo images recorded on a 7T spectrometer (Agilent, USA; TR=10000 ms, TE=17.4 ms, slice thickness=230 µm, field of view=29.4x29.4 mm^2, matrix=128x128, resolution=230x230 μm^2 zero-filled to 115x115 μm^2). Animals were anesthetized and monitored as described for stereotaxic injections. MR images were recorded for each animal before inoculation, 15 days after inoculation and then every 3 months after inoculation until 18 mpi. MR images were analyzed for voxel-based morphometry with SPM8 (Wellcome Trust Institute of Neurology, University College London, UK, (http://www.fil.ion.ucl.ac.uk/spm)) and the SPMMouse toolbox (http://spmmouse.org) as described previously[21]. Fifteen days post-inoculation images were not included in this analysis as they were only used to ensure accurate injection cannula placement and the lack of acute lesions following the surgery. Briefly, brain images were segmented into gray (GM) and white matter (WM) tissue probability maps using locally developed priors, then spatially transformed to the standard space using a GM mouse-lemur template[21]. Affine regularization was set for an average-sized template, with a bias non-uniformity cut-off FWHM of 10 mm, a 5 mm basis-function cut-off and a sampling distance of 0.3 mm. The resulting GM and WM portions were output in rigid template space and DARTEL[34] was used to create non-linearly registered maps for each subject and common templates for the cohort of animals. The warped GM portions for each subject were modulated with the Jacobian determinant from the DARTEL registration fields to preserve tissue amounts ('optimized VBM'[35]) and smoothed with a Gaussian kernel of 600 µm to produce maps for analysis. A general linear model was designed to evaluate relative changes in GM values as a function of time between the CTRL- and AD-inoculated groups. Longitudinal follow-up of each animal was taken into account in the design matrix and total intracranial volumes were taken as covariate of no interest. A two-tailed t-test contrast was performed to compare the two groups. To control for multiple comparisons, an adjusted p-value was calculated using the voxel-wise false discovery rate (FDR-corrected $p<0.05$) with extent threshold values of 10 voxels[36]. Voxels with a modulated GM value below 0.2 were not considered for statistical analysis. The operator was blinded to the group attribution during image processing.

Histology

Mouse lemurs were euthanized with an overdose of sodium pentobarbital (100 mg/kg intraperitoneally) followed by intracardiac perfusion with 4% paraformaldehyde in PBS. After overnight post-fixation, brains were cryoprotected using 15% and 30% sucrose solution. Brains were then frozen in isopentane and stored at -20°C. Forty µm-thick coronal sections of brains were cut on a sliding freezing microtome (SM2400, Leica Microsytem) and floating histological serial sections were preserved in a storage solution (glycerol 30%, ethylene glycol 30%, distilled water 30% and phosphate buffer 10%) at -20°c until use.

Immunohistochemistry

Serial sections of the entire brain were used for Aβ (4G8), tau (AT8 and AT100), glial fibrillary acidic protein (GFAP) and neuronal (NeuN) immunohistochemistry. Free-floating sections were rinsed in 0.1M PBS and then incubated in hydrogen peroxide 0.3% for 20 minutes. Human sections were used as positive controls. For 4G8 staining, 80% formic acid pre-treatment was applied for 2 minutes. Pre-treatment with PBS-Triton 0.5% (Triton X-100, Sigma Aldrich, MO, USA) and 3% BSA blocking was performed at +4°C before a 2 day-incubation with either biotinylated 4G8 (Covance, NJ, USA, 1/250), AT8 (Pierce endogen, IL, USA, 1/100), AT100 (Pierce endogen, IL, USA, 1/100), GFAP (Dako, Denmark, 1/5000), and NeuN (Abcam, Cambridge, UK, 1/2000) antibodies. Biotinylated anti-mouse or anti-rabbit secondary antibodies (IgG, Vector Laboratories, Burlingame, CA, USA) were incubated before revelation. The ABC Vectastain kit (Vector Laboratories, Burlingame, CA, USA) was used to amplify DAB revelation (DAB SK4100 kit, Vector Laboratories, Burlingame, CA, USA). Blinded qualitative evaluation of the stained sections was performed by two different operators (C.G., F.P.).

Layer thickness evaluation

NeuN-stained sections were used to evaluate the thickness of the CA1 and CA3 pyramidal layers, dentate gyrus granular layer, layer II of the entorhinal cortex, and retrosplenial cortex. CA1, CA3 and DG regions were assessed from 10 measurements per section, for 3 consecutive sections. The thickness of layer II of the entorhinal cortex was measured as the mean of 5 measurements per section for 6 consecutive sections. The thickness of the anterior retrosplenial cortex (layer I to VI) was measured on 2 consecutive sections as a mean of 5 measurements per section. All sections selected for each layer

represented the same levels along the anteroposterior axis. The operator was blinded to the group attribution during layer thickness evaluation.

Statistical analysis

Statistical analyses were performed using GraphPad Prism software (San Diego, CA, USA). Data are expressed as means ± standard error of the mean. Cognitive and motor experiments were evaluated by two-way repeated measures ANOVA (post-inoculation delay, group) followed by Bonferroni's multiple comparisons post-hoc tests. Data normality and variance homogeneity were evaluated using Shapiro-Wilk and Cochran C tests, respectively and data from behavior experiments were transformed as reciprocal in order to obtain normality and variance homogeneity. As values within CTRL-inoculated animals were very homogeneous at each time post-inoculation, we replaced 18 mpi missing data from the two CTRL animals that died by the worst values in the CTRL group at 18 mpi. EEG and neuronal layer thickness data were evaluated by Mann Whitney’s tests. Spearman's rank correlations were performed to examine relationships between EEG, neuronal layer thickness and behavioral data. The proportion of animals presenting with amyloid lesion in the CTRL and AD groups was compared with the Chi-square test. No statistical methods were used to predetermine sample size.

Legends

Figure 1. Cognitive dysfunctions in AD homogenate-inoculated mouse lemurs.

a. Pairwise visual discrimination task jumping-stand apparatus. Lemurs had to jump from a central platform to one of two boards that displayed different visual stimuli. One board gave access to a positive outcome (nest containing a reward) and the other led to a negative (and non-rewarding) outcome (fall). An increasing number of trials required to reach criterion indicates a performance decline. b. Schematic overview of the cognitive tasks. A learning task was performed before inoculation (0 months post-inoculation (mpi)). Long-term memory tasks consisted of the repetition of the discrimination task learned 6 months before. New learning tasks involving novel pairs of stimuli were performed every 6 months, after long-term memory tasks (black arrows: 6 month-long delay; grey arrows: 1 day delay). c. Progressive learning impairment in the AD-inoculated animals. Animals allocated to AD and CTRL groups had similar performance before inoculation and improved similarly at 6 mpi. Only CTRL-inoculated animals continued to improve at 12 and 18 mpi ($p<0.0001$ and $p=0.01$, respectively) and learning abilities were lower in AD-inoculated animals compared to CTRL at 12 mpi ($p=0.03$) and tended to be lower at 18 mpi ($p=0.10$). Also, the overall performance of the AD-inoculated group was significantly lower than that of CTRL group ($p=0.02$). d. In the long-term memory task, the overall performance of the AD-inoculated group and those at 6 and 18 mpi were significantly lower than those of CTRL-animals ($p=0.0002$, 0.0036, and 0.0024, respectively). e. The rotarod test did not reveal any motor dysfunction in either group. *: $p<0.05$; **: $p<0.01$; ***: $p<0.001$ ($n=6$ per group, two-way repeated measures ANOVA with Bonferroni's post-hoc tests). Error bars: standard error of the mean.

Figure 2. Neuronal activity alterations in AD-inoculated lemurs.

a-c. Evolution of EEG frequency power densities in the AD- and CTRL-inoculated groups before inoculation (a), 6 (b) and 12 (c) mpi ($n=6$ per group). b. At six mpi, the AD-inoculated group showed a decrease in delta frequency (0.5-4 Hz) and an increase in theta frequency (4-8 Hz) compared to CTRL-inoculated group ($p=0.009$ and $p=0.002$, respectively, Mann-Whitney's tests). c. At 12 mpi, the alterations in delta frequency was maintained ($p=0.009$, Mann-Whitney's tests). Alpha (8-12 Hz), sigma (12-16 Hz), and beta (16-24 Hz) frequencies were lighter in AD-inoculated group than in CTRL-inoculated group ($p=0.004$, $p=0.015$ and

p=0.009, respectively, Mann-Whitney's tests). * p<0.05; ** p<0.01. Error bars indicate standard error of the mean.

Figure 3. Gray matter loss in AD homogenate-inoculated mouse lemurs.

a. Statistical parametric heat-map depicting regions where gray matter volumes decreased in the AD group as compared to the CTRL group. Slices are spaced by 0.5mm throughout the brain (voxel-based morphometry parameters: FDR-corrected p<0.05; extent threshold k=10; heat-map represents T values). b-c. Lateral (b) and dorsal (c) 3D representations of atrophied areas. EC: Entorhinal cortex; DB: Diagonal band of Broca; Am: Amygdala; Hip: Hippocampus; nST: Nucleus stria terminalis; Fx: Fornix; Cd: Caudate nucleus; Pva: Peri-third ventricule area; IT: Inferotemporal cortex; PC: Posterior cingulate cortex; RS: Retrosplenial cortex. Dark blue clusters represent voxels with significant gray matter atrophy in posterior cingulate cortex and in retrosplenial cortex. Light blue clusters represent voxels with significant gray matter atrophy in the temporal areas of the brain (including the hippocampus, entorhinal cortex, amygdala, and the lateral and inferior temporal cortices) as well as the diagonal band of Broca, fornix and nucleus stria terminalis. Gray clusters represent other significant voxels. Red crosses display injection sites.

Figure 4. Histopathological alterations in AD -inoculated mouse lemurs.

a-b. NeuN staining of dorsal hippocampus in representative CTRL- (a) and AD-inoculated (b) animals. CA1, CA3 and dentate gyrus (DG) are highlighted. c. Comparison of the thickness of the CA1 and CA3 pyramidal layers, dentate gyrus granular layer, layer II of the entorhinal cortex and retrosplenial cortex of CTRL- and AD-inoculated animals. *: p<0.05, Mann-Whitney's test. d-h. Immunostaining of Aβ (4G8) in CTRL- (d) and AD-inoculated animals (e-h). Sparse 4G8-immunoreactivity could be detected in the parenchyma and vessels of 50% of AD-inoculated animals. Scale bars: 1 mm (a-b, d) and 50µm (insert in e and f-h). Error bars indicate standard error of the mean.

Supplementary Table 1. Schedule of the experimental protocol. mpi: months post-inoculation. MRI: Magnetic resonance imaging.

Supplementary Table 2. Human brain sample characteristics and staging. Human parietal cortex samples were obtained from two AD patients and one age-matched CTRL individual.

Supplementary Table 3. Brain regions with gray matter loss in the AD-inoculated group as compared to the CTRL-inoculated group. *: $p<0.05$; **: $p<0.01$; ***: $p<0.001$.

Extended Data Figure 1. Characterization of human brain samples and homogenates.

a-c. Immunohistochemical staining (6F3D antibody) for amyloid in the two Alzheimer samples (a-b) and in the control sample (c). Amyloid plaques are indicated with black arrows. Arrow heads correspond to amyloid angiopathy. The apparent brown background in b corresponds to extracellular diffuse amyloid deposits. d-f. Immunohistochemical staining (polyclonal anti-tau antibody) for tau lesions in the same samples. Tau positive NFTs are indicated with white arrows in the two Alzheimer samples (d-e). Most of the brown labelling corresponds to neuropil threads. Amyloid or tau lesions were not detected in the control subject (c-f). Scale bars: 50 µm. g-i. Biochemical characterization of human brain homogenates. g. $A\beta_{1-42}$ was only detected in AD brain homogenates (20% weight/volume) (ELISA). h. Typical AD shift of tau-Cter triplets in the AD samples compared to CTRL sample in Western blot (arrows). h. Pathological pS396 positive tau was only detected in AD samples by Western blot. Error bars indicate *standard error* of the mean (SEM).

Extended Data Figure 2. Correlations between cognitive abilities and EEG delta frequency (a) or thickness of CA1 hippocampal layer (b) .

a. Delta frequency measured by EEG 6 mpi was inversely correlated with long-term memory performances (Spearman's correlation test). b. The thickness of CA1 pyramidal layer was inversely correlated with learning abilities of the animals (Spearman's correlation test).

Extended Data Figure 3. Lack of glial reactivity in inoculated lemurs.

Immunostaining of astrocytes (GFAP) in the CA1 region of the hippocampus, parietal cortex (Cx) and entorhinal cortex (EC) in CTRL- and AD-inoculated animals. Regional differences are seen but qualitative evaluation did not provide evidence for changes in GFAP-immunoreactivity or astrocyte morphology between CTRL- and AD-inoculated animals. Scale bars: 100 µm.

Figures

Figure 1.

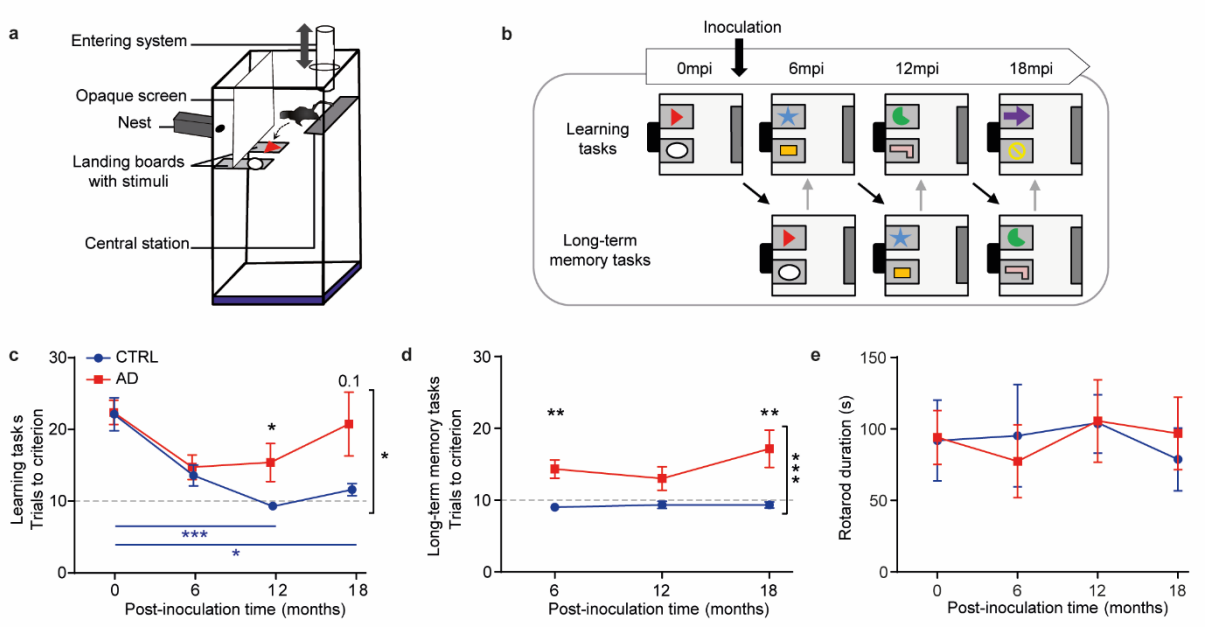

Figure 2.

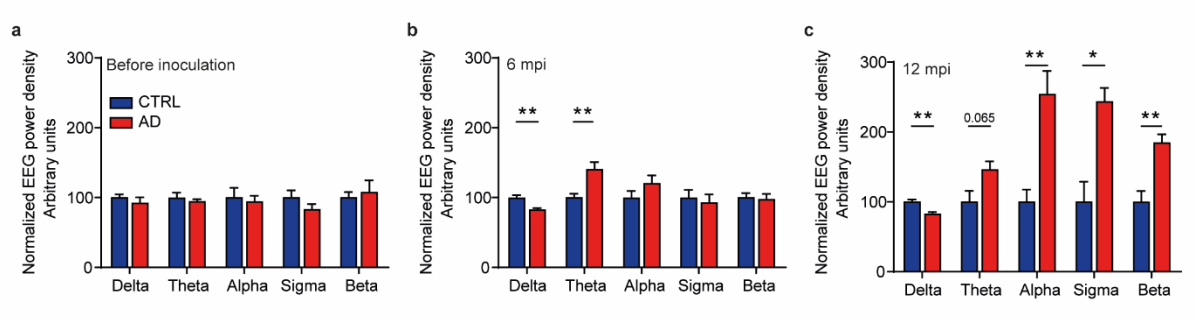
a
Before inoculation
CTRL
AD
Normalized EEG power density
Arbitrary units
300
200
100
0
Delta
Theta
Alpha
Sigma
Beta
b
6 mpi
**
**
c
12 mpi
**
0,065
**
*
**

Figure 3.

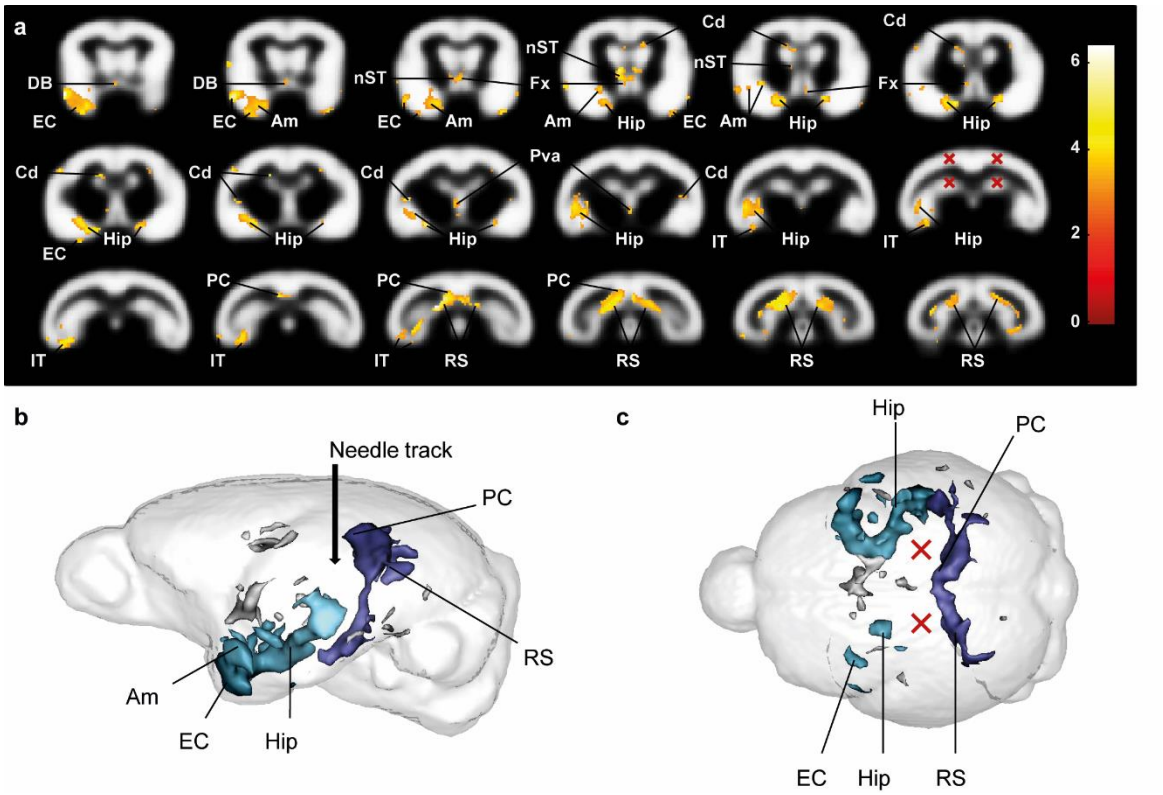
a
DB
EC
Am
nST
Fx
Hip
Cd
Pva
IT
PC
RS
6
4
2
0
b
Needle track
PC
RS
Am
EC
Hip
c
Hip
PC
EC
Hip
RS

Figure 4.

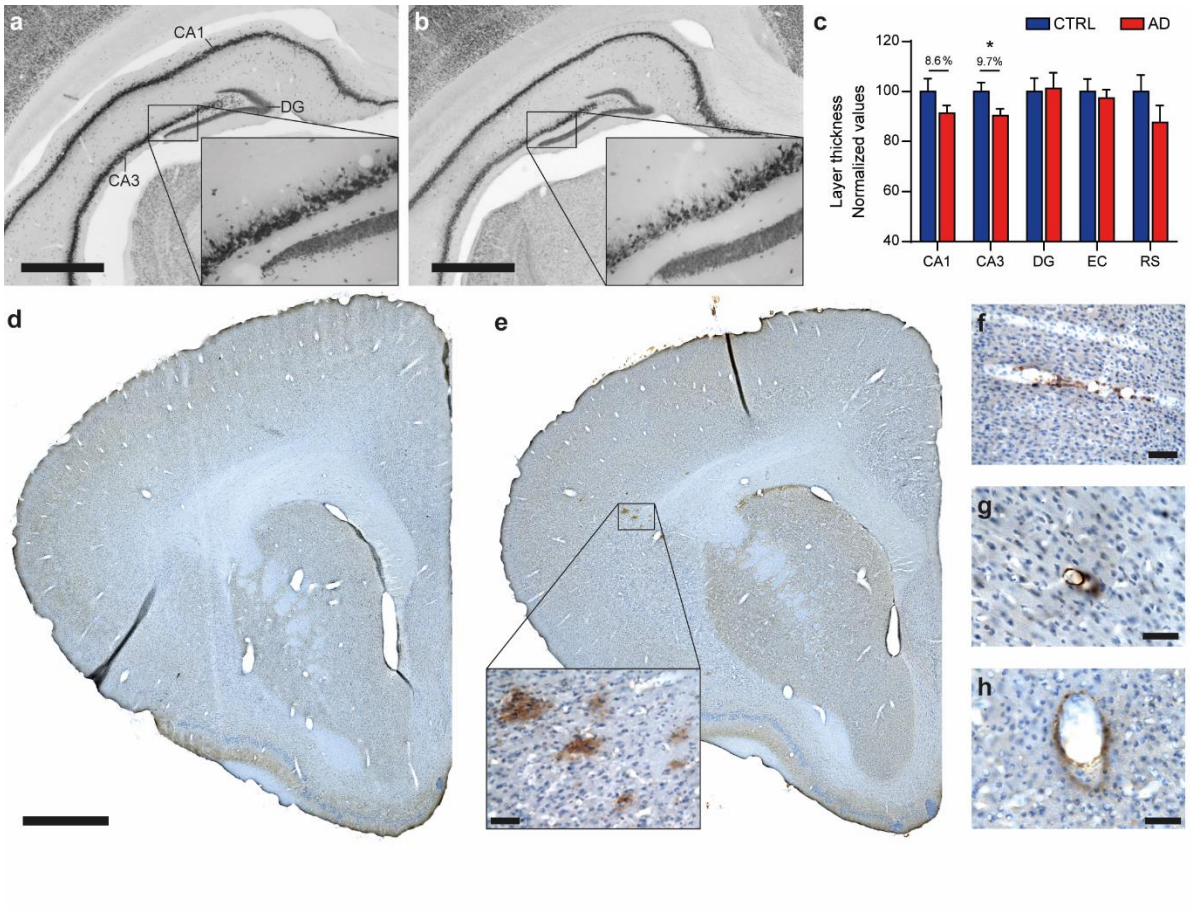
a
CA1
DG
CA3
b
c
CTRL
AD
8.6%
*
9.7%
Layer thickness
Normalized values
120
100
80
60
40
CA1
CA3
DG
EC
RS
d
e
f
g
h

Supplementary Tables

Supplementary Table 1.

Experimental protocol	Before inoculation	3mpi	6mpi	9mpi	12mpi	15mpi	18mpi
Rotarod test	X		X		X		X
Discrimination acquisition task	X		X		X		X
Long-term memory task			X		X		X
Electroencephalography	X		X		X		
MRI	X	X	X	X	X	X	X
Immunohistochemistry							X

Supplementary Table 2.

Patient	Braak stage	Thal phase	Age (years)	Post-mortem delay (hours)
AD 1	VI	5	76	10
AD 2	VI	4	83	21
CTRL	0	0	69	6

Supplementary Table 3.

Brain regions with gray matter loss in the AD- as compared to the CTRL-inoculated group	Cluster size (voxels)	Peak p-value FDR-corrected		Peak T value
Entorhinal cortex, amygdala, hippocampus and inferior temporal cortex	1562	***	0.0004	6.3952
Cingulate and retrosplenial cortices	1342	***	0.0004	6.3777
Diagonal band of Broca, fornix and nucleus and stria terminalis	184	**	0.0013	5.7422
Ventral hippocampus	103	*	0.0109	4.2790
Caudate nucleus	70	**	0.0059	4.8479
Entorhinal cortex	59	*	0.0117	4.2231
Lateral temporal cortex	55	**	0.0062	4.7998
Peri-third ventricule area	52	*	0.0112	4.2488
Inferior temporal cortex	47	*	0.0175	3.8968
Fornix and stria terminalis	33	**	0.0061	4.8140
Parietal cortex	31	**	0.0045	5.0162
Amygdala	30	*	0.0102	4.4005
Lateral temporal cortex	23	*	0.0221	3.6795
Amygdala	22	*	0.0267	3.4984
Parietal cortex	18	*	0.0227	3.6538
Amygdala	18	*	0.0255	3.5305
Inferior temporal cortex	17	*	0.0221	3.6785
Caudate nucleus	16	**	0.0067	4.7113
Fornix	15	*	0.0172	3.9105
Inferior temporal cortex	15	*	0.0193	3.7971
Caudate nucleus	14	*	0.0233	3.6270
Inferior temporal cortex	13	*	0.0234	3.6142
Inferior temporal cortex	13	*	0.0140	4.0705
Entorhinal cortex	11	*	0.0135	4.1200
Parietal cortex	10	*	0.0108	4.3009
Amygdala	10	*	0.0255	3.5285

Extended Data

Extended Data Figure 1.

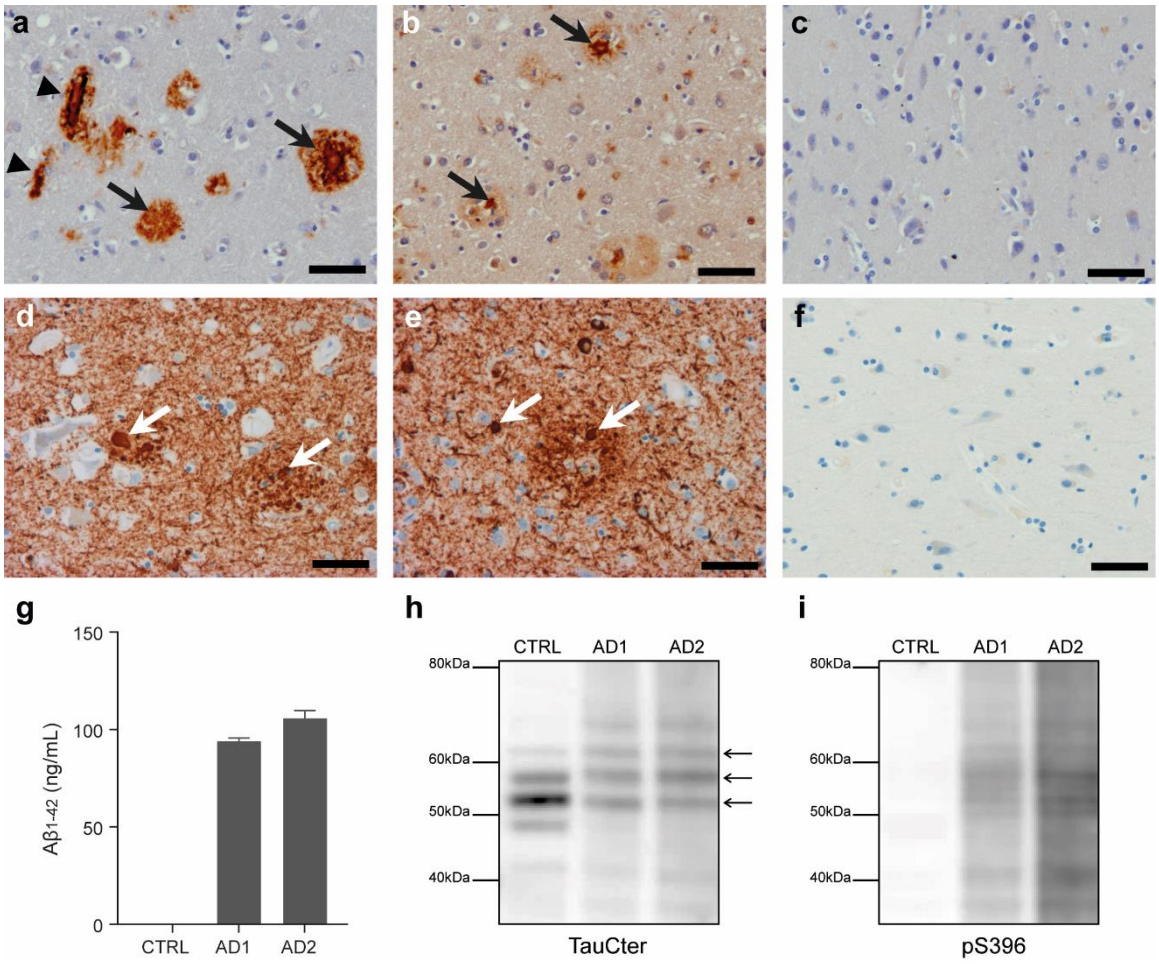

Extended Data Figure 2.

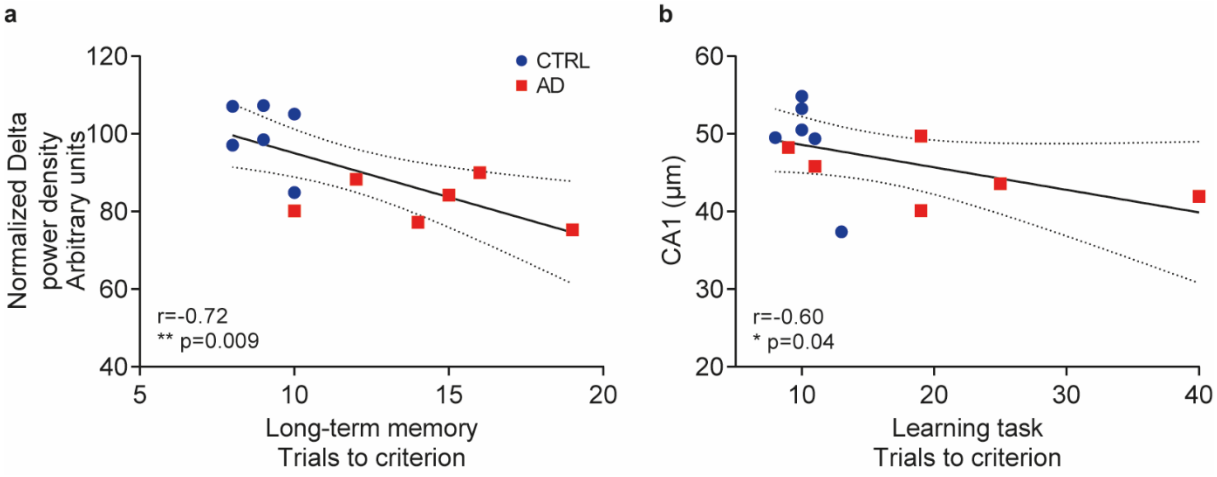

Extended Data Figure 3.

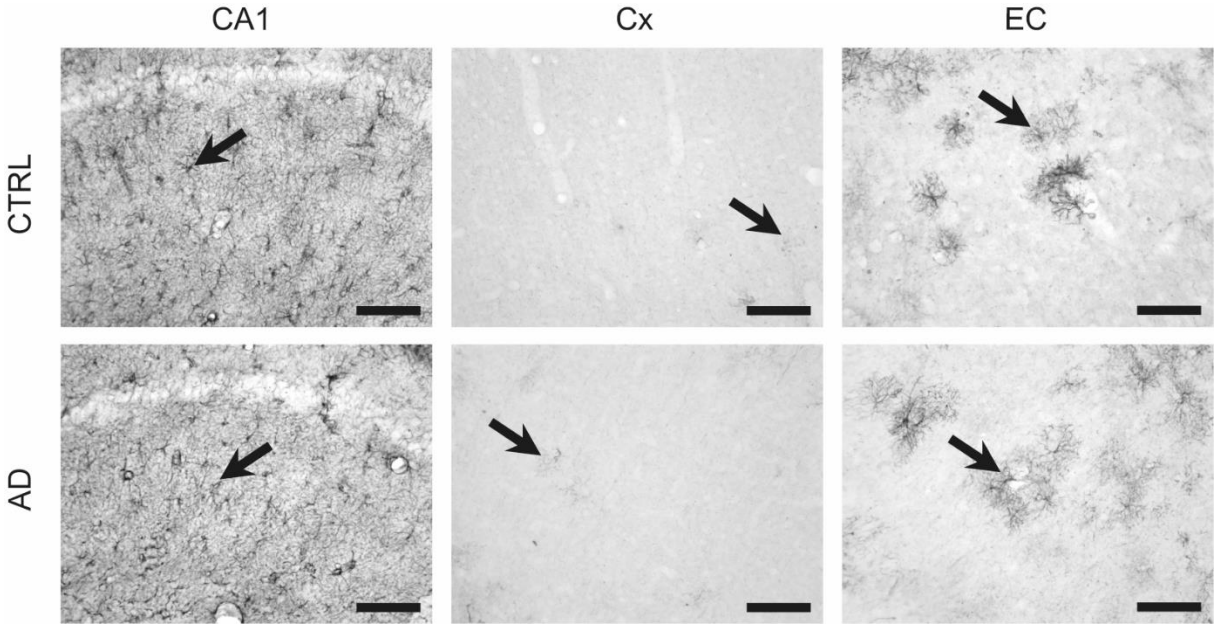

PLOS ONE

RESEARCH ARTICLE

Jumping Stand Apparatus Reveals Rapidly Specific Age-Related Cognitive Impairments in Mouse Lemur Primates

Jean-Luc Picq[1,2,3]*, Nicolas Villain[4], Charlotte Gary[2,3], Fabien Pifferi[4], Marc Dhenain[2,3]

1 Laboratoire de psychopathologie et de neuropsychologie, E.A. 2027, Université Paris 8, 2 rue de la liberté, 93000 St Denis, France, **2** Centre National de la Recherche Scientifique (CNRS), Université Paris-Sud, Université Paris-Saclay UMR 9199, Neurodegenerative Diseases Laboratory, F-92265 Fontenay-aux-Roses, France, **3** Commissariat à l'Energie Atomique et aux Energies Alternatives (CEA), Département des Sciences du Vivant (DSV), Institut d'Imagerie Biomédicale (I2BM), MIRCen, F-92265 Fontenay-aux-Roses, France, **4** CNRS UMR 7179, MNHN, Adaptive Mechanisms and Evolution (MECADEV), 1 Av du petit château, 91800 Brunoy, France

* jean_lucpicq@hotmail.com

OPEN ACCESS

Citation: Picq J-L, Villain N, Gary C, Pifferi F, Dhenain M (2015) Jumping Stand Apparatus Reveals Rapidly Specific Age-Related Cognitive Impairments in Mouse Lemur Primates. PLoS ONE 10(12): e0146238. doi: 10.1371/journal.pone.0146238

Editor: Michael Taffe, The Scripps Research Institute, UNITED STATES

Received: September 10, 2015

Accepted: December 15, 2015

Published: December 30, 2015

Data Availability Statement: All relevant data are within the paper and its Supporting Information files.

Funding: This work was supported by the Association France Alzheimer. The funder had no role in study design, data collection and analysis, decision to publish, or preparation of the manuscript.

Competing Interests: The authors have declared that no competing interests exist.

Abstract

The mouse lemur (*Microcebus murinus*) is a promising primate model for investigating normal and pathological cerebral aging. The locomotor behavior of this arboreal primate is characterized by jumps to and from trunks and branches. Many reports indicate insufficient adaptation of the mouse lemur to experimental devices used to evaluate its cognition, which is an impediment to the efficient use of this animal in research. In order to develop cognitive testing methods appropriate to the behavioral and biological traits of this species, we adapted the Lashley jumping stand apparatus, initially designed for rats, to the mouse lemur. We used this jumping stand apparatus to compare performances of young (n = 12) and aged (n = 8) adults in acquisition and long-term retention of visual discriminations. All mouse lemurs completed the tasks and only 25 trials, on average, were needed to master the first discrimination problem with no age-related differences. A month later, all mouse lemurs made progress for acquiring the second discrimination problem but only the young group reached immediately the criterion in the retention test of the first discrimination problem. This study shows that the jumping stand apparatus allows rapid and efficient evaluation of cognition in mouse lemurs and demonstrates that about half of the old mouse lemurs display a specific deficit in long-term retention but not in acquisition of visual discrimination.

Introduction

As age-related cognitive impairment has become a major health problem in our societies, the need for valid animal model to investigate the biological basis of this decline and to develop efficient treatments is a crucial concern. For about two decades, there has been a growing interest in the use of a small nonhuman primate, the grey mouse lemur (*Microcebus murinus*), for studying aging and age-associated diseases [1]. Indeed, with its mouse-like body size (body

length 12 cm, 60–120 g) rendering its breeding and housing cost-efficient, this nocturnal, rapidly maturing (puberty occurs at about 6–8 months) and short-lived (about a decade in captivity) primate offers a useful compromise between the practicalities and affordability of rodents and the evolutionary proximity to humans of monkeys or apes. This proximity was well illustrated by many studies that have brought out similarities of mouse lemurs and humans in the age-related changes occurring in brains, including amyloid plaque formation and neurofibrillary changes [2,3]; pathological tau metabolism [4]; neurochemical alterations [5]; neuronal loss in specific cerebral structures (e.g., the nucleus basalis of Meynert) [6]; iron accumulation [7]; and varying patterns of cerebral atrophy [8]. Interestingly, the atrophy of some brain regions such as septum, hippocampus or entorhinal cortex was only detected in a subcategory of aged mouse lemurs and was correlated with cognitive impairments, which suggests that it is related to pathological aging [9].

Concerning behavioral assessment, several studies have demonstrated that the pattern of age-related cognitive alteration in mouse lemurs [10,11] is strikingly reminiscent of that described in humans [12], namely a preserved procedural memory, a progressive and widespread decline in executive function and an impairment in declarative-like memory that is limited to a subpopulation of aged individuals. Nevertheless much work remains to be done in order to streamline the cognitive assessment of mouse lemurs. Indeed, many reports indicate insufficient adaptation of the mouse lemur to experimental devices mainly initially developed for rodents or large monkeys, leading to excessive duration of experimental trials and/or disproportionate elimination of individuals as non-responders during the training stages. For example, in a study by Ritchie et al. [13], more than 9 months of training were required for a single visual discrimination in a couple of animals. Regarding the rate of non-responders, high levels of attrition from 30 to more than 50% were often reported [14,15]. Moreover, a great inter-individual variability in the performance of control groups was frequently noted [16]. Such variability is likely to be more related to variable motivation or emotionality than to variable cognitive ability and can impede detection of subtle cognitive impairment in any experimental group. Recent progress was made to standardize cognitive testing in mouse lemurs by using an automated touchscreen-based procedure [17]. This approach has the main advantages of minimizing operator-subject interaction and facilitating cross-taxa comparisons as it can be used in a variety of species, including humans. The first publication on this apparatus reported that mouse lemurs need 24 days of training on average and more than 200 trials to reach the criterion of success assigned to a simple task of discrimination [17]. Another way to improve cognitive testing of mouse lemurs is to consider their specific behavioral and biological traits in order to design new devices enabling them to express their full cognitive potential. As mouse lemurs have an arboreal lifestyle and are powerful jumpers, developing apparatus and procedures allowing movements in the three-D space appears particularly well suited for an efficient behavioral testing of this species. In 1930, in order to study visual perception in rodents, Lashley designed a jumping stand apparatus [18]. To perform a discrimination task within this apparatus, rats had to jump from an elevated stand to one of two doors positioned in front of them. If the rat jumps to the correct door, the door swings open and the rat lands on a table behind and receives food or water reward. If it chooses wrongly, it strikes against the locked window and fall into a net slung beneath the apparatus. The jumping stand is rarely used today in rodents, because they are not prone to jumping and were forced to jump by being mildly shocked. On the contrary, mouse lemurs are jumping animals and our goal was to design a version of the jumping stand for lemurs. First, the test we designed was based on an elevated stand that can progressively be tilted downwardly causing a slippery slope pushing gently the mouse lemur to jump. Second, the target doors were replaced by target platforms that were stable for correct choices and

unstable, leading to the fall of the animals, for incorrect choices. In addition, a positive reward (*i.e.* the possibility to attain a safe nestbox) was maintained when the animal reached the correct platform. As underscored by Sutherland and Mackintosh [19] the jumping stand technique has the great advantage that it forces animals to look toward the stimuli before responding (usually for some time as they normally hesitate before leaping the gap) and it gives immediate positive or negative reinforcement after a correct or an incorrect jump. The main goal of the present study was to determine whether the jumping stand apparatus adapted to mouse lemurs allows obtaining fast and efficient learning and could be used as a reliable tool for testing cognition in this species.

The second goal of our study was to test whether the jumping stand apparatus can evaluate age-related cognitive alterations in mouse lemurs. The jumping stand apparatus can assess different cognitive abilities through a large panel of tasks such as simple discriminations, delayed matching (or nonmatching) to samples or shifting tasks. Acquisition and retention of simple discrimination learning task are differentially sensitive to medial temporal lobe lesions [20,21,22] and as temporal lesions are altered in a subcategory of old mouse lemurs [9], impairment was expected in retention but not in acquisition of discrimination problems. We thus designed discrimination and retention tasks based on the jumping stand apparatus to evaluate medial temporal lobe-dependent and non-medial temporal lobe-dependent cognitive performance in young and old mouse lemurs.

Materials and Methods

2.1. Ethics statement

The study was non-invasive and carried out in accordance with the European Communities Council Directive (2010/63/UE). The research was conducted under the approval of the CETEA-CEA DSV IdF ethic committee under the authorization number 12–089. In accordance with the recommendations of the Weatherall report, "The use of non-human primates in research", special attention was paid to the welfare of the animals. Neither nociceptive stimuli nor food deprivation were used during this work.

2.2. Animals

Twenty male grey mouse lemurs (*Microcebus murinus*) were evaluated. The young adult group consisted of 12 animals ranging from 3 to 4.2 years (mean age = 3.3 years) and the aged adult group consisted of 8 animals ranging from 7 to 10 years (mean age = 7.5 years). These age categories were consistent with age classification in previous studies and were based on survival data of the breeding colony which has a mean and a maximum lifespan of 56 and 120 months, respectively [1]. The animals were born and reared in the Brunoy colony (MNHN, France, licence approval N° A91.114.1). They had no previous experience with cognitive testing nor with any drug trial or experimental surgeries. The mouse lemurs, solitary foragers in the wild, were housed in individual cages to reduce stress due to capture and transport to the separate experimental room. The cages were enriched with tree branches and wooden nests (nestbox) and were kept at standard temperature (24–26°C) and relative humidity (55%). The mouse lemurs were tested during the summer-like long day length (14:10 hours light-darkness) that corresponds to the active phase of the animals. Animals were raised on fresh fruits and a laboratory daily-made mixture of cereals, milk and eggs. Water and food were given *ad libitum*. The eyes of the mouse lemurs were examined by a veterinary ophthalmologist and no anomalies were detected that would affect visual acuity.

2.3. Apparatus

Experiments were performed in a separate testing room containing the apparatus. The apparatus (see Fig 1) was a big vertical cage (height = 150 cm) made of plywood walls except the front panel that was a one-way mirror to allow observation. It was illuminated by 50-W bulb attached to the center of the cage ceiling. The mouse lemur was placed inside the cage on the center of an elevated plastic starting platform (the jumping stand) through an open-ended dark cylinder that opened in the roof of the cage. After this cylinder was gently lifted, the mouse lemur was required to jump from the elevated stand onto one of two landing platforms (15 cm x 30 cm) across a 35-cm gap. If it did not jump within one minute the starting stand was progressively tilted downwardly causing a slippery slope pushing the mouse lemur to jump. If it jumped onto the correct platform, it could pass under an opaque Plexiglass screen to access its nestbox placed behind the wall of the cage. This opaque screen prevented mouse lemurs from jumping directly to the opening of the nestbox. If it jumped onto the incorrect platform, the platform swung down and the mouse lemur fell into the bottom of the cage on a wide soft pillow to avoid any risk of injury. A small door at the base of the right wall of the cage allowed to take back the mouse lemur and to put it back on the starting platform for another trial. The correct and the incorrect platforms were distinguished by visual stimuli placed on them. The training pairs of stimuli were randomly drawn from a pool of 20 pairs. Within each pair, stimuli were chosen to be easily discriminable as the goal was to test cognitive and not visual capacities. Accordingly the two stimuli of the same pair differed both in shape, texture, brightness or pattern. Practically, they were made of different materials (cardboard, plastic, polystyrene, fabric. . .).

No food reinforcement was used. The reward for positive choices consisted in allowing the mouse lemur to reach its nestbox and then to be "home safe" for some time. This reward is particularly efficient in mouse lemurs as they are very keen to find their nestbox, due to their habit in their natural environment to make use of tree holes as vital means to evade predation, ensure thermoregulation, and park infants during food foraging [23].

2.4. Testing procedure

2.4.1. Overview of the performed tasks. Two discrimination problems (D1 and D2) and a long term-memory test (retention phase) of the first discrimination problem (D1r) were used (see Fig 2). During the first discrimination problem (D1), the mouse lemurs had to discriminate two visual stimuli. The mouse lemurs were given each day a session of a maximum of 25 trials. Testing continued until the mouse lemurs reached a criterion of eight correct choices for ten consecutive trials. The long term-memory test (D1r) was performed one month after the first discrimination problem. The following day a new discrimination problem (D2) was performed. For each test, the score was the number of errors (wrong choices leading to a fall) before reaching the criterion. One day before the first discrimination test, each mouse lemur was given a habituation session to learn the task.

2.4.2. Habituation. The habituation session was composed of seven trials. For the first four trials, only one fixed central landing platform was attached just below the nestbox opening. On trial 1, a cylindrical rod connected the jumping stand to the landing platform so that no jump was required to attain the nestbox whose opening was visible from the starting stand. On trial 2, the rod was removed so that the mouse lemur had to jump onto the central landing platform to access its nestbox. On trials 3 and 4, an opaque vertical screen was added above the middle of the landing platform masking the nestbox opening. The mouse lemur had to jump onto the central landing platform then to walk under the screen to access its

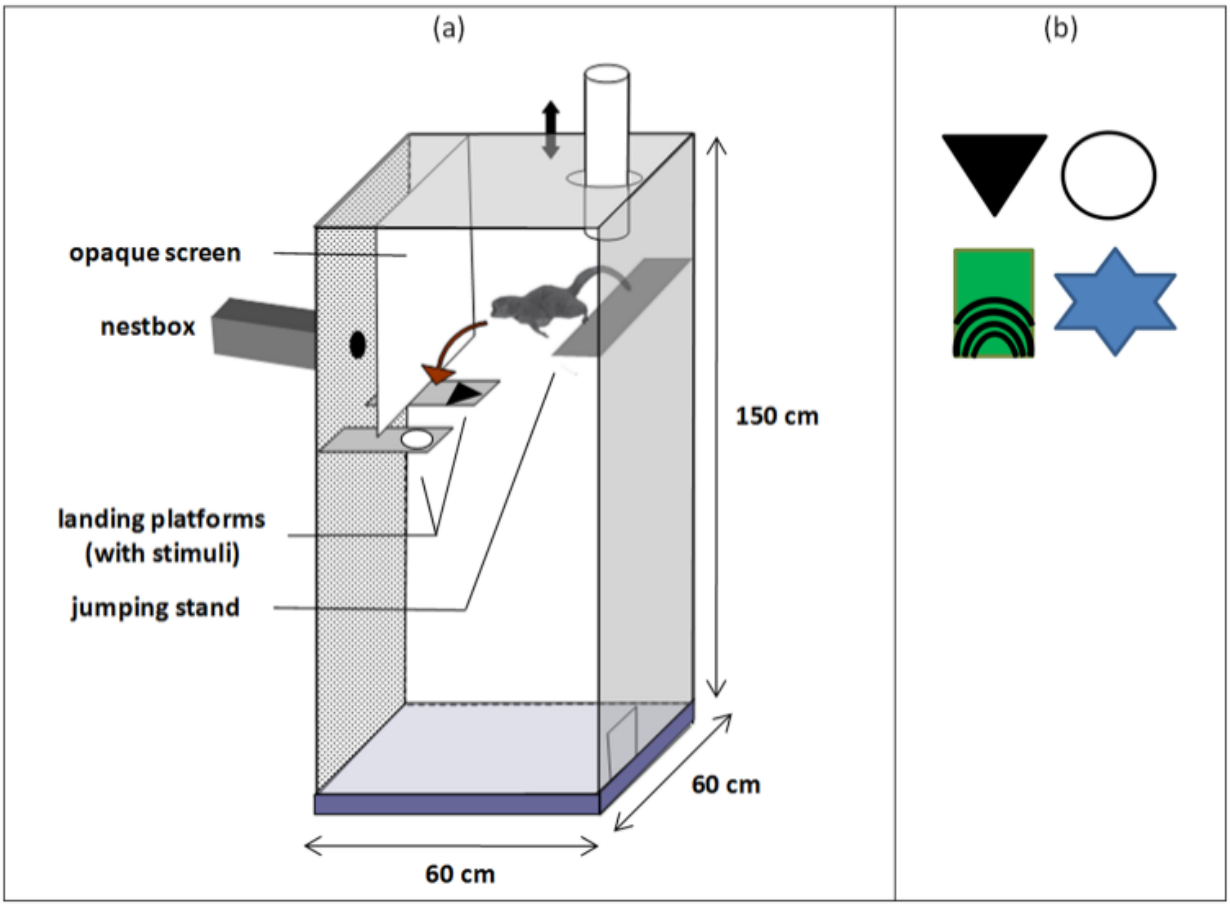

Fig 1. Jumping stand apparatus for mouse lemurs (a) and pairs of stimuli used for the two discrimination problems (b).

doi:10.1371/journal.pone.0146238.g001

nestbox. For the last three trials, the fixed landing platform was placed alternatively to the left or to the right of the nestbox opening which was masked by the opaque screen.

2.4.3. Discrimination tests. During the discrimination problems (D1, D1r, and D2), mouse lemurs were given each day a session of a maximum of 25 trials. On each trial, the mouse lemur faced two landing platforms. It had to choose the positive landing platform which gave access to a 2-min rest in its nestbox and to avoid the negative platform which resulted in the fall of the platform leading to the drop of the animal in the bottom of the cage. After a fall, the mouse lemur was left in the bottom for 20 seconds before being taking back for another trial. The discrimination was based on visual stimuli that differed in shape, texture, brightness or pattern. These stimuli (diameter about 15 cm) were interchangeably attached to the front of the landing platforms. The location of the stimuli on the right or left landing platforms was randomized with the restriction that the positive stimulus was not located on the same platform for more than three consecutive trials. Two different pairs of stimuli were selected for the two discrimination tests. One pair consisted of a black plastic triangle versus a white cardboard circle and the other pair consisted of a green rubber rectangle with black

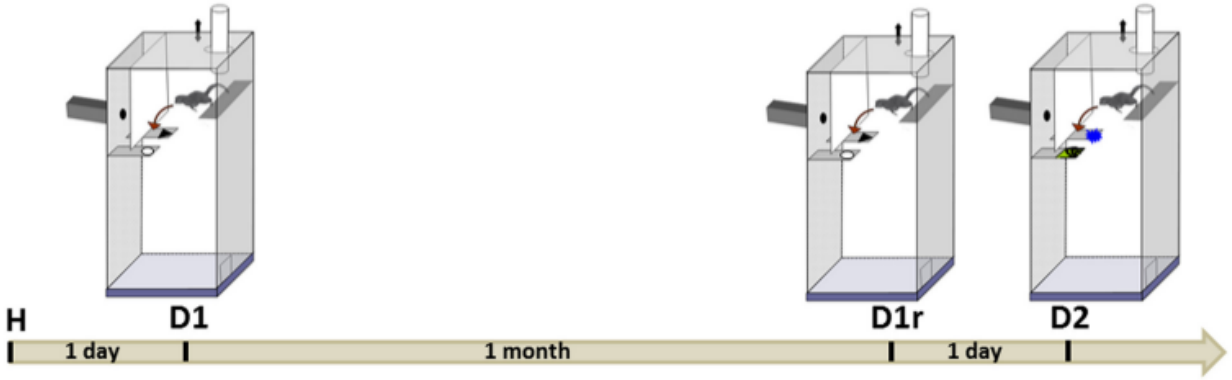

Fig 2. Timeline of tasks. H: habituation, D1: first discrimination problem, D1r: retention of the first discrimination problem, D2: second discrimination problem.

doi:10.1371/journal.pone.0146238.g002

concentric lines versus a blue star-shaped rigid paper (Fig 1b). The order of the two discrimination problems was reversed for half the animals.

2.5. Data analysis

All values are expressed as mean ± standard error of the mean (SEM). Performances between tasks (acquisition, retention, new acquisition) were compared in each age-group with paired Student's t-test analyses and performances between young and old animals on each task were compared with unpaired Student's t-test analyses. The level of statistical significance was $p < 0.05$.

Results

The general performances of young and old mouse lemurs in the D1, D1r and D2 tasks are presented in Table 1. All tested animals succeeded in acquiring the first visual discrimination (D1) in one or two sessions. The mouse lemurs needed from 13 to 41 trials to reach the criterion (median = 26 or 24 for young animals or aged animals, respectively). Thus the first discrimination could be learnt in only two days. Evaluation of the animals for the long term-memory test (D1r) or the new discrimination problem (D2) was also performed very rapidly, *i.e.* within one day (Table 1).

In the first visual discrimination (D1) the mean number of errors to criterion was 11.9 ±1.2 for the young group and 10.9 ±1.5 for the aged group (see Fig 3 and S1 Table). No group differences were observed between young and old individuals ($t = 0.53$, $p > 0.05$; Fig 3). On the retention phase of the first discrimination problem (D1r), both young and old animals succeeded faster than in the learning of the discrimination (D1) ($t = 9.68$ and 6.25, respectively,

Table 1. Mean ± SEM number of days and trials to reach the success criterion in the jumping stand apparatus. The figures in brackets indicate the score range. Attrition rate was null for each task.

	D1		D1r		D2	
	Days	Trials	Days	Trials	Days	Trials
Youngs	2 (1/2)	26±2 (13/41)	1 (1/1)	9±0 (8/10)	1 (1/1)	15±1 (9/23)
Olds	2 (1/2)	24 (14/40)	1 (1/1)	12±1 (8/18)	1 (1/1)	14±1 (10/22)

doi:10.1371/journal.pone.0146238.t001

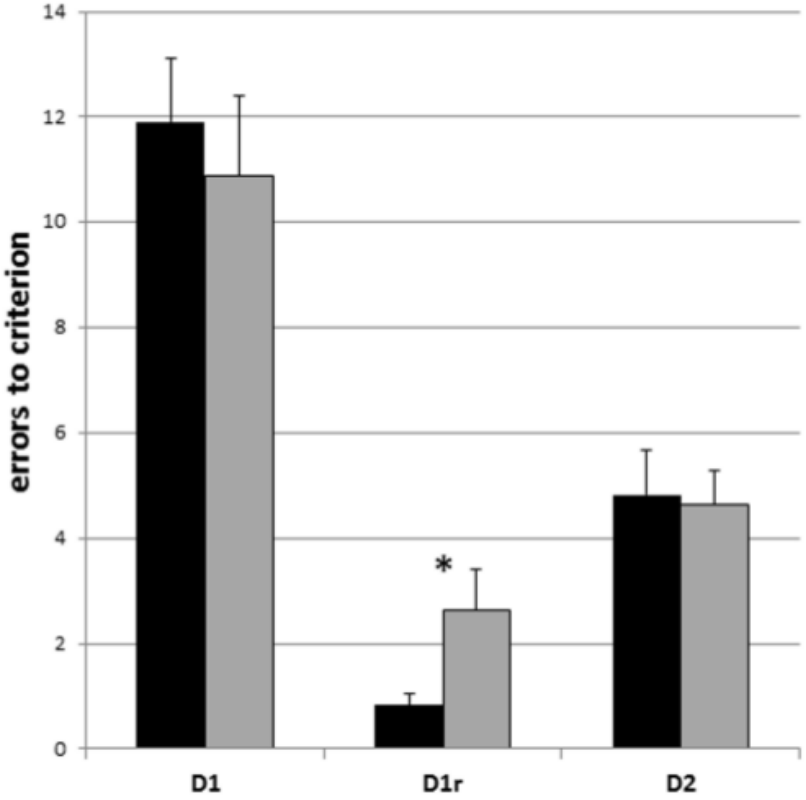

Fig 3. Mean scores on the first discrimination problem (D1), retention of the first discrimination problem (D1r) and second discrimination problem (D2) in young (black) and older (grey) adult animals. Errors bars depict SEM. * indicates a significant difference.

doi:10.1371/journal.pone.0146238.g003

$p < 0.001$). All young mouse lemurs immediately attained at least a 80% correct response level (criterion level) in the first ten trials (errors ≤ 2, mean = 0.8 ±0.2). The older animals made more errors before reaching criterion (mean = 2.6 ±0.8) than the young ones ($t = 26$, $p = 0.018$) and only half of the aged mouse lemurs succeeded in reaching the criterion in the first ten trials (Fig 3). No differences between young and aged mouse lemurs were seen on the second discrimination problem (D2, $t = 0.17$, $p > 0.05$). The performances on D2 were significantly better than those recorded on D1 for both the young and old individuals ($t = 6.72$ and 4.64, respectively, $p < 0.01$; Fig 3). The performances on D1r were significantly better than those recorded on D2 for the young individuals ($t = 5.07$, $p < 0.01$) but not for the aged individuals ($t = 2.25$, $p > 0.05$).

Discussion

The main goal of our study was to determine whether the jumping stand technique is an efficient way to test the cognitive capacities of mouse lemurs. Our findings demonstrate that naive mouse lemurs are able to master a visual discrimination task in a very small number of trials (13 to 41) after a short habituation session of only seven trials. Even though the

criterion to be reached was not the same, young adult mouse lemurs needed far fewer trials (median = 26) to acquire a pairwise discrimination in the jumping stand task than in earlier protocols involving odor discrimination [24], visual discrimination using the touchscreen procedure [17] or visual discrimination of illuminated vs. dark corridors [11], which required about 500, 200 or 80 trials, respectively. The cognitive demand being identical in all these discrimination tasks, the excellent performance of mouse lemurs in the jumping stand apparatus was likely based on sensory, motor, attentional and motivational parameters that make this procedure particularly appropriate to their biology. Indeed, in the jumping stand procedure, the visual stimuli were easily detectable and discriminable by mouse lemurs. Also attention was quickly focused on these stimuli as the mouse lemurs were strongly motivated to escape from the well-lighted and very exposed slippery stand and no other target was available. Moreover, the required jump response is a central part of the spontaneous locomotor behavior of this arboreal species. Finally, choices were instantly either rewarded (access to the nest-box) or punished (fall) making the conditioning procedure more powerful byCombining positive and negative reinforcements across trials. Moreover rewards and punishments are ecologically significant for mouse lemurs in this protocol since falling from an unstable support is a natural risk for an arboreal jumping species. In accordance with the high performances of mouse lemurs in the jumping stand, which suggests that this test procedure is relatively straightforward for this species, the attrition rate recorded in the present study over the whole experiment was zero. Given the relatively limited number of mouse lemurs (in comparison to rats or mice) available for laboratory studies, it is important that as few animals as possible have to be excluded as non-responders before completing a cognitive test battery. Another advantage of the jumping stand apparatus is that simple cognitive tasks such as visual discrimination tasks carried out in this device did not result in excessive inter-individual variability in young adult control group. Indeed most young adult mouse lemurs (11 out of 12) needed from 20 to 40 trials to reach criterion. The variability among young individuals in the present study was even far more limited in the retention test (D1r), since all mouse lemurs needed only from 8 to 10 trials to reach criterion. Thus discrimination tasks in the jumping stand device seem sufficiently sensitive to detect mild cognitive deficit in aged subjects (or in any other experimental group) and to reach statistical significance with a relatively low number of animals. Another interest of the jumping stand apparatus is that it will be easy in further studies to test separately each dimension (shape, size, texture, color, pattern) of the visual stimulus and to determine which dimension is most relevant for the mouse lemur and whether one dimension can induce age-related impairment. Moreover intra-dimensional and extra-dimensional shift tasks, which are known to be especially vulnerable to aging in primates [25,26,27], could easily be carried out.

In our study, the older mouse lemurs learned the first visual discrimination problem with a level of performance similar to that of the young ones. All aged animals performed inside the range score of the younger group. Thus the motor requirement of the jumping stand procedure was moderate enough not to impede cognitive capacity expression in aged individuals. The lack of age-related cognitive impairment in discrimination learning is consistent with previous studies in mouse lemurs [9,11,24] and has been frequently reported in rodents [28] and monkeys [29,30,31]. To the extent that such tasks can be solved on the basis of acquisition of attentional and motor biases towards individual stimuli, there are thought to mainly involve procedural memory, a form of memory well preserved in the human aging process [32,33]. Nevertheless a recent study using a touchscreen device found that aged mouse lemurs are impaired in the acquisition of a visual discrimination between two images [17]. Strong differences between the jumping stand and the touchscreen procedures concerning many

parameters such as the required motor response, the type of reinforcers used and the nature of visual stimuli to discriminate can suffice to explain the contrasting observations.

Both young and aged mouse lemurs learned the second discrimination problem (D2) much more quickly than the first one and the two age groups showed a similar level of performance. This improvement in the second problem likely relies on memory of the general rules of the discrimination task (transfer effect) in the jumping stand apparatus, supporting rapid solutions of new problems of the same class. However, although both young and old animals performed better on the retention task (D1r) than on the first discrimination (D1), the performance of the young group was better than that of the old animals in the retention task (D1r). Young animals showed a perfect recall of the specific stimulus discrimination problem a month after criterion was met. This higher level of accuracy in the retention test of the first discrimination problem cannot be ascribed to rapid acquisition of a learning set in young animals because their performance decreased in the following second discrimination problem when compared to the retention problem. This suggests that long term retention of the general rules of discrimination problems and long term retention of a specific discrimination problem have to be differentiated. Our data show that, while all the young animals were able to reach the criterion in the first ten trials of the retention test, only half of the aged animals were able to do so. The old mouse lemurs with worse scores performed as well as the young adults in both the first and the second discrimination problems. These results suggest that some aged mouse lemurs can display deficit in long term retention of a specific stimulus discrimination problem and be perfectly capable to master discrimination learning and to acquire a learning set by retaining the general rules of these tasks. This acquisition-retention distinction in discrimination tasks has been supported by experiments that demonstrated that rats with entorhinal/hippocampal lesions acquired successive discrimination problems in the same amount of time as did controls but showed marked deficits in the retention phase of these discrimination problems after long intervals of time [22]. This selective retention impairment suggests that medial temporal lobe structures are important for retaining specific visual discriminations over long delay intervals but neither for mastering a discrimination task nor for improving performance over successive discrimination problems [21,34]. This gradual gain in performance across problems is probably partly due to progressive acquisition of the procedural aspects of testing with experience and more dependent on corticostriatal circuits [35]. The present findings are consistent with previous data from our team that revealed age-related hippocampal and entorhinal atrophy in a subpopulation of aged mouse lemurs and a relationship between that atrophy and poor spatial memory performance in the circular platform test [9]. Thus we hypothesize that poor performance in the retention test of specific discrimination problems after long delays is sensitive to entorhinal/hippocampal dysfunction. The procedure described in the present study might detect aged mouse lemurs affected by pathological aging processes involving these areas. Further magnetic resonance imaging and histological evaluations of the brain of mouse lemurs tested in the jumping stand will help to explore this hypothesis.

In conclusion, the jumping stand apparatus appears to be a powerful tool for testing cognition in mouse lemurs and for exploring age-related impairment. Its efficiency can be explained because the apparatus is designed for the arboreal lifestyle of the lemurs as well as for their sensorial and behavioral skills. We suggest that it can also be adapted to evaluate cognitive abilities of other arboreal animals.

Supporting Information

S1 Table. Individual performances of the mouse lemurs.
(DOCX)

Acknowledgments

We thank Sabine Chahory (National Veterinary School of Maison-Alfort) for performing the eye examinations of the animals as well as Fabienne Aujard (CNRS UMR 7179) for critical evaluation of the manuscript.

Author Contributions

Conceived and designed the experiments: JLP. Performed the experiments: JLP NV. Analyzed the data: JLP CG MD. Contributed reagents/materials/analysis tools: JLP NV CG FP MD. Wrote the paper: JLP MD.

References

1. Languille S, Blanc S, Blin O, Canale CI, Dal-Pan A, Devau G, et al. (2012) The grey mouse lemur: A non-human primate model for ageing studies. Ageing Research Reviews 11: 150–162. doi: 10.1016/j.arr.2011.07.001 PMID: 21802530
2. Bons N, Mestre N, Petter A (1991) Senile plaques and neurofibrillary changes in the brain of an aged lemurian primate, *Microcebus murinus*. Neurobiology of Aging 13: 99–105.
3. Mestre-Francés N, Silhol S, Bons N (1996) Evolution of β-amyloid deposits in the cerebral cortex of *Microcebus murinus* lemurian primate. Alzheimer Research 2: 19–28.
4. Delacourte A, Sautière P-E, Wattez A, Mourton-Gilles C, Petter A, Bons N (1995) Biochemical characterisation of tau proteins during cerebral aging of the lemurian primate *Microcebus murinus*. Comptes Rendus de l'Académie des Sciences, Série III, Sciences de la Vie 318: 85–89.
5. Jallageas V, Privat N, Mestre-Francés N, Bons N (1998) Age-related changes in serotonergic and catecholaminergic brain systems in the lemurian primate *Microcebus murinus*. Annals of the New York Academy of Sciences 839: 628–630. PMID: 9629227
6. Mestre N, Bons N (1993) Age-related cytological changes and neuronal loss in basal forebrain cholinergic neurons in *Microcebus murinus* (Lemurian primate). Neurodegeneration 2: 25–32.
7. Dhenain M, Duyckaerts C, Michot J-L, Volk A, Picq J-L, Boller F (1998) Cerebral T2-weighted signal decrease during aging in the mouse lemur primate reflects iron accumulation. Neurobiology of Aging 19: 65–69. PMID: 9562505
8. Dhenain M, Michot JL, Privat N, Picq JL, Boller F, Duyckaerts C, et al. (2000) MRI description of cerebral atrophy in mouse lemur primates. Neurobiology of Aging 21: 81–88. PMID: 10794852
9. Picq JL, Aujard F, Volk A, Dhenain M (2012) Age-related cerebral atrophy in nonhuman primates predicts cognitive impairments. Neurobiology of Aging 33: 1096–1109. doi: 10.1016/j.neurobiolaging.2010.09.009 PMID: 20970891
10. Languille S, Lievin-Bazin A, Picq JL, Louis C, Dix S, De Barry J, et al. (2014) Deficits of psychomotor and mnesic functions across aging in mouse lemur primates. Front Behav Neurosci 8: 446. doi: 10.3389/fnbeh.2014.00446 PMID: 25620921
11. Picq JL (2007) Aging affects executive functions and memory in mouse lemur primates. Exp Gerontol 42: 223–232. PMID: 17084573
12. Gabrieli JD (1996) Memory systems analyses of mnemonic disorders in aging and age-related diseases. Proc Natl Acad Sci U S A 93: 13534–13540. PMID: 8942968
13. Ritchie K, Silhol S, Bons N (1997) Assessment of cognitive functioning in the lemurian primate *Microcebus murinus*: the development of the PAC-MM testing procedures. Alzheimer's Research 3: 37–41.
14. Trouche SG, Maurice T, Rouland S, Verdier JM, Mestre-Frances N (2010) The three-panel runway maze adapted to Microcebus murinus reveals age-related differences in memory and perseverance performances. Neurobiol Learn Mem 94: 100–106. doi: 10.1016/j.nlm.2010.04.006 PMID: 20403446
15. Vinot N, Jouin M, Lhomme-Duchadeuil A, Guesnet P, Alessandri JM, Aujard F, et al. (2011) Omega-3 fatty acids from fish oil lower anxiety, improve cognitive functions and reduce spontaneous locomotor activity in a non-human primate. PLoS One 6: e20491. doi: 10.1371/journal.pone.0020491 PMID: 21666750
16. Joly M, Michel B, Deputte B, Verdier JM (2004) Odor discrimination assessment with an automated olfactometric method in a prosimian primate, Microcebus murinus. Physiology & Behavior 82: 325–329.

17. Joly M, Ammersdorfer S, Schmidtke D, Zimmermann E (2014) Touchscreen-based cognitive tasks reveal age-related impairment in a primate aging model, the grey mouse lemur (Microcebus murinus). PLoS One 9: e109393. doi: 10.1371/journal.pone.0109393 PMID: 25299046

18. Lashley KS (1930) The mechanism of vision I. A method for the rapid analysis of pattern vision in the rat. Journal of Genetic Psychology [Name in 1930: The pedagogical seminary and journal of genetic psychology] 37: 453–460.

19. Sutherland NS, Mackintosh NJ (1971) Mechanisms of animal discrimination learning: New York: Academic Press.

20. Epp J, Keith JR, Spanswick SC, Stone JC, Prusky GT, Sutherland RJ (2008) Retrograde amnesia for visual memories after hippocampal damage in rats. Learning & memory (Cold Spring Harbor, NY) 15: 214–221.

21. Levisohn LF, Isacson O (1991) Excitotoxic lesions of the rat entorhinal cortex. Effects of selective neuronal damage on acquisition and retention of a non-spatial reference memory task. Brain Res 564: 230–244. PMID: 1810624

22. Vnek N, Gleason TC, Kromer LF, Rothblat LA (1995) Entorhinal-hippocampal connections and object memory in the rat: acquisition versus retention. J Neurosci 15: 3193–3199. PMID: 7722656

23. Kappeler PM (1998) Nests, tree holes, and the evolution of primate life histories. Am J Primatol 46: 7–33. PMID: 9730211

24. Joly M, Deputte B, Verdier JM (2006) Age effect on olfactory discrimination in a non-human primate, Microcebus murinus. Neurobiol Aging 27: 1045–1049. PMID: 15955599

25. Moore TL, Killiany RJ, Herndon JG, Rosene DL, Moss MB (2003) Impairment in abstraction and set shifting in aged rhesus monkeys. Neurobiology of Aging 24: 125–134. PMID: 12493558

26. Moore TL, Killiany RJ, Rosene DL, Prusty S, Hollander W, Moss MB (2002) Impairment of executive function induced by hypertension in the rhesus monkey (Macaca mulatta). Behavioral Neuroscience 116: 387–396. PMID: 12049319

27. Dias R, Robbins TW, Roberts AC (1997) Dissociable forms of inhibitory control within prefrontal cortex with an analog of the Wisconsin Card Sort Test: restriction to novel situations and independence from "on-line" processing. Journal of Neuroscience 17: 9285–9297. PMID: 9364074

28. Gilbert PE, Pirogovsky E, Brushfield AM, Luu TT, Tolentino JC, Renteria AF (2009) Age-related changes in associative learning for olfactory and visual stimuli in rodents. Annals of the New York Academy of Sciences 1170: 718–724. doi: 10.1111/j.1749-6632.2009.03929.x PMID: 19686218

29. Bartus RT, Dean RL, Fleming DL (1979) Aging in the rhesus monkey: effects on visual discrimination learning and reversal learning. Journal of Gerontology 34: 209–219. PMID: 108323

30. Lai ZC, Moss MB, Killiany RJ, Rosene DL, Herndon JG (1995) Executive system dysfunction in the aged monkey: spatial and object reversal learning. Neurobiology of Aging 16: 947–954. PMID: 8622786

31. Rapp PR (1990) Visual discrimination and reversal learning in the aged monkey (*Macaca mulatta*). Behavioral Neuroscience 104: 876–884. PMID: 2285486

32. Cohen NJ, Squire LR (1980) Preserved learning and retention of pattern-analyzing skill in amnesia: dissociation of knowing how and knowing that. Science 210: 207–210. PMID: 7414331

33. Squire LR (1992) Memory and the hippocampus: a synthesis from findings with rats, monkeys, and humans. Psychological Review 99: 195–231. PMID: 1594723

34. Vnek N, Rothblat LA (1996) The hippocampus and long-term object memory in the rat. J Neurosci 16: 2780–2787. PMID: 8786453

35. Mishkin M, Petri HL (1984) Memories and habits: some implications for the analysis of learning and retention. In: Squire LR, Butters N, editors. Neuropsychology of Memory: New York: Guilford. pp. 287–296.

Résumé de thèse

Partie I – Introduction générale

1.1. La maladie d'Alzheimer

La maladie d'Alzheimer (MA) est la forme la plus fréquente de démence (70% des cas, Baumgart et al., 2015). C'est une maladie progressive et terminale menant à la perte complète de l'autonomie du patient. Elle est caractérisée par une altération progressive des capacités cognitives incluant une détérioration de la mémoire.

En fonction de l'âge de déclaration des symptômes, deux types de MA, précoce ou tardive, peuvent être distingués (Blennow et al., 2006). La MA précoce est une forme génétique de la maladie associée à de nombreuses mutations de gènes impliqués dans le métabolisme du peptide β-amyloïde (Aβ) (Goate et al., 1991; Levy-Lahad et al., 1995; Schellenberg et al., 1992). La MA tardive est une maladie sporadique représentant plus de 99% des cas. D'étiologie multifactorielle, de nombreux facteurs de susceptibilité génétique et de risques environnementaux peuvent influencer le risque de MA sporadique (Reitz et al., 2011).

En neuropathologie, la MA est définie par l'agrégation dans le cerveau de deux protéines, le peptide Aβ et la protéine Tau, présentant une structure malconformée enrichie en feuillets β (Haass et Selkoe, 2007). Ces protéines malconformées s'associent et s'agrègent de manière progressive. Ces agrégats mènent à la formation de dépôts extracellulaires (amyloïdose), appelés plaques amyloïdes dans le parenchyme et angiopathie amyloïde dans les vaisseaux, et intracellulaires (tauopathie) dénommés dégénérescences neurofibrillaires, respectivement pour Aβ et Tau (Duyckaerts et al., 2009).

De nos jours, le diagnostic de MA n'est que probable du vivant du patient. Il est établi sur la base d'un examen clinique et de tests neuropsychologiques (Folstein et al., 1975; Hughes et al., 1982) et le diagnostic définitif de MA ne peut être posé que *post-mortem* (McKhann et al., 2011). Des traitements symptomatiques de la MA sont actuellement commercialisés mais n'apportent qu'un soulagement limité et temporaires des symptômes. Le développement de traitements curatifs de la MA est donc un véritable défi pour la recherche.

1.2. Les maladies à prions

Un prion, acronyme pour « PRoteinaceous Infection ONly particule » (Prusiner, 1982), est un pathogène protéique constitué de protéines malconformées. Les prions sont responsables chez

l'Homme des encéphalopathies spongiformes (maladies à prions) telles que la maladie de Creutzfeld-Jakob. Ces maladies, d'origine génétique, sporadique ou infectieuse (Colby et Prusiner, 2011), sont cliniquement caractérisées par l'apparition rapide d'une démence progressive associée à divers signes cliniques. En neuropathologie, elles sont définies par la formation de vacuoles (changement spongiformes), une neurodégénérescence et une gliose associée à l'accumulation d'une protéine malconformée riche en feuillets β (Caughey et al., 1991), la Protease-resistant Protein (PrP, Bolton et al., 1982).

Les protéines PrP malconformées peuvent transmettre leur mépliement à des protéines PrP natives (Aguzzi et Heppner, 2000) menant à la transmission et à la propagation de la maladie au sein du tissu et entre individus. Elles sont très résistantes à la dégradation (Riesner, 2003) et, par analogie à d'autres agents infectieux, peuvent présenter différentes souches sous-tendues par des conformations riches en feuillets β alternatives menant à des pathologies présentant des phénotypes différents (Colby et Prusiner, 2011).

1.3. Concepts théoriques sur les protéines amyloïdes

Les protéines Aβ, Tau et PrP font partie de la famille des protéines amyloïdes définie comme des protéines pouvant former des agrégats fibrillaires polypeptidiques avec une conformation enrichie en feuillets β (Fändrich, 2007).

La formation de ces agrégats amyloïdes est un processus progressif de polymérisation et de transconformation de protéines natives solubles (état natif) en agrégats insolubles (état amyloïde) (Eisenberg et Jucker, 2012). Les protéines natives doivent franchir une barrière énergétique pour pouvoir se méplier et progressivement se polymériser en un agrégat fibrillaire (Knowles et al., 2014). Lorsqu'un noyau constitué de l'assemblage de protéines malconformées est formé, il agit comme un patron facilitant la transconformation et l'incorporation de protéines natives (Harper et Lansbury, 1997). Ce processus, appelé nucléation, génère des agrégats de taille croissante et mène finalement à la formation de fibrilles insolubles (Kim et al., 2013).

Au vu de ce mécanisme, toutes les protéines amyloïdes sont théoriquement transmissibles car l'introduction d'un noyau de nucléation est suffisant pour déclencher la polymérisation (Eisenberg et Jucker, 2012). Jusqu'à présent cependant, seule la protéine PrP a démontré des propriétés infectieuses chez l'Homme (Prusiner, 1998).

1.4. L'hypothèse « prion » de la maladie d'Alzheimer

Depuis la découverte du caractère transmissible des prions, d'autres protéinopathies cérébrales ont été suspectées de présenter des propriétés similaires. Parmi ces maladies, il apparaît de plus en plus clairement que la MA soit initiée et propagée par le mépliement et l'agrégation des protéines Aβ et Tau de manière similaire aux prions.

Bien qu'aucune étude épidémiologique ne démontre le caractère infectieux de la MA (Beekes et al., 2014; Edgren et al., 2016), il a été récemment suggéré que l'amyloïdose soit, sous certaines conditions, transmissible à l'Homme par voie iatrogène (Jaunmuktane et al., 2015; Frontzek et al., 2016; Kovacs et al., 2016; Preusser et al., 2006).

En effet, l'inoculation d'homogénats de cerveau de patients Alzheimer (Kane et al., 2000) ou animaux atteints d'amyloïdose (Meyer-Luehmann et al., 2006) ou de tauopathie (Clavaguera et al., 2009) ainsi que d'agrégats synthétiques d'Aβ (Stöhr et al., 2014) ou Tau (Iba et al., 2013) permettent d'accélérer ou d'induire ces pathologies chez des modèles murins. Ces expériences ont montré que l'introduction de noyaux de nucléation d'Aβ ou Tau malconformés dans le cerveau est suffisante pour déclencher la pathologie chez le rongeur. En revanche, cette démonstration chez le primate reste pour l'instant peu concluante car seule une étude a montré la transmission d'une amyloïdose éparse après inoculation d'homogénats de cerveau de patient Alzheimer (Goudsmit et al., 1980 ; Baker et al., 1993 ; Brown et al., 1994; Ridley et al., 2006). Pour finir, de nombreuses caractéristiques spécifiques des protéines PrP malconformées, telles que la résistance à la dégradation (Meyer-Luehmann et al., 2006; Fritschi et al., 2014a) ou la présentation de différentes souches (Watts et al., 2014 ; Sanders et al., 2014), ont été démontrées pour les protéines Aβ et Tau malconformées (Walker et al., 2016).

Ces études suggèrent la possibilité que Aβ et Tau puissent se comporter de manière similaire à PrP et soutiennent l' « hypothèse prion » de la MA. Cependant, le fait que cette « propagation » pathologique des protéines liées à la MA entraîne le déclenchement des symptômes reste incertain (Walsh and Selkoe, 2016). En effet, dans les cas suspectés d'amyloïdose iatrogène, les autres lésions typiques de la MA, telles que les dégénérescences neurofibrillaires, n'ont pas été observées. Cela suggère que, si l'amyloïdose et la tauopathie peuvent être induites de manière infectieuse expérimentalement, le phénotype complet de la MA n'est peut-être pas transmissible. Très peu d'études ont étudié l'impact fonctionnel des

transmissions expérimentales (Kane et al., 2000 ; Stancu et al., 2015) et cette question reste pour l'instant sans réponse, en particulier chez le primate.

Objectifs de thèse

Sur la base de cette hypothèse, nous avons évalué la transmission expérimentale de certains endophénotypes de la MA à des modèles murins et primate (microcèbe murin).

Notre premier objectif était d'étudier la transmission de l'amyloïdose à deux modèles murins d'amyloïdose précoce ou tardive (2.1). Nous avons effectué des inoculations intracérébrales d'homogénats de patients Alzheimer afin d'introduire des noyaux de nucléation d'Aβ dans le cerveau de ces animaux. Nous avons évalué les capacités de nucléation et de propagation de l'amyloïdose ainsi que l'impact du modèle et de l'environnement local sur ces processus.

Notre deuxième objectif visait à préparer la transmission expérimentale à un modèle primate, le microcèbe murin (2.2). Ce modèle est intéressant car certains individus âgés peuvent développer spontanément certains endophénotypes de la MA tels que l'amyloïdose ou l'atrophie cérébrale. Ici, notre objectif était de mieux caractériser le vieillissement physiologique et pathologique du microcèbe. En premier, nous nous sommes intéressés à l'atrophie cérébrale durant le vieillissement physiologique. En second, nous avons caractérisé les lésions Aβ et Tau et évalué la proportion d'animaux présentant ce vieillissement pathologique. Ces études nous ont permis de développer des techniques utilisées pour notre troisième étude.

Pour finir, notre troisième objectif était d'évaluer la transmission expérimentale chez le microcèbe murin en nous focalisant sur les impacts fonctionnels et morphologiques de la MA (2.3). En effet, jusqu'à présent, très peu d'études ont évalué l'hypothèse selon laquelle la transmission expérimentale de la MA peut déclencher un phénotype clinique et les données humaines suggèrent que, si les pathologies Aβ et Tau pourraient suivre des mécanismes de type prion, la MA en elle-même ne serait pas transmissible. Nous avons donc étudié si l'inoculation intracérébrale d'homogénats de patients Alzheimer déclenchait des altérations cognitives et d'autres perturbations cérébrales telles que l'altération de l'activité neuronale et l'atrophie cérébrale ainsi que les lésions cardinales de la MA.

En conclusion, nous voulions complémenter des données probantes quant à la pertinence de l'hypothèse prion de la MA. Egalement, si l'amyloïdose et la tauopathie semblent être

transmissibles, aucune donnée ne supporte la possibilité d'une transmission du phénotype clinique de la MA. Au cours de cette thèse, nous nous sommes intéressés à cette question cruciale. Pour finir, la recherche préclinique est primordiale pour la compréhension des mécanismes pathologiques. Cependant, les animaux ne développent pas la MA et la mise au point de modèles plus translationnels semble indispensable pour mieux comprendre la physiopathologie de la MA.

Partie II – Etudes expérimentales

2.1. Transmission expérimentale de l'amyloïdose à des modèles murins.

Dans la littérature, les agrégats de protéines Aβ et Tau malconformés ont été montrés comme présentant des propriétés de type prion. Si l'hypothèse « prion » de la MA est correcte, l'amyloïdose et la tauopathie devraient être expérimentalement transmissibles suite à l'introduction exogène de noyaux de nucléation.

Ici, nous avons cherché à évaluer les impacts de la transmission expérimentale sur le développement de l'amyloïdose dans deux modèles murins différents. Le premier est un modèle transgénique ($APP_{Swe}PS1_{\Delta E9}$, Jankowsky et al., 2004) sur-exprimant l'Aβ humain dans toutes les structures du cerveau et développant une amyloïdose précoce et robuste dans l'ensemble du cerveau. Le deuxième est un modèle basé sur le transfert de gènes par co-injection de vecteurs viraux adéno-associés (AAV). Ce modèle permet l'expression focale dans l'hippocampe dorsal des protéines Amyloid Precursor Protein (APP) et préséniline-1 (PS1, une enzyme impliquée dans la production de l'Aβ) humaines portant des mutations impliquées dans des formes génétiques de la MA. Ce modèle diffère du premier en raison d'une expression relativement physiologique d'Aβ humaine non-mutée et locale (uniquement dans l'hippocampe dorsal, Audrain et al., 2016). Nous avons caractérisé le développement très tardif d'une amyloïdose focale et éparse dans ce modèle. Ces deux modèles nous ont permis d'étudier la transmission expérimentale de l'amyloïdose par inoculation d'homogénats de cerveaux de patients Alzheimer et l'impact de l'« hôte » sur cette transmission.

Tout d'abord, nous avons caractérisé nos échantillons humains en immunohistochimie et nos homogénats en biochimie. Nous avons utilisé trois échantillons de cortex pariétal provenant d'un individu contrôle âgé (CTRL, stade de Braak 0, phase de Thal 0) et deux patients Alzheimer (MA1 et MA2, stade de Braak VI et phases de Thal 5 et 4 respectivement).

Nous avons ensuite inoculé des homogénats de cerveaux CTRL et MA bilatéralement dans l'hippocampe de jeunes souris transgéniques $APP_{Swe}PS1_{\Delta E9}$ (8 semaines). Nous avons évalué le développement de l'amyloïdose en immunohistochimie à trois délais : 4, 8 ou 16 semaines post-inoculation. Deux autres groupes contrôles, non-injectés et injectés avec du PBS, ont également été évalués à 16 semaines post-inoculation.

Pour finir, nous avons tout d'abord co-injecté deux AAV bilatéralement dans l'hippocampe de jeunes souris sauvages (8 semaines). Nous avons ensuite caractérisé le développement de l'amyloïdose à long terme (80 semaines post-injection des AAV). Pour finir, 4 semaines après l'injection virale, nous avons inoculé aux mêmes coordonnées les homogénats de cerveaux utilisés précédemment ainsi que du PBS, comme autre groupe contrôle. Deux délais, 8 et 48 semaines post-inoculation (spi), ont été réalisés pour l'évaluation de l'amyloïdose par immunohistochimie.

Nous avons montré que l'inoculation intracérébrale d'homogénats de cerveau de patients Alzheimer accélère le développement de l'amyloïdose dans nos deux modèles, contrairement à l'inoculation d'un homogénat de patient âgé sain ou de PBS. Ces résultats suggèrent que l'accélération n'est pas induite par l'inflammation et les réponses immunitaires produites par l'injection d'homogénats de cerveau non-purifiés ou par des lésions cérébrales liées aux injections. De plus, aucune accélération n'a été observée aux temps courts (8 spi) suggérant que l'accélération observée ne reflète pas un dépôt d'Aβ inoculé. Ces résultats sont en accord avec la littérature et indiquent que la transmission de l'amyloïdose est un processus dépendant du temps (Baker et al., 1993; Eisele et al., 2009; Kane et al., 2000; Morales et al., 2012; Stöhr et al., 2012). Nos résultats, ainsi que de nombreuses études précédentes (Eisele et al., 2014; Hamaguchi et al., 2012; Kane et al., 2000; Meyer-Luehmann et al., 2006), suggèrent également que cette transmission nécessite l'introduction de noyaux de nucléation d'Aβ contenus dans les homogénats de cerveau MA. En conclusion, ces résultats complémentent de nombreuses publications montrant un rôle des agrégats d'Aβ dans la transmission expérimentale de l'amyloïdose et suggèrent un mécanisme de nucléation de type prion.

Ensuite, nous avons montré que l'hôte est un déterminant essentiel pour la modulation de la transmission expérimentale de l'amyloïdose (Eisele et al., 2014; Meyer-Luehmann et al., 2006). En effet, nous avons observé des différences entre nos modèles précoce et tardif d'amyloïdose. De plus, nous avons observé une amyloïdose singulière dans le corps calleux suite à l'administration intracérébrale d'homogénats de cerveau MA. L'accumulation

d'agrégats dans le corps calleux a été observée de façon similaire suite à l'administration intracérébrale d'échantillons contaminés par la PrP^{Sc} (Manson et al., 1999; Piccardo et al., 2007; Scott et al., 1989) mais pas dans le cas d'une administration périphérique (Gibson, 1986). Ces données suggèrent l'induction d'un phénomène spécifique de la transmission expérimentale par voie intracérébrale. Nous nous sommes également intéressés à l'effet « souche » en inoculant des homogénats provenant de deux patients Alzheimer sporadiques. En accord avec la littérature (Watts et al., 2014), nous n'avons observé aucune différence phénotypique entre ces deux inocula, suggérant qu'ils ne présentent pas de souche d'Aβ différentes. Pour finir, nous avons évalué les phénomènes de propagation de l'amyloïdose. Nous suggérons que, contrairement à Tau (Wegmann et al., 2015), l'expression d'APP est indispensable à la propagation de l'amyloïdose.

En conclusion, nos données corroborent l'hypothèse selon laquelle l'amyloïdose peut être transmise *in vivo* par des mécanismes de type prion. Plusieurs questions restent néanmoins en suspens. Bien qu'aucune étude épidémiologique ne soutienne l'hypothèse selon laquelle la MA est transmissible à l'Homme, des rapports récents suggèrent que l'amyloïdose puisse, dans certains cas, être transmissible. Jusqu'à présent, l'impact de la transmission expérimentale a été très peu étudié et il a été suggéré que le phénotype clinique de la MA ne puisse pas être transmis entre individus, contrairement aux prions.

2.2. Caractérisation du modèle primate

Afin d'étudier la question de la transmission du phénotype clinique de la MA, les modèles primates non-humains sont intéressants car ils peuvent développer des altérations liées à l'âge (Andersen et al., 1999; Dhenain et al., 2000). Nous avons étudié cette transmission chez le microcèbe murin (*Microcebus murinus*). Ce petit primate de la famille des lémuriens présente une espérance de vie maximale de 12 ans. Il est utilisé dans l'étude du vieillissement cérébral physiologique et pathologique de type Alzheimer. Afin de réaliser notre étude de transmission expérimentale, nous avons tout d'abord approfondi la caractérisation de ce modèle. Cette étude nous a aussi permis de développer de nouvelles techniques pour l'évaluation de la cognition, de l'atrophie cérébrale ainsi que de l'amyloïdose et de la tauopathie.

En lien avec cette thèse, nous avons développé un nouveau protocole d'évaluation de la cognition basé sur des discriminations visuelles appariées dans un dispositif de saut (Picq et al., 2015). Notre premier objectif était de développer un test rapide, efficace et fiable pour

l'évaluation de la cognition. En effet, les protocoles disponibles chez le microcèbe jusqu'à présent étaient fastidieux et présentaient des taux d'attrition élevés liés à des problèmes de motivation (Joly et al., 2006, 2014; Picq, 2007). Notre deuxième objectif était d'évaluer les altérations cognitives liées à l'âge chez le microcèbe. Nous avons montré que des individus âgés de plus de 6 ans développaient des altérations de la mémoire à long-terme sans déficits d'apprentissage et que de jeunes individus (moins de 4,5 ans) ne présentaient aucun trouble cognitif dans ce test. Nous avons donc validé ce test comme un outil efficace et discriminant et nous l'avons utilisé pour l'évaluation des capacités cognitives dans notre étude de transmission expérimentale.

Nous avons ensuite cherché à caractériser l'atrophie cérébrale liée au vieillissement physiologique. Pour cela, nous avons procédé à des examens en Imagerie par Résonnance Magnétique (IRM) anatomique sur une cohorte de 24 microcèbes âgés de 1 à 9 ans (6,35±2,4 ans). Nous avons analysé ces images par morphométrie voxel à voxel. Cette technique nous a permis d'évaluer statistiquement l'évolution de la matière grise en fonction du temps. En nous affranchissant des effets individuels, nous avons pu mettre en évidence l'atrophie cérébrale physiologique de ce modèle. Contrairement au vieillissement pathologique (Picq et al., 2012), nous avons observé que cette atrophie liée au vieillissement physiologique épargnait le lobe temporal ainsi que des structures non-corticales telles que l'hippocampe.

Pour finir, nous avons cherché à déterminer la proportion de microcèbes présentant des lésions Aβ et Tau, leur relation au vieillissement et leur cooccurrence dans une autre cohorte de 25 microcèbes âgés de 1 à 11 ans (7,2±2,9 ans). Nous avons déterminé que seuls des individus âgés de plus de 6 ans présentaient des lésions de type Alzheimer. Nous avons déterminé que l'amyloïdose cérébrale, sous forme de plaques amyloïdes ou d'angiopathie amyloïde, et l'accumulation de Tau hyperphosphorylée dans le soma et les prolongements neuronaux atteignaient respectivement 25% et 29% des animaux âgés de plus de 6 ans. Nous avons également observé que seuls 28,6% des animaux affectés présentaient les deux types de lésions suggérant que ces deux pathologies se développent indépendamment chez le microcèbe (Giannakopoulos et al., 1997). Pour finir, nous avons observé que similairement à d'autres primates non-humains (Cummings et al., 1996; Elfenbein et al., 2007; Heuer et al., 2012; Kimura et al., 2003; Lemere et al., 2008; Maclean et al., 2000; Struble et al., 1985), le microcèbe présente une relative résistance à l'amyloïdose et à la tauopathie car ces pathologies ne ressemblent pas aux lésions massives observées chez l'Homme.

En conclusion, nos données soutiennent l'intérêt du microcèbe comme modèle du vieillissement physiologique et pathologique de type Alzheimer. Des limites sont néanmoins observées en ce qui concerne l'intensité des pathologies Aβ et Tau. Déchiffrer les différences entre la pathologie présentée par les animaux âgés et les patients Alzheimer pourrait aider à comprendre pourquoi la MA est une maladie spécifique de l'Homme.

2.3. Transmission expérimentale d'endophénotypes de la maladie d'Alzheimer à un modèle primate

Depuis la découverte que les maladies à prions peuvent être transmises par l'inoculation de tissus affectés, l'existence d'agents transmissibles dans la MA a été suspectée. De plus en plus d'études suggèrent l'implication de mécanismes de type prion dans la physiopathologie de la MA. En effet, de manière similaire à la PrP, les pathologies Aβ et Tau sont expérimentalement transmissibles à des modèles animaux. Toutefois, jusqu'à présent, l'induction d'un phénotype clinique par la transmission expérimentale de la MA reste incertain, en particulier chez le primate (Beekes et al., 2014; Stancu et al., 2015; Walsh and Selkoe, 2016). Ceci est en opposition avec les maladies à prions, dans lesquelles la transmission expérimentale conduit à des symptômes cliniques (Brown et al., 1994; Gajdusek et al., 1967, 1968; Gibbs et al., 1968a).

Dans cette étude, nous avons cherché à répondre à ces questions. Nous avons étudié les impacts de la transmission expérimentale chez le microcèbe en nous concentrant sur des endophénotypes morphologiques et fonctionnels de la MA. Nous avons procédé à l'inoculation intracérébrale d'homogénats de cerveau de patient Alzheimer chez de jeunes microcèbes adultes (3,5±0,2ans). Nous avons réalisé des évaluations cognitives, des électroencéphalogrammes (EEG) et des IRM anatomiques jusqu'à 18 mois post-inoculation suivis d'un examen immunohistopathologique des tissus cérébraux.

Nous avons montré que l'inoculation d'homogénats de cerveau de patient Alzheimer induit des troubles de la mémoire à long-terme à un plus jeune âge que normalement détectés au cours du vieillissement. En outre, chez des animaux âgés, nous avons montré que les capacités d'apprentissage ne sont pas altérées (Picq et al., 2015). Dans notre étude, la transmission expérimentale de la MA induit des altérations de fonctions cognitives (apprentissage) normalement conservées même chez les animaux âgés souffrant de troubles cognitifs. Cette observation est particulièrement pertinente par rapport à la pathologie

humaine dans le sens où les personnes âgées peuvent présenter des déficits cognitifs légers, mais certains altérations sont spécifiques à la MA (McKhann et al., 2011).

Pour évaluer l'activité neuronale, nous avons effectué des EEG dans le cortex frontal. L'inoculation d'homogénat de cerveau MA a progressivement altéré les densités de puissance de fréquence EEG suggérant une altération de l'activité neuronale. Comme les électrodes EEG étaient placées sur le cortex frontal, éloigné des sites d'injection, l'inoculation d'homogénat de cerveau Alzheimer modifie l'activité neuronale à distance. Ce résultat suggère soit un mécanisme de propagation à partir des sites d'injection jusqu'au cortex frontal (effet local), soit un impact sur l'ensemble du réseau neuronal (effet global).

Morphologiquement, la MA est caractérisée par une atrophie cérébrale progressive qui affecte l'hippocampe et diverses structures corticales. Par rapport aux animaux inoculés avec des homogénats provenant d'un individu âgé sain, les animaux inoculés avec des homogénats de patient Alzheimer ont développé une atrophie dans les cortex cingulaire postérieur et rétrosplénial, deux zones proches des sites d'inoculation, et surtout dans d'autres régions plus lointaines comprenant l'hippocampe ventral, le cortex entorhinal, l'amygdale et le cortex temporal inférieur et latéraux. Ces résultats montrent que l'inoculation d'homogénat de cerveau Alzheimer impacte des régions distantes du site d'injection, suggérant un mécanisme de propagation.

Pour finir, nous avons réalisé un examen immunohistopathologique des tissus cérébraux. Afin d'assurer la détection de changements uniquement liés à l'inoculation sans interférence avec le vieillissement spontané, les animaux ont été euthanasiés avant 6 ans d'âge (5,0±0,2ans). Nous avons détecté de très rares plaques amyloïdes corticales et/ou une angiopathie amyloïde corticale clairsemée chez 50% des animaux du groupe Alzheimer. Aucune lésion n'a été trouvée dans le groupe Contrôle. Nos résultats suggèrent un phénomène de nucléation suite à l'inoculation d'homogénats de cerveau de patient Alzheimer. Ces lésions Aβ étaient légères par rapport à celles des patients atteints de MA et des modèles de souris transgéniques de la MA. Nous avons démontré précédemment les capacités de nucléation de nos homogénats Alzheimer dans deux modèles murins d'amyloïdose. Dans ces expériences, et en accord avec la littérature, nous avons montré que l'hôte est un paramètre critique pour la nucléation d'Aβ. Les primates non-humains âgés (Kimura et al., 2003; Lemere et al., 2008; Struble et al., 1985), y compris les microcèbes, peuvent développer des lésions Aβ parenchymales et/ou

vasculaires mais ces lésions sont plus clairsemées que chez les patients MA. Nos résultats semblent souligner encore d'avantage le rôle de l'hôte dans les mécanismes de type prion. Par ailleurs, nous n'avons détecté aucune lésion Tau. Ce résultat est cohérent avec les études réalisées chez le ouistiti (Baker et al., 1993, 1994; Maclean et al., 2000; Ridley et al., 2006) et avec les cas de suspicion d'amyloïdose iatrogène (Frontzek et al., 2016; Jaunmuktane et al., 2015; Kovacs et al., 2016; Preusser et al., 2006). En outre, une tauopathie de type Alzheimer est inhabituelle chez les primates non-humains (Heuer et al., 2012), y compris microcèbes. Par conséquent, de façon similaire à Aβ, des effets liés à l'hôte peuvent expliquer l'absence d'induction de pathologie Tau. En outre, aucun effet souche n'a été observé entre les animaux présentant des lésions Aβ inoculés avec l'un ou l'autre des patients Alzheimer. Ces résultats sont cohérents avec nos études chez la souris. Enfin, nous n'avons pas observé de réactivité astrocytaire, suggérant que l'inflammation n'est pas responsable des altérations observées.

Pour conclure, nous avons observé le développement d'altérations fonctionnelles et morphologiques semblables à celles observées dans la MA chez le microcèbe, accompagnées d'une amyloïdose subtile sans pathologie Tau. Une telle transmission en l'absence de sévères lésions neuropathologiques a été rapportée dans les maladies à prions (Lasmézas et al., 1997; Piccardo et al., 2013) mais jamais dans le contexte de la MA. Nos résultats suggèrent que les agents responsable des altérations observées puissent être des formes d'Aβ et/ou Tau non détectées en immunohistochimie et pouvant être transmises expérimentalement (Barghorn et al., 2005). En effet, des formes solubles de Aβ et Tau peuvent initier un processus d'auto-réplication *in vitro* (Dean et al., 2016; Kumar et al., 2014) et *in vivo* (Clavaguera et al., 2009; Langer et al., 2011). Il a également été montré que des formes oligomériques de la protéine Tau peuvent entraîner une nucléation sans formation de dégénérescences neurofibrillaires dans un modèle murin non symptomatique de tauopathie (Baker et al., 2016). En outre, le fait que les oligomères d'Aβ peuvent diffuser rapidement et largement dans le cerveau (Epelbaum et al., 2015) soulève la possibilité que ces noyaux de nucléation solubles puissent être responsables de la propagation d'espèces toxiques dans le cerveau. Comme ces espèces solubles ne sont généralement pas détectées par immunohistochimie (Thal et al., 2015), d'autres expériences devront être effectuées pour démontrer notre hypothèse et identifier la contribution relative des espèces solubles aux toxicités observées .

Nos résultats supportent l'hypothèse de type prion de la MA ainsi que le consensus actuel sur la toxicité des formes solubles d'Aβ et Tau. Ils soutiennent également la possibilité que

l'amyloïdose soit transmissible chez l'Homme, sous certaines conditions. En revanche, nos résultats sont en contradiction avec l'idée que les lésions liées à la MA, plutôt que la MA elle-même, puissent être soumis à des mécanismes de type prion (propagons vs prion) (Eisele and Duyckaerts, 2016; Kovacs et al., 2016). En effet, nous avons démontré qu'une pathologie de type MA peut être transmise de l'Homme à des primates. Notre étude fournit des arguments solides pour évaluer les impacts fonctionnels chez les personnes potentiellement contaminées.

Mis à part certaines conditions iatrogènes spécifiques, il n'y a aucune preuve que la MA est transmissible (Beekes et al., 2014; Edgren et al., 2016; Schmidt et al., 2012). Les connaissances actuelles favorisent l'hypothèse d'une formation endogène des premiers noyaux de nucléation d'Aβ et Tau dans le cerveau. Identifier l'origine de leur formation sera essentiel à la compréhension de la physiopathologie de la MA. Nous avons proposé que l'auto-propagation des formes solubles puisse être responsable du développement d'altérations cliniques. La démonstration de cette hypothèse sera cruciale pour comprendre leur toxicité relative et leur contribution à la pathologie symptomatique. Cette identification pourrait représenter une étape cruciale pour la compréhension de la MA et le développement de stratégies thérapeutiques efficaces. Ce nouveau paradigme fournit des preuves convaincantes quant au rôle de noyaux de nucléation d'Aβ et Tau dans l'instigation et la progression de la MA et renforce l'intérêt de cibler les formes solubles, de préférence au début de la pathologie.

Partie III – Conclusions et Perspectives

Depuis la découverte du caractère transmissible des maladies à prions, d'autres protéinopathies ont été suspectées de présenter des propriétés similaires de transmission. Parmi ces maladies, de plus en plus de données expérimentales soutiennent l'idée selon laquelle la MA est initiée et soutenue par le mépliement et l'agrégation des protéines Aβ et Tau. Ce mécanisme de « type prion » semble similaire à celui de la protéine résistante à la protéase (PrP) dans les maladies à prion (Prusiner, 1998). La transmission expérimentale est un outil utile pour évaluer l'hypothèse de type prion de la MA dans des modèles animaux. Elle nécessite l'inoculation de noyaux de nucléation d'Aβ et/ou de Tau obtenus *in vitro* ou à partir d'homogénats de cerveaux atteints. Ici, nous avons évalué la transmission expérimentale d'endophénotypes de la MA à des souris et des primates (microcèbes).

Tout d'abord, nous avons montré que l'amyloïdose est transmissible à des souris par l'inoculation intracérébrale d'homogénats de cerveau de patients souffrant de MA. Nous

avons montré que l'hôte est un modulateur de cette transmission en utilisant des modèles murins d'amyloïdose précoce et tardive. Nous avons identifié une caractéristique typique de cette transmission par voie intracérébrale (amyloïdose callosale) et suggérons qu'elle puisse être une signature de cette transmission chez le rongeur. Nous avons également montré l'absence de « phénomène de souche » chez deux patients atteints de MA sporadique et suggérons que les souches d'Aβ pourraient davantage dépendre de la séquence peptidique primaire que les souches de PrP et pourraient présenter moins de flexibilité conformationnelle (Watts et al., 2014). Enfin, nous avons étudié la propagation des lésions Aβ dans nos deux modèles et nous proposons que cette propagation dépende à la fois de l'expression d'APP et de l'agrégation spontanée. En conclusion, nos résultats soutiennent l'hypothèse de nucléation-propagation des lésions Aβ.

Nous avons ensuite caractérisé les processus de vieillissement physiologiques et pathologiques chez le microcèbe. Le vieillissement physiologique du microcèbe est accompagné d'une atrophie cérébrale liée à l'âge qui, contrairement au vieillissement pathologique, n'atteint pas le lobe temporal inférieur et de l'hippocampe. Nous avons également caractérisé la proportion de lésions histopathologiques typiques de la MA chez ces animaux et nous avons montré que, comme d'autres primates, ils présentent une certaine résistance aux deux pathologies car l'étendue de ces lésions chez les animaux atteints ne ressemblent pas aux lésions massives observées chez l'Homme.

Concernant l'hypothèse de type prion de la MA, plusieurs questions restent sans réponse. En effet, il a été suggéré que, si l'amyloïdose pouvait, sous certaines conditions, être transmissible d'Homme à Homme, le phénotype clinique n'est pas reproduit, contrastant avec les maladies à prions (Kovacs et al., 2016). En effet, il reste à déterminer si la « propagation pathogène » des protéines liées à la MA provoque l'apparition des symptômes de la MA (Walsh et Selkoe, 2016). Dans les maladies à prions, la maladie est transmisse expérimentalement de l'Homme à des primates non-humains et conduit à l'apparition des symptômes cliniques. Ici, nous avons étudié ces questions chez un primate non-humain, le Microcèbe, et démontré pour la première fois que la transmission expérimentale de la MA conduit progressivement à l'apparition de troubles cognitifs, de modifications de l'activité neuronale, et d'une atrophie cérébrale chez ces primates. Cette toxicité n'est pas associée au développement de lésions Aβ ou Tau sévères détectables en immunohistochimie. Nos résultats sont cohérents avec l'idée de plus en plus acceptée que les agrégats ne soient pas les

espèces les plus toxiques et que les assemblages solubles peuvent être responsables de la toxicité. Une telle dissociation a déjà été rapportée pour les maladies à prions (Lasmézas et al., 1997), mais jamais dans le cadre de la MA.

Nos résultats soutiennent l'hypothèse selon laquelle les assemblages solubles d'Aβ et/ou Tau peuvent s'auto-propager dans le cerveau et entrainer une importante toxicité menant à un phénotype pathologique de type MA. Cette hypothèse est étayée par des cas humains de "Suspicion of Non-Alzheimer/Amyloid Pathology" (SNAP) (Chételat et al 2016; Jack, 2014). Nous proposons que l'hypothèse de type prion de la MA ne devrait pas être limitée à l'identification d'agrégats insolubles d'Aβ et Tau et que les assemblages solubles d'Aβ et/ou Tau pourraient se propager et conduire à des conséquences fonctionnelles et morphologiques importantes. Nos résultats suggèrent un rôle pour les noyaux de nucléation d'Aβ et Tau dans l'initiation et la progression de la MA et renforce l'intérêt de cibler ces espèces, de préférence le plus précocement dans l'évolution de la pathologie.

L'hypothèse d'une auto-propagation des espèces solubles pourrait expliquer la résistance relative des microcèbes au développement des lésions Aβ et Tau malgré le développement d'une atrophie cérébrale et de déficits cognitifs au cours du vieillissement et après une transmission expérimentale. D'autres expériences sont nécessaires pour confirmer cette hypothèse. Ce modèle pourrait néanmoins permettre d'évaluer à la fois les mécanismes de type prion et de toxicité pour Aβ et Tau ainsi que leur interaction. Il pourrait également être intéressant pour l'évaluation des thérapies ciblant les espèces solubles.

En conclusion, nos résultats complètent les données récentes appuyant l'hypothèse de type prion de la MA ainsi que la suspicion d'induction iatrogène de l'amyloïdose (Frontzek et al 2016; Jaunmuktane et al, 2015; Kovacs et al 2016; Preusser et al, 2006). Contrairement à l'idée actuelle selon laquelle la MA en tant que maladie n'est pas transmissible, nous démontrons qu'une pathologie de type MA peut être transmise de l'Homme au primate. Nos résultats fournissent des arguments solides pour évaluer davantage les impacts fonctionnels chez les personnes potentiellement contaminées. Les connaissances actuelles dans ce domaine soutiennent également l'hypothèse d'une formation endogène des noyaux d'Aβ et de Tau dans le cerveau. Identifier l'origine de la formation de ces premiers noyaux et leurs mécanismes d'auto-propagation est essentiel afin de mieux comprendre la physiopathologie de la MA. Cela favorisera également le développement de stratégies thérapeutiques curatives ou, au moins, stabilisatrices si associées à une prise en charge plus précoce des patients.

Bibliography

Abbott, A. (2016). The red-hot debate about transmissible Alzheimer's. Nature *531*, 294–297.

Abelein, A., Abrahams, J.P., Danielsson, J., Gräslund, A., Jarvet, J., Luo, J., Tiiman, A., and Wärmländer, S.K.T.S. (2014). The hairpin conformation of the amyloid β peptide is an important structural motif along the aggregation pathway. J. Biol. Inorg. Chem. JBIC Publ. Soc. Biol. Inorg. Chem. *19*, 623–634.

Aguzzi, A., and Heppner, F.L. (2000). Pathogenesis of prion diseases: a progress report. Cell Death Differ. *7*, 889–902.

Ahmed, Z., Cooper, J., Murray, T.K., Garn, K., McNaughton, E., Clarke, H., Parhizkar, S., Ward, M.A., Cavallini, A., Jackson, S., et al. (2014). A novel in vivo model of tau propagation with rapid and progressive neurofibrillary tangle pathology: the pattern of spread is determined by connectivity, not proximity. Acta Neuropathol. (Berl.) *127*, 667–683.

Akiyama, H., Barger, S., Barnum, S., Bradt, B., Bauer, J., Cole, G.M., Cooper, N.R., Eikelenboom, P., Emmerling, M., Fiebich, B.L., et al. (2000). Inflammation and Alzheimer's disease. Neurobiol. Aging *21*, 383–421.

Alonso, A., Zaidi, T., Novak, M., Grundke-Iqbal, I., and Iqbal, K. (2001). Hyperphosphorylation induces self-assembly of tau into tangles of paired helical filaments/straight filaments. Proc. Natl. Acad. Sci. U. S. A. *98*, 6923–6928.

Alper, T., Cramp, W.A., Haig, D.A., and Clarke, M.C. (1967). Does the agent of scrapie replicate without nucleic acid? Nature *214*, 764–766.

Alred, E.J., Phillips, M., Berhanu, W.M., and Hansmann, U.H.E. (2015). On the lack of polymorphism in Aβ-peptide aggregates derived from patient brains. Protein Sci. Publ. Protein Soc. *24*, 923–935.

Alzheimer, A. (1907). Über eine eigenartige Erkrankung der Hirnrinde. Allg. Z. Psychiatr. Psych.-Gerichtl. Med.

Alzheimer, A., Stelzmann, R.A., Schnitzlein, H.N., and Murtagh, F.R. (1995). An English translation of Alzheimer's 1907 paper, "Uber eine eigenartige Erkankung der Hirnrinde." Clin. Anat. N. Y. N *8*, 429–431.

American Psychiatric Association (2004). DSM-4-TR (Elsevier Masson).

Andersen, A.H., Zhang, Z., Zhang, M., Gash, D.M., and Avison, M.J. (1999). Age-associated changes in rhesus CNS composition identified by MRI. Brain Res. *829*, 90–98.

Ashburner, J. (2007). A fast diffeomorphic image registration algorithm. NeuroImage *38*, 95–113.

Attems, J., Quass, M., Jellinger, K.A., and Lintner, F. (2007). Topographical distribution of cerebral amyloid angiopathy and its effect on cognitive decline are influenced by Alzheimer disease pathology. J. Neurol. Sci. *257*, 49–55.

Audrain, M., Fol, R., Dutar, P., Potier, B., Billard, J.-M., Flament, J., Alves, S., Burlot, M.-A., Dufayet-Chaffaud, G., Bemelmans, A.-P., et al. (2016). Alzheimer's disease-like APP processing in wild-type mice identifies synaptic defects as initial steps of disease progression. Mol. Neurodegener. *11*, 5.

Baker, H.F., Ridley, R.M., Duchen, L.W., Crow, T.J., and Bruton, C.J. (1993). Evidence for the experimental transmission of cerebral beta-amyloidosis to primates. Int. J. Exp. Pathol. *74*, 441.

Baker, H.F., Ridley, R.M., Duchen, L.W., Crow, T.J., and Bruton, C.J. (1994). Induction of beta (A4)-amyloid in primates by injection of Alzheimer's disease brain homogenate. Comparison with transmission of spongiform encephalopathy. Mol. Neurobiol. *8*, 25–39.

Baker, S., Polanco, J.C., and Götz, J. (2016). Extracellular Vesicles Containing P301L Mutant Tau Accelerate Pathological Tau Phosphorylation and Oligomer Formation but Do Not Seed Mature Neurofibrillary Tangles in ALZ17 Mice. J. Alzheimers Dis. JAD.

Barghorn, S., Nimmrich, V., Striebinger, A., Krantz, C., Keller, P., Janson, B., Bahr, M., Schmidt, M., Bitner, R.S., Harlan, J., et al. (2005). Globular amyloid beta-peptide oligomer - a homogenous and stable neuropathological protein in Alzheimer's disease. J. Neurochem. *95*, 834–847.

Barron, R.M., King, D., Jeffrey, M., McGovern, G., Agarwal, S., Gill, A.C., and Piccardo, P. (2016). PrP aggregation can be seeded by pre-formed recombinant PrP amyloid fibrils without the replication of infectious prions. Acta Neuropathol. (Berl.).

Barrow, C.J., Yasuda, A., Kenny, P.T., and Zagorski, M.G. (1992). Solution conformations and aggregational properties of synthetic amyloid beta-peptides of Alzheimer's disease. Analysis of circular dichroism spectra. J. Mol. Biol. *225*, 1075–1093.

Bartus, R.T. (2000). On neurodegenerative diseases, models, and treatment strategies: lessons learned and lessons forgotten a generation following the cholinergic hypothesis. Exp. Neurol. *163*, 495–529.

Basler, K., Oesch, B., Scott, M., Westaway, D., Wälchli, M., Groth, D.F., McKinley, M.P., Prusiner, S.B., and Weissmann, C. (1986). Scrapie and cellular PrP isoforms are encoded by the same chromosomal gene. Cell *46*, 417–428.

Baumgart, M., Snyder, H.M., Carrillo, M.C., Fazio, S., Kim, H., and Johns, H. (2015). Summary of the evidence on modifiable risk factors for cognitive decline and dementia: A population-based perspective. Alzheimers Dement. J. Alzheimers Assoc. *11*, 718–726.

Beekes, M., Thomzig, A., Schulz-Schaeffer, W.J., and Burger, R. (2014). Is there a risk of prion-like disease transmission by Alzheimer- or Parkinson-associated protein particles? Acta Neuropathol. (Berl.) *128*, 463–476.

Beltran, W.A., Vanore, M., Ollivet, F., Nemoz-Bertholet, F., Aujard, F., Clerc, B., and Chahory, S. (2007). Ocular findings in two colonies of gray mouse lemurs (Microcebus murinus). Vet. Ophthalmol. *10*, 43–49.

von Bergen, M., Friedhoff, P., Biernat, J., Heberle, J., Mandelkow, E.M., and Mandelkow, E. (2000). Assembly of tau protein into Alzheimer paired helical filaments depends on a local sequence motif ((306)VQIVYK(311)) forming beta structure. Proc. Natl. Acad. Sci. U. S. A. *97*, 5129–5134.

von Bergen, M., Barghorn, S., Li, L., Marx, A., Biernat, J., Mandelkow, E.M., and Mandelkow, E. (2001). Mutations of tau protein in frontotemporal dementia promote aggregation of paired helical filaments by enhancing local beta-structure. J. Biol. Chem. *276*, 48165–48174.

Bero, A.W., Yan, P., Roh, J.H., Cirrito, J.R., Stewart, F.R., Raichle, M.E., Lee, J.-M., and Holtzman, D.M. (2011). Neuronal activity regulates the regional vulnerability to amyloid-β deposition. Nat. Neurosci. *14*, 750–756.

Berriman, J., Serpell, L.C., Oberg, K.A., Fink, A.L., Goedert, M., and Crowther, R.A. (2003). Tau filaments from human brain and from in vitro assembly of recombinant protein show cross-beta structure. Proc. Natl. Acad. Sci. U. S. A. *100*, 9034–9038.

Bieschke, J., Herbst, M., Wiglenda, T., Friedrich, R.P., Boeddrich, A., Schiele, F., Kleckers, D., Lopez del Amo, J.M., Grüning, B.A., Wang, Q., et al. (2011). Small-molecule conversion of toxic oligomers to nontoxic β-sheet-rich amyloid fibrils. Nat. Chem. Biol. *8*, 93–101.

Bird, C.M., and Burgess, N. (2008). The hippocampus and memory: insights from spatial processing. Nat. Rev. Neurosci. *9*, 182–194.

Blättler, T., Brandner, S., Raeber, A.J., Klein, M.A., Voigtländer, T., Weissmann, C., and Aguzzi, A. (1997). PrP-expressing tissue required for transfer of scrapie infectivity from spleen to brain. Nature *389*, 69–73.

Blennow, K., de Leon, M.J., and Zetterberg, H. (2006). Alzheimer's disease. Lancet Lond. Engl. *368*, 387–403.

Bolton, D.C., McKinley, M.P., and Prusiner, S.B. (1982). Identification of a protein that purifies with the scrapie prion. Science *218*, 1309–1311.

Boluda, S., Iba, M., Zhang, B., Raible, K.M., Lee, V.M.-Y., and Trojanowski, J.Q. (2015). Differential induction and spread of tau pathology in young PS19 tau transgenic mice following intracerebral injections of pathological tau from Alzheimer's disease or corticobasal degeneration brains. Acta Neuropathol. (Berl.) *129*, 221–237.

Bondareff, W., Mountjoy, C.Q., Roth, M., and Hauser, D.L. (1989). Neurofibrillary degeneration and neuronal loss in Alzheimer's disease. Neurobiol. Aging *10*, 709–715.

Bondi, M.W., and Smith, G.E. (2014). Mild cognitive impairment: a concept and diagnostic entity in need of input from neuropsychology. J. Int. Neuropsychol. Soc. JINS *20*, 129–134.

Bons, N., and Mestre, N. (1993). [Similarities between cerebral amyloid plaques in aged lemurian and in human with Alzheimer's disease]. Comptes Rendus Séances Société Biol. Ses Fil. *187*, 516–525.

Bons, N., Mestre, N., and Petter, A. (1992). Senile plaques and neurofibrillary changes in the brain of an aged lemurian primate, Microcebus murinus. Neurobiol. Aging *13*, 99–105.

Bons, N., Mestre, N., Ritchie, K., Petter, A., Podlisny, M., and Selkoe, D. (1994). Identification of amyloid beta protein in the brain of the small, short-lived lemurian primate Microcebus murinus. Neurobiol. Aging *15*, 215–220.

Bons, N., Jallageas, V., Silhol, S., Mestre-Frances, N., Petter, A., and Delacourte, A. (1995). Immunocytochemical characterization of Tau proteins during cerebral aging of the lemurian primate Microcebus murinus. Comptes Rendus Académie Sci. Sér. III Sci. Vie *318*, 741–747.

Bons, N., Silhol, S., Barbié, V., Mestre-Francés, N., and Albe-Fessard, D. (1998). A stereotaxic atlas of the grey lesser mouse lemur brain (Microcebus murinus). Brain Res. Bull. *46*, 1–173.

Braak, H., and Braak, E. (1991). Neuropathological stageing of Alzheimer-related changes. Acta Neuropathol. (Berl.) *82*, 239–259.

Braak, H., and Del Tredici, K. (2011). Alzheimer's pathogenesis: is there neuron-to-neuron propagation? Acta Neuropathol. (Berl.) *121*, 589–595.

Braak, H., and Del Tredici, K. (2015). The preclinical phase of the pathological process underlying sporadic Alzheimer's disease. Brain J. Neurol. *138*, 2814–2833.

Braak, E., Braak, H., and Mandelkow, E.M. (1994a). A sequence of cytoskeleton changes related to the formation of neurofibrillary tangles and neuropil threads. Acta Neuropathol. (Berl.) *87*, 554–567.

Braak, H., Duyckaerts, C., Braak, E., and Piette, F. (1993). Neuropathological stageing of Alzheimer related changes correlates with psychometrically assessed intellectual status. Neurobiol. Aging *13*, S43–S44.

Braak, H., Braak, E., and Strothjohann, M. (1994b). Abnormally phosphorylated tau protein related to the formation of neurofibrillary tangles and neuropil threads in the cerebral cortex of sheep and goat. Neurosci. Lett. *171*, 1–4.

Braak, H., Del Tredici, K., Schultz, C., and Braak, E. (2000). Vulnerability of select neuronal types to Alzheimer's disease. Ann. N. Y. Acad. Sci. *924*, 53–61.

Braak, H., Alafuzoff, I., Arzberger, T., Kretzschmar, H., and Del Tredici, K. (2006). Staging of Alzheimer disease-associated neurofibrillary pathology using paraffin sections and immunocytochemistry. Acta Neuropathol. (Berl.) *112*, 389–404.

Brahic, M., Bousset, L., Bieri, G., Melki, R., and Gitler, A.D. (2016). Axonal transport and secretion of fibrillar forms of α-synuclein, Aβ42 peptide and HTTExon 1. Acta Neuropathol. (Berl.) *131*, 539–548.

Brouillette, J., Caillierez, R., Zommer, N., Alves-Pires, C., Benilova, I., Blum, D., De Strooper, B., and Buée, L. (2012). Neurotoxicity and memory deficits induced by soluble low-molecular-weight amyloid-β1-42 oligomers are revealed in vivo by using a novel animal model. J. Neurosci. Off. J. Soc. Neurosci. *32*, 7852–7861.

Brown, A.M., Lemkul, J.A., Schaum, N., and Bevan, D.R. (2014). Simulations of monomeric amyloid β-peptide (1-40) with varying solution conditions and oxidation state of Met35: implications for aggregation. Arch. Biochem. Biophys. *545*, 44–52.

Brown, P., Liberski, P.P., Wolff, A., and Gajdusek, D.C. (1990). Resistance of scrapie infectivity to steam autoclaving after formaldehyde fixation and limited survival after ashing at 360 degrees C: practical and theoretical implications. J. Infect. Dis. *161*, 467–472.

Brown, P., Gibbs, C.J., Rodgers-Johnson, P., Asher, D.M., Sulima, M.P., Bacote, A., Goldfarb, L.G., and Gajdusek, D.C. (1994). Human spongiform encephalopathy: the National Institutes of Health series of 300 cases of experimentally transmitted disease. Ann. Neurol. *35*, 513–529.

Brown, P., Brandel, J.-P., Sato, T., Nakamura, Y., MacKenzie, J., Will, R.G., Ladogana, A., Pocchiari, M., Leschek, E.W., and Schonberger, L.B. (2012). Iatrogenic Creutzfeldt-Jakob disease, final assessment. Emerg. Infect. Dis. *18*, 901–907.

Budka, H. (2003). Neuropathology of prion diseases. Br. Med. Bull. *66*, 121–130.

Büeler, H., Fischer, M., Lang, Y., Bluethmann, H., Lipp, H.P., DeArmond, S.J., Prusiner, S.B., Aguet, M., and Weissmann, C. (1992). Normal development and behaviour of mice lacking the neuronal cell-surface PrP protein. Nature *356*, 577–582.

Büeler, H., Aguzzi, A., Sailer, A., Greiner, R.A., Autenried, P., Aguet, M., and Weissmann, C. (1993). Mice devoid of PrP are resistant to scrapie. Cell *73*, 1339–1347.

Burgold, S., Filser, S., Dorostkar, M.M., Schmidt, B., and Herms, J. (2014). In vivo imaging reveals sigmoidal growth kinetic of β-amyloid plaques. Acta Neuropathol. Commun. *2*, 30.

Calenda, A., Jallageas, V., Silhol, S., Bellis, M., and Bons, N. (1995). Identification of a unique apolipoprotein E allele in Microcebus murinus; ApoE brain distribution and co-localization with beta-amyloid and tau proteins. Neurobiol. Dis. *2*, 169–176.

Calenda, A., Mestre-Francés, N., Czech, C., Pradier, L., Petter, A., Bons, N., and Bellis, M. (1996). Molecular cloning, sequencing, and brain expression of the presenilin 1 gene in Microcebus murinus. Biochem. Biophys. Res. Commun. *228*, 430–439.

Calenda, A., Mestre-Francés, N., Czech, C., Pradier, L., Petter, A., Perret, M., Bons, N., and Bellis, M. (1998). Cloning of the presenilin 2 cDNA and its distribution in brain of the primate, Microcebus murinus: coexpression with betaAPP and Tau proteins. Neurobiol. Dis. *5*, 323–333.

de Calignon, A., Fox, L.M., Pitstick, R., Carlson, G.A., Bacskai, B.J., Spires-Jones, T.L., and Hyman, B.T. (2010). Caspase activation precedes and leads to tangles. Nature *464*, 1201–1204.

de Calignon, A., Polydoro, M., Suárez-Calvet, M., William, C., Adamowicz, D.H., Kopeikina, K.J., Pitstick, R., Sahara, N., Ashe, K.H., Carlson, G.A., et al. (2012). Propagation of tau pathology in a model of early Alzheimer's disease. Neuron *73*, 685–697.

Carare, R.O., Hawkes, C.A., Jeffrey, M., Kalaria, R.N., and Weller, R.O. (2013). Review: cerebral amyloid angiopathy, prion angiopathy, CADASIL and the spectrum of protein elimination failure angiopathies (PEFA) in neurodegenerative disease with a focus on therapy. Neuropathol. Appl. Neurobiol. *39*, 593–611.

Caughey, B.W., Dong, A., Bhat, K.S., Ernst, D., Hayes, S.F., and Caughey, W.S. (1991). Secondary structure analysis of the scrapie-associated protein PrP 27-30 in water by infrared spectroscopy. Biochemistry (Mosc.) *30*, 7672–7680.

Check Hayden, E. (2014). Pet dogs set to test anti-ageing drug. Nature *514*, 546–546.

Chen, C., and Dong, X.-P. (2016). Epidemiological characteristics of human prion diseases. Infect. Dis. Poverty *5*, 47.

Chesser, A.S., Pritchard, S.M., and Johnson, G.V.W. (2013). Tau clearance mechanisms and their possible role in the pathogenesis of Alzheimer disease. Front. Neurol. *4*, 122.

Chételat, G., Ossenkoppele, R., Villemagne, V.L., Perrotin, A., Landeau, B., Mézenge, F., Jagust, W.J., Dore, V., Miller, B.L., Egret, S., et al. (2016). Atrophy, hypometabolism and clinical trajectories in patients with amyloid-negative Alzheimer's disease. Brain J. Neurol. *139*, 2528–2539.

Chimon, S., Shaibat, M.A., Jones, C.R., Calero, D.C., Aizezi, B., and Ishii, Y. (2007). Evidence of fibril-like β-sheet structures in a neurotoxic amyloid intermediate of Alzheimer's β-amyloid. Nat. Struct. Mol. Biol. *14*, 1157–1164.

Chiti, F., and Dobson, C.M. (2006). Protein misfolding, functional amyloid, and human disease. Annu. Rev. Biochem. *75*, 333–366.

Chui, H.C., Bondareff, W., Zarow, C., and Slager, U. (1984). Stability of neuronal number in the human nucleus basalis of Meynert with age. Neurobiol. Aging *5*, 83–88.

Clavaguera, F., Bolmont, T., Crowther, R.A., Abramowski, D., Frank, S., Probst, A., Fraser, G., Stalder, A.K., Beibel, M., Staufenbiel, M., et al. (2009). Transmission and spreading of tauopathy in transgenic mouse brain. Nat. Cell Biol. *11*, 909–913.

Clavaguera, F., Akatsu, H., Fraser, G., Crowther, R.A., Frank, S., Hench, J., Probst, A., Winkler, D.T., Reichwald, J., Staufenbiel, M., et al. (2013). Brain homogenates from human tauopathies induce tau inclusions in mouse brain. Proc. Natl. Acad. Sci. *110*, 9535–9540.

Clavaguera, F., Hench, J., Lavenir, I., Schweighauser, G., Frank, S., Goedert, M., and Tolnay, M. (2014). Peripheral administration of tau aggregates triggers intracerebral tauopathy in transgenic mice. Acta Neuropathol. (Berl.) *127*, 299–301.

Clavaguera, F., Hench, J., Goedert, M., and Tolnay, M. (2015). Invited review: Prion-like transmission and spreading of tau pathology. Neuropathol. Appl. Neurobiol. *41*, 47–58.

Cobb, N.J., and Surewicz, W.K. (2009). Prion diseases and their biochemical mechanisms. Biochemistry (Mosc.) *48*, 2574–2585.

Cohen, M.L., Kim, C., Haldiman, T., ElHag, M., Mehndiratta, P., Pichet, T., Lissemore, F., Shea, M., Cohen, Y., Chen, W., et al. (2015). Rapidly progressive Alzheimer's disease features distinct structures of amyloid-β. Brain J. Neurol. *138*, 1009–1022.

Colby, D.W., and Prusiner, S.B. (2011). Prions. Cold Spring Harb. Perspect. Biol. *3*, a006833.

Coleman, P.D., and Yao, P.J. (2003). Synaptic slaughter in Alzheimer's disease. Neurobiol. Aging *24*, 1023–1027.

Collinge, J., Whitfield, J., McKintosh, E., Beck, J., Mead, S., Thomas, D.J., and Alpers, M.P. (2006). Kuru in the 21st century--an acquired human prion disease with very long incubation periods. Lancet Lond. Engl. *367*, 2068–2074.

Corder, E.H., Saunders, A.M., Strittmatter, W.J., Schmechel, D.E., Gaskell, P.C., Small, G.W., Roses, A.D., Haines, J.L., and Pericak-Vance, M.A. (1993). Gene dose of apolipoprotein E type 4 allele and the risk of Alzheimer's disease in late onset families. Science *261*, 921–923.

Cordonnier, C., and van der Flier, W.M. (2011). Brain microbleeds and Alzheimer's disease: innocent observation or key player? Brain J. Neurol. *134*, 335–344.

Cork, L.C., Powers, R.E., Selkoe, D.J., Davies, P., Geyer, J.J., and Price, D.L. (1988). Neurofibrillary tangles and senile plaques in aged bears. J. Neuropathol. Exp. Neurol. *47*, 629–641.

Cotman, C.W., and Head, E. (2008). The canine (dog) model of human aging and disease: dietary, environmental and immunotherapy approaches. J. Alzheimers Dis. JAD *15*, 685–707.

Cummings, J.L. (2000). Cholinesterase inhibitors: A new class of psychotropic compounds. Am. J. Psychiatry *157*, 4–15.

Cummings, B.J., Head, E., Ruehl, W., Milgram, N.W., and Cotman, C.W. (1996). The canine as an animal model of human aging and dementia. Neurobiol. Aging *17*, 259–268.

Cummings, J.L., Morstorf, T., and Zhong, K. (2014). Alzheimer's disease drug-development pipeline: few candidates, frequent failures. Alzheimers Res. Ther. *6*, 37.

Dean, D.N., Pate, K.M., Moss, M.A., and Rangachari, V. (2016). Conformational Dynamics of Specific Aβ Oligomers Govern Their Ability To Replicate and Induce Neuronal Apoptosis. Biochemistry (Mosc.) *55*, 2238–2250.

Delacourte, A., Sautière, P.E., Wattez, A., Mourton-Gilles, C., Petter, A., and Bons, N. (1995). Biochemical characterization of Tau proteins during cerebral aging of the lemurian primate Microcebus murinus. Comptes Rendus Académie Sci. Sér. III Sci. Vie *318*, 85–89.

Dhenain, M., Michot, J.L., Privat, N., Picq, J.L., Boller, F., Duyckaerts, C., and Volk, A. (2000). MRI description of cerebral atrophy in mouse lemur primates. Neurobiol. Aging *21*, 81–88.

Dhenain, M., Chenu, E., Hisley, C.K., Aujard, F., and Volk, A. (2003). Regional atrophy in the brain of lissencephalic mouse lemur primates: measurement by automatic histogram-based segmentation of MR images. Magn. Reson. Med. *50*, 984–992.

Dierks, T., Perisic, I., Frölich, L., Ihl, R., and Maurer, K. (1991). Topography of the quantitative electroencephalogram in dementia of the Alzheimer type: relation to severity of dementia. Psychiatry Res. *40*, 181–194.

Domert, J., Rao, S.B., Agholme, L., Brorsson, A.-C., Marcusson, J., Hallbeck, M., and Nath, S. (2014). Spreading of amyloid-β peptides via neuritic cell-to-cell transfer is dependent on insufficient cellular clearance. Neurobiol. Dis. *65*, 82–92.

Driscoll, I., Davatzikos, C., An, Y., Wu, X., Shen, D., Kraut, M., and Resnick, S.M. (2009). Longitudinal pattern of regional brain volume change differentiates normal aging from MCI. Neurology *72*, 1906–1913.

Duffy, P., Wolf, J., Collins, G., DeVoe, A.G., Streeten, B., and Cowen, D. (1974). Letter: Possible person-to-person transmission of Creutzfeldt-Jakob disease. N. Engl. J. Med. *290*, 692–693.

Dujardin, S., Lécolle, K., Caillierez, R., Bégard, S., Zommer, N., Lachaud, C., Carrier, S., Dufour, N., Aurégan, G., Winderickx, J., et al. (2014a). Neuron-to-neuron wild-type Tau protein transfer through a trans-synaptic mechanism: relevance to sporadic tauopathies. Acta Neuropathol. Commun. *2*, 14.

Dujardin, S., Bégard, S., Caillierez, R., Lachaud, C., Delattre, L., Carrier, S., Loyens, A., Galas, M.-C., Bousset, L., Melki, R., et al. (2014b). Ectosomes: a new mechanism for non-exosomal secretion of tau protein. PloS One *9*, e100760.

Duran-Aniotz, C., Morales, R., Moreno-Gonzalez, I., Hu, P.P., and Soto, C. (2013). Brains from non-Alzheimer's individuals containing amyloid deposits accelerate Aβ deposition in vivo. Acta Neuropathol. Commun. *1*, 76.

Duran-Aniotz, C., Morales, R., Moreno-Gonzalez, I., Hu, P.P., Fedynyshyn, J., and Soto, C. (2014). Aggregate-depleted brain fails to induce Aβ deposition in a mouse model of Alzheimer's disease. PloS One *9*, e89014.

Duyckaerts, C., Hauw, J.J., Piette, F., Rainsard, C., Poulain, V., Berthaux, P., and Escourolle, R. (1985). Cortical atrophy in senile dementia of the Alzheimer type is mainly due to a decrease in cortical length. Acta Neuropathol. (Berl.) *66*, 72–74.

Duyckaerts, C., Bennecib, M., Grignon, Y., Uchihara, T., He, Y., Piette, F., and Hauw, J.J. (1997a). Modeling the relation between neurofibrillary tangles and intellectual status. Neurobiol. Aging *18*, 267–273.

Duyckaerts, C., Uchihara, T., Seilhean, D., He, Y., and Hauw, J.J. (1997b). Dissociation of Alzheimer type pathology in a disconnected piece of cortex. Acta Neuropathol. (Berl.) *93*, 501–507.

Duyckaerts, C., Delatour, B., and Potier, M.-C. (2009). Classification and basic pathology of Alzheimer disease. Acta Neuropathol. (Berl.) *118*, 5–36.

Eanes, E.D., and Glenner, G.G. (1968). X-ray diffraction studies on amyloid filaments. J. Histochem. Cytochem. Off. J. Histochem. Soc. *16*, 673–677.

Edgren, G., Hjalgrim, H., Rostgaard, K., Lambert, P., Wikman, A., Norda, R., Titlestad, K.-E., Erikstrup, C., Ullum, H., Melbye, M., et al. (2016). Transmission of Neurodegenerative Disorders Through Blood Transfusion: A Cohort Study. Ann. Intern. Med.

Eisele, Y.S., and Duyckaerts, C. (2016). Propagation of Aß pathology: hypotheses, discoveries, and yet unresolved questions from experimental and human brain studies. Acta Neuropathol. (Berl.) *131*, 5–25.

Eisele, Y.S., Bolmont, T., Heikenwalder, M., Langer, F., Jacobson, L.H., Yan, Z.-X., Roth, K., Aguzzi, A., Staufenbiel, M., Walker, L.C., et al. (2009). Induction of cerebral beta-amyloidosis: intracerebral versus systemic Abeta inoculation. Proc. Natl. Acad. Sci. U. S. A. *106*, 12926–12931.

Eisele, Y.S., Obermuller, U., Heilbronner, G., Baumann, F., Kaeser, S.A., Wolburg, H., Walker, L.C., Staufenbiel, M., Heikenwalder, M., and Jucker, M. (2010). Peripherally Applied A -Containing Inoculates Induce Cerebral -Amyloidosis. Science *330*, 980–982.

Eisele, Y.S., Fritschi, S.K., Hamaguchi, T., Obermüller, U., Füger, P., Skodras, A., Schäfer, C., Odenthal, J., Heikenwalder, M., Staufenbiel, M., et al. (2014). Multiple factors contribute to the peripheral induction of cerebral β-amyloidosis. J. Neurosci. Off. J. Soc. Neurosci. *34*, 10264–10273.

Eisenberg, D., and Jucker, M. (2012). Review: The Amyloid State of Proteins in Human Diseases. Cell *148*, 1188–1203.

Elfenbein, H.A., Rosen, R.F., Stephens, S.L., Switzer, R.C., Smith, Y., Pare, J., Mehta, P.D., Warzok, R., and Walker, L.C. (2007). Cerebral beta-amyloid angiopathy in aged squirrel monkeys. Histol. Histopathol. *22*, 155–167.

Epelbaum, S., Youssef, I., Lacor, P.N., Chaurand, P., Duplus, E., Brugg, B., Duyckaerts, C., and Delatour, B. (2015). Acute amnestic encephalopathy in amyloid-β oligomer-injected mice is due to their widespread diffusion in vivo. Neurobiol. Aging *36*, 2043–2052.

Falcon, B., Cavallini, A., Angers, R., Glover, S., Murray, T.K., Barnham, L., Jackson, S., O'Neill, M.J., Isaacs, A.M., Hutton, M.L., et al. (2015). Conformation determines the seeding potencies of native and recombinant Tau aggregates. J. Biol. Chem. *290*, 1049–1065.

Fändrich, M. (2007). On the structural definition of amyloid fibrils and other polypeptide aggregates. Cell. Mol. Life Sci. CMLS *64*, 2066–2078.

Feinstein, S.C., and Wilson, L. (2005). Inability of tau to properly regulate neuronal microtubule dynamics: a loss-of-function mechanism by which tau might mediate neuronal cell death. Biochim. Biophys. Acta *1739*, 268–279.

Fjell, A.M., Walhovd, K.B., Fennema-Notestine, C., McEvoy, L.K., Hagler, D.J., Holland, D., Brewer, J.B., and Dale, A.M. (2009). One-year brain atrophy evident in healthy aging. J. Neurosci. Off. J. Soc. Neurosci. *29*, 15223–15231.

Flach, K., Hilbrich, I., Schiffmann, A., Gärtner, U., Krüger, M., Leonhardt, M., Waschipky, H., Wick, L., Arendt, T., and Holzer, M. (2012). Tau oligomers impair artificial membrane integrity and cellular viability. J. Biol. Chem. *287*, 43223–43233.

Fleischman, D.A., and Gabrieli, J. (1999). Long-term memory in Alzheimer's disease. Curr. Opin. Neurobiol. *9*, 240–244.

Folstein, M.F., Folstein, S.E., and McHugh, P.R. (1975). "Mini-mental state". A practical method for grading the cognitive state of patients for the clinician. J. Psychiatr. Res. *12*, 189–198.

Forny-Germano, L., Lyra e Silva, N.M., Batista, A.F., Brito-Moreira, J., Gralle, M., Boehnke, S.E., Coe, B.C., Lablans, A., Marques, S.A., Martinez, A.M.B., et al. (2014). Alzheimer's disease-like pathology induced by amyloid-β oligomers in nonhuman primates. J. Neurosci. Off. J. Soc. Neurosci. *34*, 13629–13643.

Frandemiche, M.L., De Seranno, S., Rush, T., Borel, E., Elie, A., Arnal, I., Lanté, F., and Buisson, A. (2014). Activity-dependent tau protein translocation to excitatory synapse is disrupted by exposure to amyloid-beta oligomers. J. Neurosci. Off. J. Soc. Neurosci. *34*, 6084–6097.

Franklin, E.E., Perrin, R.J., Vincent, B., Baxter, M., Morris, J.C., Cairns, N.J., and Alzheimer's Disease Neuroimaging Initiative (2015). Brain collection, standardized neuropathologic assessment, and comorbidity in Alzheimer's Disease Neuroimaging Initiative 2 participants. Alzheimers Dement. J. Alzheimers Assoc. *11*, 815–822.

Fraser, P.E., McLachlan, D.R., Surewicz, W.K., Mizzen, C.A., Snow, A.D., Nguyen, J.T., and Kirschner, D.A. (1994). Conformation and fibrillogenesis of Alzheimer A beta peptides with selected substitution of charged residues. J. Mol. Biol. *244*, 64–73.

Freer, R., Sormanni, P., Vecchi, G., Ciryam, P., Dobson, C.M., and Vendruscolo, M. (2016). A protein homeostasis signature in healthy brains recapitulates tissue vulnerability to Alzheimer's disease. Sci. Adv. *2*, e1600947.

Friedhoff, P., von Bergen, M., Mandelkow, E.M., Davies, P., and Mandelkow, E. (1998). A nucleated assembly mechanism of Alzheimer paired helical filaments. Proc. Natl. Acad. Sci. U. S. A. *95*, 15712–15717.

Friedrich, R.P., Tepper, K., Rönicke, R., Soom, M., Westermann, M., Reymann, K., Kaether, C., and Fändrich, M. (2010). Mechanism of amyloid plaque formation suggests an intracellular basis of Abeta pathogenicity. Proc. Natl. Acad. Sci. U. S. A. *107*, 1942–1947.

Fritschi, S.K., Cintron, A., Ye, L., Mahler, J., Bühler, A., Baumann, F., Neumann, M., Nilsson, K.P.R., Hammarström, P., Walker, L.C., et al. (2014a). Aβ seeds resist inactivation by formaldehyde. Acta Neuropathol. (Berl.) *128*, 477–484.

Fritschi, S.K., Langer, F., Kaeser, S.A., Maia, L.F., Portelius, E., Pinotsi, D., Kaminski, C.F., Winkler, D.T., Maetzler, W., Keyvani, K., et al. (2014b). Highly potent soluble amyloid-β seeds in human Alzheimer brain but not cerebrospinal fluid. Brain J. Neurol. *137*, 2909–2915.

Frontzek, K., Lutz, M.I., Aguzzi, A., Kovacs, G.G., and Budka, H. (2016). Amyloid-β pathology and cerebral amyloid angiopathy are frequent in iatrogenic Creutzfeldt-Jakob disease after dural grafting. Swiss Med. Wkly. *146*, w14287.

Frost, B., Ollesch, J., Wille, H., and Diamond, M.I. (2009). Conformational diversity of wild-type Tau fibrils specified by templated conformation change. J. Biol. Chem. *284*, 3546–3551.

Fukutani, Y., Cairns, N.J., Shiozawa, M., Sasaki, K., Sudo, S., Isaki, K., and Lantos, P.L. (2000). Neuronal loss and neurofibrillary degeneration in the hippocampal cortex in late-onset sporadic Alzheimer's disease. Psychiatry Clin. Neurosci. *54*, 523–529.

Gajdusek, D.C., Gibbs, C.J., Jr, and Alpers, M. (1967). Transmission and passage of experimenal "kuru" to chimpanzees. Science *155*, 212–214.

Gajdusek, D.C., Gibbs, Clarence J., Asher, D.M., and David, E. (1968). Transmission of Experimental Kuru to the Spider Monkey (Ateles geoffreyi). Science 693.

Gambetti, P., Dong, Z., Yuan, J., Xiao, X., Zheng, M., Alshekhlee, A., Castellani, R., Cohen, M., Barria, M.A., Gonzalez-Romero, D., et al. (2008). A novel human disease with abnormal prion protein sensitive to protease. Ann. Neurol. *63*, 697–708.

Gandy, S., DeMattos, R.B., Lemere, C.A., Heppner, F.L., Leverone, J., Aguzzi, A., Ershler, W.B., Dai, J., Fraser, P., Hyslop, P.S.G., et al. (2004). Alzheimer A beta vaccination of rhesus monkeys (Macaca mulatta). Alzheimer Dis. Assoc. Disord. *18*, 44–46.

Gandy, S., Simon, A.J., Steele, J.W., Lublin, A.L., Lah, J.J., Walker, L.C., Levey, A.I., Krafft, G.A., Levy, E., Checler, F., et al. (2010). Days to criterion as an indicator of toxicity associated with human Alzheimer amyloid-beta oligomers. Ann. Neurol. *68*, 220–230.

Garcia-Alloza, M., Robbins, E.M., Zhang-Nunes, S.X., Purcell, S.M., Betensky, R.A., Raju, S., Prada, C., Greenberg, S.M., Bacskai, B.J., and Frosch, M.P. (2006). Characterization of amyloid deposition in the APPswe/PS1dE9 mouse model of Alzheimer disease. Neurobiol. Dis. *24*, 516–524.

Gellermann, G.P., Byrnes, H., Striebinger, A., Ullrich, K., Mueller, R., Hillen, H., and Barghorn, S. (2008). Abeta-globulomers are formed independently of the fibril pathway. Neurobiol. Dis. *30*, 212–220.

Genovese, C.R., Lazar, N.A., and Nichols, T. (2002). Thresholding of statistical maps in functional neuroimaging using the false discovery rate. NeuroImage *15*, 870–878.

George, S., Rönnbäck, A., Gouras, G.K., Petit, G.H., Grueninger, F., Winblad, B., Graff, C., and Brundin, P. (2014). Lesion of the subiculum reduces the spread of amyloid beta pathology to interconnected brain regions in a mouse model of Alzheimer's disease. Acta Neuropathol. Commun. *2*, 17.

Ghoshal, N., García-Sierra, F., Wuu, J., Leurgans, S., Bennett, D.A., Berry, R.W., and Binder, L.I. (2002). Tau conformational changes correspond to impairments of episodic memory in mild cognitive impairment and Alzheimer's disease. Exp. Neurol. *177*, 475–493.

Giaccone, G., Verga, L., Finazzi, M., Pollo, B., Tagliavini, F., Frangione, B., and Bugiani, O. (1990). Cerebral preamyloid deposits and congophilic angiopathy in aged dogs. Neurosci. Lett. *114*, 178–183.

Giannakopoulos, P., Silhol, S., Jallageas, V., Mallet, J., Bons, N., Bouras, C., and Delaère, P. (1997). Quantitative analysis of tau protein-immunoreactive accumulations and beta amyloid protein deposits in the cerebral cortex of the mouse lemur, Microcebus murinus. Acta Neuropathol. (Berl.) *94*, 131–139.

Giannitrapani, D., Collins, J., and Vassiliadis, D. (1991). The EEG spectra of Alzheimer's disease. Int. J. Psychophysiol. Off. J. Int. Organ. Psychophysiol. *10*, 259–269.

Gibbs, C.J., Gajdusek, D.C., Asher, D.M., Alpers, M.P., Beck, E., Daniel, P.M., and Matthews, W.B. (1968a). Creutzfeldt-Jakob disease (spongiform encephalopathy): transmission to the chimpanzee. Science *161*, 388–389.

Gibbs, C.J., Jr, Gajdusek, D.C., Asher, D.M., Alpers, M.P., Beck, E., Daniel, P.M., and Matthews, W.B. (1968b). Creutzfeldt-Jakob disease (spongiform encephalopathy): transmission to the chimpanzee. Science *161*, 388–389.

Gibson, P.H. (1986). Distributions of amyloid plaques in four regions of the brains of mice infected with scrapie by intracerebral and intraperitoneal routes of injection. Acta Neuropathol. (Berl.) *69*, 322–325.

Giffard, B., Laisney, M., Mézenge, F., de la Sayette, V., Eustache, F., and Desgranges, B. (2008). The neural substrates of semantic memory deficits in early Alzheimer's disease: clues from semantic priming effects and FDG-PET. Neuropsychologia *46*, 1657–1666.

Giri, M., Zhang, M., and Lü, Y. (2016). Genes associated with Alzheimer's disease: an overview and current status. Clin. Interv. Aging *11*, 665–681.

Glenner, G.G., and Wong, C.W. (1984). Alzheimer's disease: initial report of the purification and characterization of a novel cerebrovascular amyloid protein. Biochem. Biophys. Res. Commun. *120*, 885–890.

Goate, A., Chartier-Harlin, M.C., Mullan, M., Brown, J., Crawford, F., Fidani, L., Giuffra, L., Haynes, A., Irving, N., and James, L. (1991). Segregation of a missense mutation in the amyloid precursor protein gene with familial Alzheimer's disease. Nature *349*, 704–706.

Godyń, J., Jończyk, J., Panek, D., and Malawska, B. (2016). Therapeutic strategies for Alzheimer's disease in clinical trials. Pharmacol. Rep. PR *68*, 127–138.

Goedert, M., Spillantini, M.G., Cairns, N.J., and Crowther, R.A. (1992). Tau proteins of Alzheimer paired helical filaments: abnormal phosphorylation of all six brain isoforms. Neuron *8*, 159–168.

Golomb, J., de Leon, M.J., Kluger, A., George, A.E., Tarshish, C., and Ferris, S.H. (1993). Hippocampal atrophy in normal aging. An association with recent memory impairment. Arch. Neurol. *50*, 967–973.

Gómez-Isla, T., Hollister, R., West, H., Mui, S., Growdon, J.H., Petersen, R.C., Parisi, J.E., and Hyman, B.T. (1997). Neuronal loss correlates with but exceeds neurofibrillary tangles in Alzheimer's disease. Ann. Neurol. *41*, 17–24.

Good, C.D., Johnsrude, I.S., Ashburner, J., Henson, R.N., Friston, K.J., and Frackowiak, R.S. (2001). A voxel-based morphometric study of ageing in 465 normal adult human brains. NeuroImage *14*, 21–36.

Götz, J., and Ittner, L.M. (2008). Animal models of Alzheimer's disease and frontotemporal dementia. Nat. Rev. Neurosci. *9*, 532–544.

Goudsmit, J., Morrow, C.H., Asher, D.M., Yanagihara, R.T., Masters, C.L., Gibbs, C.J., and Gajdusek, D.C. (1980). Evidence for and against the transmissibility of Alzheimer disease. Neurology *30*, 945–950.

Greenamyre, J.T., Maragos, W.F., Albin, R.L., Penney, J.B., and Young, A.B. (1988). Glutamate transmission and toxicity in Alzheimer's disease. Prog. Neuropsychopharmacol. Biol. Psychiatry *12*, 421–430.

Griffith, J.S. (1967). Self-replication and scrapie. Nature *215*, 1043–1044.

Grothe, M.J., Ewers, M., Krause, B., Heinsen, H., and Teipel, S.J. (2014). Basal forebrain atrophy and cortical amyloid deposition in nondemented elderly subjects. Alzheimers Dement. *10*, S344–S353.

Güntert, A., Döbeli, H., and Bohrmann, B. (2006). High sensitivity analysis of amyloid-beta peptide composition in amyloid deposits from human and PS2APP mouse brain. Neuroscience *143*, 461–475.

Guo, J.L., and Lee, V.M.-Y. (2011). Seeding of normal Tau by pathological Tau conformers drives pathogenesis of Alzheimer-like tangles. J. Biol. Chem. *286*, 15317–15331.

Gylys, K.H., Fein, J.A., Yang, F., Wiley, D.J., Miller, C.A., and Cole, G.M. (2004). Synaptic changes in Alzheimer's disease: increased amyloid-beta and gliosis in surviving terminals is accompanied by decreased PSD-95 fluorescence. Am. J. Pathol. *165*, 1809–1817.

Haass, C., and De Strooper, B. (1999). The presenilins in Alzheimer's disease--proteolysis holds the key. Science *286*, 916–919.

Haass, C., and Selkoe, D.J. (2007). Soluble protein oligomers in neurodegeneration: lessons from the Alzheimer's amyloid beta-peptide. Nat. Rev. Mol. Cell Biol. *8*, 101–112.

Halliday, G.M., Double, K.L., Macdonald, V., and Kril, J.J. (2003). Identifying severely atrophic cortical subregions in Alzheimer's disease. Neurobiol. Aging *24*, 797–806.

Hamaguchi, T., Eisele, Y.S., Varvel, N.H., Lamb, B.T., Walker, L.C., and Jucker, M. (2012). The presence of Aβ seeds, and not age per se, is critical to the initiation of Aβ deposition in the brain. Acta Neuropathol. (Berl.) *123*, 31–37.

Hanger, D.P., Anderton, B.H., and Noble, W. (2009). Tau phosphorylation: the therapeutic challenge for neurodegenerative disease. Trends Mol. Med. *15*, 112–119.

Hansen, R.A., Gartlehner, G., Webb, A.P., Morgan, L.C., Moore, C.G., and Jonas, D.E. (2008). Efficacy and safety of donepezil, galantamine, and rivastigmine for the treatment of Alzheimer's disease: a systematic review and meta-analysis. Clin. Interv. Aging *3*, 211–225.

Hardy, J., and Selkoe, D.J. (2002). The amyloid hypothesis of Alzheimer's disease: progress and problems on the road to therapeutics. Science *297*, 353–356.

Harold, D., Abraham, R., Hollingworth, P., Sims, R., Gerrish, A., Hamshere, M.L., Pahwa, J.S., Moskvina, V., Dowzell, K., Williams, A., et al. (2009). Genome-wide association study identifies variants at CLU and PICALM associated with Alzheimer's disease. Nat. Genet. *41*, 1088–1093.

Harper, J.D., and Lansbury, P.T., Jr (1997). Models of amyloid seeding in Alzheimer's disease and scrapie: mechanistic truths and physiological consequences of the time-dependent solubility of amyloid proteins. Annu. Rev. Biochem. *66*, 385–407.

Harper, J.D., Wong, S.S., Lieber, C.M., and Lansbury, P.T. (1997). Observation of metastable Abeta amyloid protofibrils by atomic force microscopy. Chem. Biol. *4*, 119–125.

Hasegawa, M. (2016). Molecular Mechanisms in the Pathogenesis of Alzheimer's disease and Tauopathies-Prion-Like Seeded Aggregation and Phosphorylation. Biomolecules *6*.

Haute Autorité de Santé (2011). Recommandation de bonne pratique: Maladie d'Alzheimer et maladies apparentées: diagnostic et prise en charge.

Head, E. (2011). Neurobiology of the aging dog. Age Dordr. Neth. *33*, 485–496.

Heilbronner, G., Eisele, Y.S., Langer, F., Kaeser, S.A., Novotny, R., Nagarathinam, A., Aslund, A., Hammarström, P., Nilsson, K.P.R., and Jucker, M. (2013). Seeded strain-like transmission of β-amyloid morphotypes in APP transgenic mice. EMBO Rep. *14*, 1017–1022.

Heuer, E., Rosen, R.F., Cintron, A., and Walker, L.C. (2012). Nonhuman primate models of Alzheimer-like cerebral proteopathy. Curr. Pharm. Des. *18*, 1159–1169.

van der Hiele, K., Vein, A.A., Reijntjes, R.H.A.M., Westendorp, R.G.J., Bollen, E.L.E.M., van Buchem, M.A., van Dijk, J.G., and Middelkoop, H.A.M. (2007a). EEG correlates in the spectrum of cognitive decline. Clin. Neurophysiol. *118*, 1931–1939.

van der Hiele, K., Vein, A.A., van der Welle, A., van der Grond, J., Westendorp, R.G.J., Bollen, E.L.E.M., van Buchem, M.A., van Dijk, J.G., and Middelkoop, H.A.M. (2007b). EEG and MRI correlates of mild cognitive impairment and Alzheimer's disease. Neurobiol. Aging *28*, 1322–1329.

Holmes, B.B., DeVos, S.L., Kfoury, N., Li, M., Jacks, R., Yanamandra, K., Ouidja, M.O., Brodsky, F.M., Marasa, J., Bagchi, D.P., et al. (2013). Heparan sulfate proteoglycans mediate internalization and propagation of specific proteopathic seeds. Proc. Natl. Acad. Sci. U. S. A. *110*, E3138-3147.

Holtzman, D.M., Morris, J.C., and Goate, A.M. (2011). Alzheimer's disease: the challenge of the second century. Sci. Transl. Med. *3*, 77sr1.

Hsia, A.Y., Masliah, E., McConlogue, L., Yu, G.Q., Tatsuno, G., Hu, K., Kholodenko, D., Malenka, R.C., Nicoll, R.A., and Mucke, L. (1999). Plaque-independent disruption of neural circuits in Alzheimer's disease mouse models. Proc. Natl. Acad. Sci. U. S. A. *96*, 3228–3233.

Hsu, Y.-Y., Schuff, N., Du, A.-T., Mark, K., Zhu, X., Hardin, D., and Weiner, M.W. (2002). Comparison of Automated and Manual MRI Volumetry of Hippocampus in Normal Aging and Dementia. J. Magn. Reson. Imaging JMRI *16*, 305–310.

Hu, W., Zhang, X., Tung, Y.C., Xie, S., Liu, F., and Iqbal, K. (2016). Hyperphosphorylation determines both the spread and the morphology of tau pathology. Alzheimers Dement. J. Alzheimers Assoc.

Hu, X., Crick, S.L., Bu, G., Frieden, C., Pappu, R.V., and Lee, J.-M. (2009). Amyloid seeds formed by cellular uptake, concentration, and aggregation of the amyloid-beta peptide. Proc. Natl. Acad. Sci. U. S. A. *106*, 20324–20329.

Huang, C., Wahlund, L., Dierks, T., Julin, P., Winblad, B., and Jelic, V. (2000). Discrimination of Alzheimer's disease and mild cognitive impairment by equivalent EEG sources: a cross-sectional and longitudinal study. Clin. Neurophysiol. Off. J. Int. Fed. Clin. Neurophysiol. *111*, 1961–1967.

Hughes, C.P., Berg, L., Danziger, W.L., Coben, L.A., and Martin, R.L. (1982). A new clinical scale for the staging of dementia. Br. J. Psychiatry J. Ment. Sci. *140*, 566–572.

Hyman, B.T., Phelps, C.H., Beach, T.G., Bigio, E.H., Cairns, N.J., Carrillo, M.C., Dickson, D.W., Duyckaerts, C., Frosch, M.P., Masliah, E., et al. (2012). National Institute on Aging–Alzheimer's Association guidelines for the neuropathologic assessment of Alzheimer's disease. Alzheimers Dement. J. Alzheimers Assoc. *8*, 1–13.

Iba, M., Guo, J.L., McBride, J.D., Zhang, B., Trojanowski, J.Q., and Lee, V.M.-Y. (2013). Synthetic tau fibrils mediate transmission of neurofibrillary tangles in a transgenic mouse model of Alzheimer's-like tauopathy. J. Neurosci. Off. J. Soc. Neurosci. *33*, 1024–1037.

Iba, M., McBride, J.D., Guo, J.L., Zhang, B., Trojanowski, J.Q., and Lee, V.M.-Y. (2015). Tau pathology spread in PS19 tau transgenic mice following locus coeruleus (LC) injections of synthetic tau fibrils is determined by the LC's afferent and efferent connections. Acta Neuropathol. (Berl.) *130*, 349–362.

Imran, M., and Mahmood, S. (2011). An overview of human prion diseases. Virol. J. *8*, 1.

Infarinato, F., Rahman, A., Del Percio, C., Lamberty, Y., Bordet, R., Richardson, J.C., Forloni, G., Drinkenburg, W., Lopez, S., Aujard, F., et al. (2015). On-Going Frontal Alpha Rhythms Are Dominant in Passive State and Desynchronize in Active State in Adult Gray Mouse Lemurs. PloS One *10*, e0143719.

Irwin, D.J., Abrams, J.Y., Schonberger, L.B., Leschek, E.W., Mills, J.L., Lee, V.M.-Y., and Trojanowski, J.Q. (2013). Evaluation of potential infectivity of Alzheimer and Parkinson disease proteins in recipients of cadaver-derived human growth hormone. JAMA Neurol. *70*, 462–468.

Iwata, N., Tsubuki, S., Takaki, Y., Watanabe, K., Sekiguchi, M., Hosoki, E., Kawashima-Morishima, M., Lee, H.J., Hama, E., Sekine-Aizawa, Y., et al. (2000). Identification of the major Abeta1-42-degrading catabolic pathway in brain parenchyma: suppression leads to biochemical and pathological deposition. Nat. Med. *6*, 143–150.

Jack, C.R. (2014). PART and SNAP. Acta Neuropathol. (Berl.) *128*, 773–776.

Jack, C.R., and Holtzman, D.M. (2013). Biomarker modeling of Alzheimer's disease. Neuron *80*, 1347–1358.

Jack, C.R., Petersen, R.C., Xu, Y.C., Waring, S.C., O'Brien, P.C., Tangalos, E.G., Smith, G.E., Ivnik, R.J., and Kokmen, E. (1997). Medial Temporal Atrophy on MRI in Normal Aging and Very Mild Alzheimer's Disease. Neurology *49*, 786–794.

Jack, C.R., Petersen, R.C., Xu, Y., O'Brien, P.C., Smith, G.E., Ivnik, R.J., Tangalos, E.G., and Kokmen, E. (1998). Rate of medial temporal lobe atrophy in typical aging and Alzheimer's disease. Neurology *51*, 993–999.

Jack, C.R., Dickson, D.W., Parisi, J.E., Xu, Y.C., Cha, R.H., O'Brien, P.C., Edland, S.D., Smith, G.E., Boeve, B.F., Tangalos, E.G., et al. (2002). Antemortem MRI findings correlate with hippocampal neuropathology in typical aging and dementia. Neurology *58*, 750–757.

Jack, C.R., Bennett, D.A., Blennow, K., Carrillo, M.C., Feldman, H.H., Frisoni, G.B., Hampel, H., Jagust, W.J., Johnson, K.A., Knopman, D.S., et al. (2016). A/T/N: An unbiased descriptive classification scheme for Alzheimer disease biomarkers. Neurology *87*, 539–547.

Jackson, S.J., Kerridge, C., Cooper, J., Cavallini, A., Falcon, B., Cella, C.V., Landi, A., Szekeres, P.G., Murray, T.K., Ahmed, Z., et al. (2016). Short Fibrils Constitute the Major Species of Seed-Competent Tau in the Brains of Mice Transgenic for Human P301S Tau. J. Neurosci. Off. J. Soc. Neurosci. *36*, 762–772.

Jankowsky, J.L., Fadale, D.J., Anderson, J., Xu, G.M., Gonzales, V., Jenkins, N.A., Copeland, N.G., Lee, M.K., Younkin, L.H., Wagner, S.L., et al. (2004). Mutant presenilins specifically elevate the levels of the 42 residue beta-amyloid peptide in vivo: evidence for augmentation of a 42-specific gamma secretase. Hum. Mol. Genet. *13*, 159–170.

Jarrett, J.T., and Lansbury, P.T. (1993). Seeding "one-dimensional crystallization" of amyloid: a pathogenic mechanism in Alzheimer's disease and scrapie? Cell *73*, 1055–1058.

Jarrett, J.T., Berger, E.P., and Lansbury, P.T. (1993). The carboxy terminus of the beta amyloid protein is critical for the seeding of amyloid formation: implications for the pathogenesis of Alzheimer's disease. Biochemistry (Mosc.) *32*, 4693–4697.

Jaunmuktane, Z., Mead, S., Ellis, M., Wadsworth, J.D.F., Nicoll, A.J., Kenny, J., Launchbury, F., Linehan, J., Richard-Loendt, A., Walker, A.S., et al. (2015). Evidence for human transmission of amyloid-β pathology and cerebral amyloid angiopathy. Nature *525*, 247–250.

Jeganathan, S., von Bergen, M., Brutlach, H., Steinhoff, H.-J., and Mandelkow, E. (2006). Global hairpin folding of tau in solution. Biochemistry (Mosc.) *45*, 2283–2293.

Jelic, V., Johansson, S.-E., Almkvist, O., Shigeta, M., Julin, P., Nordberg, A., Winblad, B., and Wahlund, L.-O. (2000). Quantitative electroencephalography in mild cognitive impairment: longitudinal changes and possible prediction of Alzheimer's disease. Neurobiol. Aging *21*, 533–540.

Johnstone, E.M., Chaney, M.O., Norris, F.H., Pascual, R., and Little, S.P. (1991). Conservation of the sequence of the Alzheimer's disease amyloid peptide in dog, polar bear and five other mammals by cross-species polymerase chain reaction analysis. Brain Res. Mol. Brain Res. *10*, 299–305.

Joly, M., Deputte, B., and Verdier, J.-M. (2006). Age effect on olfactory discrimination in a non-human primate, Microcebus murinus. Neurobiol. Aging *27*, 1045–1049.

Joly, M., Ammersdörfer, S., Schmidtke, D., and Zimmermann, E. (2014). Touchscreen-based cognitive tasks reveal age-related impairment in a primate aging model, the grey mouse lemur (Microcebus murinus). PloS One *9*, e109393.

Jonsson, T., Stefansson, H., Steinberg, S., Jonsdottir, I., Jonsson, P.V., Snaedal, J., Bjornsson, S., Huttenlocher, J., Levey, A.I., Lah, J.J., et al. (2013). Variant of TREM2 associated with the risk of Alzheimer's disease. N. Engl. J. Med. *368*, 107–116.

Josephs, K.A., Whitwell, J.L., Ahmed, Z., Shiung, M.M., Weigand, S.D., Knopman, D.S., Boeve, B.F., Parisi, J.E., Petersen, R.C., Dickson, D.W., et al. (2008). Beta-amyloid burden is not associated with rates of brain atrophy. Ann. Neurol. *63*, 204–212.

Jucker, M., and Walker, L.C. (2013). Self-propagation of pathogenic protein aggregates in neurodegenerative diseases. Nature *501*, 45–51.

Jyoti, A., Plano, A., Riedel, G., and Platt, B. (2015). Progressive age-related changes in sleep and EEG profiles in the PLB1Triple mouse model of Alzheimer's disease. Neurobiol. Aging *36*, 2768–2784.

Kalaria, R.N. (1997). Cerebrovascular degeneration is related to amyloid-beta protein deposition in Alzheimer's disease. Ann. N. Y. Acad. Sci. *826*, 263–271.

Kane, M.D., Lipinski, W.J., Callahan, M.J., Bian, F., Durham, R.A., Schwarz, R.D., Roher, A.E., and Walker, L.C. (2000). Evidence for seeding of beta -amyloid by intracerebral infusion of Alzheimer brain extracts in beta -amyloid precursor protein-transgenic mice. J. Neurosci. Off. J. Soc. Neurosci. *20*, 3606–3611.

Karch, C.M., Jeng, A.T., and Goate, A.M. (2012). Extracellular Tau Levels Are Influenced by Variability in Tau That Is Associated with Tauopathies. J. Biol. Chem. *287*, 42751–42762.

Kayed, R., Head, E., Thompson, J.L., McIntire, T.M., Milton, S.C., Cotman, C.W., and Glabe, C.G. (2003). Common structure of soluble amyloid oligomers implies common mechanism of pathogenesis. Science *300*, 486–489.

Kelly, J.J. (1987). Polyneuropathies Associated with Plasma Cell Dyscrasias. Semin. Neurol. *7*, 30.

Kfoury, N., Holmes, B.B., Jiang, H., Holtzman, D.M., and Diamond, M.I. (2012). Trans-cellular propagation of Tau aggregation by fibrillar species. J. Biol. Chem. *287*, 19440–19451.

Kim, W., and Hecht, M.H. (2008). Mutations enhance the aggregation propensity of the Alzheimer's A beta peptide. J. Mol. Biol. *377*, 565–574.

Kim, J., Basak, J.M., and Holtzman, D.M. (2009). The role of apolipoprotein E in Alzheimer's disease. Neuron *63*, 287–303.

Kim, Y.E., Hipp, M.S., Bracher, A., Hayer-Hartl, M., and Ulrich Hartl, F. (2013). Molecular Chaperone Functions in Protein Folding and Proteostasis. Annu. Rev. Biochem. *82*, 323–355.

Kimura, N., Tanemura, K., Nakamura, S., Takashima, A., Ono, F., Sakakibara, I., Ishii, Y., Kyuwa, S., and Yoshikawa, Y. (2003). Age-related changes of Alzheimer's disease-associated proteins in cynomolgus monkey brains. Biochem. Biophys. Res. Commun. *310*, 303–311.

Kimura, T., Whitcomb, D.J., Jo, J., Regan, P., Piers, T., Heo, S., Brown, C., Hashikawa, T., Murayama, M., Seok, H., et al. (2014). Microtubule-associated protein tau is essential for long-term depression in the hippocampus. Philos. Trans. R. Soc. Lond. B. Biol. Sci. *369*, 20130144.

King, M.E., Ahuja, V., Binder, L.I., and Kuret, J. (1999). Ligand-dependent tau filament formation: implications for Alzheimer's disease progression. Biochemistry (Mosc.) *38*, 14851–14859.

Kirkitadze, M.D., Condron, M.M., and Teplow, D.B. (2001). Identification and characterization of key kinetic intermediates in amyloid beta-protein fibrillogenesis. J. Mol. Biol. *312*, 1103–1119.

Knowles, T.P.J., Vendruscolo, M., and Dobson, C.M. (2014). The amyloid state and its association with protein misfolding diseases. Nat. Rev. Mol. Cell Biol. *15*, 384–396.

Kodali, R., Williams, A.D., Chemuru, S., and Wetzel, R. (2010). Abeta(1-40) forms five distinct amyloid structures whose beta-sheet contents and fibril stabilities are correlated. J. Mol. Biol. *401*, 503–517.

Koenig, T., Prichep, L., Dierks, T., Hubl, D., Wahlund, L.O., John, E.R., and Jelic, V. (2005). Decreased EEG synchronization in Alzheimer's disease and mild cognitive impairment. Neurobiol. Aging *26*, 165–171.

Kondo, A., Shahpasand, K., Mannix, R., Qiu, J., Moncaster, J., Chen, C.-H., Yao, Y., Lin, Y.-M., Driver, J.A., Sun, Y., et al. (2015). Antibody against early driver of neurodegeneration cis P-tau blocks brain injury and tauopathy. Nature *523*, 431–436.

Köpke, E., Tung, Y.C., Shaikh, S., Alonso, A.C., Iqbal, K., and Grundke-Iqbal, I. (1993). Microtubule-associated protein tau. Abnormal phosphorylation of a non-paired helical filament pool in Alzheimer disease. J. Biol. Chem. *268*, 24374–24384.

Koss, D.J., Drever, B.D., Stoppelkamp, S., Riedel, G., and Platt, B. (2013). Age-dependent changes in hippocampal synaptic transmission and plasticity in the PLB1Triple Alzheimer mouse. Cell. Mol. Life Sci. *70*, 2585–2601.

Kovacs, G.G., and Gelpi, E. (2012). Clinical Neuropathology Practice News 3-2012: the "ABC" in AD – revised and updated guideline for the neuropathologic assessment of Alzheimer's disease. Clin. Neuropathol. *31*, 116–118.

Kovacs, G.G., Lutz, M.I., Ricken, G., Ströbel, T., Höftberger, R., Preusser, M., Regelsberger, G., Hönigschnabl, S., Reiner, A., Fischer, P., et al. (2016). Dura mater is a potential source of Aβ seeds. Acta Neuropathol. (Berl.) *131*, 911–923.

Kraska, A., Dorieux, O., Picq, J.-L., Petit, F., Bourrin, E., Chenu, E., Volk, A., Perret, M., Hantraye, P., Mestre-Frances, N., et al. (2011). Age-associated cerebral atrophy in mouse lemur primates. Neurobiol. Aging *32*, 894–906.

Kraska, A., Santin, M.D., Dorieux, O., Joseph-Mathurin, N., Bourrin, E., Petit, F., Jan, C., Chaigneau, M., Hantraye, P., Lestage, P., et al. (2012). In vivo cross-sectional characterization of cerebral alterations induced by intracerebroventricular administration of streptozotocin. PloS One *7*, e46196.

Kretzschmar, H. (2009). Brain banking: opportunities, challenges and meaning for the future. Nat Rev Neurosci *10*, 70–78.

Kretzschmar, H.A., Prusiner, S.B., Stowring, L.E., and DeArmond, S.J. (1986). Scrapie prion proteins are synthesized in neurons. Am. J. Pathol. *122*, 1–5.

Kuchibhotla, K.V., Wegmann, S., Kopeikina, K.J., Hawkes, J., Rudinskiy, N., Andermann, M.L., Spires-Jones, T.L., Bacskai, B.J., and Hyman, B.T. (2014). Neurofibrillary tangle-bearing neurons are functionally integrated in cortical circuits in vivo. Proc. Natl. Acad. Sci. U. S. A. *111*, 510–514.

Kumar, A., Pate, K.M., Moss, M.A., Dean, D.N., and Rangachari, V. (2014). Self-Propagative Replication of A[beta] Oligomers Suggests Potential Transmissibility in Alzheimer Disease. PLoS ONE.

Kurz, A., Altland, K., Lautenschlager, N., Zimmer, R., Busch, R., Gerundt, I., Lauter, H., and Müller, U. (1996). Apolipoprotein E type 4 allele and Alzheimer's disease: effect on age at onset and relative risk in different age groups. J. Neurol. *243*, 452–456.

Lam, H.T., Graber, M.C., Gentry, K.A., and Bieschke, J. (2016). Stabilization of α-Synuclein Fibril Clusters Prevents Fragmentation and Reduces Seeding Activity and Toxicity. Biochemistry (Mosc.) *55*, 675–685.

Lambert, J.-C., Heath, S., Even, G., Campion, D., Sleegers, K., Hiltunen, M., Combarros, O., Zelenika, D., Bullido, M.J., Tavernier, B., et al. (2009). Genome-wide association study identifies variants at CLU and CR1 associated with Alzheimer's disease. Nat. Genet. *41*, 1094–1099.

Lambert, M.P., Barlow, A.K., Chromy, B.A., Edwards, C., Freed, R., Liosatos, M., Morgan, T.E., Rozovsky, I., Trommer, B., Viola, K.L., et al. (1998). Diffusible, nonfibrillar ligands derived from Abeta1-42 are potent central nervous system neurotoxins. Proc. Natl. Acad. Sci. U. S. A. *95*, 6448–6453.

Landreh, M., Sawaya, M.R., Hipp, M.S., Eisenberg, D.S., Wüthrich, K., and Hartl, F.U. (2016). The formation, function and regulation of amyloids: insights from structural biology. J. Intern. Med.

Langer, F., Eisele, Y.S., Fritschi, S.K., Staufenbiel, M., Walker, L.C., and Jucker, M. (2011). Soluble Aβ seeds are potent inducers of cerebral β-amyloid deposition. J. Neurosci. Off. J. Soc. Neurosci. *31*, 14488–14495.

Languille, S., Blanc, S., Blin, O., Canale, C.I., Dal-Pan, A., Devau, G., Dhenain, M., Dorieux, O., Epelbaum, J., Gomez, D., et al. (2012). The grey mouse lemur: a non-human primate model for ageing studies. Ageing Res. Rev. *11*, 150–162.

Lannfelt, L., Bogdanovic, N., Appelgren, H., Axelman, K., Lilius, L., Hansson, G., Schenk, D., Hardy, J., and Winblad, B. (1994). Amyloid precursor protein mutation causes Alzheimer's disease in a Swedish family. Neurosci. Lett. *168*, 254–256.

Lasagna-Reeves, C.A., Castillo-Carranza, D.L., Sengupta, U., Sarmiento, J., Troncoso, J., Jackson, G.R., and Kayed, R. (2012a). Identification of oligomers at early stages of tau aggregation in Alzheimer's disease. FASEB J. Off. Publ. Fed. Am. Soc. Exp. Biol. *26*, 1946–1959.

Lasagna-Reeves, C.A., Castillo-Carranza, D.L., Sengupta, U., Guerrero-Munoz, M.J., Kiritoshi, T., Neugebauer, V., Jackson, G.R., and Kayed, R. (2012b). Alzheimer brain-derived tau oligomers propagate pathology from endogenous tau. Sci. Rep. *2*, 700.

Lasmézas, C.I., Deslys, J.P., Robain, O., Jaegly, A., Beringue, V., Peyrin, J.M., Fournier, J.G., Hauw, J.J., Rossier, J., and Dormont, D. (1997). Transmission of the BSE agent to mice in the absence of detectable abnormal prion protein. Science *275*, 402–405.

Lee, J., Culyba, E.K., Powers, E.T., and Kelly, J.W. (2011a). Amyloid-β forms fibrils by nucleated conformational conversion of oligomers. Nat. Chem. Biol. *7*, 602–609.

Lee, J., Culyba, E.K., Powers, E.T., and Kelly, J.W. (2011b). Amyloid-β forms fibrils by nucleated conformational conversion of oligomers. Nat. Chem. Biol. *7*, 602–609.

Legname, G., Baskakov, I.V., Nguyen, H.-O.B., Riesner, D., Cohen, F.E., DeArmond, S.J., and Prusiner, S.B. (2004). Synthetic Mammalian Prions. Science 673.

Lei, P., Ayton, S., Moon, S., Zhang, Q., Volitakis, I., Finkelstein, D.I., and Bush, A.I. (2014). Motor and cognitive deficits in aged tau knockout mice in two background strains. Mol. Neurodegener. *9*, 29.

Lemere, C.A., Beierschmitt, A., Iglesias, M., Spooner, E.T., Bloom, J.K., Leverone, J.F., Zheng, J.B., Seabrook, T.J., Louard, D., Li, D., et al. (2004). Alzheimer's disease abeta vaccine reduces central nervous system abeta levels in a non-human primate, the Caribbean vervet. Am. J. Pathol. *165*, 283–297.

Lemere, C.A., Oh, J., Stanish, H.A., Peng, Y., Pepivani, I., Fagan, A.M., Yamaguchi, H., Westmoreland, S.V., and Mansfield, K.G. (2008). Cerebral amyloid-beta protein accumulation with aging in cotton-top tamarins: a model of early Alzheimer's disease? Rejuvenation Res. *11*, 321–332.

Levy-Lahad, E., Wasco, W., Poorkaj, P., Romano, D.M., Oshima, J., Pettingell, W.H., Yu, C.E., Jondro, P.D., Schmidt, S.D., and Wang, K. (1995). Candidate gene for the chromosome 1 familial Alzheimer's disease locus. Science *269*, 973–977.

Li, W., Wu, Y. 'e, Min, F., Li, Z., Huang, J., and Huang, R. (2010). A nonhuman primate model of Alzheimer's disease generated by intracranial injection of amyloid-β42 and thiorphan. Metab. Brain Dis. *25*, 277–284.

Liao, Y.C., Lebo, R.V., Clawson, G.A., and Smuckler, E.A. (1986). Human prion protein cDNA: molecular cloning, chromosomal mapping, and biological implications. Science *233*, 364–367.

Liberski, P.P. (2012). Historical overview of prion diseases: a view from afar. Folia Neuropathol *50*, 1–12.

Liu, L., Drouet, V., Wu, J.W., Witter, M.P., Small, S.A., Clelland, C., and Duff, K. (2012). Trans-synaptic spread of tau pathology in vivo. PloS One *7*, e31302.

Liu, P., Reed, M.N., Kotilinek, L.A., Grant, M.K.O., Forster, C.L., Qiang, W., Shapiro, S.L., Reichl, J.H., Chiang, A.C.A., Jankowsky, J.L., et al. (2015). Quaternary Structure Defines a Large Class of Amyloid-β Oligomers Neutralized by Sequestration. Cell Rep. *11*, 1760–1771.

Lowes-Hummel, P., Gertz, H.J., Ferszt, R., and Cervos-Navarro, J. (1989). The basal nucleus of Meynert revised: the nerve cell number decreases with age. Arch. Gerontol. Geriatr. *8*, 21–27.

Lu, J.-X., Qiang, W., Yau, W.-M., Schwieters, C.D., Meredith, S.C., and Tycko, R. (2013). Molecular structure of β-amyloid fibrils in Alzheimer's disease brain tissue. Cell *154*, 1257–1268.

Lu, P.J., Wulf, G., Zhou, X.Z., Davies, P., and Lu, K.P. (1999). The prolyl isomerase Pin1 restores the function of Alzheimer-associated phosphorylated tau protein. Nature *399*, 784–788.

Lue, L.F., Kuo, Y.M., Roher, A.E., Brachova, L., Shen, Y., Sue, L., Beach, T., Kurth, J.H., Rydel, R.E., and Rogers, J. (1999). Soluble amyloid beta peptide concentration as a predictor of synaptic change in Alzheimer's disease. Am. J. Pathol. *155*, 853–862.

Luo, J., Wärmländer, S.K.T.S., Gräslund, A., and Abrahams, J.P. (2016). Reciprocal Molecular Interactions between the Aβ Peptide Linked to Alzheimer's Disease and Insulin Linked to Diabetes Mellitus Type II. ACS Chem. Neurosci. *7*, 269–274.

Mabbott, N.A., and MacPherson, G.G. (2006). Prions and their lethal journey to the brain. Nat. Rev. Microbiol. *4*, 201–211.

Maccioni, R.B., Farías, G., Morales, I., and Navarrete, L. (2010). The revitalized tau hypothesis on Alzheimer's disease. Arch. Med. Res. *41*, 226–231.

Maclean, C.J., Baker, H.F., Ridley, R.M., and Mori, H. (2000). Naturally occurring and experimentally induced beta-amyloid deposits in the brains of marmosets (Callithrix jacchus). J. Neural Transm. Vienna Austria 1996 *107*, 799–814.

Maheswaran, S., Barjat, H., Rueckert, D., Bate, S.T., Howlett, D.R., Tilling, L., Smart, S.C., Pohlmann, A., Richardson, J.C., Hartkens, T., et al. (2009). Longitudinal regional brain volume changes quantified in normal aging and Alzheimer's APP x PS1 mice using MRI. Brain Res. *1270*, 19–32.

Mander, B.A., Marks, S.M., Vogel, J.W., Rao, V., Lu, B., Saletin, J.M., Ancoli-Israel, S., Jagust, W.J., and Walker, M.P. (2015). β-amyloid disrupts human NREM slow waves and related hippocampus-dependent memory consolidation. Nat. Neurosci. *18*, 1051–1057.

Manson, J.C., Jamieson, E., Baybutt, H., Tuzi, N.L., Barron, R., McConnell, I., Somerville, R., Ironside, J., Will, R., Sy, M.S., et al. (1999). A single amino acid alteration (101L) introduced into murine PrP dramatically alters incubation time of transmissible spongiform encephalopathy. EMBO J. *18*, 6855–6864.

Maphis, N., Xu, G., Kokiko-Cochran, O.N., Jiang, S., Cardona, A., Ransohoff, R.M., Lamb, B.T., and Bhaskar, K. (2015). Reactive microglia drive tau pathology and contribute to the spreading of pathological tau in the brain. Brain J. Neurol. *138*, 1738–1755.

Marr, R.A., and Hafez, D.M. (2014). Amyloid-beta and Alzheimer's disease: the role of neprilysin-2 in amyloid-beta clearance. Front. Aging Neurosci. *6*.

Martin, L., Latypova, X., and Terro, F. (2011). Post-translational modifications of tau protein: implications for Alzheimer's disease. Neurochem. Int. *58*, 458–471.

Marzesco, A.-M., Flötenmeyer, M., Bühler, A., Obermüller, U., Staufenbiel, M., Jucker, M., and Baumann, F. (2016). Highly potent intracellular membrane-associated Aβ seeds. Sci. Rep. *6*, 28125.

Masters, C.L., Simms, G., Weinman, N.A., Multhaup, G., McDonald, B.L., and Beyreuther, K. (1985). Amyloid plaque core protein in Alzheimer disease and Down syndrome. Proc. Natl. Acad. Sci. U. S. A. *82*, 4245–4249.

Mastrianni, J.A. (2010). The genetics of prion diseases. Genet. Med. Off. J. Am. Coll. Med. Genet. *12*, 187–195.

Mattia, D., Babiloni, F., Romigi, A., Cincotti, F., Bianchi, L., Sperli, F., Placidi, F., Bozzao, A., Giacomini, P., Floris, R., et al. (2003). Quantitative EEG and dynamic susceptibility contrast MRI in Alzheimer's disease: a correlative study. Clin. Neurophysiol. Off. J. Int. Fed. Clin. Neurophysiol. *114*, 1210–1216.

Mattson, M.P. (2004). Pathways towards and away from Alzheimer's disease. Nature *430*, 631–639.

Mattsson, N., Tosun, D., Insel, P.S., Simonson, A., Jack, C.R., Beckett, L.A., Donohue, M., Jagust, W., Schuff, N., Weiner, M.W., et al. (2014). Association of brain amyloid-β with cerebral perfusion and structure in Alzheimer's disease and mild cognitive impairment. Brain J. Neurol. *137*, 1550–1561.

Mawuenyega, K.G., Sigurdson, W., Ovod, V., Munsell, L., Kasten, T., Morris, J.C., Yarasheski, K.E., and Bateman, R.J. (2010). Decreased clearance of CNS beta-amyloid in Alzheimer's disease. Science *330*, 1774.

Mayer, G., Nitsch, R., and Hoyer, S. (1990). Effects of changes in peripheral and cerebral glucose metabolism on locomotor activity, learning and memory in adult male rats. Brain Res. *532*, 95–100.

Mayeux, R., Stern, Y., and Spanton, S. (1985). Heterogeneity in dementia of the Alzheimer type: evidence of subgroups. Neurology *35*, 453–461.

McKhann, G., Drachman, D., Folstein, M., Katzman, R., Price, D., and Stadlan, E.M. (1984). Clinical diagnosis of Alzheimer's disease: report of the NINCDS-ADRDA Work Group under the auspices of Department of Health and Human Services Task Force on Alzheimer's Disease. Neurology *34*, 939–944.

McKhann, G.M., Knopman, D.S., Chertkow, H., Hyman, B.T., Jack, C.R., Kawas, C.H., Klunk, W.E., Koroshetz, W.J., Manly, J.J., Mayeux, R., et al. (2011). The diagnosis of dementia due to Alzheimer's disease: recommendations from the National Institute on Aging-Alzheimer's Association workgroups on diagnostic guidelines for Alzheimer's disease. Alzheimers Dement. J. Alzheimers Assoc. *7*, 263–269.

McLaurin, J., Yang, D., Yip, C.M., and Fraser, P.E. (2000). Review: modulating factors in amyloid-beta fibril formation. J. Struct. Biol. *130*, 259–270.

McLean, C.A., Cherny, R.A., Fraser, F.W., Fuller, S.J., Smith, M.J., Beyreuther, K., Bush, A.I., and Masters, C.L. (1999). Soluble pool of Abeta amyloid as a determinant of severity of neurodegeneration in Alzheimer's disease. Ann. Neurol. *46*, 860–866.

Mestre-Francés, N., Keller, E., Calenda, A., Barelli, H., Checler, F., and Bons, N. (2000). Immunohistochemical analysis of cerebral cortical and vascular lesions in the primate Microcebus murinus reveal distinct amyloid beta1-42 and beta1-40 immunoreactivity profiles. Neurobiol. Dis. *7*, 1–8.

Meyer, V., Dinkel, P.D., Rickman Hager, E., and Margittai, M. (2014). Amplification of Tau fibrils from minute quantities of seeds. Biochemistry (Mosc.) *53*, 5804–5809.

Meyer-Luehmann, M., Stalder, M., Herzig, M.C., Kaeser, S.A., Kohler, E., Pfeifer, M., Boncristiano, S., Mathews, P.M., Mercken, M., Abramowski, D., et al. (2003). Extracellular amyloid formation and associated pathology in neural grafts. Nat. Neurosci. *6*, 370–377.

Meyer-Luehmann, M., Coomaraswamy, J., Bolmont, T., Kaeser, S., Schaefer, C., Kilger, E., Neuenschwander, A., Abramowski, D., Frey, P., Jaton, A.L., et al. (2006). Exogenous induction of cerebral beta-amyloidogenesis is governed by agent and host. Science *313*, 1781–1784.

Mhatre, S.D., Tsai, C.A., Rubin, A.J., James, M.L., and Andreasson, K.I. (2015). Microglial malfunction: the third rail in the development of Alzheimer's disease. Trends Neurosci. *38*, 621–636.

Miller, J.A., Woltjer, R.L., Goodenbour, J.M., Horvath, S., and Geschwind, D.H. (2013). Genes and pathways underlying regional and cell type changes in Alzheimer's disease. Genome Med. *5*, 48.

Miners, J.S., Barua, N., Kehoe, P.G., Gill, S., and Love, S. (2011). Aβ-degrading enzymes: potential for treatment of Alzheimer disease. J. Neuropathol. Exp. Neurol. *70*, 944–959.

Mirbaha, H., Holmes, B.B., Sanders, D.W., Bieschke, J., and Diamond, M.I. (2015). Tau Trimers Are the Minimal Propagation Unit Spontaneously Internalized to Seed Intracellular Aggregation. J. Biol. Chem. *290*, 14893–14903.

Mirra, S.S., Heyman, A., McKeel, D., Sumi, S.M., Crain, B.J., Brownlee, L.M., Vogel, F.S., Hughes, J.P., van Belle, G., and Berg, L. (1991). The Consortium to Establish a Registry for Alzheimer's Disease (CERAD). Part II. Standardization of the neuropathologic assessment of Alzheimer's disease. Neurology *41*, 479–486.

Mittermeier, R.A., Ganzhorn, J.U., Konstant, W.R., Glander, K., Tattersall, I., Groves, C.P., Rylands, A.B., Hapke, A., Ratsimbazafy, J., Mayor, M.I., et al. (2008). Lemur Diversity in Madagascar. Int. J. Primatol. *29*, 1607–1656.

Mohamed, N.-V., Herrou, T., Plouffe, V., Piperno, N., and Leclerc, N. (2013). Spreading of tau pathology in Alzheimer's disease by cell-to-cell transmission. Eur. J. Neurosci. *37*, 1939–1948.

de la Monte, S.M. (1989). Quantitation of cerebral atrophy in preclinical and end-stage Alzheimer's disease. Ann. Neurol. *25*, 450–459.

Montine, T.J., Phelps, C.H., Beach, T.G., Bigio, E.H., Cairns, N.J., Dickson, D.W., Duyckaerts, C., Frosch, M.P., Masliah, E., Mirra, S.S., et al. (2012). National Institute on Aging-Alzheimer's Association guidelines for the neuropathologic assessment of Alzheimer's disease: a practical approach. Acta Neuropathol. (Berl.) *123*, 1–11.

Morales, R., Abid, K., and Soto, C. (2007). The prion strain phenomenon: Molecular basis and unprecedented features. Biochim. Biophys. Acta *1772*, 681–691.

Morales, R., Duran-Aniotz, C., Castilla, J., Estrada, L.D., and Soto, C. (2012). De novo induction of amyloid-β deposition in vivo. Mol. Psychiatry *17*, 1347–1353.

Morales, R., Bravo-Alegria, J., Duran-Aniotz, C., and Soto, C. (2015). Titration of biologically active amyloid–β seeds in a transgenic mouse model of Alzheimer's disease. Sci. Rep. *5*.

Mori, H., Kondo, J., and Ihara, Y. (1987). Ubiquitin is a component of paired helical filaments in Alzheimer's disease. Science *235*, 1641–1644.

Morley, J.E., Farr, S.A., Banks, W.A., Johnson, S.N., Yamada, K.A., and Xu, L. (2010). A physiological role for amyloid-beta protein:enhancement of learning and memory. J. Alzheimers Dis. JAD *19*, 441–449.

Morriss-Andrews, A., and Shea, J.-E. (2015). Computational studies of protein aggregation: methods and applications. Annu. Rev. Phys. Chem. *66*, 643–666.

Mukrasch, M.D., Bibow, S., Korukottu, J., Jeganathan, S., Biernat, J., Griesinger, C., Mandelkow, E., and Zweckstetter, M. (2009). Structural polymorphism of 441-residue tau at single residue resolution. PLoS Biol. *7*, e34.

Nelson, P.T., Greenberg, S.G., and Saper, C.B. (1994). Neurofibrillary tangles in the cerebral cortex of sheep. Neurosci. Lett. *170*, 187–190.

Nelson, R., Sawaya, M.R., Balbirnie, M., Madsen, A.O., Riekel, C., Grothe, R., and Eisenberg, D. (2005). Structure of the cross-beta spine of amyloid-like fibrils. Nature *435*, 773–778.

Némoz-Bertholet, F., and Aujard, F. (2003). Physical activity and balance performance as a function of age in a prosimian primate (Microcebus murinus). Exp. Gerontol. *38*, 407–414.

Nestor, P.J., Fryer, T.D., and Hodges, J.R. (2006). Declarative memory impairments in Alzheimer's disease and semantic dementia. NeuroImage *30*, 1010–1020.

Neve, R.L., Harris, P., Kosik, K.S., Kurnit, D.M., and Donlon, T.A. (1986). Identification of cDNA clones for the human microtubule-associated protein tau and chromosomal localization of the genes for tau and microtubule-associated protein 2. Brain Res. *387*, 271–280.

Newell, A.J., Sue, L.I., Scott, S., Rauschkolb, P.K., Walker, D.G., Potter, P.E., and Beach, T.G. (2003). Thiorphan-induced neprilysin inhibition raises amyloid beta levels in rabbit cortex and cerebrospinal fluid. Neurosci. Lett. *350*, 178–180.

Nizhnikov, A.A., Antonets, K.S., and Inge-Vechtomov, S.G. (2015). Amyloids: from pathogenesis to function. Biochem. Mosc. 1127.

Norrby, E. (2011). Prions and protein-folding diseases: Review: Prions and protein-folding diseases. J. Intern. Med. *270*, 1–14.

Novotny, R., Langer, F., Mahler, J., Skodras, A., Vlachos, A., Wegenast-Braun, B.M., Kaeser, S.A., Neher, J.J., Eisele, Y.S., Pietrowski, M.J., et al. (2016). Conversion of Synthetic A to In Vivo Active Seeds and Amyloid Plaque Formation in a Hippocampal Slice Culture Model. J. Neurosci. *36*, 5084–5093.

Otzen, D.E. (2013). The Amyloid Phenomenon and Its Significance. Amyloid Fibrils Prefibrillar Aggreg. Mol. Biol. Prop. 1.

Palop, J.J., and Mucke, L. (2010). Amyloid-β Induced Neuronal Dysfunction in Alzheimer's Disease: From Synapses toward Neural Networks. Nat. Neurosci. *13*, 812–818.

Pan, K.M., Baldwin, M., Nguyen, J., Gasset, M., Serban, A., Groth, D., Mehlhorn, I., Huang, Z., Fletterick, R.J., and Cohen, F.E. (1993). Conversion of alpha-helices into beta-sheets features in the formation of the scrapie prion proteins. Proc. Natl. Acad. Sci. U. S. A. *90*, 10962–10966.

Papegaey, A., Eddarkaoui, S., Deramecourt, V., Fernandez-Gomez, F.-J., Pantano, P., Obriot, H., Machala, C., Anquetil, V., Camuzat, A., Brice, A., et al. (2016). Reduced Tau protein expression is associated with frontotemporal degeneration with progranulin mutation. Acta Neuropathol. Commun. *4*.

Paravastu, A.K., Qahwash, I., Leapman, R.D., Meredith, S.C., and Tycko, R. (2009). Seeded growth of beta-amyloid fibrils from Alzheimer's brain-derived fibrils produces a distinct fibril structure. Proc. Natl. Acad. Sci. U. S. A. *106*, 7443–7448.

Patterson, K.R., Remmers, C., Fu, Y., Brooker, S., Kanaan, N.M., Vana, L., Ward, S., Reyes, J.F., Philibert, K., Glucksman, M.J., et al. (2011). Characterization of prefibrillar Tau oligomers in vitro and in Alzheimer disease. J. Biol. Chem. *286*, 23063–23076.

Pattison, I., and Jones, K. (1967). The possible nature of the transmissible agent of scrapie.

Paxinos, G., and Franklin, K.B. (2004). The mouse brain in stereotaxic coordinates (Gulf Professional Publishing).

Peeraer, E., Bottelbergs, A., Van Kolen, K., Stancu, I.-C., Vasconcelos, B., Mahieu, M., Duytschaever, H., Ver Donck, L., Torremans, A., Sluydts, E., et al. (2015). Intracerebral injection of preformed synthetic tau fibrils initiates widespread tauopathy and neuronal loss in the brains of tau transgenic mice. Neurobiol. Dis. *73*, 83–95.

Perez, S.E., Sherwood, C.C., Cranfield, M.R., Erwin, J.M., Mudakikwa, A., Hof, P.R., and Mufson, E.J. (2016). Early Alzheimer's disease-type pathology in the frontal cortex of wild mountain gorillas (Gorilla beringei beringei). Neurobiol. Aging *39*, 195–201.

Perez-Nievas, B.G., Stein, T.D., Tai, H.-C., Dols-Icardo, O., Scotton, T.C., Barroeta-Espar, I., Fernandez-Carballo, L., de Munain, E.L., Perez, J., Marquie, M., et al. (2013). Dissecting phenotypic traits linked to human resilience to Alzheimer's pathology. Brain J. Neurol. *136*, 2510–2526.

Perret, M. (1997). Change in photoperiodic cycle affects life span in a prosimian primate (Microcebus murinus). J. Biol. Rhythms *12*, 136–145.

Petersen, R.C. (2004). Mild cognitive impairment as a diagnostic entity. J. Intern. Med. *256*, 183–194.

Petersen, R.C., Jack, C.R., Xu, Y.C., Waring, S.C., O'Brien, P.C., Smith, G.E., Ivnik, R.J., Tangalos, E.G., Boeve, B.F., and Kokmen, E. (2000). Memory and MRI-based hippocampal volumes in aging and AD. Neurology *54*, 581–587.

Petkova, A.T. (2005). Self-Propagating, Molecular-Level Polymorphism in Alzheimer's -Amyloid Fibrils. Science *307*, 262–265.

Philipson, O., Lord, A., Lalowski, M., Soliymani, R., Baumann, M., Thyberg, J., Bogdanovic, N., Olofsson, T., Tjernberg, L.O., Ingelsson, M., et al. (2012). The Arctic amyloid-β precursor protein (AβPP) mutation results in distinct plaques and accumulation of N- and C-truncated Aβ. Neurobiol. Aging *33*, 1010.e1-13.

Piccardo, P., Manson, J.C., King, D., Ghetti, B., and Barron, R.M. (2007). Accumulation of prion protein in the brain that is not associated with transmissible disease. Proc. Natl. Acad. Sci. U. S. A. *104*, 4712–4717.

Piccardo, P., King, D., Telling, G., Manson, J.C., and Barron, R.M. (2013). Dissociation of Prion Protein Amyloid Seeding from Transmission of a Spongiform Encephalopathy. J. Virol. *87*, 12349–12356.

Piccini, A., Russo, C., Gliozzi, A., Relini, A., Vitali, A., Borghi, R., Giliberto, L., Armirotti, A., D'Arrigo, C., Bachi, A., et al. (2005). beta-amyloid is different in normal aging and in Alzheimer disease. J. Biol. Chem. *280*, 34186–34192.

Picq, J.L. (1995). Effects of aging upon recent memory in Microcebus murinus. Aging Milan Italy *7*, 17–22.

Picq, J.-L. (2007). Aging affects executive functions and memory in mouse lemur primates. Exp. Gerontol. *42*, 223–232.

Picq, J.-L., Aujard, F., Volk, A., and Dhenain, M. (2012). Age-related cerebral atrophy in nonhuman primates predicts cognitive impairments. Neurobiol. Aging *33*, 1096–1109.

Picq, J.-L., Villain, N., Gary, C., Pifferi, F., and Dhenain, M. (2015). Jumping Stand Apparatus Reveals Rapidly Specific Age-Related Cognitive Impairments in Mouse Lemur Primates. PloS One *10*, e0146238.

Pifferi, F., Terrien, J., Marchal, J., Dal-Pan, A., Djelti, F., Hardy, I., Chahory, S., Cordonnier, N., Desquilbet, L., Hurion, N., et al. (2016). Caloric restriction increases lifespan at the expense of brain integrity in a primate species. Submitted.

Piras, A., Collin, L., Grüninger, F., Graff, C., and Rönnbäck, A. (2016). Autophagic and lysosomal defects in human tauopathies: analysis of post-mortem brain from patients with familial Alzheimer disease, corticobasal degeneration and progressive supranuclear palsy. Acta Neuropathol. Commun. *4*, 22.

Pozueta, J., Lefort, R., and Shelanski, M.L. (2013). Synaptic changes in Alzheimer's disease and its models. Neuroscience *251*, 51–65.

Prayson, R.A. (2012). Neuropathology (Elsevier Health Sciences).

Preusser, M., Ströbel, T., Gelpi, E., Eiler, M., Broessner, G., Schmutzhard, E., and Budka, H. (2006). Alzheimer-type neuropathology in a 28 year old patient with iatrogenic Creutzfeldt-Jakob disease after dural grafting. J. Neurol. Neurosurg. Psychiatry *77*, 413–416.

Prusiner, S.B. (1982). Novel Proteinaceous Infectious Particles Cause Scrapie. Science 136.

Prusiner, S.B. (1998). Prions. Proc. Natl. Acad. Sci. *95*, 13363–13383.

Puzzo, D., Privitera, L., Leznik, E., Fà, M., Staniszewski, A., Palmeri, A., and Arancio, O. (2008). Picomolar amyloid-beta positively modulates synaptic plasticity and memory in hippocampus. J. Neurosci. Off. J. Soc. Neurosci. *28*, 14537–14545.

Rahman, A., Languille, S., Lamberty, Y., Babiloni, C., Perret, M., Bordet, R., Blin, O.J., Jacob, T., Auffret, A., Schenker, E., et al. (2013). Sleep deprivation impairs spatial retrieval but not spatial learning in the non-human primate grey mouse lemur. PloS One *8*, e64493.

Rajendran, L., Honsho, M., Zahn, T.R., Keller, P., Geiger, K.D., Verkade, P., and Simons, K. (2006). Alzheimer's disease beta-amyloid peptides are released in association with exosomes. Proc. Natl. Acad. Sci. U. S. A. *103*, 11172–11177.

Reitz, C., Brayne, C., and Mayeux, R. (2011). Epidemiology of Alzheimer disease. Nat. Rev. Neurol. *7*, 137–152.

Ridley, R.M., Baker, H.F., Windle, C.P., and Cummings, R.M. (2006). Very long term studies of the seeding of beta-amyloidosis in primates. J. Neural Transm. Vienna Austria 1996 *113*, 1243–1251.

Riesner, D. (2003). Biochemistry and structure of PrP(C) and PrP(Sc). Br. Med. Bull. *66*, 21–33.

Rogaeva, E.A., Fafel, K.C., Song, Y.Q., Medeiros, H., Sato, C., Liang, Y., Richard, E., Rogaev, E.I., Frommelt, P., Sadovnick, A.D., et al. (2001). Screening for PS1 mutations in a referral-based series of AD cases: 21 novel mutations. Neurology *57*, 621–625.

Rönnbäck, A., Sagelius, H., Bergstedt, K.D., Näslund, J., Westermark, G.T., Winblad, B., and Graff, C. (2012). Amyloid neuropathology in the single Arctic APP transgenic model affects interconnected brain regions. Neurobiol. Aging *33*, 831.e11-19.

Rosen, R.F., Fritz, J.J., Dooyema, J., Cintron, A.F., Hamaguchi, T., Lah, J.J., LeVine, H., Jucker, M., and Walker, L.C. (2012). Exogenous seeding of cerebral β-amyloid deposition in βAPP-transgenic rats. J. Neurochem. *120*, 660–666.

Roux, F., and Uhlhaas, P.J. (2014). Working memory and neural oscillations: α-γ versus θ-γ codes for distinct WM information? Trends Cogn. Sci. *18*, 16–25.

Rudinskiy, N., Hawkes, J.M., Wegmann, S., Kuchibhotla, K.V., Muzikansky, A., Betensky, R.A., Spires-Jones, T.L., and Hyman, B.T. (2014). Tau pathology does not affect experience-driven single-neuron and network-wide Arc/Arg3.1 responses. Acta Neuropathol. Commun. *2*, 63.

Russell, M.J., Bobik, M., White, R.G., Hou, Y., Benjamin, S.A., and Geddes, J.W. (1996). Age-specific onset of beta-amyloid in beagle brains. Neurobiol. Aging *17*, 269–273.

Ryu, J.K., and McLarnon, J.G. (2009). A leaky blood-brain barrier, fibrinogen infiltration and microglial reactivity in inflamed Alzheimer's disease brain. J. Cell. Mol. Med. *13*, 2911–2925.

Salat, D.H., Buckner, R.L., Snyder, A.Z., Greve, D.N., Desikan, R.S.R., Busa, E., Morris, J.C., Dale, A.M., and Fischl, B. (2004). Thinning of the cerebral cortex in aging. Cereb. Cortex N. Y. N 1991 *14*, 721–730.

Saman, S., Kim, W., Raya, M., Visnick, Y., Miro, S., Saman, S., Jackson, B., McKee, A.C., Alvarez, V.E., Lee, N.C.Y., et al. (2012). Exosome-associated tau is secreted in tauopathy models and is selectively phosphorylated in cerebrospinal fluid in early Alzheimer disease. J. Biol. Chem. *287*, 3842–3849.

Sams-Dodd, F. (2006). Strategies to optimize the validity of disease models in the drug discovery process. Drug Discov. Today *11*, 355–363.

Sanders, D.W., Kaufman, S.K., DeVos, S.L., Sharma, A.M., Mirbaha, H., Li, A., Barker, S.J., Foley, A.C., Thorpe, J.R., Serpell, L.C., et al. (2014). Distinct tau prion strains propagate in cells and mice and define different tauopathies. Neuron *82*, 1271–1288.

Sawiak, S.J., Picq, J.-L., and Dhenain, M. (2014). Voxel-based morphometry analyses of in vivo MRI in the aging mouse lemur primate. Front. Aging Neurosci. *6*, 82.

Schellenberg, G.D., Bird, T.D., Wijsman, E.M., Orr, H.T., Anderson, L., Nemens, E., White, J.A., Bonnycastle, L., Weber, J.L., and Alonso, M.E. (1992). Genetic linkage evidence for a familial Alzheimer's disease locus on chromosome 14. Science *258*, 668–671.

Schmidt, C., Karch, A., Korth, C., and Zerr, I. (2012). On the issue of transmissibility of Alzheimer disease: a critical review. Prion *6*, 447–452.

Schöll, M., Lockhart, S.N., Schonhaut, D.R., O'Neil, J.P., Janabi, M., Ossenkoppele, R., Baker, S.L., Vogel, J.W., Faria, J., Schwimmer, H.D., et al. (2016). PET Imaging of Tau Deposition in the Aging Human Brain. Neuron *89*, 971–982.

Schultz, C., Hubbard, G.B., Rüb, U., Braak, E., and Braak, H. (2000). Age-related progression of tau pathology in brains of baboons. Neurobiol. Aging *21*, 905–912.

Scott, M., Foster, D., Mirenda, C., Serban, D., Coufal, F., Wälchli, M., Torchia, M., Groth, D., Carlson, G., DeArmond, S.J., et al. (1989). Transgenic mice expressing hamster prion protein produce species-specific scrapie infectivity and amyloid plaques. Cell *59*, 847–857.

Selenica, M.-L.B., Brownlow, M., Jimenez, J.P., Lee, D.C., Pena, G., Dickey, C.A., Gordon, M.N., and Morgan, D. (2013). Amyloid oligomers exacerbate tau pathology in a mouse model of tauopathy. Neurodegener. Dis. *11*, 165–181.

Selkoe, D.J. (2002). Alzheimer's disease is a synaptic failure. Science *298*, 789–791.

Selkoe, D.J. (2008). Soluble oligomers of the amyloid beta-protein impair synaptic plasticity and behavior. Behav. Brain Res. *192*, 106–113.

Selkoe, D.J., and Hardy, J. (2016). The amyloid hypothesis of Alzheimer's disease at 25 years. EMBO Mol. Med. *8*, 595–608.

Selkoe, D.J., Bell, D.S., Podlisny, M.B., Price, D.L., and Cork, L.C. (1987). Conservation of brain amyloid proteins in aged mammals and humans with Alzheimer's disease. Science *235*, 873–877.

Sepulcre, J., Sabuncu, M.R., Becker, A., Sperling, R., and Johnson, K.A. (2013). In vivo characterization of the early states of the amyloid-beta network. Brain J. Neurol. *136*, 2239–2252.

Sergeant, N., Delacourte, A., and Buée, L. (2005). Tau protein as a differential biomarker of tauopathies. Biochim. Biophys. Acta BBA - Mol. Basis Dis. *1739*, 179–197.

Serrano-Pozo, A., Mielke, M.L., Gómez-Isla, T., Betensky, R.A., Growdon, J.H., Frosch, M.P., and Hyman, B.T. (2011). Reactive glia not only associates with plaques but also parallels tangles in Alzheimer's disease. Am. J. Pathol. *179*, 1373–1384.

Shamy, J.L.T., Buonocore, M.H., Makaron, L.M., Amaral, D.G., Barnes, C.A., and Rapp, P.R. (2006). Hippocampal volume is preserved and fails to predict recognition memory impairment in aged rhesus monkeys (Macaca mulatta). Neurobiol. Aging *27*, 1405–1415.

Shankar, G.M., Bloodgood, B.L., Townsend, M., Walsh, D.M., Selkoe, D.J., and Sabatini, B.L. (2007). Natural oligomers of the Alzheimer amyloid-beta protein induce reversible synapse loss by modulating an NMDA-type glutamate receptor-dependent signaling pathway. J. Neurosci. Off. J. Soc. Neurosci. *27*, 2866–2875.

Shankar, G.M., Li, S., Mehta, T.H., Garcia-Munoz, A., Shepardson, N.E., Smith, I., Brett, F.M., Farrell, M.A., Rowan, M.J., Lemere, C.A., et al. (2008). Amyloid-beta protein dimers isolated directly from Alzheimer's brains impair synaptic plasticity and memory. Nat. Med. *14*, 837–842.

Šimić, G., Babić Leko, M., Wray, S., Harrington, C., Delalle, I., Jovanov-Milošević, N., Bažadona, D., Buée, L., de Silva, R., Di Giovanni, G., et al. (2016). Tau Protein Hyperphosphorylation and Aggregation in Alzheimer's Disease and Other Tauopathies, and Possible Neuroprotective Strategies. Biomolecules *6*, 6.

Simmons, L.K., May, P.C., Tomaselli, K.J., Rydel, R.E., Fuson, K.S., Brigham, E.F., Wright, S., Lieberburg, I., Becker, G.W., and Brems, D.N. (1994). Secondary structure of amyloid beta peptide correlates with neurotoxic activity in vitro. Mol. Pharmacol. *45*, 373–379.

Simpson, I.A., Chundu, K.R., Davies-Hill, T., Honer, W.G., and Davies, P. (1994). Decreased concentrations of GLUT1 and GLUT3 glucose transporters in the brains of patients with Alzheimer's disease. Ann. Neurol. *35*, 546–551.

Sipe, J.D., Benson, M.D., Buxbaum, J.N., Ikeda, S., Merlini, G., Saraiva, M.J.M., and Westermark, P. (2014). Nomenclature 2014: Amyloid fibril proteins and clinical classification of the amyloidosis. Amyloid Int. J. Exp. Clin. Investig. Off. J. Int. Soc. Amyloidosis *21*, 221–224.

Small, G.W., Bookheimer, S.Y., Thompson, P.M., Cole, G.M., Huang, S.-C., Kepe, V., and Barrio, J.R. (2008). Current and future uses of neuroimaging for cognitively impaired patients. Lancet Neurol. *7*, 161–172.

Smith, D.E., Rapp, P.R., McKay, H.M., Roberts, J.A., and Tuszynski, M.H. (2004). Memory impairment in aged primates is associated with focal death of cortical neurons and atrophy of subcortical neurons. J. Neurosci. Off. J. Soc. Neurosci. *24*, 4373–4381.

Sorbi, S., Bird, E.D., and Blass, J.P. (1983). Decreased pyruvate dehydrogenase complex activity in Huntington and Alzheimer brain. Ann. Neurol. *13*, 72–78.

Soto, C. (2003). Unfolding the role of protein misfolding in neurodegenerative diseases. Nat. Rev. Neurosci. *4*, 49–60.

Sperling, R.A., Aisen, P.S., Beckett, L.A., Bennett, D.A., Craft, S., Fagan, A.M., Iwatsubo, T., Jack, C.R., Kaye, J., Montine, T.J., et al. (2011). Toward defining the preclinical stages of Alzheimer's disease: recommendations from the National Institute on Aging-Alzheimer's Association workgroups on diagnostic guidelines for Alzheimer's disease. Alzheimers Dement. J. Alzheimers Assoc. *7*, 280–292.

Spirig, T., Ovchinnikova, O., Vagt, T., and Glockshuber, R. (2014). Direct evidence for self-propagation of different amyloid-β fibril conformations. Neurodegener. Dis. *14*, 151–159.

Stahl, N., and Prusiner, S.B. (1991). Prions and prion proteins. FASEB J. *5*, 2799–2807.

Stancu, I.-C., Vasconcelos, B., Ris, L., Wang, P., Villers, A., Peeraer, E., Buist, A., Terwel, D., Baatsen, P., Oyelami, T., et al. (2015). Templated misfolding of Tau by prion-like seeding along neuronal connections impairs neuronal network function and associated behavioral outcomes in Tau transgenic mice. Acta Neuropathol. (Berl.) *129*, 875–894.

Stöhr, J., Watts, J.C., Mensinger, Z.L., Oehler, A., Grillo, S.K., DeArmond, S.J., Prusiner, S.B., and Giles, K. (2012). Purified and synthetic Alzheimer's amyloid beta (Aβ) prions. Proc. Natl. Acad. Sci. U. S. A. *109*, 11025–11030.

Stöhr, J., Condello, C., Watts, J.C., Bloch, L., Oehler, A., Nick, M., DeArmond, S.J., Giles, K., DeGrado, W.F., and Prusiner, S.B. (2014). Distinct synthetic Aβ prion strains producing different amyloid deposits in bigenic mice. Proc. Natl. Acad. Sci. U. S. A. *111*, 10329–10334.

Streit, W.J., Mrak, R.E., and Griffin, W.S.T. (2004). Microglia and neuroinflammation: a pathological perspective. J. Neuroinflammation *1*, 14.

Struble, R.G., Price, D.L., Cork, L.C., and Price, D.L. (1985). Senile plaques in cortex of aged normal monkeys. Brain Res. *361*, 267–275.

Sunde, M., Serpell, L.C., Bartlam, M., Fraser, P.E., Pepys, M.B., and Blake, C.C.. (1997). Regular article: Common core structure of amyloid fibrils by synchrotron X-ray diffraction11Edited by F. E. Cohen. J. Mol. Biol. *273*, 729–739.

Takahashi, M., Miyata, H., Kametani, F., Nonaka, T., Akiyama, H., Hisanaga, S., and Hasegawa, M. (2015). Extracellular association of APP and tau fibrils induces intracellular aggregate formation of tau. Acta Neuropathol. (Berl.) *129*, 895–907.

Tan, C.-C., Yu, J.-T., Wang, H.-F., Tan, M.-S., Meng, X.-F., Wang, C., Jiang, T., Zhu, X.-C., and Tan, L. (2014). Efficacy and safety of donepezil, galantamine, rivastigmine, and memantine for the treatment of Alzheimer's disease: a systematic review and meta-analysis. J. Alzheimers Dis. JAD *41*, 615–631.

Tanaka, M., Collins, S.R., Toyama, B.H., and Weissman, J.S. (2006). The physical basis of how prion conformations determine strain phenotypes. Nature *442*, 585–589.

Tannenholz, L., Jimenez, J.C., and Kheirbek, M.A. (2014). Local and regional heterogeneity underlying hippocampal modulation of cognition and mood. Front. Behav. Neurosci. *8*, 147.

Teipel, S.J., Flatz, W.H., Heinsen, H., Bokde, A.L.W., Schoenberg, S.O., Stöckel, S., Dietrich, O., Reiser, M.F., Möller, H.-J., and Hampel, H. (2005). Measurement of basal forebrain atrophy in Alzheimer's disease using MRI. Brain J. Neurol. *128*, 2626–2644.

Terry, R.D., Masliah, E., Salmon, D.P., Butters, N., DeTeresa, R., Hill, R., Hansen, L.A., and Katzman, R. (1991). Physical basis of cognitive alterations in Alzheimer's disease: synapse loss is the major correlate of cognitive impairment. Ann. Neurol. *30*, 572–580.

Thal, D.R., Rüb, U., Orantes, M., and Braak, H. (2002a). Phases of A beta-deposition in the human brain and its relevance for the development of AD. Neurology *58*, 1791–1800.

Thal, D.R., Ghebremedhin, E., Rüb, U., Yamaguchi, H., Del Tredici, K., and Braak, H. (2002b). Two types of sporadic cerebral amyloid angiopathy. J. Neuropathol. Exp. Neurol. *61*, 282–293.

Thal, D.R., Ghebremedhin, E., Orantes, M., and Wiestler, O.D. (2003). Vascular Pathology in Alzheimer Disease: Correlation of Cerebral Amyloid Angiopathy and Arteriosclerosis/Lipohyalinosis with Cognitive Decline. J. Neuropathol. Exp. Neurol. *62*, 1287–1301.

Thal, D.R., Griffin, W.S.T., de Vos, R.A.I., and Ghebremedhin, E. (2008). Cerebral amyloid angiopathy and its relationship to Alzheimer's disease. Acta Neuropathol. (Berl.) *115*, 599–609.

Thal, D.R., Walter, J., Saido, T.C., and Fändrich, M. (2015). Neuropathology and biochemistry of Aβ and its aggregates in Alzheimer's disease. Acta Neuropathol. (Berl.) *129*, 167–182.

de la Torre, J.C. (2000). Critically attained threshold of cerebral hypoperfusion: the CATCH hypothesis of Alzheimer's pathogenesis. Neurobiol. Aging *21*, 331–342.

de la Torre, J.C. (2016). Cerebral perfusion enhancing interventions: A new strategy for the prevention of Alzheimer dementia. Brain Pathol. Zurich Switz.

Trouche, S.G., Maurice, T., Rouland, S., Verdier, J.-M., and Mestre-Francés, N. (2010). The three-panel runway maze adapted to Microcebus murinus reveals age-related differences in memory and perseverance performances. Neurobiol. Learn. Mem. *94*, 100–106.

Ubhi, K., Rockenstein, E., Doppler, E., Mante, M., Adame, A., Patrick, C., Trejo, M., Crews, L., Paulino, A., Moessler, H., et al. (2009). Neurofibrillary and neurodegenerative pathology in APP-transgenic mice injected with AAV2-mutant TAU: neuroprotective effects of Cerebrolysin. Acta Neuropathol. (Berl.) *117*, 699–712.

Van der Jeugd, A., Hochgräfe, K., Ahmed, T., Decker, J.M., Sydow, A., Hofmann, A., Wu, D., Messing, L., Balschun, D., D'Hooge, R., et al. (2012). Cognitive defects are reversible in inducible mice expressing pro-aggregant full-length human Tau. Acta Neuropathol. (Berl.) *123*, 787–805.

Vehmas, A.K., Kawas, C.H., Stewart, W.F., and Troncoso, J.C. (2003). Immune reactive cells in senile plaques and cognitive decline in Alzheimer's disease. Neurobiol. Aging *24*, 321–331.

Vemuri, P., Whitwell, J.L., Kantarci, K., Josephs, K.A., Parisi, J.E., Shiung, M.S., Knopman, D.S., Boeve, B.F., Petersen, R.C., Dickson, D.W., et al. (2008). Antemortem MRI based STructural Abnormality iNDex (STAND)-scores correlate with postmortem Braak neurofibrillary tangle stage. NeuroImage *42*, 559–567.

Viola, K.L., and Klein, W.L. (2015). Amyloid β oligomers in Alzheimer's disease pathogenesis, treatment, and diagnosis. Acta Neuropathol. (Berl.) *129*, 183–206.

Violet, M., Delattre, L., Tardivel, M., Sultan, A., Chauderlier, A., Caillierez, R., Talahari, S., Nesslany, F., Lefebvre, B., Bonnefoy, E., et al. (2014). A major role for Tau in neuronal DNA and RNA protection in vivo under physiological and hyperthermic conditions. Front. Cell. Neurosci. *8*, 84.

Walker, L.C., Kitt, C.A., Schwam, E., Buckwald, B., Garcia, F., Sepinwall, J., and Price, D.L. (1987). Senile plaques in aged squirrel monkeys. Neurobiol. Aging *8*, 291–296.

Walker, L.C., Callahan, M.J., Bian, F., Durham, R.A., Roher, A.E., and Lipinski, W.J. (2002). Exogenous induction of cerebral beta-amyloidosis in betaAPP-transgenic mice. Peptides *23*, 1241–1247.

Walker, L.C., Schelle, J., and Jucker, M. (2016). The Prion-Like Properties of Amyloid-β Assemblies: Implications for Alzheimer's Disease. Cold Spring Harb. Perspect. Med. *6*.

Walsh, D.M., and Selkoe, D.J. (2016). A critical appraisal of the pathogenic protein spread hypothesis of neurodegeneration. Nat. Rev. Neurosci. *17*, 251–260.

Walsh, D.M., Hartley, D.M., Kusumoto, Y., Fezoui, Y., Condron, M.M., Lomakin, A., Benedek, G.B., Selkoe, D.J., and Teplow, D.B. (1999). Amyloid beta-protein fibrillogenesis. Structure and biological activity of protofibrillar intermediates. J. Biol. Chem. *274*, 25945–25952.

Wang, Y., and Mandelkow, E. (2016). Tau in physiology and pathology. Nat. Rev. Neurosci. *17*, 5–21.

Watts, J.C., Condello, C., Stöhr, J., Oehler, A., Lee, J., DeArmond, S.J., Lannfelt, L., Ingelsson, M., Giles, K., and Prusiner, S.B. (2014). Serial propagation of distinct strains of Aβ prions from Alzheimer's disease patients. Proc. Natl. Acad. Sci. U. S. A. *111*, 10323–10328.

Webb, T.E.F., Poulter, M., Beck, J., Uphill, J., Adamson, G., Campbell, T., Linehan, J., Powell, C., Brandner, S., Pal, S., et al. (2008). Phenotypic heterogeneity and genetic modification of P102L inherited prion disease in an international series. Brain *131*, 2632–2646.

Wegmann, S., Medalsy, I.D., Mandelkow, E., and Müller, D.J. (2013). The fuzzy coat of pathological human Tau fibrils is a two-layered polyelectrolyte brush. Proc. Natl. Acad. Sci. U. S. A. *110*, E313-321.

Wegmann, S., Maury, E.A., Kirk, M.J., Saqran, L., Roe, A., DeVos, S.L., Nicholls, S., Fan, Z., Takeda, S., Cagsal-Getkin, O., et al. (2015). Removing endogenous tau does not prevent tau propagation yet reduces its neurotoxicity. EMBO J. *34*, 3028–3041.

Westergard, L., Christensen, H.M., and Harris, D.A. (2007). The cellular prion protein (PrP(C)): its physiological function and role in disease. Biochim. Biophys. Acta *1772*, 629–644.

Wetzel, R. (2006). Kinetics and thermodynamics of amyloid fibril assembly. Acc. Chem. Res. *39*, 671–679.

White, J.D., Eimerbrink, M.J., Hayes, H.B., Hardy, A., Van Enkevort, E.A., Peterman, J.L., Chumley, M.J., and Boehm, G.W. (2016). Hippocampal Aβ expression, but not phosphorylated tau, predicts cognitive deficits following repeated peripheral poly I:C administration. Behav. Brain Res. *313*, 219–225.

Whitehouse, P.J. (1987). Neurotransmitter receptor alterations in Alzheimer disease: a review. Alzheimer Dis. Assoc. Disord. *1*, 9–18.

Whitehouse, P.J., Price, D.L., Clark, A.W., Coyle, J.T., and DeLong, M.R. (1981). Alzheimer disease: Evidence for selective loss of cholinergic neurons in the nucleus basalis. Ann. Neurol. *10*, 122–126.

Whitwell, J.L. (2010). Progression of atrophy in Alzheimer's disease and related disorders. Neurotox. Res. *18*, 339–346.

Whitwell, J.L., Josephs, K.A., Murray, M.E., Kantarci, K., Przybelski, S.A., Weigand, S.D., Vemuri, P., Senjem, M.L., Parisi, J.E., Knopman, D.S., et al. (2008). MRI correlates of neurofibrillary tangle pathology at autopsy: a voxel-based morphometry study. Neurology *71*, 743–749.

WHO, G. (Switzerland) (2003). WHO manual for surveillance of human transmissible spongiform encephalopathies including variant Creutzfeldt-Jakob disease.

Will, R.G., Ironside, J.W., Zeidler, M., Cousens, S.N., Estibeiro, K., Alperovitch, A., Poser, S., Pocchiari, M., Hofman, A., and Smith, P.G. (1996). A new variant of Creutzfeldt-Jakob disease in the UK. Lancet Lond. Engl. *347*, 921–925.

Wille, H., Drewes, G., Biernat, J., Mandelkow, E.M., and Mandelkow, E. (1992). Alzheimer-like paired helical filaments and antiparallel dimers formed from microtubule-associated protein tau in vitro. J. Cell Biol. *118*, 573–584.

Wischik, C.M., Novak, M., Thøgersen, H.C., Edwards, P.C., Runswick, M.J., Jakes, R., Walker, J.E., Milstein, C., Roth, M., and Klug, A. (1988). Isolation of a fragment of tau derived from the core of the paired helical filament of Alzheimer disease. Proc. Natl. Acad. Sci. U. S. A. *85*, 4506–4510.

Wisniewski, T., Lalowski, M., Bobik, M., Russell, M., Strosznajder, J., and Frangione, B. (1996). Amyloid beta 1-42 deposits do not lead to Alzheimer's neuritic plaques in aged dogs. Biochem. J. *313 (Pt 2)*, 575–580.

Wolf, D., Grothe, M., Fischer, F.U., Heinsen, H., Kilimann, I., Teipel, S., and Fellgiebel, A. (2014). Association of basal forebrain volumes and cognition in normal aging. Neuropsychologia *53*, 54–63.

Wolff, M., Unuchek, D., Zhang, B., Gordeliy, V., Willbold, D., and Nagel-Steger, L. (2015). Amyloid β Oligomeric Species Present in the Lag Phase of Amyloid Formation. PloS One *10*, e0127865.

Wu, J.W., Herman, M., Liu, L., Simoes, S., Acker, C.M., Figueroa, H., Steinberg, J.I., Margittai, M., Kayed, R., Zurzolo, C., et al. (2013). Small Misfolded Tau Species Are Internalized via Bulk Endocytosis and Anterogradely and Retrogradely Transported in Neurons. J. Biol. Chem. *288*, 1856–1870.

Wu, J.W., Hussaini, S.A., Bastille, I.M., Rodriguez, G.A., Mrejeru, A., Rilett, K., Sanders, D.W., Cook, C., Fu, H., Boonen, R.A.C.M., et al. (2016). Neuronal activity enhances tau propagation and tau pathology in vivo. Nat. Neurosci.

Xiao, X., Cali, I., Yuan, J., Cracco, L., Curtiss, P., Zeng, L., Abouelsaad, M., Gazgalis, D., Wang, G.-X., Kong, Q., et al. (2015). Synthetic Aβ peptides acquire prion-like properties in the brain. Oncotarget *6*, 642–650.

Xu, G., Ran, Y., Fromholt, S.E., Fu, C., Yachnis, A.T., Golde, T.E., and Borchelt, D.R. (2015). Murine Aβ over-production produces diffuse and compact Alzheimer-type amyloid deposits. Acta Neuropathol. Commun. *3*, 72.

Yamada, K., Cirrito, J.R., Stewart, F.R., Jiang, H., Finn, M.B., Holmes, B.B., Binder, L.I., Mandelkow, E.-M., Diamond, M.I., Lee, V.M.-Y., et al. (2011). In vivo microdialysis reveals age-dependent decrease of brain interstitial fluid tau levels in P301S human tau transgenic mice. J. Neurosci. Off. J. Soc. Neurosci. *31*, 13110–13117.

Yamada, K., Holth, J.K., Liao, F., Stewart, F.R., Mahan, T.E., Jiang, H., Cirrito, J.R., Patel, T.K., Hochgräfe, K., Mandelkow, E.-M., et al. (2014). Neuronal activity regulates extracellular tau in vivo. J. Exp. Med. *211*, 387–393.

Ye, L., Fritschi, S.K., Schelle, J., Obermüller, U., Degenhardt, K., Kaeser, S.A., Eisele, Y.S., Walker, L.C., Baumann, F., Staufenbiel, M., et al. (2015a). Persistence of Aβ seeds in APP null mouse brain. Nat. Neurosci. *18*, 1559–1561.

Ye, L., Hamaguchi, T., Fritschi, S.K., Eisele, Y.S., Obermüller, U., Jucker, M., and Walker, L.C. (2015b). Progression of Seed-Induced Aβ Deposition within the Limbic Connectome. Brain Pathol. Zurich Switz. *25*, 743–752.

Zahn, R., Liu, A., Lührs, T., Riek, R., von Schroetter, C., López García, F., Billeter, M., Calzolai, L., Wider, G., and Wüthrich, K. (2000). NMR solution structure of the human prion protein. Proc. Natl. Acad. Sci. U. S. A. *97*, 145–150.

Zarow, C., Vinters, H.V., Ellis, W.G., Weiner, M.W., Mungas, D., White, L., and Chui, H.C. (2005). Correlates of hippocampal neuron number in Alzheimer's disease and ischemic vascular dementia. Ann. Neurol. *57*, 896–903.

Zhang, Y., Li, P., Feng, J., and Wu, M. (2016). Dysfunction of NMDA receptors in Alzheimer's disease. Neurol. Sci. Off. J. Ital. Neurol. Soc. Ital. Soc. Clin. Neurophysiol. *37*, 1039–1047.

Zhu, S., Shala, A., Bezginov, A., Sljoka, A., Audette, G., and Wilson, D.J. (2015). Hyperphosphorylation of intrinsically disordered tau protein induces an amyloidogenic shift in its conformational ensemble. PloS One *10*, e0120416.

Zilka, N., Filipcik, P., Koson, P., Fialova, L., Skrabana, R., Zilkova, M., Rolkova, G., Kontsekova, E., and Novak, M. (2006). Truncated tau from sporadic Alzheimer's disease suffices to drive neurofibrillary degeneration in vivo. FEBS Lett. *580*, 3582–3588.

Zipser, B.D., Johanson, C.E., Gonzalez, L., Berzin, T.M., Tavares, R., Hulette, C.M., Vitek, M.P., Hovanesian, V., and Stopa, E.G. (2007). Microvascular injury and blood-brain barrier leakage in Alzheimer's disease. Neurobiol. Aging *28*, 977–986.

Appendix

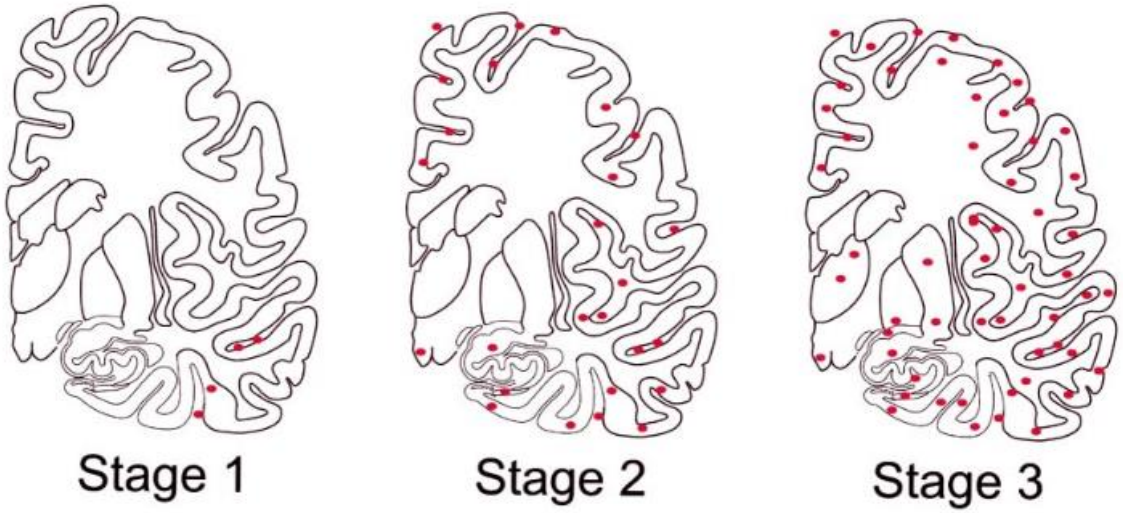

Appendix 1. **Representation of cerebral amyloid angiopathy (CAA) stages.** CAA changes starts in a few neocortical areas (leptomeningeal and cortical vessels, stage 1) then reaches the hippocampus, amygdala, hypothalamus, midbrain and cerebellum (stage 2) and finally basal ganglia, thalamus, basal forebrain and lower brainstem (stage 3). Adapted from (Thal et al., 2003).

A

A	Thal phases	B	Braak stages	C	CERAD
0	0	0	None	0	None
1	1 or 2	1	I or II	1	Sparse
2	3	2	III or IV	2	Moderate
3	4 or 5	3	V or VI	3	Frequent

B

A	C	B		
		0 or 1	2	3
0	0	Not	Not	Not
1	0 or 1	Low	Low	Low
	2 or 3	Low	Intermediate	Intermediate
2	Any C	Low	Intermediate	Intermediate
3	0 or 1	Low	Intermediate	Intermediate
	2 or 3	Low	Intermediate	High

Appendix 2. **"ABC" Score for Level of AD Neuropathological Change.** A. Correspondence of ABC score to Thal phases (A), Braak stages (B) and CERAD (C). B. ABC scores and AD neuropathological change level. Adapted from (Hyman et al., 2012).

GWAS Gene	Chromosomal Location	Function	Cellular Localization
APOE4	19q13.2	Lipid processing pathway	Cytoplasm, endosome
TREM2	6p21.1	Immune response/ anti-inflammatory	Plasma membrane
CD33	19q13.3	Immune response/ endocytosis	Plasma membrane
CR1	1q32	Immune response/ complement system	Plasma membrane
CLU	8p21–p12	Lipid processing pathway/immune response/complement system	Cytoplasm, extracellular space
MS4A4E/6A	11q12.1–q12.2	Immune response	Plasma membrane
ABCA7	19p13.3	Lipid processing pathway/immune response/complement system	Plasma membrane
MEF2C	5q14.3	Immune response/ endocytosis	Nuclear/ cytoplasm
INPP5D	2q37.1	Immune response	Cytoplasm
HLA-DR5/ DR1	6q21.3	Immune response	Plasma membrane, extracellular space
EPHA1	7q34	Immune response/ endocytosis	Plasma membrane
PICALM	11q14	Endocytosis*	Golgi apparatus, vesicle, nuclear
BIN1	2q14	Endocytosis*	Nuclear, cytoplasm
PTK2B	8p21.1	Endocytosis*	Plasma membrane, nuclear, cytoplasm
CASS4	20q13.31	Cytoskeleton/ axonal transport*	Cytoskeleton

Appendix 3. **Genetic risk factors of AD**. From (Mhatre et al., 2015).

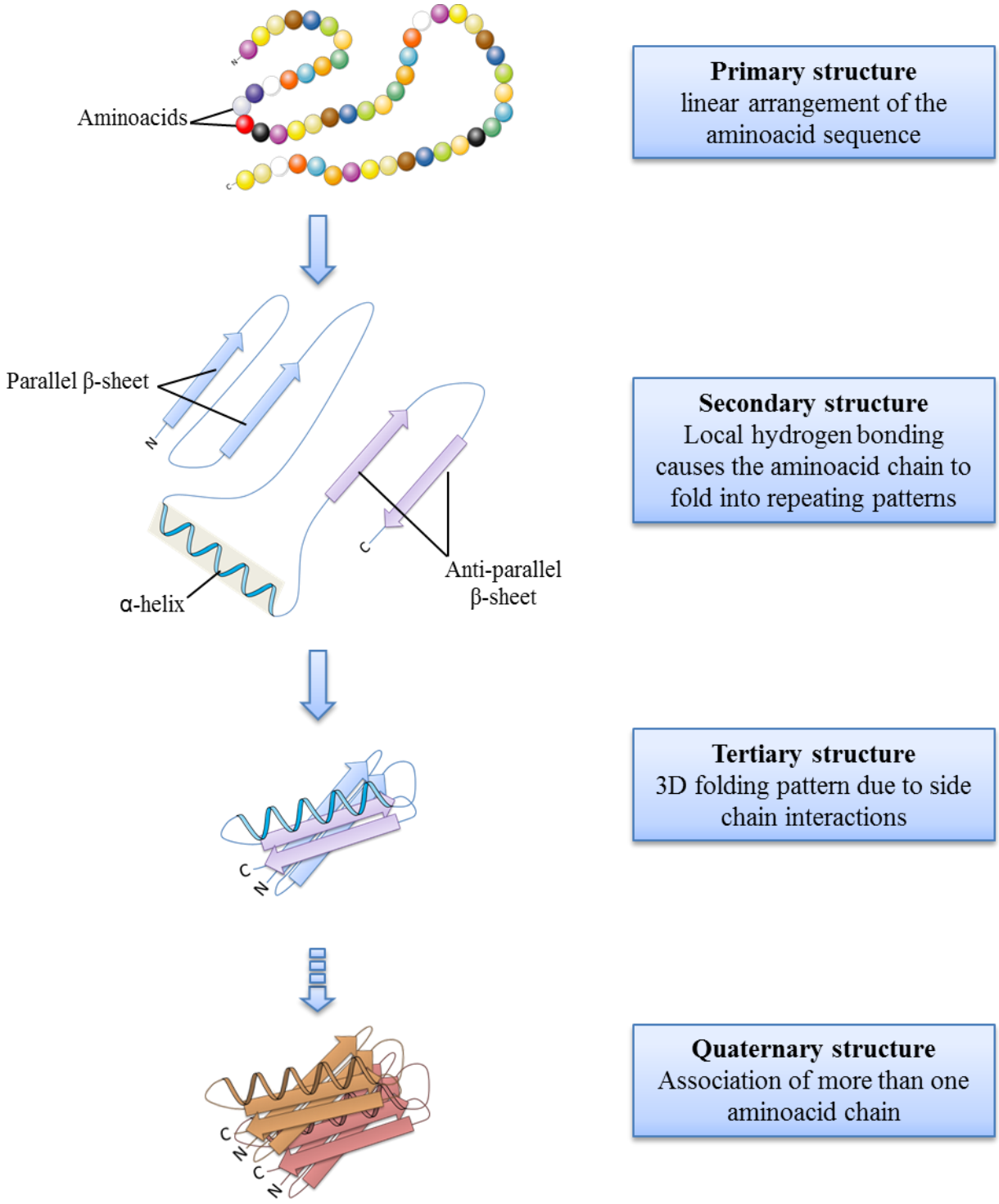

Appendix 4. **Structures responsible for protein folding into a specific conformation.**

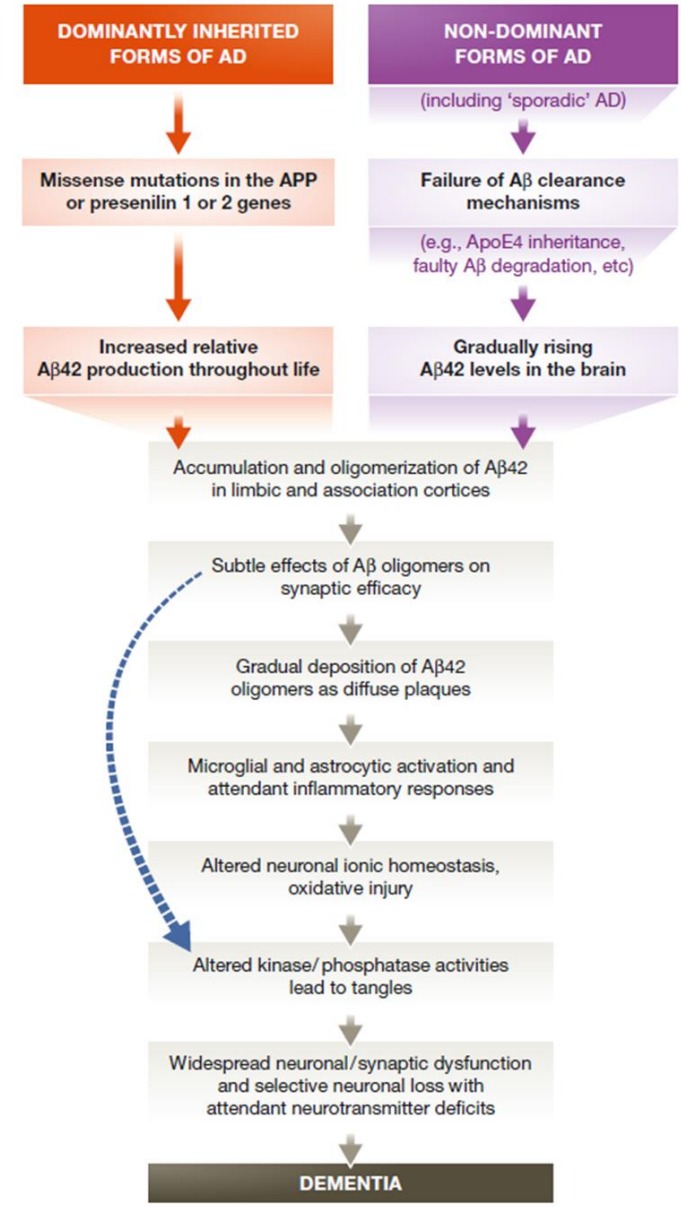

Appendix 5. **Amyloid cascade hypothesis.** The curved blue arrow indicates that Aβ oligomers may directly injure synapses and neurites of neurons, in addition to activating microglia and astrocytes. From (Selkoe and Hardy, 2016).

Appendix 6. **Comparison of Aβ human and mouse sequences.** Three aminoacid residues 5, 10 and 13 differing are underlined in bold. Adapted from (Xu et al., 2015).

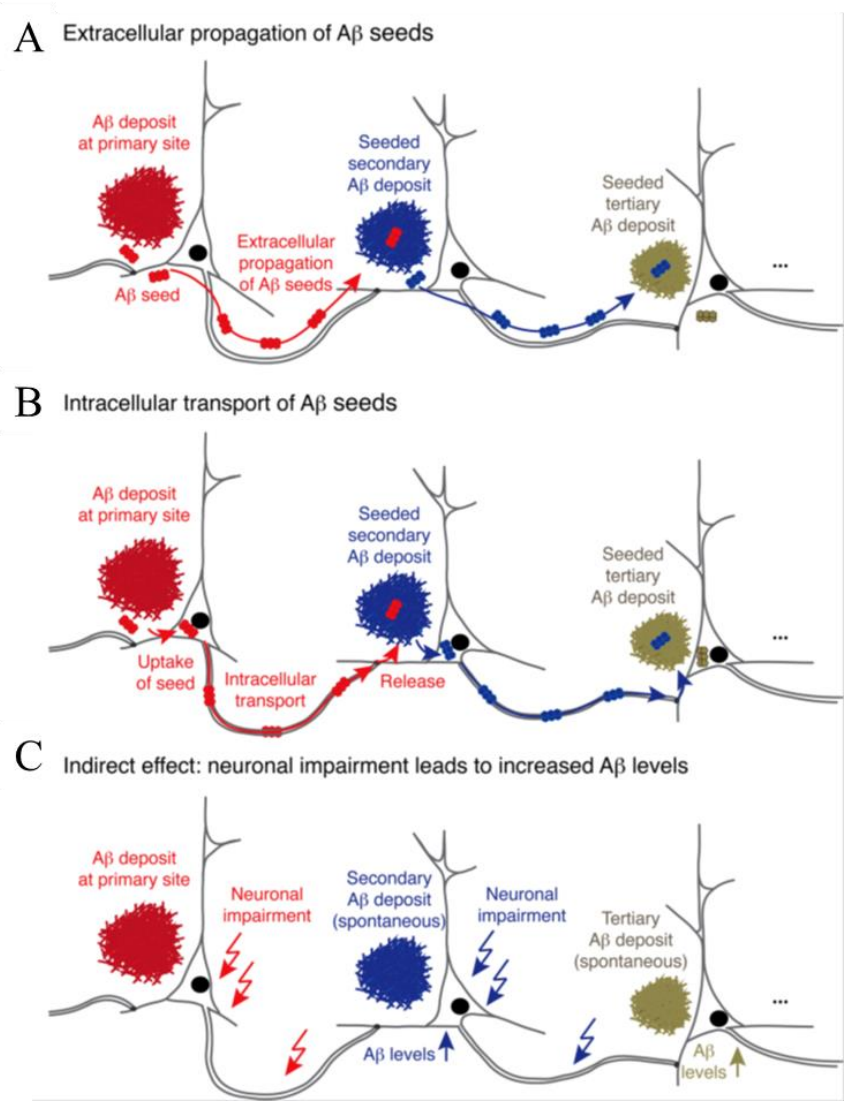

Appendix 7. **Proposed hypotheses for the propagation of Aβ pathology.** Initial Aβ seeds and deposits (in red) spontaneously form in a permissive environment created, for example, by the local increase of Aβ concentration. A. As they are present in the extracellular space, spreading could occur by diffusion through the parenchyma, via the blood or along neuroanatomical connections. B. Cellular uptake, intracellular transport, and release of Aβ seeds at the synapse could spread Aβ pathology within neuronal networks. C. Non prion-like mechanisms should also be considered. Aβ–induced neuronal impairments could lead to adaptive signals resulting, for example, in an increase of Aβ secretion at the synapse or induce its production at the projection site leading to spontaneous Aβ nucleation in connected areas without Aβ seeds diffusion or transport. These three hypotheses are not to be considered exclusive. From (Eisele and Duyckaerts, 2016).

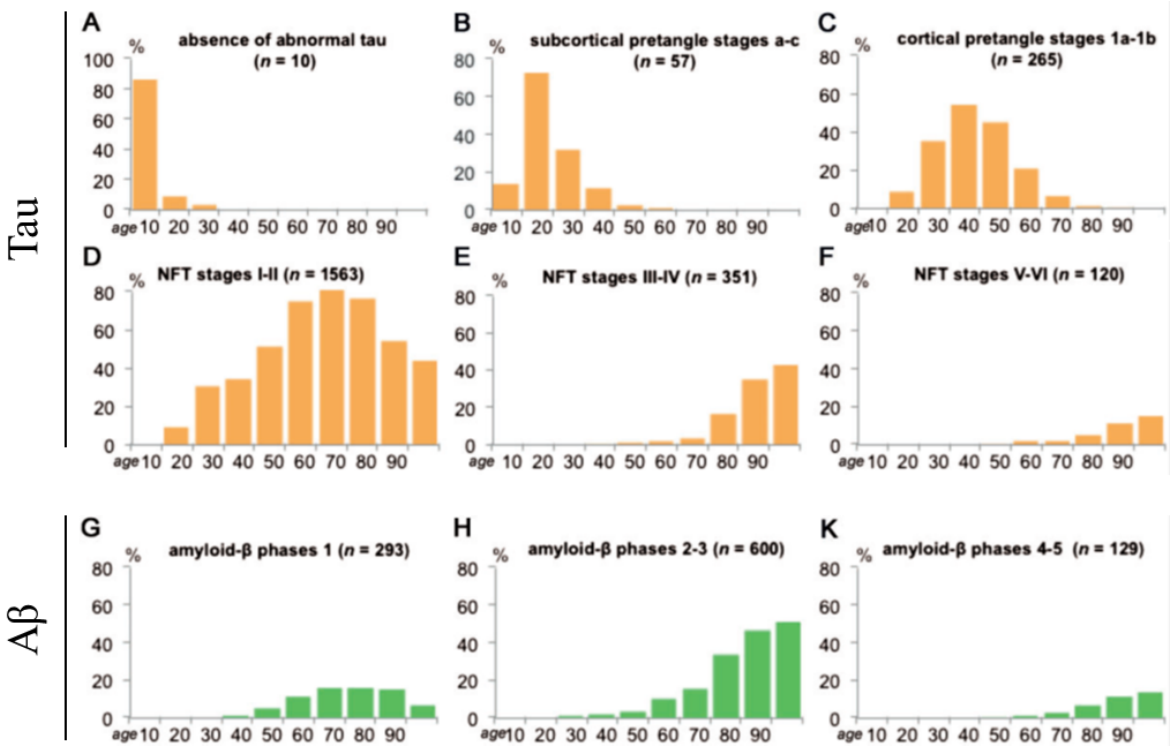

Appendix 8. **Occurrence of Tau and Aβ pathologies by decade.** A. Abnormal Tau is virtually detected in all adult brains (absence of abnormal Tau only represent 0.4% of all cases). B. Subtle subcortical non-fibrillar abnormal tau pathology in axons and pretangle formation as a function of age. C. Cortical non-fibrillar inclusions in the transentorhinal cortex. D. Braak stages I-II as a function of age. E. Braak stages III-IV as a function of age. F. Braak stages V-VI as a function of age. G. Amyloid plaques in the inferior temporal neocortex (phase 1) as a function of age. H. Amyloid plaques in the entire neocortex (phase 2) and in subcortical portions of the forebrain (phase 3) as a function of age. K. Amyloid plaques into mesencephalic components (phase 4) and in the reticular formation and the cerebellum (phase 5) as a function of age. Adapted from (Braak and Del Tredici, 2015).

Titre : Transmission expérimentale d'endophénotypes de la maladie d'Alzheimer à des modèles murins et primates.

Mots clés : Maladie d'Alzheimer, transmission expérimentale, prion, modèles animaux, endophénotypes

Résumé : La maladie d'Alzheimer (MA) est caractérisée par l'accumulation de protéines β-amyloïde (Aβ) et Tau malconformées. L'hypothèse que la MA soit transmissible de manière similaire à celles des maladies à prion est un sujet d'intense recherche. L'objectif de cette thèse est d'étudier la transmission des endophénotypes de la maladie d'Alzheimer par l'inoculation intracérébrale d'homogénats de patients souffrant de MA.

Tout d'abord, nous avons montré que la transmission expérimentale de la MA accélère l'amyloïdose dans des modèles murins d'amyloïdose génétique précoce et tardive. Ensuite, nous avons observé le développement d'altérations fonctionnelles et morphologiques semblables à celles observées dans la MA chez le primate microcèbe (*Microcebus murinus*) et accompagnées d'une amyloïdose subtile sans pathologie Tau. Une telle transmission en l'absence de sévères lésions neuropathologiques a été rapportée dans les maladies à prions mais jamais dans le contexte de la MA. Nos résultats suggèrent que les agents responsable des altérations observées puissent être des formes d'Aβ et/ou Tau non détectées en immunohistochimie et pouvant être transmises expérimentalement.

En conclusion, nos résultats supportent l'hypothèse de type prion de la MA et le consensus actuel sur la toxicité des formes solubles d'Aβ et Tau. Pour finir, ils soutiennent la possibilité que l'amyloïdose soit transmissible chez l'Homme sous certaines conditions et appellent à l'évaluation des impacts fonctionnels chez les sujets à risque de contamination.

Title: Experimental transmission of Alzheimer's disease endophenotypes to murine and primate models.

Keywords: Alzheimer's disease, experimental transmission, prion, animal models, endophenotypes

Abstract: Alzheimer's disease (AD) is characterized by the accumulation of misfolded β-amyloid (Aβ) and Tau proteins. There has been longstanding interest as to whether AD might be transmissible similarly to prion diseases. Our objective was to study the transmissibility of AD endophenotypes after AD brain intracerebral inoculation in mice and primates.

First, we showed that AD experimental transmission accelerated Aβ pathology in two rodent models of early or late genetic β-amyloidosis. Then, we focused on a primate model of sporadic AD, the mouse lemur (*Microcebus murinus*). AD-inoculated adult lemurs progressively developed cognitive impairments, neuronal activity alterations and cerebral atrophy. AD-inoculated mouse lemurs also developed subtle β-amyloidosis in the absence of Tau pathology, 18 months after inoculation. The transmission of an AD-like pathology in the absence of severe neuropathological lesions is striking. Such observations have already been reported for prion diseases but never in the context of AD. Our results suggest that agents leading to AD-like alterations may be non immunohistopathological-detectable forms of Aβ or Tau proteins and be transmitted experimentally.

In conclusion, our results support the "prion-like" hypothesis of AD and provide further arguments for a dichotomy between the toxicity of deposited and soluble assemblies of Aβ or Tau proteins. Finally, they complement recent evidence supporting iatrogenic β-amyloidosis in humans and provide strong arguments to evaluate functional outcomes in potentially contaminated individuals.

Université Paris-Saclay
Espace Technologique / Immeuble Discovery
Route de l'Orme aux Merisiers RD 128 / 91190 Saint-Aubin, France